WILEY-VCH

Max Appl

Ammonia

Principles and Industrial Practice

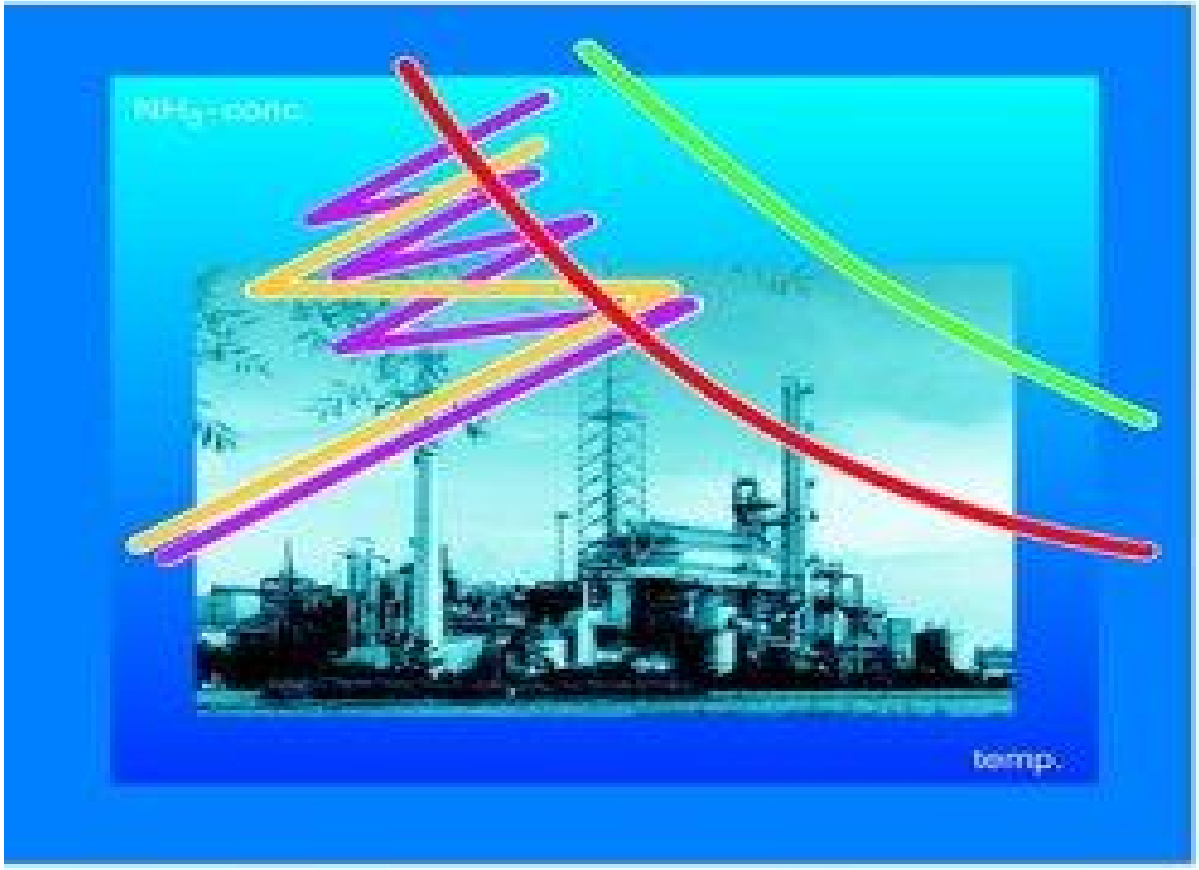

Contents

1. Introduction

The name ammonia for the nitrogen–hydrogen compound NH_3 is derived from the oasis Ammon (today Siwa) in Egypt, where Ammonia salts were already known in ancient times and also the Arabs were aware of ammonium carbonate. For a long time only the "sal ammoniacum" was available. Free ammonia was prepared much later (PRIESTLEY, 1774).

In nature ammonia, NH_3 occurs almost exclusively in the form of ammonium salts. Natural formation of ammonia is primarily by decomposition of nitrogen-containing organic materials or through volcanic activity. Ammonium chloride can deposite at the edges of smoldering, exposed coal beds (already observed in Persia before 900 A. D.). Similar deposits can be found at volcanoes, for example, Vesuvius and Etna in Italy. Ammonia and its oxidation products, which combine to form ammonium nitrate and nitrite, are produced from nitrogen and water vapor by electrical discharges in the atmosphere. These ammonium salts supply a significant proportion of the nitrogen needed by growing plants when eventually deposited on the earth's surface. Ammonia and its salts are also byproducts of commercial processing (gasification, coking) of fuels such as coal, lignite and peat (see Fig. 1) Other sources of nitrogen compounds are exhausts from industrial, power-generation, and automotive sectors.

Following the discovery of the nature and value of mineral fertilization by LIEBIG in 1840, nitrogen compounds were used in increasing quantities as an ingredient of mineral fertilizers. At the end of the last century ammonia was recovered in coke oven plants and gas works as a byproduct of the destructive distillation of coal. The produced ammonium sulfate was used as fertilizer. Since these sources of nitrogen were limited in quantity they did not suffice for fertilization. Therefore, it was necessary to use saltpeter from natural deposits in Chile. The earliest source of synthetic nitrogen compunds as fertilizers was the Frank–Caro calcium cyanamide process from 1898 onwards. But the supply was far from sufficient and scientists were concerned with the possibility of future famine because of insufficient agricultural yields. In September

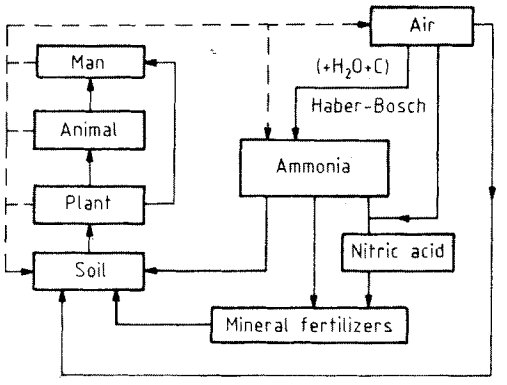

Figure 1. The nitrogen cycle

1898, in his famous presidential speech to the British Association of Advanced Science, SIR WILLIAM CROOKS adressed the problem and concluded with the prophetic words: "It is the chemist who must come to the rescue of the threatened communities. It is through the laboratory that starvation may ultimately be turned into plenty. Before we are in the grip of actual dearth the chemist will step in and postpone the days of famine to so distant a period that we, our sons and grandsons may live without undue solicitude for the future."

The development of the synthesis of ammonia from its elements is therefore a landmark in the history of industrial chemistry. But this process did not only solve a fundamental problem in securing our food supply by economic production of fertilizers in quantity but also opened a new phase of industrial chemistry by laying the foundations for subsequent high-pressure processes like methanol synthesis, oxo synthesis, Fischer–Tropsch process, coal liquefaction, and Reppe reactions. The technical experience and process know-how gained thereby had an enormous influence on the further development of chemical engineering, metallurgy, process control, fabrication and design of reactors, apparatus, and of course on the theory and practice of heterogeneous catalysis.

Process technology and chemical engineering as we understand it today began with the successful realization of the technical ammonia synthesis. Continuous production with high space velocities and space yields combined with the ammonia oxidation process developed immediately thereafter enabled chemical industry for the first time to compete successfully with a cheap natural bulk product, namely, sodium nitrate from Chile. The synthesis of ammonia thus became exemplary for all subsequent chemical mass production processes.

The development of the ammonia production process was also beginning of systematic catalytic research and widespread use of catalysts in industrial chemistry. Many subsequent achievments in theoretical understanding and practical application of heterogeneous catalysis have their roots in the ammonia synthesis reaction with probably can be considered to be the best understood catalytic process, as demonstrated by the enormous number of publications.

Today ammonia is the second largest synthetic chemical product; more than 90 % of world consumption is manufactured from the elements nitrogen and hydrogen in a catalytic process originally developed by FRITZ HABER and CARL BOSCH using a promoted iron catalyst discovered by ALWIN MITTASCH. Since the early days there has been no fundamental change in this process. Even today the synthesis section of every ammonia plant has the same basic configuration as the first plants. A hydrogen–nitrogen mixture reacts over the iron catalyst (today's formulation differs little from the original) at elevated temperature in the range of 400–500 °C (originally up to 600 °C) and pressures above 100 bar with recycle of the unconverted part of the synthesis gas and separation of the ammonia product under high pressure.

BOSCH was already well aware that the production of a pure hydrogen–nitrogen mixture is largest single contributor to the total production cost of ammonia [1]. So, in contrast to the synthesis reaction, dramatic changes happened over the years in the

technology of synthesis-gas generation, and industrial ammonia processes differ today mainly with respect to synthesis-gas preparation and purification. The elements nitrogen and hydrogen are abundantly available in the form of air and water, from which they can be separated by physical methods and/or chemical reactions using almost exclusively fossil energy. The predominant fossil fuels are natural gas, liquified petroleum gas (LPG), naphtha, and higher petroleum fractions; coal or coke is used today only under special economic and geographical conditions (China, India, South Africa). Recovery of ammonia as byproduct of other production processes, e.g., coke ovens, is no longer of great importance.

Of course, some of the hydrogen comes also from the hydrocarbons themselves (methane has the highest content), and the carbon acts as a reducing agent for water and in some processes may also facilitate the separation of oxygen from nitrogen by formation of carbon dioxide, which can be removed by various operations.

As the ammonia sythesis is the very heart of every ammonia production and is also from a historical point of view the most interesting section it seems to be justified to discuss the fundamentals and the catalysis of this reaction separately and at first.

After this the various techniques used in the individual process steps of industrial ammonia production will be reviewed: gas generation and feedstock pretreatment, carbon monoxide shift conversion, gas purification, compression, and ammonium synthesis. Next the concept and philosophy of integrated single–train ammonia plants will be presented, followed by a review of the commercial processes presently marketed by the various licensors and engineering contractors and of some options for modernization of older plants. Separate chapters are included for the following subjects: integration of other production processes; material considerations for equipment fabrication; handling, storage and transport of ammonia; quality specifications and analysis; environmental, safety and health aspects; chemical reactions and uses; economic aspects; future prospects.

2. Historical Development

The driving force in the search for methods of nitrogen fixation, of course, was to produce fertilizers. In principle there are three ways of breaking the bond of the nitrogen molecule and fixing the element in a compound:

1) To combine the atmospheric elements nitrogen and oxygen directly to form nitric oxides
2) To combine nitrogen and hydrogen to give ammonia
3) To use compounds capable of fixing nitrogen in their structure under certain reaction conditions.

A vast amount of research in all three directions led to commercial processes for each of them: the electric arc process, the cyanamid process, and ammonia synthesis, which finally displaced the other two and rendered them obsolete.

The availability of cheap hydrolelectric power in Norway and the United States stimulated the development of the *electric arc process.* Air was passed through an electric arc which raised its temperature to 3000 °C, where nitrogen and oxygen combine to give nitric oxide. In 1904 CHRISTIAN BIRKELAND performed successful experiments and, together with SAM EYDE, an industrial process was developed and a commercial plant was built, which by 1908 was already producing 7000 t of fixed nitrogen. Working in parallel, SCHOENHERR at BASF developed a different electric arc furnace in 1905. The Norwegeans and BASF combined forces in 1912 to build a new commercial plant in Norway. However, since at this time pilot-plant operation of ammonia synthesis was already successful, BASF withdrew from this joint venture soon after. Nevertheless, the Norwegian plants operated throughout World War I and had total production of 28 000 t/a of fixed nitrogen with a power consumption of 210 000 kW [2]. The specific energy consumption was tremendous: 60 000 kW per tonne of fixed nitrogen. Had this electricity been generated from fossil fuels this figure would correspond to about 600 GJ/t nitrogen, which is about 17 times the consumption of an advanced steam-reforming ammonia plant in 1996.

The cyanamide process, [2]–[5], developed by FRANK and CARO in 1898, was commercially established by 1910. Calcium carbide, formed from coke and lime in a carbide furnace [6], reacts with nitrogen to give calcium cyanamide, which can be decomposed with water to yield ammonia. The process was energetically very inefficient, consuming 190 GJ per tonne of ammonia. Some other routes via barium cyanide produced from barytes, coke and nitrogen, or using the formation of titanium nitride were investigated in Ludwigshafen by BOSCH and MITTASCH but did not appear promising. In 1934, 11 % of world's fixed nitrogen production (about 2×10^6 t/a) [7] was still based on the cyanamid process, and some plants even continued to operate after World War II.

After Berthollet proved in 1784 that ammonia consists of nitrogen and hydrogen and was also able to establish the approximate ratio between these elements, many

experiments in the 1800s were aimed at its *direct synthesis*, but remained unsuccessful [8]–[10]. One of the reasons for the lack of success was the limited knowledge of thermodynamics and the incomplete understanding of the law of mass action and chemical equilibrium. It was the new science of physical chemistry, which developed rapidly in the late 1800s, that enabled chemists to investigate ammonia formation more systematically.

Around 1900 FRITZ HABER began to investigate the ammonia equilibrium [11] at atmospheric pressure and found minimal ammonia concentrations at around 1000 °C (0.012 %). Apart from HABER, OSTWALD and NERNST were also closely involved in the ammonia synthesis problem, but a series of mistakes and misunderstandings occurred during the research. For example, OSTWALD withdrew a patent application for an iron ammonia synthesis catalyst because of an erroneous experiment, while NERNST concluded that commercial ammonia synthesis was not feasible in view of the low conversion he found when he first measured the equilibrium at 50 – 70 bar [12] – [14].

After a controversy with NERNST, HABER repeated his measurements at atmospheric pressure and subsequently at higher pressures [15]–[18], overcoming his colleague's preoccupation with the unfavorable equilibrium concentrations. HABER concluded that much higher pressures had to be employed and that, perhaps more importantly, a recycle process was necessary.

The amount of ammonia formed in a single pass of the synthesis gas over the catalyst is much too small to be of interest for an economic production. HABER therefore recycled the unconverted synthesis gas. After separating the ammonia by condensation under synthesis pressure and supplementing with fresh synthesis gas to make up for the portion converted to ammonia, the gas was recirculated by means of a circulation compressor to the catalyst-containing reactor. This process, described in the patent DRP 235 421 (1908), became the basis for the industrial manufacture of ammonia and since then the same principle has found widespread application in numerous high-pressure processes. HABER also anticipated the preheating of the synthesis gas to reaction temperature (at that time 600 °C) by heat exchange with the hot exhaust gas from the reactor, the temperature of which would be raised by the exothermic ammonia formation reaction sufficiently (about 18 °C temperature rise for a 1 % increase of the ammonia concentration in converted synthesis gas).

HABER's recycle idea changed the static conception of process engineering in favor of a more dynamic approach. For the first time reaction kinetics were considered as well as the thermodynamics of the system. In addition to the chemical equilibrium, HABER recognized that for industrial realization, reaction rate was a determining factor. Instead of simple yield in a once-through process, which was the usual focus of chemists at that time, he concentrated on space–time yield. Figure 2 illustrates this consideration of equilibrium concentration in combination with space–time yield by comparing ammonia synthesis as a recycle process with the SO_2 oxidation process as a once-through operation.

In 1908 HABER approached BASF (Badische Anilin & Soda Fabrik at that time) to seek support for his work and to discuss the possibilities for the realization of an

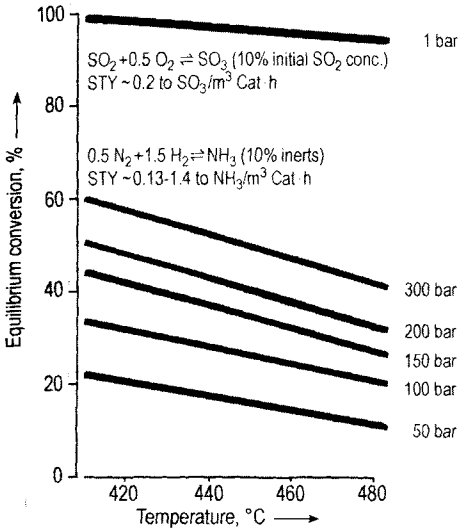

Figure 2. Equilibrium conversion and space time yield for NH_3 and SO_3 production

industrial process. His successful demonstration in April 1909 of a small laboratory scale ammonia plant having all the features described above finally convinced the BASF representatives, and the company's board decided to pursue the technical development of the process with all available resources. In an unprecedented achievement, CARL BOSCH, together with a team of dedicated and highly skilled co-workers, succeeded in developing a commercial process in less than five years [1], [19]–[25]. The first plant started production at Oppau in September 1913 and had a daily capacity of 30 t of ammonia. Expansions increased the capacity to about 250 t/d in 1916/17 and a second plant with a capacity of 36 000 t/a went on stream in 1917 in Leuna. Further stepwise expansions, finally reaching 240 000 t/a, already decided in 1916, came in full production only after World War I [3]. After World War I ammonia plants were built in England, France, Italy and many other countries based on a BASF license or own process developments, with modified process parameters, but using the same catalyst. Figure 3 shows with the example of the BASF plant what the plants looked like in these years. Synthesis gas production was performed from coke by using water gas generators and producer gas generators in parallel. Coal (e.g., lignite) was gasified in Leuna in the subsequently introduced Winkler generators, the first example of fluidized-bed technology. Progress in cryogenic air separation plants with respect to reliability and capacity made it possible to switch the gasification processes from air to oxygen as time went on. Shift conversion was already performed on iron oxide chromium oxide catalysts, water scrubbing was used for CO_2 removal, and residual CO was removed by a copper liquid wash. Gasification, desulfurization, and shift conversion were at normal pressure, CO_2 removal at 25 bar, and copper liquid wash and synthesis at 300 bar. Ammonia was removed from the loop by condensation (from early 1920 onwards; before that by water scrubbing as aqueous ammonia).

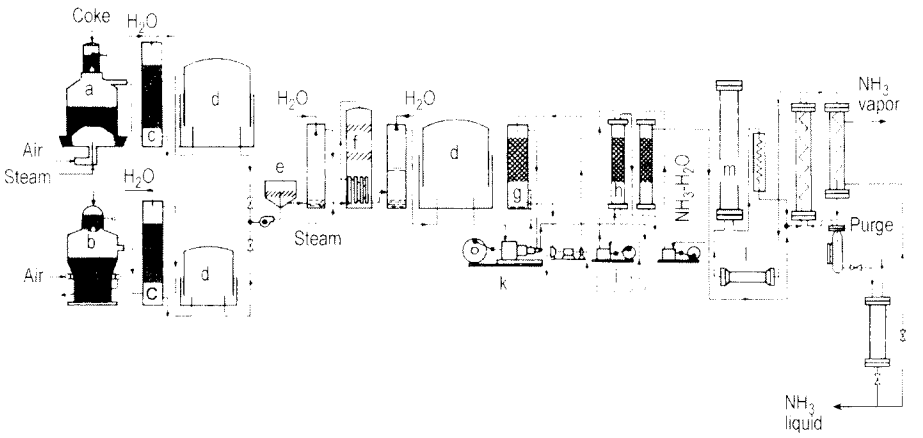

Figure 3. Simplified flow sheet of a coke-based ammonia plant in the 1930s
a) Watergas generator, b) Producer gas generation, c) Scrubber, d) Gas holders, e) Sulfur removal, f) Shift converter g) CO_2 removal, h) CO removal (Co-liq.), i) Copper liq. regeneration, k) Syngas compressor, l) Circulation pump, m) Ammonia converter

Up to the end of World War II, plant capacities were expanded by installing parallel lines of 70 – 120 t/d units, and synthesis-gas generation continued to be based on coal until the 1950s, of course, with improved and now continuously operating designs, as for example the so-called "Abstichgenerator" of BASF [26]. With growing availability of cheap petrochemical feedstocks and novel cost-saving gasification processes (steam reforming and partial oxidation) a new age dawned in the ammonia industry. The development started in the USA, where steam reforming of natural gas was used for synthesis gas production. This process was originally developed by BASF and greatly improved by ICI, who extended it to naphtha feedstocks. Before natural gas became available in large quantities in Europe, partial oxidation of heavy oil fractions was used in several plants. The next revolution in the ammonia industry was the advent of the single-train steam reforming ammonia plants, pioneered by M. W. KELLOGG and others. The design philosophy was to use a single-train for large capacities (no parallel lines) and to be as far as possible energetically self-sufficient (no energy import) by having a high degree of energy integration (process steps in surplus supplying those in deficit). Only through this innovative plant concept with its drastic reduction in feedstock consumption and investment costs, could the enormous increase in world capacity in the following years became possible. Increasing competition and rising feedstock prices in the 1970s and 1980s forced industry and engineering companies to improve the processes further.

The LCA process of ICI (Section 5.1.4.3.) and the KRES/KAAP process (Section 5.1.4.3.), which is the first process since 1913 to use a non-iron synthesis catalyst, are recent advances that make a radical breakaway from established technology.

A short survey of the history of ammonia process technology can be found in [14], [24], [27].

3. Fundamentals of the Synthesis Reaction

3.1. Physical Properties of Ammonia

Molecular Properties. Corresponding to its nuclear charge number, the nitrogen atom possesses seven shell electrons. One electron pair in in the ground state 1 *s* (K shell), and five electrons are distributed over the four orbitals with the principal quantum number 2 (L shell). Of these, one electron pair occupies the 2 *s* level and three unpaired electrons, respectively, a half of the remaining three levels, $2p_x$, $2p_y$, $2p_z$. The unpaired electrons can enter into electron-pair bonds with the 1 *s* electron of three hydrogen atoms. Thus, the three half occupied orbitals of the L shell become about fully accupied (formation of an octet of the neon type in accordance with the octet theory of Lewis–Langmuir).

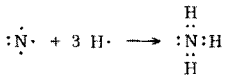

The nitrogen atom is at the apex of a pyramid above the plane of the three hydrogen atoms, which are arranged in an equilateral triangle. The H–N–H bond angle is about 107 ° [28]. Although covalent, the nitrogen–hydrogen bonds have a polar contribution because of a stronger electronegativity of nitrogen relative to hydrogen. Because of polarization of the bonds and the unsymmetrical molecular arrangement, the ammonia molecule has a considerable dipole moment, 1.5 D [29].

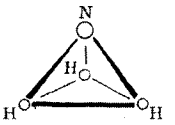

As the ammonia molecule possesses the same electron configuration as water (isosterism) and similar bond angles (water vapor bond angle 105 °, dipole moment 1.84 D), ammonia and water behave similarly in many reactions. Ammonia and water are diamagnetic. The dielectric constant of liquid ammonia is about 15 and greater than those of the most condensed gases; therefore, liquid ammonia has a considerable ability to dissolve many substances. The ammonia molecule, with its free electron pair, can combine with a proton.

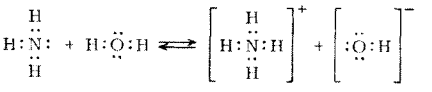

In the resulting ammonium ion, the nitrogen atom is situated in the middle of a

terahedron whose corners are occupied by hydrogen atoms. The four hydrogen atoms are equivalent in their behaviour. According to LINUS PAULING, the positive excess charge is distributed about equally over all five atoms.

Physical Data. The results of comprehensive investigations of the physical properties of ammonia have been published in [30] and [31]. Both papers provide numerous equations for physical properties derived from published data, the laws of thermodynamics, and statistical evaluation. These equations are supplemented by lists and tables of thermodynamic quantities and an extensive collection of literature references.

Moreover, data an physical properties and the comples systems important in synthesis may be found in [32]–[35], and of course, in the well-known tabulations *Landolt-Börnstein* [36] and *Handbuch der Kältetechnik* [37], among others. The most important physical data are compiled in Table 1.

***p–V–T* Data.** The $p-V-T$ data in Table 2 are calculated from the equations in [31] and further data in [30], [32]–[37]. Measured $p-V-T$ values for liquid ammonia in the pressure range from 7 to 180 MPa (70–1800 bar) and at temperatures from –20 °C to 40 °C may be found in [38]. Detailed information on compressibility gained from experimental data can be found in [40]–[44]. An equation of state for liquid ammonia is given in [45]; for a more simple form, see [35]. Further data may be found in references [46]–[48]. Properties of liquid ammonia from –50 to 65 °C and from saturation pressure up to 370 bar are reported in [49].

Caloric Data. Enthalpy and entropy of solid ammonia are given in [32]. Enthalpy and entropy may be calculated by the equations in [31]. Further data are given in [37], [50] and [32]–[37]. An enthalpy log$p$ diagram can be found in [37].

Specific Heat. In the range of –45 °C to 50 °C the specific heat (in kJ kg^{-1}K^{-1}) of liquid ammonia can be calculated by using the Equation (1):

$$c_p = -3.787 + 0.0949\,T - 0.3734 \times 10^{-3}\,T^2 + 0.5064 \times 10^{-6}\,T^3 \qquad (1)$$

where $T = \vartheta + 273.15$

Assuming ammonia to be an ideal gas in the range 300–2000 K the following Equation (2) represents the specific heat:

$$c_p = 1.4780 + 2.09307 \times 10^{-3}T - 2.0019 \times 10^{-7}\,T^2 - 8.07923 \times 10^{-11}\,T^3 \qquad (2)$$

The values of the specific heat at constant pressure in Table 3 have been calculated according to [31] and have been extrapolated to 500 °C using data from [31]. Further data can be found in [32]–[36], [52] and [53].

Properties of Saturated Ammonia Liquid and Vapor. Table 4 is derived from [31]. Further data may be found in [30], [34], [36] and [37]. For calculations from reduced data, among others, see [2], [54].

Table 1. Properties of ammonia

M_r	17.0312
Molecular volume	
(at 0 °C, 101.3 kPa)	22.08 L/mol
Gas constant R	0.48818 kPa m^3 kg^{-1} K^{-1}
Liquid density	
(at 0 °C, 101.3 kPa)	0.6386 g/cm^3
Gas density	
(at 0 °C, 101.3 kPa)	0.7714 g/L
Liquid density	
(at –33.43 °C, 101.3 kPa)	0.682 g/cm^3
Gas density	
(at –33.43 °C, 101.3 kPa)	0.888 g/L
Critical pressure	11.28 MPa
Critical temperature	132.4 °C
Critical density	0.235 g/cm^3
Critical volume	4.225 cm^3/g
Critical compressibility	0.242
Critical thermal conductivity	0.522 kJ K^{-1} h^{-1} m^{-1}
Critical viscosity	23.90 × 10^{-3} mPa · s
Melting point (triple point)	–77.71 °C
Heat of fusion (at 101.3 kPa)	332.3 kJ/kg
Vapor pressure (triple point)	6.077 kPa
Boiling point (at 101.3 kPa)	–33.43 °C
Heat of vaporization	
(at 101.3 kPa)	1370 kJ/kg
Standard enthalpy of	
formation (gas at 25 °C)	–46.22 kJ/mol
Standard entropy	
(gas at 25 °C, 101.3 kPa)	192.731 J mol^{-1} K^{-1}
Free enthalpy of formation	
(gas at 25 °C, 101.3 kPa)	–16.391 kJ/mol
Net heating value, *LHV*	18.577 kJ/g
Gross heating value, *HHV*	22.543 kJ/g
Electrical conductivity	
(at –35 °C), very pure	1 × 10^{-11} $\Omega^{-1}cm^{-1}$
Commercial	3 × 10^{-5} $\Omega^{-1}cm^{-1}$
Ignition temperature acc.	
to DIN 51794	651 °C
Explosive limits	
NH_3– O_2 mixture	
(at 20 °C, 101.3 kPa)	15–79 vol% NH_3
NH_3–air mixture	
(at 0 °C, 101.3 kPa)	16–27 vol% NH_3
(at 100 °C, 101.3 kPa)	15.5–28 vol% NH_3

Vapor–Liquid Equilibria for the Ammonia, Hydrogen, Nitrogen, Argon, Methane System (Fig. 4). Because of the great importance of absorption processes in synthesis loop engineering (see Section 4.5.6), these binary and multicomponent systems have been experimentally and theoretically reinvestigated several times. The updates are based mainly on thermodynamic relationships in combination with equations of state.

In [58] various publications are compared with one another and equilibrium methods for the ranges 273–323 K and 4.9–49 MPa (49 to 490 bar) are reported. Inves-

Table 2. Specific volume of ammonia in L/kg

p,MPa	Temperature, °C											
	−33	−20	−10	0	10	20	50	100	150	200	250	300
0.1	1172.001	1235.492	1284.303	1333.094	1381.870	1430.634	1576.882	1820.589	2064.339	2308.163	2552.061	2796.020
0.5	1.467	1.503	1.533	1.566	257.613	269.524	303.259	356.206	407.353	457.602	507.299	556.610
1	1.466	1.503	1.533	1.565	1.600	1.638	144.981	173.883	200.728	226.667	252.117	277.272
2	1.465	1.501	1.531	1.563	1.598	1.636	64.713	82.476	97.322	111.121	124.391	137.352
3	1.464	1.500	1.530	1.562	1.596	1.634	1.772	51.740	62.785	72.589	81.818	90.721
4	1.463	1.499	1.528	1.560	1.594	1.631	1.768	36.088	45.448	53.305	60.532	67.414
5	1.462	1.498	1.527	1.558	1.592	1.629	1.764	26.361	34.981	41.713	47.754	53.432
6	1.461	1.497	1.526	1.557	1.590	1.627	1.760	19.379	27.944	33.968	39.229	44.109
7	1.460	1.495	1.524	1.555	1.589	1.625	1.756	2.171	22.859	28.422	33.137	37.449
8	1.459	1.494	1.523	1.554	1.587	1.623	1.752	2.151	18.986	24.251	28.565	32.455
10	1.458	1.492	1.520	1.551	1.583	1.618	1.745	2.115	13.375	18.385	22.163	25.467
15	1.453	1.486	1.514	1.543	1.574	1.608	1.727	2.048	4.321	10.478	13.632	16.176
20	1.448	1.481	1.508	1.536	1.566	1.599	1.712	1.999	2.780	6.534	9.408	11.574
25	1.443	1.475	1.501	1.529	1.558	1.590	1.697	1.959	2.516	4.474	6.957	8.863
30	1.438	1.470	1.496	1.522	1.551	1.581	1.684	1.926	2.376	3.540	5.443	7.113
35	1.434	1.465	1.490	1.516	1.544	1.573	1.672	1.898	2.282	3.094	4.494	5.922
40	1.429	1.460	1.484	1.510	1.537	1.565	1.660	1.873	2.211	2.839	3.893	5.088
45	1.424	1.454	1.479	1.504	1.530	1.557	1.650	1.850	2.155	2.670	3.497	4.491
50	1.419	1.449	1.473	1.498	1.523	1.550	1.639	1.830	2.108	2.547	3.221	4.054
55	1.414	1.444	1.468	1.492	1.517	1.543	1.630	1.811	2.068	2.453	3.020	3.727
60	1.409	1.439	1.462	1.486	1.511	1.536	1.620	1.794	2.033	2.377	2.865	3.476

Table 3. Specific heat of ammonia at constant pressure in kJ kg^{-1} K^{-1}

p, MPa	Temperature, °C													
	−33	−20	−10	0	10	20	50	100	150	200	250	300	400	500
0.1	2.324	2.236	2.197	2.175	2.163	2.159	2.174	2.240	2.328	2.422	2.518	2.612	2.797	2.966
0.5	4.468	4.528	4.572	4.618	2.673	2.553	2.383	2.339	2.385	2.459	2.542	2.628	2.815	2.981
1	4.466	4.526	4.569	4.615	4.668	4.736	2.707	2.470	2.456	2.504	2.574	2.653	2.838	2.998
2	4.462	4.521	4.563	4.607	4.659	4.725	3.785	2.787	2.611	2.597	2.636	2.696	2.886	3.028
3	4.458	4.516	4.557	4.600	4.651	4.714	5.039	3.216	2.788	2.697	2.701	2.742	2.934	3.060
4	4.454	4.511	4.552	4.594	4.642	4.703	5.014	3.832	2.994	2.805	2.769	2.788	2.981	3.091
5	4.450	4.506	4.546	4.587	4.634	4.693	4.991	4.826	3.236	2.923	2.840	2.837	3.028	3.121
6	4.446	4.501	4.541	4.580	4.626	4.683	4.969	6.854	3.526	3.050	2.916	2.887	3.067	3.168
7	4.442	4.497	4.535	4.574	4.618	4.673	4.947	6.776	3.882	3.190	2.994	2.939	3.069	3.203
8	4.439	4.492	4.530	4.567	4.610	4.664	4.927	6.551	4.330	3.342	3.077	2.992	3.155	3.238
10	4.432	4.484	4.520	4.555	4.595	4.645	4.889	6.215	5.724	3.695	3.255	3.103	3.242	3.304
15	4.415	4.463	4.496	4.527	4.561	4.603	4.806	5.701	20.410	4.965	3.776	3.407	3.470	3.463
20	4.400	4.444	4.474	4.501	4.530	4.566	4.736	5.396	8.827	6.899	4.399	3.739	3.644	3.607
25	4.387	4.427	4.454	4.477	4.502	4.532	4.676	5.187	6.826	8.074	5.046	4.080	3.812	3.734
30	4.376	4.412	4.435	4.456	4.477	4.502	4.624	5.032	6.048	7.426	5.543	4.397	3.980	3.861
35	4.367	4.399	4.419	4.436	4.454	4.475	4.578	4.912	5.614	6.605	5.741	4.652	4.104	3.967
40	4.361	4.387	4.404	4.418	4.432	4.450	4.538	4.814	5.330	6.033	5.693	4.818	4.229	4.074
45	4.358	4.377	4.391	4.402	4.413	4.427	4.502	4.734	5.128	5.643	5.539	4.894	4.310	4.159
50	4.359	4.369	4.379	4.387	4.395	4.407	4.469	4,665	4.975	5.365	5.364	4.903	4.392	4.244
55	4.367	4.363	4.369	4.374	4.379	4.388	4,440	4.607	4.855	5.157	5.202	4.873	4.442	4.301
60	4.385	4.360	4.361	4.362	4.365	4.370	4.413	4.556	4.757	4.996	5.060	4.824	4.492	4.359

Table 4. Properties of saturated ammonia liquid and vapor

t, °C	p, kPa	Specific volume		Enthalpy		Heat of vaporization,	Entropy	
		Liquid, L/kg	Vapor, L/kg	Liquid, kJ/kg	Vapor, kJ/kg	kJ/kg	Liquid, kJ kg^{-1}K^{-1}	Vapor, kJ kg^{-1}K^{-1}
−40	71.72	1.4490	1551.6	180.53	1568.7	1388.1	0.8479	6.8017
−35	93.14	1.4620	1215.4	202.80	1576.5	1373.1	0.9423	6.7105
−30	119.49	1.4754	962.9	225.19	1584.1	1358.9	1.0352	6.6241
−25	151.54	1.4892	770.95	247.69	1591.5	1343.8	1.1266	6.5419
−20	190.16	1.5035	623.31	270.31	1598.6	1328.3	1.2166	6.4637
−15	236.24	1.5184	508.49	293.05	1605.4	1312.4	1.3053	6.3890
−10	290.77	1.5337	418.26	315.91	1611.9	1296.0	1.3927	6.3175
− 5	354.77	1.5496	346.68	338.87	1618.0	1279.1	1.4787	6.2488
0	429.35	1.5660	289.39	361.96	1623.6	1261.7	1.5636	6.1826
5	515.65	1.5831	243.16	385.17	1628.9	1243.8	1.6473	6.1188
10	614.86	1.6009	205.55	408.51	1633.7	1225.2	1.7299	6.0571
15	728.24	1.6194	174.74	432.01	1638.1	1206.1	1.8116	5.9972
20	857.08	1.6387	149.31	455.67	1642.0	1186.3	1.8922	5.9390
25	1002.7	1.6590	128.19	479.52	1645.3	1165.8	1.9721	5.8822
30	1166.6	1.6801	110.54	503.57	1648.1	1144.5	2.0512	5.8267
35	1350.0	1.7023	95.699	527.86	1650.3	1122.4	2.1295	5.7722
40	1554.6	1.7257	83.150	522.40	1651.9	1099.5	2.2075	5.7185
45	1781.7	1.7505	72.484	577.22	1652.8	1075.6	2.2849	5.6656
50	2033.0	1.7766	63.373	602.36	1653.0	1050.6	2.3619	5.6131

tigations of binary systems are reported in [56] and [59]–[66] and equations and compilations in [56], [67], and [68], among others. The basis for the saturation concentration (Table 5) and solubilities in liquid ammonia (Table 6) are unpublished BASF calculations produced with the help of the Lee–Kesler equation of state [69] and publications [56], [57]. The ammonia content of the gas may be calculated with the formulas from [63].

A mutual interaction of solubilities exists in all multicomponent systems. The interaction with methane is pronounced. This interdependence is treated in detail in [56], [59], [70] and [71].

Surface Tension. The following equation (Eq. 3), from [72], represents the surface tension of ammonia (σ in Nm^{-1}) over the range −50 to 50 °C.

$$\sigma = 26.55 \times 10^{-3} - 2.3 \times 10^{-4}\,\vartheta \qquad (3)$$

Experimental data are given in [73]. The surface tension of aqueous ammonia solutions over the ranges 0.1–1.2 MPa (1–12 bar) and 20–100 °C can be found in [74].

Dynamic Viscosity. A survey on dynamic viscosity data for the ranges 30–250 °C and 0.1–80 MPa (1–800 bar) appears in [34]; further data occur in [75] and [76]. Experimental viscosity data and correlating equations for the range 448–598 K and for pressures up to 12.1 MPa (121 bar) can be found in [77]. Generalized equations for viscosity calculations on refrigerants are presented in [78].

Figure 4. Equilibrium solubilities (K factors) for argon (A), hydrogen (B), nitrogen (C), hydrogen:nitrogen 3:1 (D), and methane:nitrogen in liquid ammonia (E), F shows the dependance of the methane partial pressure ($p \cdot \gamma CH_4$) on the concentration of methane dissolved in the liquidm χCH_4, for three different gas mixture A – C and E according to [55], F according to [56], D was developed from data reported in [57]

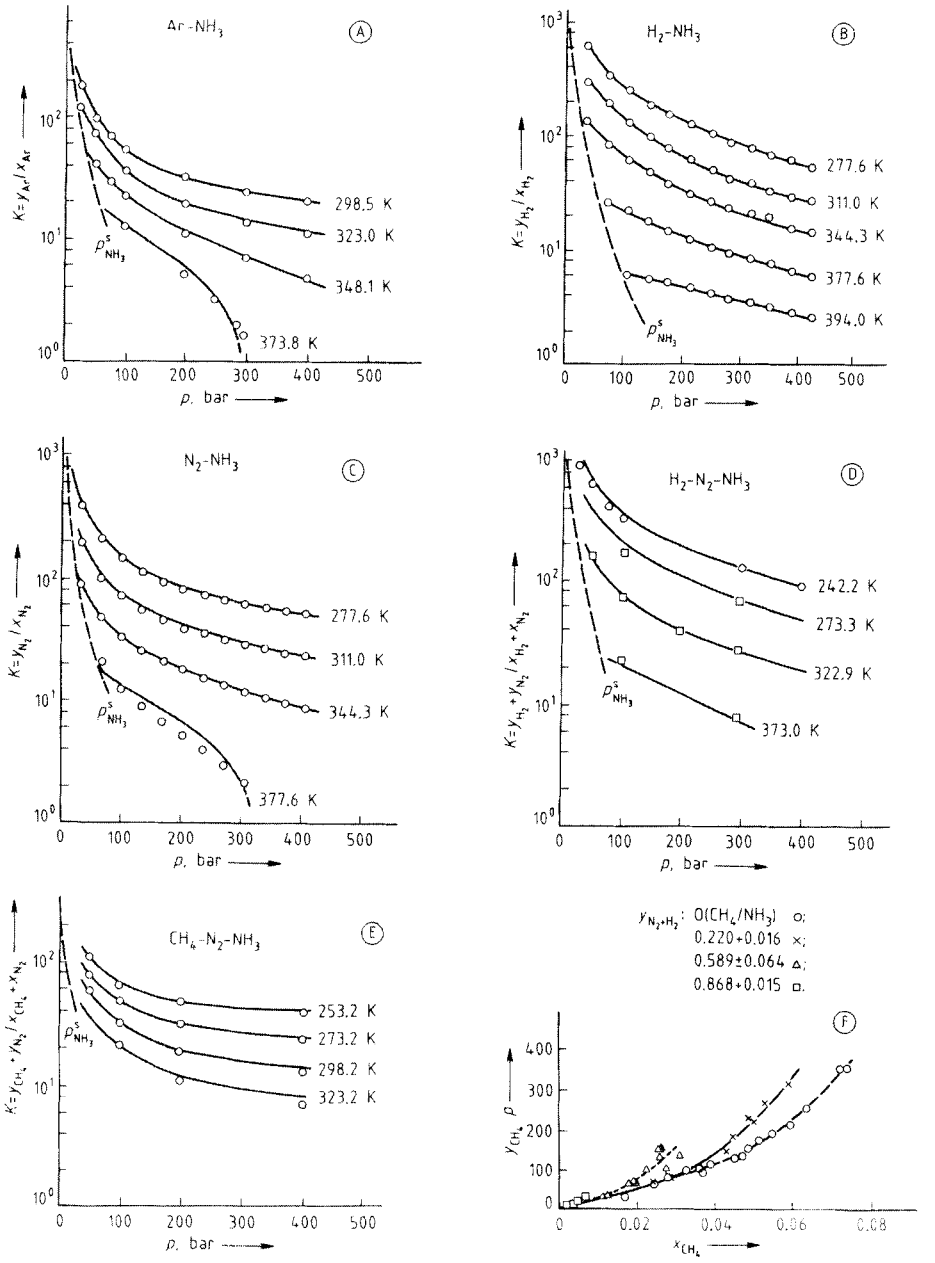

Table 5. Ammonia concentration at saturation in 1:3 mixtures of nitrogen and hydrogen, in vol%

t, °C	p, MPa							
	5	10	15	20	30	40	50	100
−30	2.9	1.7	1.34	1.15	0.95	0.9	0.87	0.8
−20	4.6	2.70	2.05	1.58	1.5	1.38	1.3	1.2
−10	6.8	4.06	3.10	2.63	2.22	2.03	1.94	1.75
0	10.0	5.80	4.50	3.80	3.20	2.90	2.75	2.5
10	15.0	8.25	6.40	5.36	4.50	4.05	3.84	3.55
20	19.6	11.4	8.6	7.35	6.05	5.55	5.25	4.9
30	20.0	15.2	11.5	9.80	8.20	7.50	7.10	6.70
40	26.5	20.0	15.0	14.0	10.75	9.80	9.40	9.0

Table 6. Solubility of hydrogen and nitrogen in liquid ammonia for 1:3 mixtures of nitrogen and hydrogen in cm^3 gas/g NH_3 (STP)

t, °C		Total pressure, MPa							
		5	10	15	20	30	40	50	100
−30	N_2	0.632	1.161	1.637	2.036	2.743	3.291	3.754	5.317
	H_2	1.291	2.598	3.896	5.157	7.554	8.625	12.380	22.287
−20	N_2	0.864	1.438	2.036	2.568	3.452	4.195	4.195	8.852
	H_2	1.581	3.167	4.759	6.248	9.294	12.518	15.219	33.945
−10	N_2	0.922	1.730	2.488	3.129	4.258	5.207	6.027	8.853
	H_2	1.845	3.869	5.756	7.623	11.444	14.954	18.349	33.945
0	N_2	1.081	2.088	2.994	3.811	5.269	6.457	7.532	11.218
	H_2	2.215	4.560	6.956	9.163	13.740	18.220	22.461	41.863
10	N_2	1.226	2.461	3.583	4.564	6.342	7.800	9.190	14.085
	H_2	2.585	5.490	8.360	11.178	16.590	22.056	27.300	51.783
20	N_2	1.372	2.874	4.414	5.415	7.654	8.303	11.285	17.733
	H_2	2.969	6.423	9.970	13.338	20.142	26.731	33.310	63.530
30	N_2	1.505	3.315	4.954	6.418	9.169	11.619	13.968	22.528
	H_2	3.300	7.557	11.719	15.711	24.272	32.343	40.396	79.345
40	N_2	1.584	3.717	5.767	7.647	10.967	13.954	16.852	28.527
	H_2	3.631	8.761	13.745	18.916	28.028	39.127	49.451	97.253

The following, from [72], is a formula for interpolation along the vapor pressure curve for liquid ammonia (viscosity η in N s m^{-2}):

$$\eta = 1.949 \times 10^{-4} - 1.72 \times 10^{-10}\,\vartheta + 7 \times 10^{-6}\,\vartheta^2 \quad (4)$$

An interpolation formula for ammonia vapor for the temperature range −20 to 150 °C at 0.098 MPa is given in [72]:

$$\eta = 9.83 \times 10^{-6} + 2.75 \times 10^{-8}\,\vartheta + 2.8 \times 10^{-11}\,\vartheta^2 \quad (5)$$

Reference [79] reports viscosity measurements for the hydrogen–ammonia system; [80] for nitrogen–ammonia, oxygen–ammonia, methane–ammonia, and ethylene–ammonia; and [81] for argon–ammonia.

Thermal Conductivity. In [82], experimental data and calculation methods for ammonia liquid and vapor for the ranges 0.1–49 MPa (1–490 bar) and 20–177 °C

Table 7. Table for determining the percentage ammonia content of aqueous solutions from the density at 15 °C

Density, g/cm³	Ammonia content	Density, g/cm³	Ammonia content
1.000	0.00	0.935	17.12
0.995	1.14	0.930	18.64
0.990	2.31	0.925	20.18
0.985	3.55	0.920	21.75
0.980	4.80	0.915	23.35
0.975	6.05	0.910	24.99
0.970	7.31	0.905	26.64
0.965	8.59	0.900	28.33
0.960	9.91	0.895	30.03
0.955	11.32	0.890	31.73
0.950	12.74	0.885	33.67
0.945	14.17	0.880	35.60
0.940	15.63		

are reported. The anomaly in the thermal conductivity at the critical point is discussed in full detail. A nomogram for these data appears in [83]. A third-degree equation for the range 358 – 925 K can be found in [84]. For the liquid phase the following formula may be used to interpolate in the range from –10 to 100 °C [72] (thermal conductivity λ in W m^{-1} K^{-1}):

$$\lambda = 0.528 - 1.669 \times 10^{-2}\,\vartheta - 6.2 \times 10^{-6}\,\vartheta^2 \qquad (6)$$

Also from [72] is the formula for ammonia vapor at 101.3 kPa and –20 to 150 °C:

$$\lambda = 0.0217 + 1.17 \times 10^{-4}\,\vartheta + 1.87 \times 10^{-2}\,\vartheta^2 \qquad (7)$$

The thermal conductivities of gas mixtures of ammonia with argon, neon, hydrogen, and methane are reported in [80] and [85] – [87].

Solubility in Water. Tables 7 and 8 and Figures 5 and 6 show miscellaneous information. General physicochemical and chemical engineering handbooks can be consulted for further data.

Reference [88] gives $p - V - T$ values for ammonia containing up to 0.5 wt % water at pressures in the range 113 – 221 kPa.

3.2. Thermodynamic Data of the Reaction

Ammonia synthesis proceeds according to the following reaction (8):

$$0.5\ N_2 + 1.5\ H_2 \rightleftharpoons NH_3 \qquad \Delta H_{298} = -46.22\ \text{kJ/mol} \qquad (8)$$

To fix a kilogram of nitrogen in ammonia requires reacting 2.4 m³ (STP) of hydrogen and 0.8 m³ (STP) of nitrogen. About 3.27 MJ of heat is evolved. Table 9 is a

Table 8. Heat of solution of ammonia in water, in kJ/mol NH_3

t, °C	Mixture ratio (moles of water per mole ammonia)						
	1	2.33	4	9	19	49	99
0	30.69	34.25	35.17	35.80	36.22	36.47	36.09
20	27.38	32.87	33.66	34.50	34.67	34.83	34.92
40	24.53	31.99	32.91	33.62	33.87	33.95	34

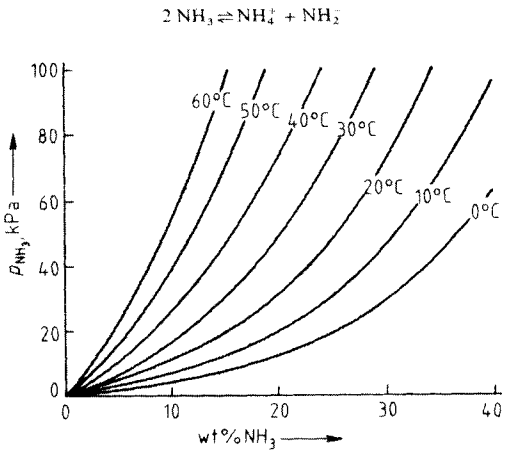

Figure 5. Ammonia partial pressure in aqueous ammonia solutions

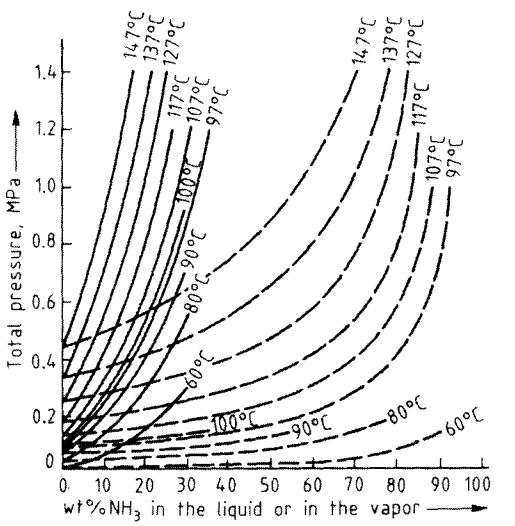

Figure 6. Total vapor pressure and composition of the liquid (——) and vapor (– – –) in the system NH_3–H_2O
Isotherms.

Table 9. Thermodynamic data for the reaction 0.5 N_2+1.5 $H_2 \rightarrow NH_3$ at atmospheric pressure

	t, K							
	300	400	500	600	700	800	900	1000
ΔH, kJ	−46.35	− 48.48	−50.58	−52.04	−53.26	−54.28	−55.06	−55.68
ΔS, J/K	−99.35	−105.63	−110.03	−112.71	−114.55	−115.89	−116.77	−117.48
$\Delta G/T$, J/K	−55.22	−15.66	8.88	26.25	38.48	48.02	55.56	61.81
$c_{p,\,NH_3}$, J mol^{-1}K^{-1}	35.52	38.80	41.97	45.04	47.98	50.80	53.49	56.03
$c_{p,\,H_2}$, J mol^{-1}K^{-1}	28.868	29.199	29.278	29.341	29.454	29.634	29.89	30.216
$c_{p,\,N_2}$, J mol^{-1}K^{-1}	29.144	29.270	29.601	30.132	30.777	31.451	32.117	32.724

compilation of the most important thermodynamic data for the reaction at atmospheric pressure.

Chemical Equilibrium. The reaction equilibrium has been investigated experimentally and theoretically many times. Today, values for the equilibrium constant are available for pressures up to 350 MPa (3500 bar).

GILLESPIE and BEATTIE [89] (see also [33]) were by far the most successful experimentally in establishing a firm basis for an analytical expression of the equilibrium constant in the range of industrial interest. The values in Tables 10 and 11 were calculated using their equation. A detailed description, with literature data and many tables, appears in [33]. A description of the equilibrium using the REDLICH–KWONG equation of state is given in [90].

Heat of Reaction. HABER investigated the heat of reaction at atmospheric pressure [91]. Numerous authors have estimated the pressure dependence under various assumptions. Today, most people use the Gillespie–Beattie equation [92]. This equation was used in calculating the values in Table 12. For further data see, for example, [33]. Reference [93] contains test results for the range 120–200 MPa (1200–2000 bar) and 450–525 °C. Additional literature can be found in [94].

Physical Properties of the Reactants. Various authors have measured the $p-V-T$ behavior of nitrogen, hydrogen, and 3:1 hydrogen–nitrogen mixtures. Reference [33] contains a survey. For the specific heat, thermal conductivity, and viscosity of the reactants, see [95], [96]. It is to be noted that heats of mixing must be considered for synthesis gas. This applies especially for high pressures and low temperatures. Reference [97] gives viscosities of hydrogen–nitrogen and hydrogen–ammonia mixtures.

Table 10. Ammonia content (in mol %) in equilibrium synthesis gas; $N_2:H_2=1:3$

t, °C	p_{abs}, MPa										
	5	10	20	30	40	50	60	70	80	90	100
300	39.38	52.79	66.43	74.20	79.49	83.38	86.37	88.72	90.61	92.14	93.39
310	36.21	49.63	63.63	71.75	77.35	81.51	84.73	87.29	89.35	91.03	92.42
320	33.19	46.51	60.79	69.23	75.12	79.53	82.98	85.74	87.98	89.83	91.35
330	30.33	43.45	57.92	66.64	72.79	77.46	81.13	84.09	86.52	88.52	90.20
340	27.64	40.48	55.04	63.99	70.39	75.29	79.18	82.34	84.95	87.12	88.94
350	25.12	37.60	52.17	61.31	67.93	73.04	77.14	80.49	83.28	85.62	87.59
360	22.79	34.84	49.33	58.61	65.41	70.72	75.01	78.55	81.52	84.02	86.15
370	20.64	32.21	46.53	55.89	62.85	68.33	72.80	76.52	79.66	82.33	84.61
380	18.67	29.71	43.79	53.19	60.26	65.89	70.53	74.42	77.72	80.54	82.97
390	16.87	27.36	41.12	50.50	57.66	63.41	68.19	72.23	75.69	78.67	81.25
400	15.23	25.15	38.53	47.86	55.06	60.91	65.81	69.99	73.59	76.71	79.43
410	13.74	23.08	36.04	45.26	52.47	58.39	63.40	67.69	71.42	74.68	77.54
420	12.40	21.16	33.65	42.72	49.91	55.87	60.96	65.36	69.20	72.58	75.57
430	11.19	19.38	31.37	40.26	47.39	53.37	58.50	62.99	66.93	70.43	73.53
440	10.10	17.74	29.20	37.87	44.92	50.88	56.05	60.60	64.63	68.22	71.43
450	9.12	16.23	27.15	35.57	42.50	48.43	53.61	58.20	62.29	65.97	69.28
460	8.24	14.84	25.21	33.36	40.16	46.03	51.19	55.80	59.95	63.69	67.08
470	7.46	13.57	23.39	31.26	37.89	43.67	48.81	53.42	57.60	61.39	64.85
480	6.75	12.41	21.69	29.55	35.71	41.38	46.46	51.06	55.25	59.09	62.60
490	6.12	11.36	20.10	27.34	33.61	39.16	44.17	48.74	52.92	56.78	60.33
500	5.56	10.39	18.61	25.54	31.60	37.02	41.94	46.46	50.62	54.48	58.06
510	5.05	9.52	17.24	23.84	29.68	34.95	39.77	44.22	48.36	52.20	55.80
520	4.59	8.72	15.96	22.24	27.86	32.97	37.68	42.05	46.13	49.96	53.55
530	4.19	8.00	14.77	20.74	26.13	31.07	35.65	39.94	43.96	47.75	51.32
540	3.82	7.34	13.68	19.34	24.49	29.26	33.71	37.89	41.84	45.58	49.13
550	3.49	6.74	12.67	18.02	22.95	27.54	31.85	35.92	39.79	43.47	46.97
560	3.20	6.20	11.74	16.80	21.49	25.90	30.06	34.02	37.80	41.41	44.86
570	2.93	5.70	10.88	15.65	20.13	24.35	28.37	32.20	35.88	39.41	42.81
580	2.69	5.26	10.09	14.59	18.84	22.88	26.75	30.46	34.04	37.48	40.81
590	2.47	4.85	9.36	13.60	17.64	21.50	25.22	28.80	32.26	35.62	38.87
600	2.28	4.48	8.69	12.69	16.52	20.20	23.76	27.22	30.57	33.83	37.00

3.3. General Aspects

Usually, a system having an exothermic heat of reaction under operating conditions should react spontaneously. However, to form ammonia from hydrogen and nitrogen molecules, significant energy input is required for the nitrogen molecule to achieve the activated state. This is because of its high dissociation energy of 941 kJ/mol, which is considerably higher than that of hydrogen. The Gibbs free energy for the dissociation reaction was determinded as $N_2 \rightleftharpoons 2N$ $\Delta F^0_{298} = 911$ kJ/Mol. The distance between the triply bonded nitrogen atoms of 1.098 Å is rather short. The first ionization energy is 1503 kJ/mol.

Because of the high dissociation energy the direct formation of oxides is "endergonisch" [98]. They are thermodynamically unstable compared to N_2 and O_2, which explains why the oxidation route for nitrogen fixation was not competitive.

Table 11. Equilibrium ammonia content (in mol%) in the presence of inert gases (2.5 mol% Ar; 7.5 mol% CH_4); N_2:H_2=1:3

t, °C	p_{abs}, MPa										
	5	10	20	30	40	50	60	70	80	90	100
300	32.11	43.10	54.27	60.62	64.95	68.12	70.56	72.49	74.03	75.28	76.31
310	29.52	40.51	51.98	58.63	63.20	66.59	69.22	71.31	72.99	74.37	75.51
320	27.05	37.96	49.66	56.57	61.38	64.98	67.79	70.04	71.87	73.38	74.63
330	24.71	35.46	47.32	54.45	59.48	63.29	66.28	68.70	70.67	72.31	73.68
340	22.51	33.03	44.96	52.30	57.52	61.52	64.69	67.27	69.39	71.16	72.65
350	20.46	30.68	42.62	50.11	55.51	59.68	63.02	65.76	68.03	69.93	71.54
360	18.56	28.42	40.30	47.90	53.46	57.79	61.29	64.18	66.59	68.63	70.36
370	16.80	26.27	38.01	45.69	51.37	55.85	59.49	62.52	65.08	67.24	69.10
380	15.19	24.33	35.77	43.48	49.26	53.86	57.64	60.81	63.49	65.79	67.77
390	13.72	22.31	33.59	41.29	47.14	51.85	55.74	59.03	61.84	64.27	66.36
400	12.39	20.50	31.48	39.13	45.02	49.81	53.81	57.21	60.14	62.68	64.89
410	11.18	18.81	29.44	37.01	42.91	47.76	51.84	55.34	58.38	61.03	63.35
420	10.08	17.24	27.49	34.93	40.83	45.71	49.86	53.44	56.57	59.32	61.75
430	9.10	15.79	25.62	32.92	38.77	43.67	47.86	51.52	54.73	57.57	60.09
440	8.21	14.45	23.85	30.97	36.75	41.64	45.87	49.58	52.86	55.78	58.39
450	7.41	13.22	22.17	29.09	34.78	39.65	43.88	47.63	50.97	53.96	56.65
460	6.70	12.09	20.59	27.29	32.87	37.68	41.92	45.68	49.06	52.11	54.87
470	6.06	11.05	19.10	25.56	31.02	35.77	39.97	43.75	47.16	50.25	53.06
480	5.49	10.11	17.71	23.92	29.23	33.90	38.06	41.83	45.25	48.38	51.24
490	4.97	9.24	16.41	22.36	27.51	32.08	36.20	39.94	43.36	46.51	49.40
500	4.51	8.46	15.19	20.89	25.87	30.33	34.37	38.08	41.49	44.64	47.56
510	4.10	7.74	14.07	19.50	24.30	28.64	32.61	36.26	39.65	42.79	45.72
520	3.73	7.09	13.02	18.19	22.81	27.02	30.89	34.49	37.84	40.97	43.90
530	3.40	6.50	12.05	16.96	21.39	25.46	29.24	32.76	36.07	39.17	42.09
540	3.10	5.97	11.16	15.81	20.05	23.98	27.65	31.09	34.34	37.41	40.31
550	2.83	5.48	10.33	14.73	18.79	22.57	26.12	29.48	32.66	35.68	38.56
560	2.59	5.04	9.57	13.73	17.60	21.23	24.67	27.93	31.04	34.01	36.84
570	2.38	4.64	8.87	12.79	16.48	19.96	23.28	26.44	29.47	32.38	35.17
580	2.18	4.27	8.22	11.92	15.43	18.76	21.95	25.01	27.96	30.80	33.54
590	2.01	3.94	7.63	11.12	14.44	17.63	20.69	23.65	26.51	29.28	31.96
600	1.85	3.64	7.08	10.37	13.52	16.56	19.50	22.35	25.12	27.81	30.43

The only reactions of molecular nitrogen at ambient temperature are the formation of lithium nitride Li_3N, reactions with certain transition metal complexes, and nitrogen fixation with nitrogenase in the bacteria of the root nodules of legumes and in blue algae (Sections 14.1.1 and 14.1.2). Above 500 °C nitrogen reacts with some elements, especially with metals (nitride formation).

According to estimates [99], the homogenous reaction of nitrogen with hydrogen to form ammonia in the gas phase requires an activation energy of 230 – 420 kJ/mol. For purely thermal energy supply with a favorable collision yield, this activation barrier requires temperatures well above 800 – 1200 K to achieve measurable reaction rates. However, at such high temperatures and industrially reasonable pressures, the theoretically achievable ammonia yield is extremely small because of the unfavorable position of the thermodynamic equilibrium. In fact, all older attempts to combine molecular nitrogen purely thermally with atomic or molecular hydrogen failed. On the other

Table 12. Heat of reaction ΔH (in kJ) for the reaction $0.5\ N_2+1.5\ H_2 \rightarrow NH_3$, from [89]

t, °C	p_{abs}, MPa										
	0 (ideal)	10	20	30	40	50	60	70	80	90	100
0	44.39	55.20	66.02	76.84	87.66	98.47	109.29	120.11	130.92	141.74	152.56
25	44.92	53.48	62.03	70.59	79.15	87.70	96.26	104.82	113.38	121.93	130.49
50	45.44	52.37	59.30	66.23	73.16	80.09	87.02	93.95	100.88	107.80	114.73
75	45.96	51.69	57.41	63.14	68.86	74.58	80.31	86.03	91.76	97.48	103.20
100	46.47	51.28	56.10	60.91	65.72	70.53	75.34	80.16	84.97	89.78	94.59
125	46.97	51.08	55.19	59.29	63.40	67.51	71.62	75.72	79.83	83.94	88.04
150	47.46	51.02	54.57	58.12	61.68	65.23	68.78	72.34	75.89	79.44	83.00
175	47.95	51.06	54.17	57.28	60.39	63.50	66.61	69.72	72.83	75.94	79.05
200	48.42	51.17	53.92	56.68	59.43	62.18	64.93	67.69	70.44	73.19	75.94
225	48.88	51.34	53.80	56.26	58.71	61.17	63.63	66.09	68.55	71.01	73.47
250	49.33	51.54	53.76	55.97	58.19	60.40	62.62	64.84	67.05	69.27	71.48
275	49.76	51.77	53.79	55.80	57.81	59.82	61.84	63.85	65.86	67.87	69.88
300	50.18	52.02	53.86	55.70	57.54	59.38	61.22	63.06	64.90	66.74	68.59
325	50.59	52.28	53.98	55.67	57.37	59.06	60.75	62.45	64.14	65.83	67.53
350	50.99	52.55	54.12	55.69	57.26	58.82	60.39	61.96	63.53	65.10	66.66
375	51.36	52.82	54.28	55.74	57.20	58.66	60.12	61.58	63.04	64.49	65.95
400	51.73	53.09	54.46	55.82	57.18	58.55	59.91	61.28	62.64	64.00	65.37
425	52.07	53.35	54.64	55.92	57.20	58.48	59.76	61.04	62.32	63.60	64.88
450	52.40	53.61	54.82	56.03	57.23	58.44	59.65	60.86	62.06	63.27	64.48
475	52.71	53.86	55.00	56.14	57.29	58.43	59.57	60.72	61.86	63.00	64.14
500	53.01	54.09	55.18	56.26	57.35	58.43	59.52	60.60	61.69	62.78	63.86
525	53.28	54.31	55.35	56.38	57.42	58.45	59.48	60.52	61.55	62.58	63.62
550	53.53	54.52	55.51	56.50	57.48	58.47	59.46	60.45	61.44	62.42	63.41
575	53.76	54.71	55.66	56.60	57.55	58.50	59.44	60.39	61.33	62.28	63.23
600	53.98	54.88	55.79	56.70	57.61	58.52	59.43	60.34	61.24	62.15	63.06

hand, both ammonia and hydrazine result from reacting atomic nitrogen with atomic hydrogen [99].

At pressures above 200 MPa (2000 bar), the synthesis of ammonia proceeds even in the absence of specific catalysts. At such extreme pressures the vessel walls appear to catalyze the formation of ammonia.

In the homogeneous phase under thermodynamically favorable temperature conditions, the formation of ammonia may be forced by employing other forms of energy, such as electrical energy or ionizing radiation. The principal difficulty with these so-called plasma processes, which also impedes their economic use, is that the energy supplied is useful only in part for ammonia formation. A greater part is transformed in primary collision and exothermic secondary processes into undesirable heat or unusable incidental radiation.

In the catalytic combination of nitrogen and hydrogen, the molecules lose their translational degrees of freedom by fixation on the catalyst surface. This drastically reduces the required energy of activation, for example, to 103 kJ/mol on iron [100]. The reaction may then proceed in the temperature range 250–400 °C. In 1972, it was discovered that electron donor–acceptor (EDA) complexes permit making ammonia with measurable reaction rate at room temperature.

The following discussion concentrates mainly on the ammonia synthesis reaction over iron catalysts and refers only briefly to reactions with non-iron catalysts. Iron catalysts which are generally used until today in commercial production units are composed in unreduced form of iron oxides (mainly magnetite) and a few percent of Al, Ca, and K; other elements such as Mg and Si may also be present in small amounts. Activation is usually accomplished in situ by reduction with synthesis gas. Prereduced catalysts are also commercially available.

Numerous investigations have been performed to elucidate the mechanism of catalytic reaction of nitrogen and hydrogen to form ammonia. References [101]–[104] give reviews of the older and some of the newer literature. During the past two decades a large variety of surface science techniques involving Auger electron spectroscopy, X-ray photoelectron spectroscopy, work-function measurements, temperature-programmed adsorption and desorption, scanning tunnelling microscopy, and others have been developed [105], [106]. Many of these methods are based on interaction of slow electrons, ions, or neutral particles and exhibit high sensitivity to surface structures. With these powerful tools the kinetics of nitrogen and hydrogen adsorption and desorption could be investigated, and it was also possible to identify adsorbed intermediates. The results of these experiments allow the mechanism of ammonia synthesis in the pressure range of industrial interest to be elucidated [107]–[110].

As with every catalytic gas-phase reaction, the course of ammonia synthesis by the Haber–Bosch process can be divided into the following steps:

1) Transport of the reactants by diffusion and convection out of the bulk gas stream, through a laminar boundary layer, to the outer surface of the catalyst particles, and further through the pore system to the inner surface (pore walls)
2) Adsorption of the reactants (and catalyst poisons) on the inner surface
3) Reaction of the adsorbed species, if need be with participation by hydrogen from the gas phase, to form activated intermediate compounds
4) Desorption of the ammonia formed into the gas phase
5) Transport of the ammonia through the pore system and the laminar boundary layer into the bulk gas stream

Only the portion of the sequence that occurs on the catalyst surface is significant for the intrinsic catalytic reaction. Of special importance is the adsorption of nitrogen. This assumption is decisive in representing the synthesis reaction kinetics. The transport processes occurring in the pores of the catalyst in accordance with the classical laws of diffusion are of importance in industrial synthesis (see also Sections 3.5 and 3.6).

3.4. Mechanism of the Intrinsic Reaction

Earlier studies [111]–[120] had already suggested that on iron catalysts nitrogen adsorption and dissociation can be regarded as the rate-determining step for the intrinsic reaction. This has now been fully confirmed by microkinetic simulations based on the results of surface science studies [107], [121], [122]. In single-crystal experiments it was found that the activation energy for dissociative nitrogen adsorption is not constant; it increases as the surface becomes increasingly covered with adsorbed nitrogen species. Under reaction conditions it can attain values of 63–84 kJ/mol [109], [112], [113], [123] which are typical for ammonia synthesis. In the case of nitrogen the first step seems to be an adsorption in molecular state followed by chemisorption in the atomic state. From experimental results it was concluded that for hydrogen a direct transition from the gaseous H_2 molecule into the chemisorbed H_{ad} is most likely, and evidence for the stepwise hydrogenation of surface nitrogen atomic species was found. In IR spectroscopic investigations, NH and NH_2 species were identified [124], and secondary ion emissions detecting NH^+ also confirmed the presence of NH species on the surface [125]. It was further shown that at lower temperatures nitrogen becomes adsorbed only in the molecular state, but subsequently dissociates when the temperature is raised. Isotopic experiments with $^{30}N_2$ and $^{29}N_2$ showed that the surface species resulting from low-temperature adsorption was molecular, whereas that from high-temperature adsorption was atomic [126]. Ammonia synthesis is highly sensitive to the orientation of the different crystal planes of iron in the catalyst [127]–[131]. Measurements on defined single crystal surfaces of pure iron performed under ultrahigh vacuum [132]–[134] clearly showed that Fe(111) is the most active surface. This was also demonstrated by the rate of ammonia formation on five different crystallographic planes for unpromoted iron at 20 bar, as shown in Figure 7.

Activation energy, reactivity, adhesion coefficient (the probability that a nitrogen molecule striking the surface will be adsorbed dissociatively) and work function show a clear dependence on surface orientation [135], [136]:

Ammonia synthesis activity:
(111) > (211) > (100) > (210) > (110)
Activation energy of nitrogen adsorption:
(111) > (100) > (110)
Work function:
(210) > (111) > (211) > (100) > (110)
Surface roughness:
(210) > (111) > (211) > (100) > (110)

Ultrahigh-vacuum experiments with single crystals show that the activation energy of nitrogen adsorption at zero coverage increases from about zero for Fe(111) to 21 kJ/mol for Fe(100) and 27 kJ/mol for Fe(110) [107], [112], [137]–[139]. These values increase significantly for higher coverage [138], [139]. Adsorption and desorption

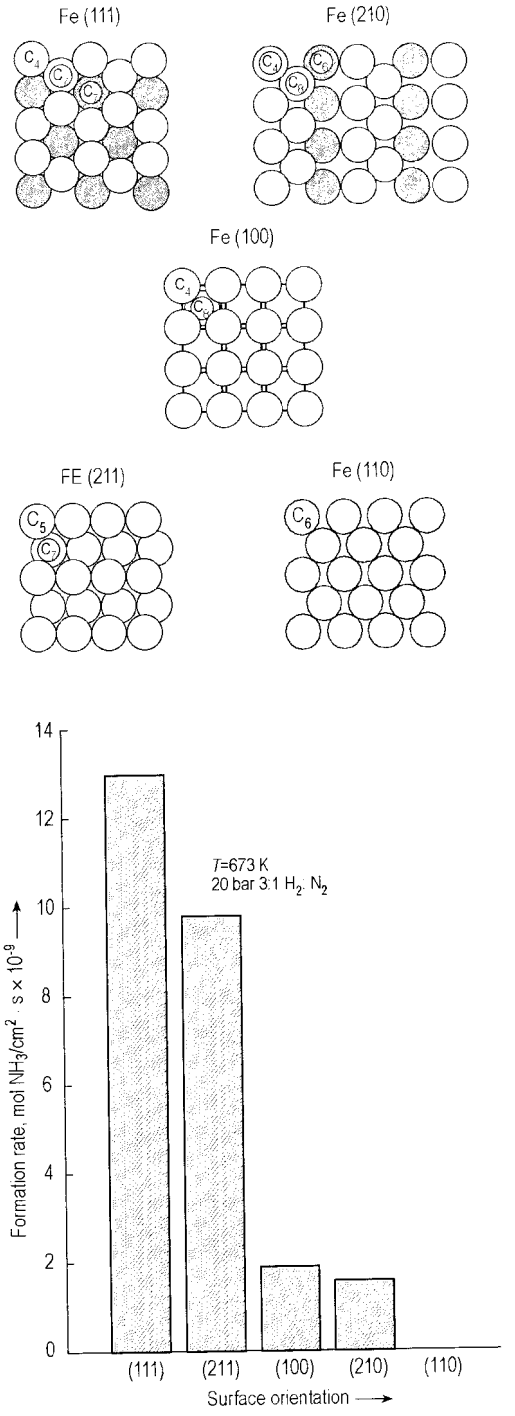

Figure 7. Ammonia formation rate on different iron surfaces [122], [135]

under higher pressure on finely dispersed catalyst indicate that the reaction is highly activated. Activation energy is 100 kJ/mol under these conditions with high coverage. [111], [140]. According to [137], [138] adsorption on the planes Fe(111) and Fe(110) is associated with a regrouping of the surface atoms.

A possible explanation for the high activity of faces (111) and (211) is that these are the only surfaces which expose C_7 sites (iron with seven nearest neighbors) to the reactant gases. There are theoretical arguments [141] that highly coordinated surface atoms should show increased catalytic activity due to low-energy charge fluctuations in the *d*-bands of these highly coordinated atoms. This argument might probably be the key for the special role of C_7 sites. Other reasons discussed are based on charge transfer and interaction of iron *d*-bands with antibonding 2 π^* orbitals of nitrogen [142].

Promotion with potassium of single iron crystals enhances the sticking probability for nitrogen dissociation much more on the Fe(100) and (110) than on the Fe(111) (factors 280, ca. 1000 and 8, respectively) to the effect that the differences in surface orientation disappear [143]. A similar effect was not found for the ammonia synthesis at 20 bar and catalyst temperature of 400 °C: only a two-fold increase of the ammonia formation rate was measured for Fe(111) and Fe(100), and the face (110) was found to be inactive with and without potassium [135]. Other experiments [144] show that even the least active face Fe(110) becomes as active for the synthesis as Fe(111) after addition of alumina with subsequent annealing with oxygen and water vapor. A proposed mechanism for these findings — backed by X-ray photoelectron spectroscopy, temperature programmed desorption and electron microscopy — assumes that first alumina forms an iron aluminate $FeAl_2O_4$ on the surface. This new surface then may serve as a template on which iron grows with (111) and (211) orientation upon exposure to the synthesis-gas mixture in the reaction [145].

Based on these experimental results a reaction scheme for the ammonia synthesis may be formulated comprising the following sequence of individual steps [107]:

$$H_2 + * \rightleftharpoons 2\,H_{ad} \tag{9}$$
$$N_2 + * \rightleftharpoons N_{2,ad} \tag{10}$$
$$N_{2,ad} \rightleftharpoons 2\,N_{ad} \tag{11}$$
$$N_{ad} + H_{ad} \rightleftharpoons NH_{ad} \tag{12}$$
$$NH_{ad} + H_{ad} \rightleftharpoons NH_{2,ad} \tag{13}$$
$$NH_{2,ad} + H_{ad} \rightleftharpoons NH_{3,ad} \tag{14}$$
$$NH_{3,ad} \rightleftharpoons NH_3 + * \tag{15}$$

The progress of the reaction may be described in the form of an energy profile, as shown in Figure 8. Industrial ammonia synthesis in the homogeneous gas phase is not feasible because of the high dissociation energies for the initial steps. The reaction over a catalyst avoids this problem since the energy gain associated with the surface atom bonds overcompensates these dissociation energies and the first steps have actually become exothermic.

Dissociative nitrogen adsorption remains nevertheless the rate-determinating step, not so much on account of its activation barrier but rather because of the very

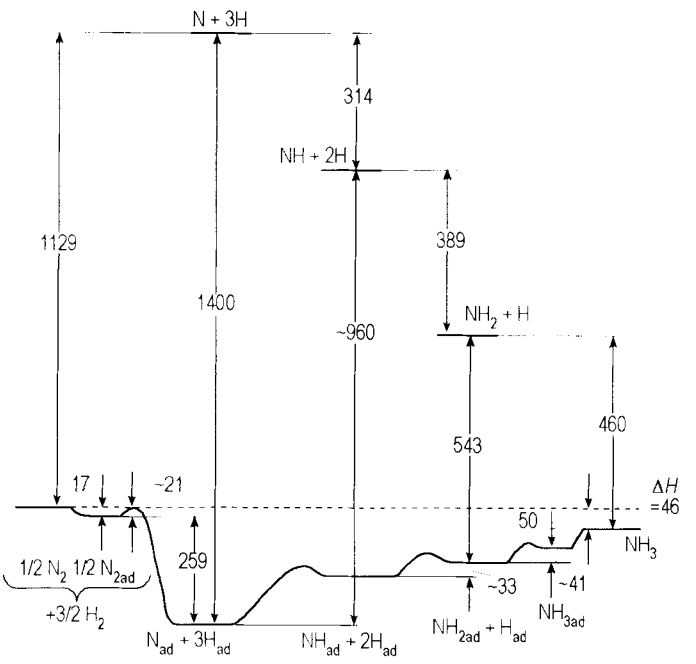

Figure 8. Schematic energy profile of the progress of ammonia synthesis on Fe (energies in kJ/mol) [107]

unfavorable pre-exponential factor in its rate constant. The subsequent hydrogenation steps are energetically uphill, but the energy differences involved can easily be overcome at the temperatures (ca. 700 K) used in industrial ammonia synthesis. It is, however, quite apparent that the rate-controlling step would switch from dissociative nitrogen adsorption to hydrogenation of adsorbed atomic nitrogen species if the temperature were lowered sufficiently because of these differences in activation energy.

Some critics [146] of the above energy diagram question the low net activation barrier from the gas phase. The arguments are based on an analysis of activation energies from early measurements of the nitrogen adsorption kinetics on singly (Al_2O_3) promoted catalysts and on the results of experiments with supersonic molecular beams [147], [148].

An attempt to explain these differences is given in [149]. In more recent investigations of the adsorbed nitrogen species [150]–[153] a second molecularly adsorbed species was detected. This so-called α state was interpreted as a bridge-bonded species with electron donation from the surface to the antibonding π levels of N_2, whereas the γ state is regarded as a terminally bound species. Thus the following picture (16) for the nitrogen adsorption emerges:

$$N_2 \rightarrow S^*- N_2\ (\gamma \text{ state}) \rightarrow S^*-N_2 -S^*\ (\alpha \text{ state}) \rightarrow 2\ S^*-N\ (\beta \text{ state}) \qquad (16)$$

where S* denotes a surface atom.

For industrial catalysts made by careful reduction of magnetite fused with nonreducible oxide promoters the important role of the (111) face seems to be confirmed [154]. However, the question whether the active industrial catalyst exposes mostly (111) faces remains unresolved. If not, further improvements of the catalyst are at least theoretically possible [155]. A critical evaluation of our present knowledge of the reaction mechanism was recently made by SCHLÖGL [156].

Other reaction mechanisms have been debated for reaction temperatures below 330 °C [130], [157], [158]–[169]. These propose participation of diatomic nitrogen, or of adsorption complexes containing diatomic nitrogen, in the rate-determining step (see [101], [102] for further literature).

NIELSEN et al. investigated ammonia synthesis on a commercial Topsøe catalyst, KM IR, over a wide temperature range. They found evidence that a different reaction mechanism predominates below and above 330 °C [170]. Also, at low temperatures, chemisorbed hydrogen blocks the catalyst surface [171]. The latter finding is in agreement with the observations of ERTL's group [123].

Reaction Mechanism on Non-Iron Catalysts. Non-iron systems which exhibit some potential to catalyze ammonia synthesis can be divided into the following groups [172]:

- Platinum group metals such as Ru, Os Ir, Pt (no nitrides)
- Mn, Co, Ni, Tc, Rh and their alloys (no nitride formation under synthesis conditions)
- Mn, Mo, V (present as nitrides under the reaction conditions)

In the non-iron systems the rate-determining step is also dissociative adsorption of nitrogen and the catalyst effectivity seems to be primarily dictated by the activation energy of the dissociation reaction [172]. This is somewhat surprising in view of the marked differences in the heats of adsorption of nitrogen and the adsorption activation energy. This even holds for tungsten, which has no significant activation energy and a high adsorption enthalpy for nitrogen, so that hydrogenation of adsorbed atomic nitrogen could be expected to be the rate-determining step. The factor common with the iron catalyst is the structure sensitivity.

The only system which seems to be promising for industrial application is ruthenium promoted with rubidium on graphite as carrier (see Section 3.6.2.3). Further information on structure, activity and reaction mechanism of non-iron catalysts is given in [102], [172]–[175]. Specific references: vanadium [176], uranium [177], molybdenum [178]–[180], tungsten [181].

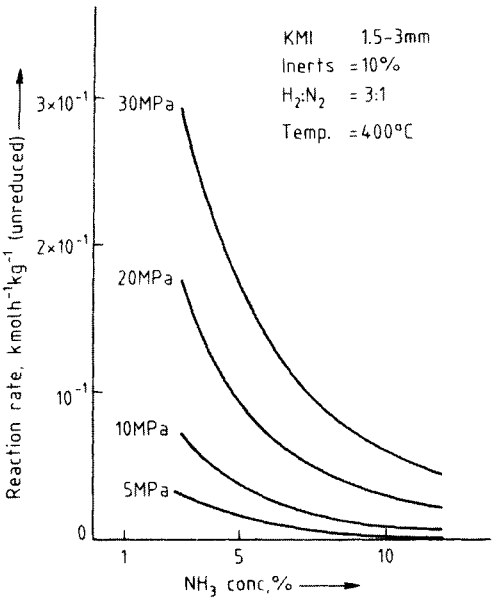

Figure 9. Reaction rate for NH_3 synthesis. Dependence on the ammonia concentration at various pressures.

3.5. Kinetics

Knowledge of the reaction kinetics is important for designing industrial ammonia synthesis reactors, for determining the optimal operating conditions, and for computer control of ammonia plants. This means predicting the technical dependence on operating variables of the rate of formation of ammonia in an integral catalyst volume element of a converter.

High pressure promotes a high rate of ammonia formation; high ammonia concentration in the synthesis gas (recycle gas) restricts it (Fig. 9). High temperatures accelerate ammonia formation but imply a lower value of the equilibrium ammonia concentration and so a lower driving force. Therefore, the rate of formation at first increases with rising temperature but then goes through a maximum as the system approaches thermodynamic equilibrium (Fig. 10). A similar situation exists for the dependence of the reaction rate on the ratio of the hydrogen and nitrogen partial pressures; with lower temperature, the maximum rate shifts to a lower hydrogen–nitrogen ratio (Fig. 11). Figure 11 presents data obtained using a commercial iron catalyst, Topsøe KMIR. The data show a sharp drop in reaction rate with declining temperature at $H_2/N_2 = 3:1$ ratio in contrast to a $H_2/N_2 = 1:1$ ratio. This may be attributed to a hindering effect of adsorbed hydrogen at low temperature [171].

Equations for describing ammonia synthesis under industrial operating conditions must represent the influence of the temperature, the pressure, the gas composition, and the equilibrium composition. Moreover, they must also take into consideration the dependence of the ammonia formation rate on the concentration of catalyst poisons and the influence of mass-transfer resistances, which are significant in industrial ammonia synthesis.

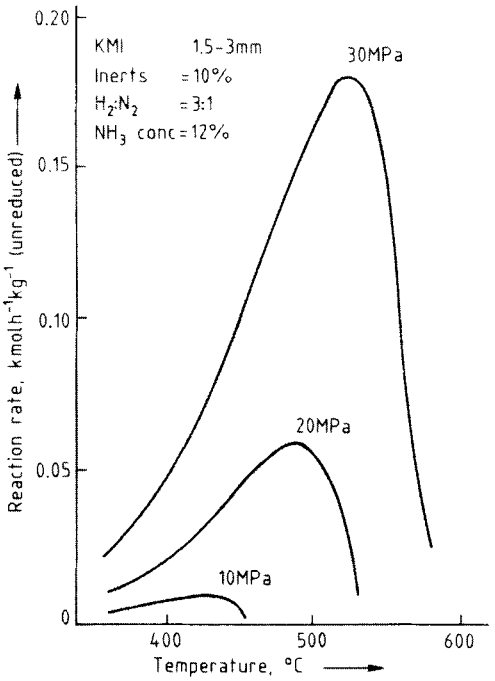

Figure 10. Reaction rate for NH_3 synthesis. Dependence on the temperature at various pressures.

Since the beginning of commercial ammonia synthesis, a large number of different kinetic equations have been suggested, emanating in each case from a proposed reaction mechanism or from empirical evaluations. A critical review of the data and equations published up to 1959 appears in [182]. A discussion of kinetics proposed up to 1970, insofar as they have been based on measurements in the operating range of commercial interest, can be found in [157]. An evaluation of present knowledge is given in [107], [121], [183], [184].

Contradictory data on the kinetics of ammonia synthesis, especially in the earlier literature, in some circumstances may reflect a lack of attention to the influence of impurities in the gas. If oxygen compounds are present in the synthesis gas, reversible poisoning of the adsorbing areas, in accordance with an equilibrium depending on the temperature and the water vapor–hydrogen partial pressure ratio, must be taken into account when developing rate equations (see also Section 3.6.1.5).

Experimental Measurements of Reaction Kinetics. The reaction expressions discussed in the following model the intrinsic reaction on the catalyst surface, free of mass-transfer restrictions. Experimental measurements, usually made with very fine particles, are described by theoretically deduced formulas, the validity of which is tested experimentally by their possibility for extrapolation to other reaction conditions. Commonly the isothermal integral reactor is used with catalyst crushed to a size of 0.5–1.5 mm to avoid pore diffusion restriction and heat-transfer resistance in the catalyst particles. To exclude maldistribution effects and back mixing, a high ratio of

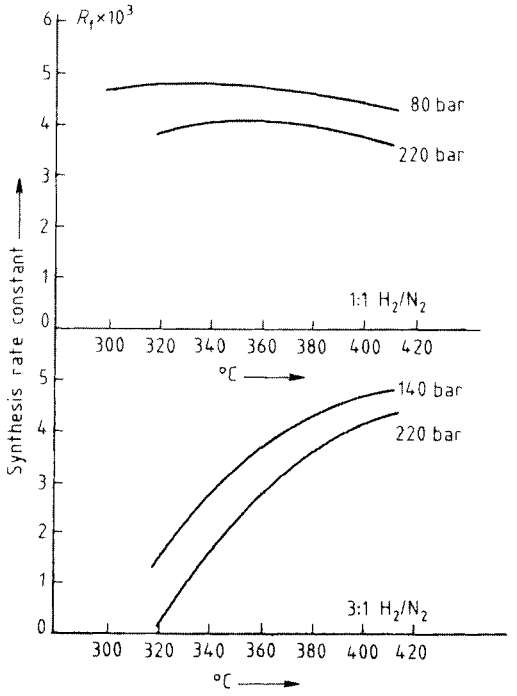

Figure 11. Ammonia synthesis rate constant dependence on hydrogen–nitrogen ratio

bed length to bed diameter is chosen. Sometimes the catalyst is also diluted with inert material. In some investigations, differential reactors were used. To exclude any poisoning by the synthesis gas, very pure reactants were prepared by decomposition of anhydrous ammonia [183].

Classical Expressions for Ammonia Synthesis Kinetics. The first expression useful for engineering purposes was the Temkin–Pyzhev Equation (17) proposed in 1940 [185], [186]. It is based on the assumption that dissociative adsorption is the rate-determining step, that hydrogen and ammonia have no significant influence on nitrogen adsorption, and that the kinetics of nitrogen adsorption and desorption can be described adequately by Elovich-type adsorption on an energetically inhomogeneous surface. For many years this kinetic expression was the basic design equation for ammonia converters. Values for the factors α between 0.5 [187]–[189] and 0.75 [33], [190], [191] were used. A problem with this equation was that the α values (reaction order) were dependent on temperature, and the rate constants on pressure [170], [190]–[194]. More serious (not so much for industrial purposes, where the converter feed has always a certain ammonia content) was the fact that for zero ammonia content, as in some laboratory measurements, the equation gives an infinitely high reaction rate. To avoid this, a simpler expression (Eq. 18) was often used [192], [193].

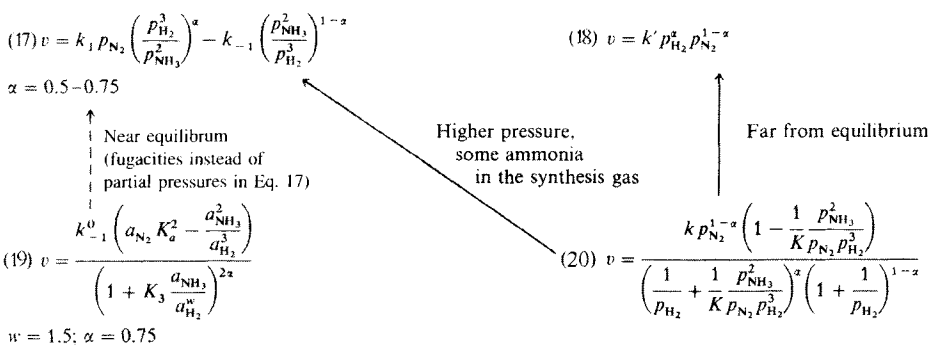

An important modification was made by TEMKIN [195] who incorporated hydrogen addition to the adsorbed nitrogen as a second rate-determining step (Eq. 20). ICI demonstrated that this equation gives a better fit with experimental data [196]. It was also shown later that the original Equation (17) is a simplified form of a more general model which can be derived from the concept of energetically homogeneous (Langmuir–Hinshelwood adsorption isotherm) as well as for heterogeneous surfaces (Elovich-type isotherm). The applicability of a particular equation resulting from this concept also depends on the state of reduction of the catalyst [194] and the type of promoter [197]. Equation (19), used by NIELSEN et al. [198], is a combination of these model equations, developed by OZAKI et al. [199], that uses fugacities instead of partial pressures. A similar equation is found in [200]. Additionally, a number of modified equations were proposed and tested with existing experimental data and industrial plant results [201]–[204]. Near the thermodynamical equilibrium, Equation (19) transforms into Equation (17) [157], [170].

Surface science based ammonia kinetics [107], [108], [183], [184] are presently still viewed as an academic exercise rather than as a practical tool for engineering. The large amount of available data on nitrogen and hydrogen adsorption from ultrahigh-vacuum studies on clean iron surfaces, acquired with all the modern spectroscopic techniques, has prompted some research groups, such as BOWKER et al. [205], [206] and STOLTZE and NØRSKOW [207], [208], to attempt the generation of a kinetic expression for ammonia synthesis from a detailed microscopic model of the reaction mechanism consisting of a number of discrete steps at molecular and atomic level. Potential energy diagrams for the various intermediate steps and species, were set up and Arrhenius expressions for each single step with known or estimated values for all pre-factors and activation energies were formulated. The best results have been achieved so far by calculating the overall rate from the rate of dissociation of the adsorbed nitrogen and equilibrium constants for all other reaction steps. The adsorption–desorption equilibria were treated with approximation of competitive Langmuir-type adsorption and by evaluation of the partition functions for the gaseous and adsorbed species. The data from single-crystal experiments for potassium-promoted

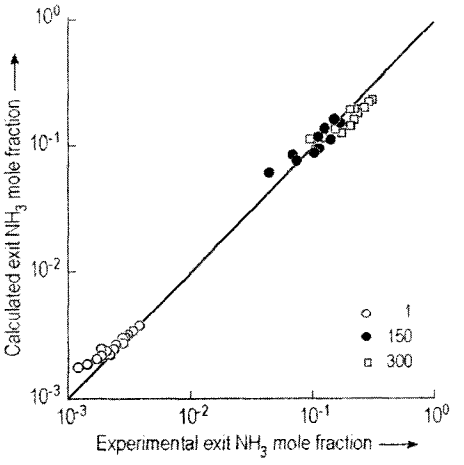

Figure 12. Comparison of ammonia concentrations calculated from surface science kinetics with experimentally measured values [208], [210]

Fe(111) surface were used for the rate of the dissociative nitrogen adsorption. Comparison of the calculated ammonia yields with those determined experimentally on a commercial Topsøe KM1 catalyst showed an agreement within a factor better **than** 2. Figure 12 demonstrates these encouraging results. These conclusions have been confirmed by calculations results of another independent group [121], [209].

To compete with the empirical models (Temkin and improved expressions) for the best fit to experimental data cannot be the prime objective of the microkinetic approaches. Rather, they are means of checking whether our knowledge and understanding of the elementary steps correspond to the reality of catalysts under industrial synthesis conditions.

Transport Phenomena. For practical application, the above kinetic equations have to be modified to make allowance for mass and energy transfer since the reaction rates actually observed in a commercial converter are lower. One aspect is interparticle mass transfer and heat transfer through the stagnant film which surrounds the catalyst particles. The high velocity of the gas passing through the converter creates sufficient turbulence to keep the film thickness rather small in relation to the catalyst grain size. For this reason the largest concentration gradient (with respect to the concentration in the bulk gas stream) is within the catalyst particles. Since the thermal conductivity of the iron catalysts is much higher than that of the synthesis gas, the major temperature difference is in the external gas film, while the catalyst particles themselves operate under approximately isothermal conditions. As can be seen from Table 13 the differences in temperature and ammonia concentration between the bulk gas stream and the external catalyst surface are small. It also appears that the effects are oppositely directed and will partly compensate each other. So it can be concluded that their combined influence on the reaction rate is negligible compared to inaccuracies of the experimental data for the intrinsic catalyst activity [183].

Table 13. Mass and heat transfer effects at the external surface of catalyst particle

Position in catalyst bed, vol% from inlet	NH_3 concentration in bulk gas, mol%	NH_3 concentration at catalyst surface, mol%	Temperature in bulk gas, °C	Temperature at catalyst surface, °C
0	2.500	2.592	400.0	401.4
20	4.500	4.288	428.1	429.5
40	5.960	6.045	455.1	456.5
60	7.000	7.778	481.9	483.2
80	9.300	9.361	505.5	506.6
100	10.500	10.536	522.7	523.3

For the particle sizes used in industrial reactors ($\geq$ 1.5 mm), intraparticle transport of the reactants and ammonia to and from the active inner catalyst surface may be slower than the intrinsic reaction rate and therefore cannot be neglected. The overall reaction can in this way be considerably limited by ammonia diffusion through the pores within the catalysts [211]. The ratio of the actual reaction rate to the intrinsic reaction rate (absence of mass transport restriction) has been termed as pore effectiveness factor E. This is often used as a correction factor for the rate equation constants in the engineering design of ammonia converters.

For pore diffusion resistances in reactions having moderate heat evolution, the following phenomena characteristically hold true in industrial ammonia synthesis [212]: in the temperature range in which transport limitation is operative, the apparent energy of activation falls to about half its value at low temperatures; the apparent activation energy and reaction order, as well as the ammonia production per unit volume of catalyst, decrease with increasing catalyst particle size [211], [213]–[215]. For example at the gas inlet to a TVA converter, the effective rate of formation of ammonia on 5.7-mm particles is only about a quarter of the rate measured on very much smaller grains (Fig. 13) [157].

Mathematical models [216] for calculating these effectiveness factors involve simultaneous differential equations, which on account of the complex kinetics of ammonia synthesis cannot be solved analytically. Exact numerical integration procedures, as adopted by various research groups [157], [217]–[219], are rather troublesome and time consuming even for a fast computer. A simplification [220] can be used which can be integrated analytically when the ammonia kinetics are approximated by a pseudo-first-order reaction [214], [215], [221], according to the Equation (21):

$$r = k_v \left(c_{NH_3,\,\text{equilibrium}} - c_{NH_3}\right) \tag{21}$$

For this case, the pore effectiveness factor E is a function of the so-called Thiele modulus m (Eq. 22) [222]:

$$E = \frac{3}{m}\left[\frac{1}{\operatorname{tgh} m} - \frac{1}{m}\right] \tag{22}$$

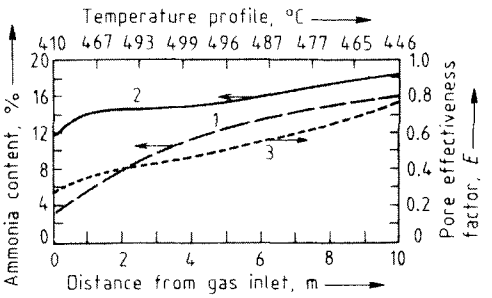

Figure 13. Ammonia content in the bulk stream (1) and in the catalyst pores (at $r = 0.5\ R$) (2) and pore effectiveness factor, E (3)
21.4 MPa; 12% inerts; SV = 15000 h^{-1}; particle diameter, $2R = 5.7$ mm

The Thiele modulus m is defined by Equation (23):

$$m = \frac{d_{eff}}{2}\sqrt{\frac{k_v}{D_{eff}}} \tag{23}$$

where

d_{eff} =	effective particle diameter
D_{eff} =	effective diffusion coefficient of ammonia in the catalyst particle
k_v =	reaction rate constant referred to a unit of particle volume
tgh =	tangens hyperbolicus

The practical application of kinetic equations to the mathematical calculation of ammonia synthesis converters is described in [196], [217], [223]–[229].

3.6. Catalysts

The ammonia synthesis catalyst may be viewed as the heart of an ammonia plant. For a given operating pressure and desired production, it determines the operating temperature range, recycle gas flow, and refrigeration requirement. As a result, it directly fixes vessel and exchanger design in the synthesis loop. It also indirectly influences the makeup gas purity requirement, and so the operating pressure, and capital cost, and energy consumption for synthesis gas production and purification. Although the proportionate cost of catalysts compared to the total cost of a modern ammonia synthesis plant is negligible, the economics of the total process are determined considerably by the performance of the ammonia catalyst [230].

Industrial catalysts for ammonia synthesis must satisfy the following requirements:

1) High *catalyst activity* at the lowest possible reaction temperatures in order to take advantage of the favorable thermodynamic equilibrium situation at low temperatures. Average commercial catalysts yield about 25 vol% ammonia when operating at 40 MPa (400 bar) and 480 °C catalyst end temperature, which corresponds to a 535 °C equilibrium temperature. With catalysts that would function at a reaction temperature about 100 K lower, a yield of 45 vol% ammonia can be expected with

the same approach to equilibrium, or the pressure may be reduced to 15 MPa (compare Tables 9 and 10).

2) The highest possible *insensitivity to oxygen- and chlorine-containing catalyst poisons,* which may be present in even the very effectively purified synthesis gas of a modern process (see Sections 3.6.1.5, and 4.3.2). In assessing the newly developed catalyst systems recommended for operation at very low temperatures (see Section 3.6.2.3), it must be kept in mind that the effect of poisons, for example, oxygen compounds, may become more severe as temperature declines (see Fig. 25).
3) *Long life,* which is determined essentially by resistance to thermal degradation and to irreversible poisoning (see Section 3.6.1.5). In older high-pressure plants (60 – 100 MPa), catalyst life was a big issue; because the catalysts in these plants showed a markedly reduced life owing to the severe operating conditions, the necessary downtime for removing, replacing, and reducing the catalyst had a considerable effect on the ammonia manufacturing cost. In modern single-train ammonia plants, conventional iron catalysts achieve service lifetimes up to 14 years.
4) *Mechanical Strength.* Insufficient pressure and abrasion resistance may lead to an excessive increase in converter pressure drop, and so to a premature plant shutdown. For example, mechanical disintegration during operation along with oxygen sensitivity thwarted the industrial application of uranium carbide catalysts [231].
5) Because of the high and increasing world demand for ammonia, a *reliable primary raw material source.* For example, osmium, which was planned as the first industrial catalyst, is so scarce that, in 1910, as a precautionary measure for this option, BASF had secured almost the total world supply [231].

The ammonia synthesis catalyst problem has been more intensively studied than the catalysis of any other industrial reaction. At BASF, A. MITTASCH et al. started a tremendous experimental programm, in which up to 1911 more than 2500 different formulations were tested in more than 6500 runs. They checked almost all elements of the periodic table for their suitability as ammonia catalysts [8], [232]. The experiments were fially brought to a close in 1922 after a total of 22 000 tests. From these experiments came a series of technical findings, for example, concerning the relationships between catalytic effectiveness and the strength of the nitrogen bond and reducibility, or relating to the mechanism of opposing activation or inactivation in doubly promoted systems.

In principle, metals or metal alloys are suitable as ammonia catalysts, above all those from the transition-metal group [233] (Table 14). Metals or metal compounds for which the chemisorption energy of nitrogen is neither too high nor too low show the greatest effectiveness (Figs. 14, 15), [234], [235], but only the magnetite-based catalyst proved suitable for industrial use.

Table 14. Effectiveness of various elements as catalysts, promoters, or catalyst poisons

	Catalysts	Promoters	Poisons
I		Li, Na, K, Rb, Cs	
II		Be, Mg, Ca, Ba, Sr	Cd, Zn
III	Ce and rare earths	Al, Y, La, Ce and rare earths	B, Tl
IV	(Ti), (Zr)	Si, Ti, Zr, Th	Sn, Pb, C
V	(V)	Nb, Ta	P, As, Bi
VI	(Cr), Mo, W, U	Cr, Mo, W, U	O, S, Se, Te
VII	(Mn), Re		F, Cl, Br, J
VIII	Fe, Ni, Co, Ru, (Rh), Os, (Ir)		

Table 15. Effect of various elements or their oxides on the activity of iron catalysts in ammonia synthesis

a)	positive: Al, Ba, Be, Ca, Ce, Cr, Er, K, La, Li, Mg, Mn, Mo, Na, Nb, Nd, Rb, Sm, Sr, Ta, Th, Ti, U, V, W, Y, Zr
b)	negative: As, B, Bi, Br, C, Cd, Cl, F, J, P, Pb, S, Sb, Sn, Te, Tl, Zn
c)	doubtful: Au, Co, Cu, Hg, Ir, Ni, Os, Pd, Pt, Si

3.6.1. Classical Iron Catalysts

From the early days of ammonia production to the present, the only catalysts that have been used have been iron catalysts promoted with nonreducible oxides. Recently, a ruthenium-based catalyst promoted with rubidium has found industrial application. The basic composition of iron catalysts is still very similar to that of the first catalyst developed by BASF.

The catalytic activity of iron was already known well before the advent of industrial ammonia synthesis. RAMSAY and YOUNG used metallic iron for decomposing ammonia. PERMAN [236], as well as HABER and OORDT [237], conducted the first catalytic synthesis experiments with iron at atmospheric pressure. NERNST [12] used elevated pressures of 5–7 MPa. Pure iron showed noticeable initial activity which, however, could be maintained for longer operating periods only with extremely pure synthesis gas.

The ammonia synthesis catalyst problem could be considered solved when the catalytic effectiveness of iron in conversion and its onstream life were successfully and substantially improved by adding reduction-resistant metal oxides [232] (Table 15). The iron catalysts promoted with aluminum and potassium oxides proved to be most serviceable [238]. Later, calcium was added as the third activator. Development work in the United States from 1922 can be found in [239].

Modern catalysts additionally contain other promoters that were present in the older catalysts only as natural impurities from the raw materials. Onstream life and performance were enhanced considerably by optimizing the component ratios (Section 3.6.1.1), conditions of preparation (Section 3.6.1.3), and catalyst particle size and form (Section 3.6.1.2). The high-purity gas of modern processes and the trend to lower

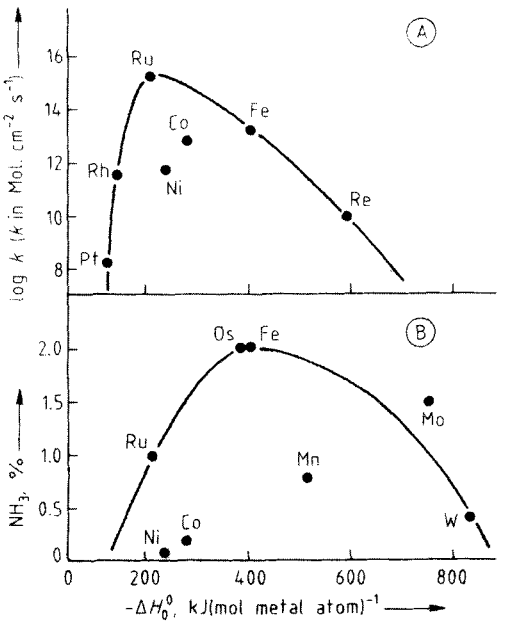

Figure 14. The rate constants of ammonia decomposition (A) on and the ammonia synthesis capacities (B) of metals as a function of $-\Delta H_0^0$. (Mol. denotes molecule, mol denotes mole)

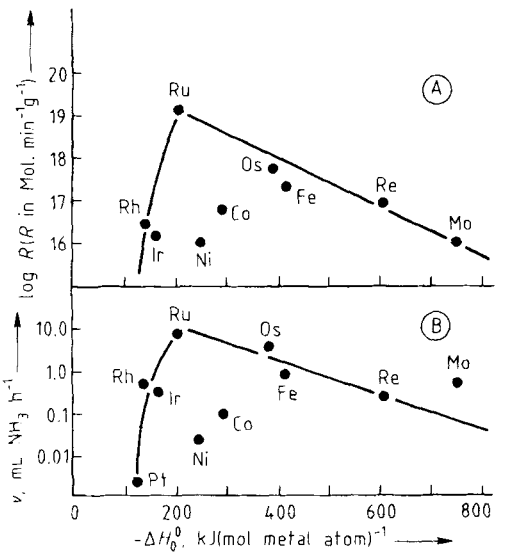

Figure 15. Catalytic activity of carbon-supported metals promoted by metallic potassium as a function of $-\Delta H_0^0$.
A) The rate of isotopic equilibration of N_2 at 623 K, 20 kPa of p_{N_2} (Mol. denotes molecule, mol denotes mole);
B) The rate of ammonia synthesis at 523 K, 80 kPa of total pressure

synthesis pressures especially favor the development of more active and easily reducible types of catalysts, at some sacrifice in temperature stability and resistance to poisons. To some extent even today, ammonia plant operating conditions and types of converters (Section 4.5.3) can differ greatly one from another. Thus, individual catalyst manufacturers now offer several catalyst types in various particle size distributions, in oxidic and prereduced states.

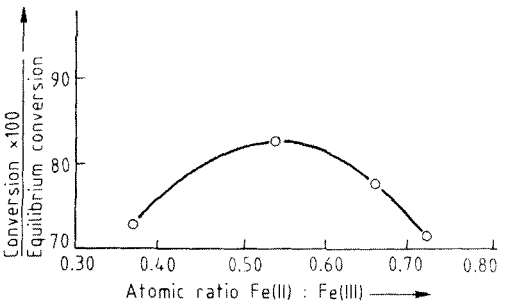

Figure 16. Dependence of the ammonia yield on the degree of oxidation of the iron in the unreduced catalyst

3.6.1.1. Composition

Table 16 gives a composition survey of commercial ammonia catalysts in the years 1964–1966. The principal component of oxidic catalysts is more or less stoichiometric magnetite, Fe_3O_4, which transforms after reduction into the catalytically active form of α-iron.

The degree of oxidation of industrial catalysts has a considerable influence on their catalytic properties. MITTASCH in 1909 established that catalysts manufactured by reducing a magnetite phase were superior to those prepared from other oxides. For industrial catalysts, the highest ammonia yields are observed with an Fe(II)–Fe(III) ratio of 0.5–0.6, about the degree of oxidation of stoichiometrically composed magnetite [240]–[242] (Fig. 16). To obtain optimal catalyst composition, careful control of the manufacturing process, especially the melting conditions, which determine the oxygen content, is necessary.

In general, the catalysts contain varying quantities of the oxides of aluminum, potassium, calcium, magnesium, and silicon as promoters. Patents recommend adding sodium [243], beryllium [244], vanadium [245], uranium [246], or platinum [247]. Reference [248] describes cesium-containing catalysts. Catalysts patented by Lummus [249] and Ammonia Casale [250] contain cerium as additional promoter. ICI [251] has developed a cobalt-containing catalyst, as has Grande Paroisse [252].

Nature of the Surface of Commercial Iron Catalysts. Freshly reduced commercial iron catalysts that contain aluminum, potassium, and calcium oxides as basic promoters consist of approximately 30-nm primary crystallites; the spaces between them form an interconnecting system of pores. Besides a maximum at a pore radius of about 10 nm that originates on reduction of the Fe_3O_4 (magnetite) phase of the nonporous oxidic catalyst, the pore distribution curve (Fig. 17) generally shows a peak at 25–50 nm that is formed on reduction of the wustite phase [157], [253]. The pore volume measures 0.09–0.1 cm^3/g; with an apparent density of 4.8–4.9 g/cm^3, accordingly, the pores represent 44–46% of the volume of a catalyst granule [33]. The surface of the walls of the pores, the so-called inner surface, amounts to about 15 m^2/g.

Table 16. Examples of commercial ammonia catalysts from the years 1964 – 1966. Values for the composition in weight%. The numbers at the beginning of the lines are keyed to the catalyst origin.

Origin, type	Fe total	FeO	Fe_2O_3	Al_2O_3	MgO	SiO_2	CaO	K_2O	Other	Particle size, mm	Bulk density, kg/L
1	68.6	36.07	57.85	3.30	0.09	0.75	2.13	1.13	–	2 – 4	2.37
2 normal	60.0	32.91	60.18	2.90	0.37	0.35	2.80	0.54	–	4 – 10	2.94
2	68.2	31.30	62.53	2.90	0.30	0.35	1.65	0.97	–	6 – 10	2.80
2 HT	66.9	32.47	59.18	2.95	1.55	0.40	2.95	0.50	–	6 – 10	2.80
2 prereduced	88.1			3.70	0.43	0.45	3.60	0.70	–	6 – 10	2.30
3	71.3	39.22	58.2	1.80	0.18	0.27	1.43	0.89	–	2 – 4	2.86
4	66.3	22.27	49.0	0.59	4.47	0.77	0.65	0.50	0.7 Cr_2O_3		
4 prereduced	90.6			0.10	6.08	1.23	0.10	0.86	1.05 Cr_2O_3		
5	71.5	33.0	65.5	2.96	1.55	–	0.20	0.01	–		
6 (1964)	69.5	23.85		3.15	0.26	0.40	1.85	1.10	–	3 – 9	2.71
6 (1966)	66.9			2.73	0.29	0.43	1.84	1.15	–	5 – 10	2.73
7 prereduced	90.4			3.12	1.00	0.46	0.25	0.58	0.4 MnO	5/5	2.55
8	68.4	35.35		3.16	0.56	0.50	3.54	0.58	–	2 – 4	2.61
9	70.0	32.14		3.17	0.28	0.10	2.40	0.32	–	2 – 4	2.81
10	70.8	33.62		1.58	0.28	1.14	0.67	1.57	–	2 – 4	2.66
11 normal (1964)	66.7	35.95	56.97	3.27	0.67	0.55	3.00	0.65	–		
11 (1966)	68.2	38.70	54.60	2.42	0.35	0.64	2.85	0.58	–		
11 normal (1964)				3.0	0.3	0.5	2.0	1.0	–		
11 (1966)	69.5	38.20	56.70	2.34	0.35	0.57	1.85	0.57	–		
11 HT	66.3	38.22	52.38	2.94	3.56	0.30	2.66	0.63	–		
11 prereduced	84.9			3.62	0.43	0.94	4.70	0.68	–	5 – 11	2.11
12				3.9	4.0	0.8	2.3	1.8	–		
13		23.15		2.9	0.1	0.42	3.12	0.52	–		
14				4		0.7	3	1			

Table 17. Composition by volume of an industrial ammonia catalyst in comparison to the surface composition before and after reduction (an approximately 10^{-4} cm^2 size typical surface). Numerical values in atomic % [109]

	Fe	K	Al	Ca	O
Volume composition	40.5	0.35	2.0	1.7	53.2
Surface composition before reduction	8.6	36.1	10.7	4.7	40.0
Surface composition after reduction	11.0	27.0	17.0	4.0	41.0

The composition of the outermost atomic layers of the pore walls deviates considerably from the overall average concentrations. Auger electron spectroscopic (AES) measurements on an industrial catalyst (BASF S 6-10) have shown that a significant enrichment of the promoters into the surface results using the unreduced as well as the reduced catalyst [109] (see Table 17). The free iron surface of the reduced BASF catalyst [109] and Topsøe catalyst KM-I [254] comprises only a fraction of the total surface, as could be deduced from the results of prior investigations [157], [255]–[261].

The aluminum oxide promoter exists partly in the form of larger crystallites and, moreover, is relatively homogeneously distributed over the iron area of the surface, although with low concentration [109], [254]. After reduction, about 1 wt% of the alumina also remains statistically distributed in the form of $FeAl_2O_4$ molecular groups built into the α-iron lattice of the reduced catalyst [262], [263]. According to [109] the potassium, in the form of a K + O adsorbed layer, covers about 20–50% of the iron surface. According to [253], [254], a correlation exists between the distribution of the potassium and that of aluminum and/or silicon. Calcium oxide segregates, essentially at the grain boundaries, into separate regions, probably as a mixture of the silicate and ferrite [110]. Auger spectroscopic investigations on reduced BASF and Topsøe catalysts reveal large local differences in composition [109], [253]. Large, apparently homogeneous regions that have originated from reduction of Fe_3O_4 crystallites alternate with nonhomogeneous regions that are formed by the reduction of FeO crystals or consist of amorphous phases [253].

Extensive studies in the last decade have provided a more refined picture of the morphology of the active catalyst (reduced state) and its precursor (oxidic state). A review is given in [156], [264]. With methods such as scanning transmission electron microscopy (TEM) and electron microdiffraction a textural hierarchy has been modeled. Macroscopic particles in the reduced catalyst are confined by fracture lines running through a system of blocks consisting of stacks of slabs in parallel orientation. This structure is already preformed in the preparation of the catalyst precursor, and in the reduction process a further subdivision of the slabs into even smaller platelets might occur. This texture is stabilized by structural promoters, which act as spacers and "glue", separating neighboring platelets and thus providing voids for the interconnection of the pore system. There is also evidence that the basal plane of many platelets has the Fe(111) orientation [154], [264].

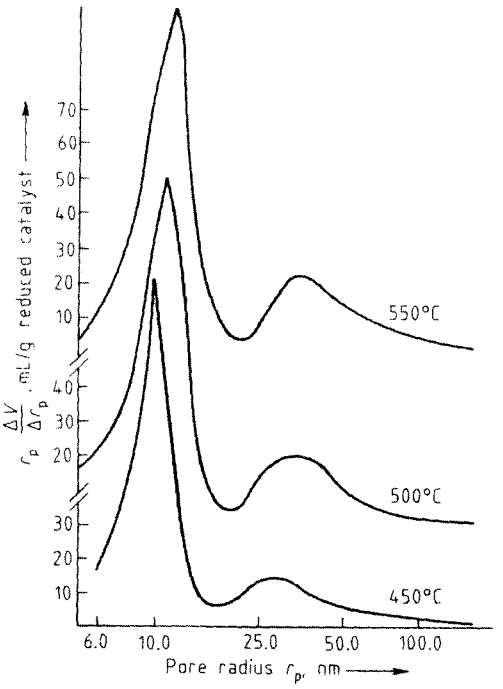

Figure 17. Pore size distribution of a commercial catalyst after reduction at various temperatures [253]

Influence of the Promoters. Promoters can be classified in different groups according to the specific action of the metal oxides:

Structural stabilizers, such as Al_2O_3, produce a high inner surface during reduction and stabilize it under thermal stress by restraining iron crystallite growth [144], [242], [265]. The ability of the various metal oxides to create a high specific surface decreases in the following order [266]:

$$Al_2O_3 > TiO_2 > Cr_2O_3 > MgO > MnO = CaO > SiO_2 > BeO$$

So-called *electronic promoters,* such as the alkali oxides, enhance the specific activity (based on a unit surface) of iron–alumina catalysts. However, they reduce the inner surface or lower the temperature stability and the resistance to oxygen-containing catalyst poisons [267], [268]. In the alkali-metal series, the promoter effect increases with increasing atomic radius, and the destructive effect with decreasing atomic radius [269]. In striving to improve the activity or stability of iron catalysts, a multitude of structural and electronic promoters has been investigated in recent years, among them rare-earth oxides [270], [271], such as Sm_2O_3 [272], Ho_2O_3, Dy_2O_3, and Er_2O_3 [273].

Promoter oxides that are reduced to the metal during the activation process and form an alloy with the iron (see also Section 3.6.2.1) are a special group. Among those in use industrially, cobalt is of special interest [274], [275].

The effect of a given promoter depends on concentration and on the type of promoter combination and the operating conditions, especially the reaction temperature and the synthesis gas purity [245], [267], [269], [276]–[279].

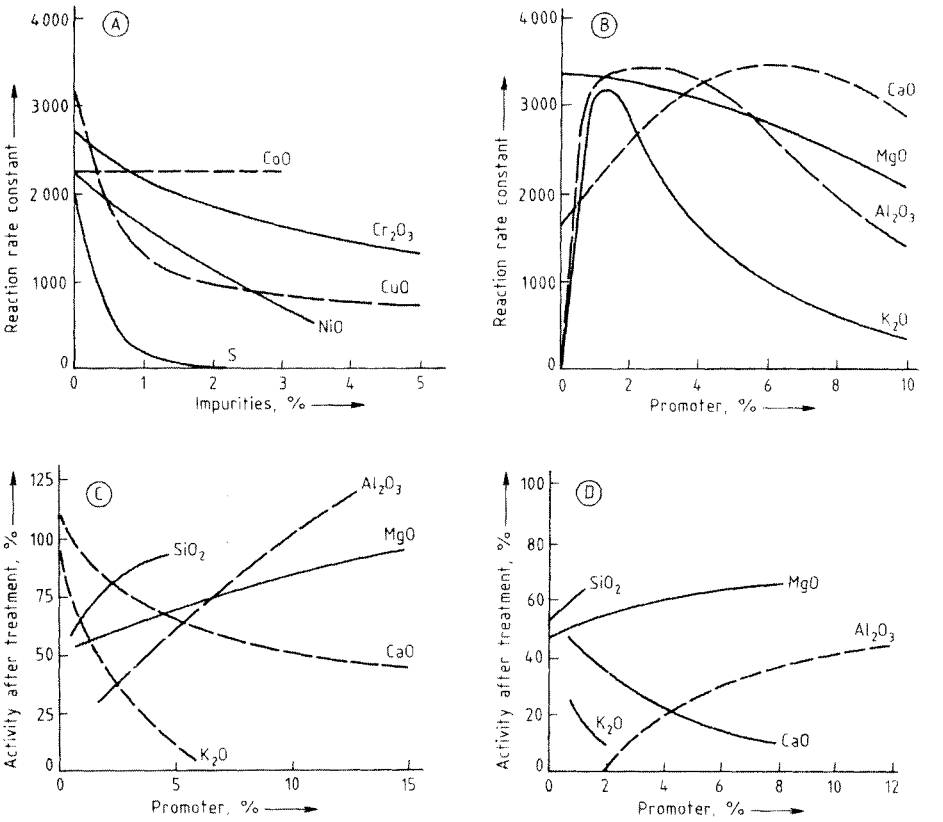

Figure 18. Dependence of the catalyst activity on various factors
A) Concentration of impurities; B) Concentration of promoters; C) Overheating to 700 °C with increasing promoter concentrations; D) Poisoning with water at increasing promoter concentrations

A graphic picture is conveyed in [269] of how the activity of a quadruply promoted (4% Al_2O_3, 1% K_2O, 1% CaO, 1% SiO_2) catalyst changes with varying promoter concentration and operating conditions (Fig. 18). Under normal operating conditions [14–45 MPa, 380–550 °C, 10 000–20 000 $m^3m^{-3}h^{-1}$ (STP)], the optimal activity corresponds to a composition of 2.5–3.5% CaO, 2.3–5.0% Al_2O_3, 0.8–1.2% K_2O, and 0–1.2% SiO_2 (Fig. 18 B). Raising or lowering the concentration of a particular oxide causes a reduction in activity. Changes in the potassium and aluminum oxide concentrations have an especially strong influence. Adding magnesium oxide decreases the catalyst performance. If before the test the catalyst is overheated at 700 °C for 72 h (Fig. 18 C) or poisoned with 2000 cm^3 water vapor per cubic meter of gas at 550 °C (Fig. 18 D), the optimum composition shifts to higher Al_2O_3 and SiO_2 and lower K_2O and CaO concentrations. Magnesium oxide addition now shows a favorable effect.

For ammonia plants operating at pressures up to 35 MPa (350 bar), catalyst end temperatures of 520–530 °C maximum, and with highly purified synthesis gas, the preferred catalysts contain 2.5–4.0% Al_2O_3, 0.5–1.2% K_2O, 2.0–3.5% CaO, 0–1.0% MgO, and a natural content of about 0.2–0.5% SiO_2 [242]. Less active but more

poison- and temperature-resistant catalysts containing up to 3.6% magnesium oxide were recommended for older plants, for example, classical Casale plants, which operated at up to 80 MPa (800 bar) pressure and in which catalyst end temperature reached 650 °C (see for example [33]). An industrial catalyst for operating temperatures up to 550 °C is stabilized against deterioration by 2–5% V_2O_5 besides 3.5–4.0% Al_2O_3, 2.0–2.5% CaO, and 0.7% K_2O [245]. For higher operating temperatures, still higher V_2O_5 contents are recommended. Silicon dioxide additions shift the optimum potassium oxide concentration to higher values [267]. For example, the Bulgarian catalyst K-31 contains 3.9% Al_2O_3, 2.3% CaO, 0.4% MgO, 0.8% SiO_2, and 1.8% K_2O. An older Norsk Hydro catalyst, besides the usual additives, contained 1.14% SiO_2 and 1.57% K_2O. The ICI catalyst with composition 5.2% CoO, 1.9% CaO, 0.8% K_2O, 2.5% Al_2O_3, 0.2% MgO, 0.5% SiO_2, remainder Fe_3O_4, is substantially more active than the conventional cobalt-free catalysts [251], [280]. Reducing the synthesis pressure and/or the synthesis temperature should enable application of the Lummus [249], [281] and Ammonia Casale [250] cerium-containing catalysts.

The effect of the promoters on the rate of reduction and the temperature required for reducing the iron oxide phase is also significant in industrial practice. The structural promoters, such as Al_2O_3, lower the rate of reduction [264], [282], [283]. Magnesium oxide-activated iron, said to be thermally stable up to 650 °C, needs a higher reduction temperature than aluminum oxide-promoted iron catalyst [284]. Greater differences in reducibility have also been observed in commercial catalysts with similar chemical composition [285] and in connection with particular oxide phases, such as $CaFe_3O_5$ and FeO [285]–[287]. Early work [288] referred to the rough parallels between the reducibility and the thermal stability of catalysts. All published experience appears to demonstrate that it is not possible to combine in a catalyst high thermal stability with easy reducibility and high activity at low temperatures. Hence it may be advantageous to use a combination of active and thermally-resistant catalysts in the same converter.

Mechanism of the Promoter Effect. The action of the so-called structural promoters (stabilizers), such as Al_2O_3, is closely associated with their solubilities in the iron oxide matrix of the unreduced catalyst or with the capability of the regular crystallizing magnetite to form solid solutions with iron–aluminum spinels [33], [289]–[291]. The solid solutions of Fe_3O_4 and the spinel $FeAl_2O_4$ have a miscibility gap below 850 °C [292]; at 500 °C, the solubility limit in the magnetite mixed crystal is a maximum of 7.5% $FeAl_2O_4$, i.e., 3% Al_2O_3, referred to iron. Higher alumina contents lead to separation into two phases, whereby only the portion dissolved in the magnetite phase appears to be responsible for the specific promoter action of alumina [255], [256], [293]. According to [294], there exists a close connection with the mechanism of the reduction which consists schematically of the following partial steps [295]:

1) Phase-boundary reaction of hydrogen with oxygen ions of the magnetite lattice, with formation of water vapor and release of electrons

2) Formation of metallic iron nuclei by combination the electrons with Fe^{2-} ions
3) Diffusion of Fe^{2+} ions and electrons to the nuclei and growth of the nuclei to iron crystals of various size

A more detailed discussion of the reduction mechanism is given in Section 3.6.1.4.

In the presence of dissolved aluminum ions, at not too high a temperature, the diffusion rate of the iron ions in the magnetite lattice is low. Hence, nucleus formation proceeds rapidly relative to crystal growth. Therefore, small iron crystallites, about 30 nm, form with correspondingly large specific surfaces. The aluminum probably remains partly in the iron crystallite in the form of very small $FeAl_2O_4$ areas statistically distributed over the lattice [262], [263], [294], [296], where an $FeAl_2O_4$ molecule occupies seven α Fe lattice positions [101].

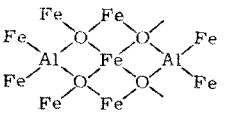

According to this concept, the stabilizer function of alumina reduces to paracrystalline lattice defects; an analogous effect is to be expected with Cr_2O_3, Sc_2O_3, etc. [262], [296]. Another theory is based on the observation that during reduction part of the alumina precipitates with other promoters into the surface of the iron crystallite in a molecularly dispersed distribution [258], [297] or in small islands [254]. This "patchy" monolayer of alumina acts like a "spacer" between iron atoms of neighboring crystallites and prevents sintering by means of a "skin" effect [263]. (See also [101], [110], [253].)

Insofar as small crystals of nonreducible oxides dispersed on the internal interfaces of the basic structural units (platelets) will stabilize the active catalyst surface Fe(111), the paracrystallinity hypothesis will probably hold true. But the assumption that this will happen on a molecular level on each basic structural unit is not true. The unique texture and anisotropy of the ammonia catalyst is a thermodynamically metastable state. Impurity stabilization (structural promotion) kinetically prevents the transformation of platelet iron into isotropic crystals by Ostwald ripening [154]. Thus the primary function of alumina is to prevent sintering by acting as a spacer, and in part it may also contribute to stabilizing the Fe(111) faces [155], [156], [298].

Calcium oxide, which also acts as a structural promoter [253] has a limited solubility in magnetite. It tends to stretch the magnetite lattice [101]. In the main, on cooling the magnetite melt, it separates at the grain boundaries as $CaFe_3O_5$ (at very rapid cooling rates) [285] and, in the presence of SiO_2, forms poorly reducible intermediate layers of calcium ferrite and silicates [253], [286]. In the reduced catalysts, it segregates between the iron crystallites [260], [299] and so possibly prevents sintering together at high operating temperatures. One may also presume that by partial neutralization of the "acid" components by calcium, more potassium is made available for activating the iron [196].

Potassium is likewise scarcely soluble in magnetite because of its ionic size [100]. In the unreduced catalysts, separate potassium- and iron-rich regions were found [109]. The appearance of a $K_2Fe_{22}O_{34}$ phase besides an unidentified phase, however, has been proved [300]. According to [301], during reduction, the emerging K_2O migrates to the iron crystallite surface. While doing this it reacts with the more or less homogeneously distributed aluminum (silicon) compounds. In this way, it is distributed over the iron phase. In the reduced catalysts, the potassium exists as a K + O adsorption layer that covers about 20 – 50 % of the iron surface [109]. According to [259], [302], potassium associates partly with the alumina in the surface, partly as KOH with iron [303]. It was found that the enhancement of the catalysts' specific activity by potassium oxide is accompanied by a decrease in the electron work function [302], [304], [305]. The promoting effect of potassium seems to be based on two factors which probably act simultaneously. One mechanism is the lowering of the activation energy for the dissociative adsorption of nitrogen [101], [109]. The explanation is based on an electrostatic model [107], [142], [306]. As indicated by the strong decrease in the work function upon potassium adsorption, there is a considerable electronic charge transfer to the substrate, which creates a $M^{\delta-} - K^{\delta+}$ dipole. A nitrogen molecule adsorbed near such a site will experience a more pronounced back-bonding effect from the metal to its antibonding π orbitals. This will increase the bond strength to the metal and further weaken the N – N bond, as can be seen from a further reduction of the N – N stretching frequency [307]. The other effect consists of lowering the adsorption energy of ammonia, which avoids hindering of nitrogen adsorption by blocking (poisoning) of the catalyst surface by adsorbed ammonia molecules [99], [109]; hence, potassium oxide ought to improve the catalyst performance less at low than at higher operating pressures [190], [308].

The negative effect of K_2O concentrations higher than about 0.58 % has not been explained unequivocally [144]. With increasing potassium concentration, this manifests itself by the increasing size of the average iron crystallite or the decreasing specific surface in the reduced catalyst [267], [300]. Since potassium oxide prevents the formation of solid solutions between alumina and magnetite to a certain extent [309], the recrystallization-promoting effect of higher K_2O concentrations may be attributed to a lowering of the portion of alumina dissolved in the magnetite phase [300]. Remarks in [301] and [310] reveal another possible interpretation: the K_2O located at the phase boundary surface and not bound to acid or amphoteric oxides may be converted by water vapor concentrations over 10^{-2} pm in the synthesis gas into potassium hydroxide or by hydrogen into potassium and potassium hydroxide, which would exist in molten form at operating conditions [301], [303].

An extensive review on promoters can be found in [108], and [156] provides a critical discussion of present theoretical interpretations of the promoter effects.

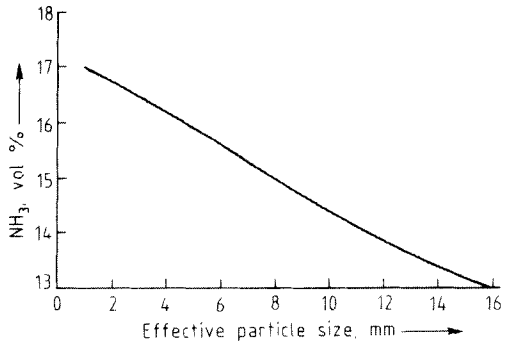

Figure 19. Influence of the particle size on the ammonia production (BASF catalyst).
25 MPa; SV = 12 000 $m^3m^{-3}h^{-1}$ (STP); gas composition (vol %): N_2 20.59, H_2 60.06, NH_3 2.55, Ar 5, CH_4 10

3.6.1.2. Particle Size and Shape

The choice of particle size and shape of commercial ammonia catalysts is determined mainly by two factors:

1) Catalyst performance
2) Pressure drop

From the standpoint of space–time yield, it is desirable to use the finest possible particle, which, practically speaking, is about 1–2 mm (Fig. 19); however, with decreasing particle size, the pressure drop and the risk of destructive fluidization of the catalyst increase (Fig. 20).

For processes operating at pressures of 25–45 MPa (250–450 bar) and at space velocities of 8000–20 000 $m^3m^{-3}h^{-1}$ (STP) a grain size of 6–10 mm is preferred. Larger granulations, for example, 8–15 mm or 14–20 mm, are used only in plants where the lowest possible pressure drop is essential because of very high gas velocities. In catalyst zones in which the ammonia formation rate is so high that the allowable temperature limits are exceeded, it may be advantageous to use coarse particles for suppressing the reaction. Radial-flow converters and the horizontal crossflow Kellogg converter (Fig. 91), which operate at comparatively low gas velocities [311], allow the use of small granulations (1.5–3 or 2–4 mm) with optimal use of the converter volume. Fluidized-bed processes, which have been explored especially in the Soviet Union, have so far been unsuccessful [312], [313].

Two effects cause the low production capacity of coarse-grained catalyst: first, large grain size retards transport of the ammonia from the particle interior into the bulk gas stream, because this proceeds only by slow diffusion through the pore system. Slow ammonia diffusion inhibits the rate of reaction. At the high reaction rate typical for the converter inlet layer, only a surface layer of the catalyst grains, about 1–2 mm thick, participates in the reaction.

The second effect is a consequence of the fact that a single catalyst grain in the oxidic state is reduced from the outside to the interior of the particle [314]: the water vapor produced in the grain interior by reduction comes into contact with already reduced

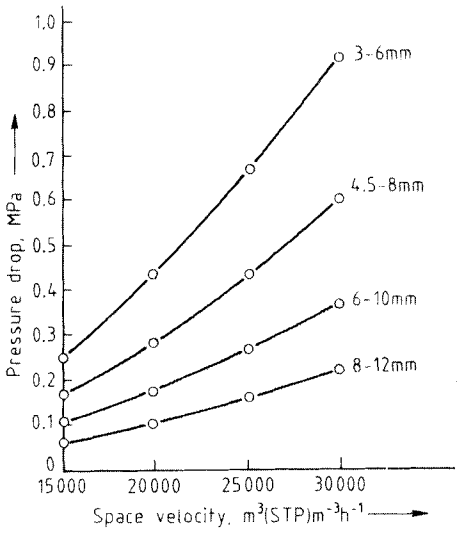

Figure 20. Pressure drop in the catalyst bed for various catalyst particle size ranges, from [33]. Depth of the catalyst bed, 7 m; reaction pressure 27.1 MPa; reaction temperature 450 °C

catalyst on its way to the particle outer surface; this induces a severe recrystallization [33]. The effect is very significant. As an example, if the particle size increases from about 1 to 8 mm, the inner surface decreases from 11 – 16 m^2/g to 3 – 8 m^2/g [315].

To allow for the influence of various particle shapes and size distributions within a defined sieve fraction, in lay-out calculations it is customary to employ an effective particle diameter, d_{eff}, as nominal size [32]. The diameter d_{eff} is defined as the ratio of equivalent diameter Λ and a form factor ψ. Λ is equal to the diameter of a sphere with a volume equal to the (average) volume of the particles, and ψ is the average ratio of the particle surface to the surface of a sphere of equal volume.

Table 18 shows the relation between the catalyst size classification, the equivalent particle diameter, and the percentage saving in catalyst or converter volume relative to the 6 – 10 mm standard size [280].

An irregular grain shape, for example with a shape factor of 1.5, has a more favorable effective activity for the individual particle and for radial intermixing of mass and heat in an industrial converter [316] than a more cubic or spherical shape, with a shape factor close to one. According to a patent by Chemie Linz AG [317], the catalyst particle ought to be 2 – 20 times as long as it is broad, preferably 5 – 10 mm long and 1 – 2 mm thick (broad). On the other hand, regular shapes have the advantages of greater abrasion resistance and lower pressure drop (see Fig. 21) [318].

The advantages of regular catalyst shapes and the need to compensate for the above-described negative effects of larger grain size by a system of macropores in the oxidic and reduced catalyst stimulated various attempts to manufacture shaped, macroporous catalysts. Various manufacturing techniques have been proposed [319] – [328]. As an example, magnetite is melted with the additives at high temperature (> 1600 °C) and the melt is cooled, broken, and ground to powder. After water is added and, if required, a binding agent, such as bentonite [327], or a promoter salt, such as cerium

Table 18. Effect of catalyst size on catalyst volume

Catalyst size classification, mm	Approximate equivalent particle diameter, mm	Relative catalyst volume, %
6–10	7.5	100
4.5–8	5.5–6.5	92–95
3.6	4.5–4.7	88–90
1.5–3	2.0–2.2	80–82
1–1.5	1.2–1.3	77–79

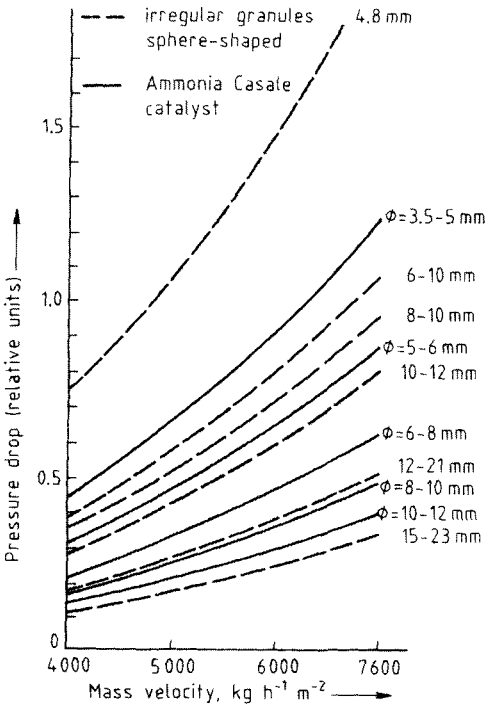

Figure 21. Comparison of the Ammonia Casale spherical catalyst and irregularly shaped catalyst [280]

nitrate [250], the powder is pelletized. The pellets subsequently are dried and sintered in an inert atmosphere at higher temperatures (about 1350 °C).

The application of macroporous catalysts ought to be especially useful for very low synthesis pressures and in plants in which large catalyst particles must be used for reasons of low pressure drop. For example, the performance of the macroporous Topsøe catalyst KMG 6 mm at 5 MPa synthesis pressure is said to be at least equivalent to KM I 1.5–3 mm and distinctly superior to KM I 6–10 mm [329].

3.6.1.3. Catalyst-Precursor Manufacture

The term "ammonia catalyst" commonly refers to the oxidic form consisting of magnetite and oxidic promoters. In fact this is only the catalyst precursor which is

transformed into the active catalyst composed of α-iron and promoters by reduction with synthesis gas, usually in situ. The reduction step is very important for catalyst performance.

The first effective catalysts were made by the oxygen-melt process. The purest possible iron (e.g., Swedish charcoal iron), together with the additives, was burned to Fe_3O_4 in a stream of oxygen. This process was largely replaced by melt processes in which natural or, less frequently, synthetic magnetite, together with the activators, was melted electrically or in electric arc furnaces [241], [330]. The cooled melt is ground to the proper granulation and reduced with hydrogen–nitrogen mixtures.

A process developed by Farbenfabriken (formerly Friedrich Bayer) had only local significance and is today only of historical interest. Complex iron cyanides were decomposed thermally in the presence of hydrogen. The hydrodecomposition proceeds via the carbide and nitride, finally to α iron. This is activated in the well-known manner by reduction-resistant metal oxides. The so-called Mont Cenis process employed such catalysts [331]. Repeatedly described as a means of manufacture, although only in the scientific literature, is coprecipitation of the catalyst components, for example, from aqueous solutions of the metal salts, with subsequent calcining and reduction [332]–[335]. With magnesium oxide as support, very small (under 10 nm) iron particles are obtained with high specific iron surfaces [335], similar to those obtained by exchange of magnesium ions by iron ions in the surfaces of magnesium hydroxy carbonate crystals [335], [336]. Granulation and sintering techniques have been used for the preparation of shaped macroporous iron catalysts, described in Section 3.6.1.2, which, however, have not gained industrial importance.

Impregnating the pore surface of prereduced passivated catalysts is a possibility for incorporating promoters into iron ammonia catalysts. A United Kingdom patent [337], by way of example, claims catalysts manufactured by impregnating the reduced catalysts with cerium salts. Improving the performance and life of industrial catalysts by radioactivity and X rays [338], treatment with ultrasound [339], [340], mechanical treatment [341], or high-frequency, alternating-field heating [342] has been attempted also.

The superiority of the catalyst manufacturing processes that use a molten iron oxide stage is mainly due to the fact that above 1000 °C in air, magnetite, Fe_3O_4, is the thermodynamically stable oxide phase of iron [8], [343]. Magnetite leads to especially efficient catalysts, and its electrical conductivity allows the use of economical electrical melting processes.

In 1996 the prices of commercial ammonia catalysts were about 2 $/lb (7 DM/kg) for oxidic and about 5.5 $/lb (20 DM/kg) for prereduced. Therefore, they are among the least expensive catalysts.

Operating conditions in the individual manufacturing steps — proportioning and mixing the raw materials, melting, cooling, crushing or if necessary grinding and preforming, and reduction — influence the quality of the finished catalyst (Fig. 22) [230].

The raw materials — usually, natural magnetite, lime, potash, and alumina — must, as far as possible, be free of catalyst poisons (see Section 3.6.1.5). Many ores have too high a content of free or bound silica, which can be lowered with magnetic separators [344]. Melting is accomplished in electrical resistance or induction furnaces (arc furnaces in the past) operating at 1600–2000 °C. The walls of these furnaces should

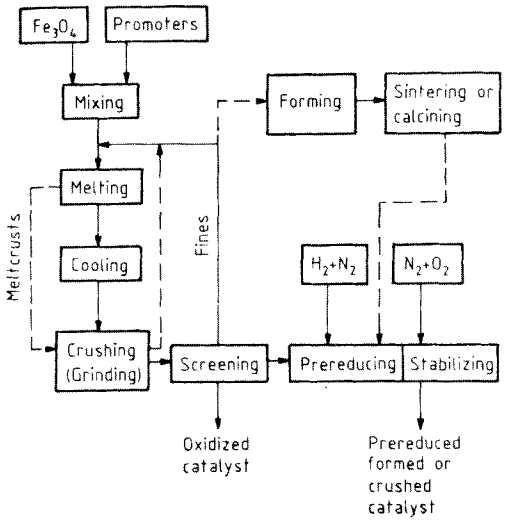

Figure 22. Ammonia catalyst manufacture

consist of a weakly basic tamping material indifferent to the melt, such as magnesium oxide, which is also an activating component of the catalyst [345]. A homogeneous distribution of the promoters in the magnetite melt and a degree of oxidation at or under that of stoichiometric magnetite should be obtained. This is said to be promoted by initially overheating to temperatures up to 3500 °C [346] (Fig. 23). It is claimed to be advantageous to bring the promoters into the melt as common chemical compounds that are isomorphous with magnetite [347].

Induction furnaces are optimal for the melting operation. Their good temperature control permits accurate adjustment of the degree of oxidation. Since the melt is held in constant turbulent motion by the magnetic field produced in the primary coil, it is well mixed, even for short melt times. In comparison to the most frequently used resistance furnaces, plant cost and power consumption are higher.

Another important factor in catalyst manufacture is the melt cooling rate, which is affected by the design and dimensions of the ingot molds. Quenching or fast cooling in thin sheets leads to a less abrasion-resistant, sharp-edged chip after crushing. Very slow cooling results in a more cubic chip, but with inferior catalyst quality (Fig. 23). In practice, slow cooling is avoided.

With falling temperature, both the solubility of the activator oxides (see Section 3.6.1.1) in magnetite and the rate of adjustment to the new phase equilibrium decline. Therefore, by rapid cooling of the melt the activator oxide distribution can be frozen in a condition corresponding to that of a higher temperature [348]. According to [285], there may exist relationships between the melt cooling rate, the appearance of certain phases, and the reducibility of the catalysts.

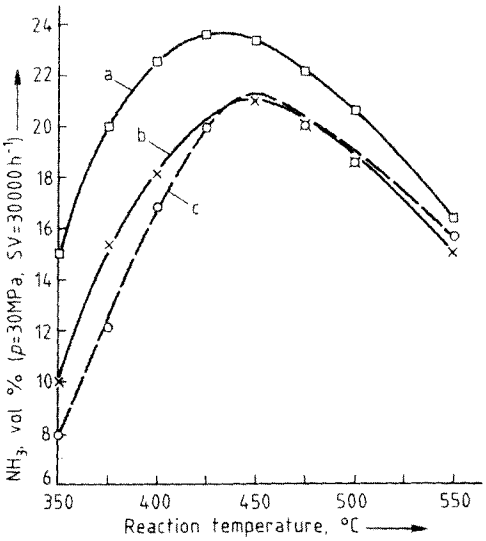

Figure 23. Effect of the melting temperature and rate of cooling of the melt on the activity of ammonia catalysts
a) Melt overheated to 3500 °C (rapid cooling); b) Melt temperature 1800–2000 °C (rapid cooling); c) Melt temperature 1800–2000 °C (slow cooling)

3.6.1.4. Catalyst Reduction

The reduction of oxidic catalyst is generally effected with synthesis gas. The magnetite is converted into a highly porous, high surface area, highly catalytically active form of α-iron. The promoters, with the exception of cobalt, are not reduced [33].

To ensure maximum effectiveness of the catalyst, a defined reduction procedure must be followed. Above all, it is important to hold the partial pressure of the resulting water vapor as low as possible and to insure that the water vapor does not come into contact with regions that have already been reduced [359]. High temperature and high water vapor partial pressure markedly accelerate premature catalyst aging by recrystallization. Therefore, the reduction should be carried out at high gas velocities [about 5000–15 000 $m^3m^{-3}h^{-1}$ (STP)], at the lowest temperatures sufficient for complete reduction, and at not too high pressures (7–12 MPa in low-pressure, 25–30 MPa in high-pressure plants) to hold the exothermic formation of ammonia under better control during the reduction. When the reduction of the oxidic catalyst is carried out in the production plants, long reduction times are needed at low temperatures and low pressures with a consequential loss of production.

In practice, the reduction temperature is raised stepwise by using the exothermic heat of ammonia formation. The progress of the reduction is controlled according to the catalyst temperature and the water concentration by adjustment of the synthesis gas flow. As a rough guideline, the water content of the gas effluent from the catalyst should not exceed 2–3 g/m^3 (STP). Under these conditions, depending on its size and operating pressure, a synthesis converter with a fresh load of oxidic catalyst attains its full production capacity in 4–10 d.

The minimum temperatures necessary for reduction are somewhat different for the various catalyst types. Catalysts conventionally employed in medium-pressure plants

may be reduced from about 340 to 390 °C, although a slow induction period starts somewhat lower. Generally, temperatures above 440 °C are required to complete the reduction.

The reducibility of industrial catalysts is dependent on both the combination of promoters and the degree of oxidation. The FeO (wustite) phase is reduced faster and at lower temperatures than the Fe_3O_4 (magnetite) phase [285]. According to [285], the rather considerable differences in the reduction rates of commercial catalysts with similar compositions may be attributed to differences in manufacturing methods or operating conditions. Commonly, the manufacturers hold these in strict secrecy.

Some older publications deal with the influence of catalyst granulation on the optimum reducing conditions [349]. Directions for reduction in multibed converters that combine fine- and coarse-grained catalyst appear in [350]. The influence of the hydrogen/nitrogen ratio during reduction on the catalyst performance after reduction is discussed in [351].

The influence of the reduction conditions (gas flow rate, temperature in the range 300 – 600 °C, nitrogen content in the hydrogen in the range 0 – 100 %) on the production capacity of an ammonia catalyst has been investigated [352].

The gas/solid reaction between magnetite and hydrogen has been studied in great detail by rate measurements, microscopy, and X-ray diffraction [353] – [356]; a summary is given in [156] and [264]. According to one model, on an atomic scale the reaction is controlled by two processes:

1) Metallic iron is formed from wustite (Eq. 24) by direct chemical reaction controlled in the initial phase by the reaction rate (activation energy ca. 65 kJ/mol) and in the final stage by diffusion processes involving hydrogen and water on the reaction site:

$$FeO + H_2 \longrightarrow Fe + H_2O \tag{24}$$

2) The chemical reaction creates an iron(II) ion concentration gradient in the solid. This gradient leads to a rapid diffusion of iron(II) ions from magnetite through wustite to the chemical reaction interface, where they are reduced and precipitated as iron nuclei. This is made possible by the structural defects of the wustite. The precipitation of further wustite nuclei on the magnetite/wustite reaction interface seems to be effected by ion/electron diffusion processes rather than by direct contact of magnetite with hydrogen [357] (Eqs. 25, 26):

$$O^{2-} + H_2 \longrightarrow H_2O + 2\ e^- \tag{25}$$

$$Fe_3O_4 + Fe^{2+} + 2\ e^- \longrightarrow 4\ FeO \tag{26}$$

The topotactic reduction process leads to a core and shell structure which is visible under the optical microscope and is shown schematically in Figure 24 (a). Figure 24 (b) shows the wustite/magnetite interface as observed by electron microscopy [264]. This concept was developed for single-crystal magnetite grains, but the shell and core model is also discussed for commercial polycrystalline catalysts [264], [358]. But this model seems to contain too many simplifications [156]. For example, it is difficult to explain with this model why water diffusing through porous iron in contact with oxo anions

would not reoxidize it. Therefore it might be viewed more as a formal description rather than a mechanical approximation. A more detailed atomistic view of the reduction reaction indicates that migration of electrons and reactants through intrinsic and extrinsic defects will control the kinetics of the reaction. Information in this respect was gained from metallurgical reduction processes [1470]–[1473]. According to this, a gradient in chemical potential of the iron ions is required for a satisfactory progress of the reaction. This gradient is established by iron metal nuclei which are formed from metastable wuestite existing in the mosaic-like crystals of the precursor. Consequently there should be no homogeneous topotactic reaction interface, as assumed in the shell and core model. According to the alternative model, the active catalyst should not grow as a shell around a core of percursor material but as a core within an oxidic matrix. Reaction equations for this reaction may formulated as follows (Eqs. 27–31) [156], [1472], [1473].

$$4\ O^{-2} + 4\ H_2 \longrightarrow 4\ H_2O + 2\ e^- \tag{27}$$

$$Fe_3O_4 + Fe^{2+} + 2\ e^- \longrightarrow 4\ FeO \tag{28}$$

$$4\ FeO \longrightarrow 4\ Fe^{2+} + 4\ O^{2-} \tag{29}$$

$$4\ Fe^{2+} \longrightarrow 8\ e^- + 4\ Fe \tag{30}$$

Overall reaction:

$$4Fe_3O_4 + 4\ Fe + 4\ H_2O \longrightarrow 4\ Fe + 4\ H_2O \tag{31}$$

The equation of the overall reaction suggests the process is at least in some formal way autocatalytic. As all atoms of the activated catalyst should move through the matrix, there will be no structural correlation on an atomic scale between the starting material (precursor) and the product (active catalyst). In contrast to the simple core and shell model, a reproduction of the oxide morphology of the precursor could not be expected for the final reduced catalyst. An explanation of how the desired iron platalet microstructure could be formed is seen in the topochemistry of the iron nuclei which result from a decomposition of wuestite into iron and platalets of secondary magnetite. The presence of wuestite is thus thought to be essential. According to SCHÖGL [156] this could be a first hint of a difference between normal iron and "ammonia iron". Information on the reduction kinetics, including industrial catalysts, can be found in [154], [156], [314], [360], [364]–[367]. Newer findings also seem to question the shell and core model with the topotactic reaction interface [156].

Prereduced, stabilized catalyst types, introduced on the market some years ago, have gained a considerable market share. Prereduced catalysts have the full pore structure of active catalysts, although the pore surface has been oxidized to a depth of a few atomic layers to make these catalysts nonpyrophoric.

Reactivating such catalysts usually takes only 30–40 h. Ammonia formation begins at substantially lower temperatures, so that altogether the downtime of a production unit is reduced markedly. This and further advantages, such as reducing the risk of damaging the catalyst during activation by too high a local concentration of water, the

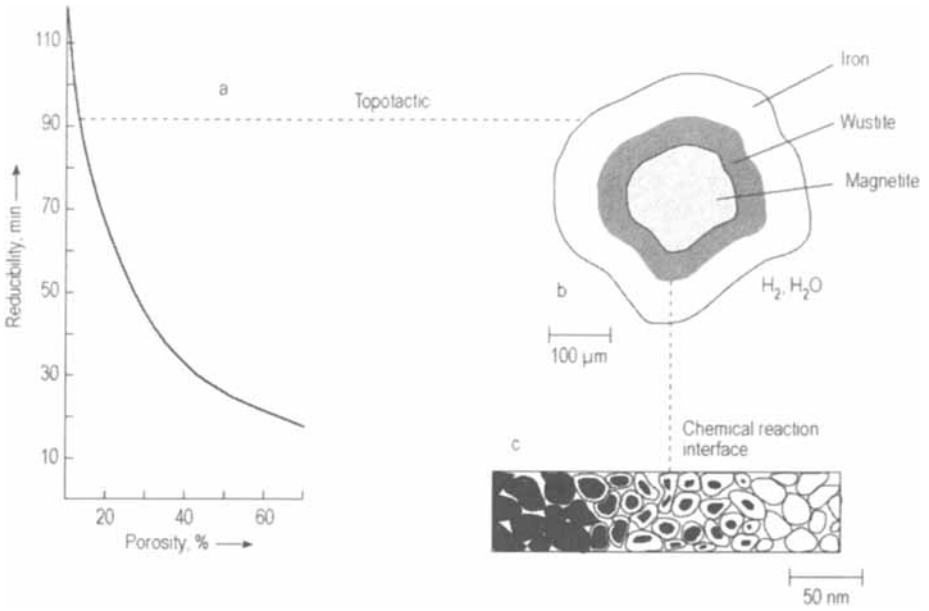

Figure 24. Core and shell mechanism of catalyst reduction [264]
a) Reducibility of catalyst under standard conditions as a function of its porosity; b) Core and shell structure of catalyst; c) Reaction interface

quantitatively lower yield of aqueous ammonia solution (which can be added to the production), as well as the roughly 20% lower bulk weight (which reduces the design loadings and costs of the internals of large converter units), make using prereduced catalysts increasingly attractive, especially in single-train plants, in spite of higher prices. The somewhat inferior mechanical strength is a disadvantage that requires special care when a charge is being loaded into the converter.

Reduced catalyst is pyrophoric in the atmosphere; therefore, it has to be stabilized by passivating the surface with oxygen after the reduction with hydrogen/nitrogen mixture at low to moderate pressure before it can be removed from the reduction reactor for packing and shipping. Usually, the method recommended by BURNETT is used. The reduced charge is treated with nitrogen containing 100 – 1000 ppm oxygen at 50 – 70 °C (maximum 95 °C) and a pressure of 0.1 – 0.2 MPa (1 – 2 bar) and up [368]. The reducible oxygen content of the prereduced catalyst ranges between 2 and 7%. Part of this is only loosely bound and is removed in reactivation even below 200 – 300 °C.

Detailed data on the manufacturing steps most important to the catalyst performance, reduction, prereduction, passivating, and reactivation, appear in [33], including a discussion of the most important literature in this field.

3.6.1.5. Catalyst Poisons

The activity of an ammonia synthesis catalyst may be lowered by certain substances, commonly referred to as poisons. These substances can be minor gaseous constituents of the synthesis gas or solids introduced into the catalysts during the manufacturing procedure, derived from impurities in the natural magnetite from which the catalyst is made. These latter should not play a major role with catalysts from manufacturers of repute and are not discussed in detail in this section because of the proprietary nature of the production processes. General measures to avoid this sort of contamination include selecting a rather pure magnetite, the application of pre-treatment processes, and the use of high-purity promoters. The melting process itself may also contribute to minimizing the content of some minor impurities. For gaseous poisons in the synthesis gas, a distinction can be made between permanent poisons that cause irreversible damage to the catalyst and temporary poisons which lower the activity while present in the synthesis gas. In contrast to temporary poisons, permanent poisons can be detected on the catalyst by chemical analysis. Oxygen-containing compounds such as H_2O, CO, CO_2 and O_2 are the most common temporary poisons encountered in ammonia synthesis.

Oxygen compounds have a reversible effect on iron catalysts at not too high temperatures. That is, the activity of a damaged catalyst may be practically completely restored by reduction with clean synthesis gas. Equivalent concentrations of oxygen compounds, for example, 100 ppm of O_2 or CO_2 and 200 ppm CO or H_2O, lead to the same degree of poisoning, presumably because as soon as they enter the catalyst bed they rapidly and completely transform into H_2O [33]. The damage depends approximately linearly on the quantity of adsorbed water taken up by the catalyst [369], which is proportional to $\sqrt{p_{H_2O}}\sqrt{p_{H_2}}$ [370]. Corresponding to the adsorption equilibrium, the degree of poisoning therefore rises with growing partial pressure ratio, p_{H_2O}/p_{H_2} and falls with increasing temperature.

Under the assumption of a displacement equilibrium (Eq. 32) in accordance with

$$(N_2)_{ads} + H_2O_{gas} + 2\ H_{2gas} \leftrightharpoons (O)_{ads} + 2\ NH_3 \tag{32}$$

I. A. SMIRNOV et al. set up a rate equation for ammonia synthesis [371], [372] that takes the effect of water vapor into consideration over a wide range of temperature and pressure:

$$v = \frac{k_1 p_{N_2} - k_2 p_{NH_3}^2/p_{H_2}^3}{\left(p_{NH_3}^2/p_{H_2}^2 + C p_{H_2O}/p_{H_2}\right)^{1/2}} \tag{33}$$

and found the values of C listed in Table 19.

A more recent investigation [373]–[375] proposed multiplying the rate equation by a correction factor $1-\Theta$, where $\Theta = a + bT + cT \ln X_{H_2O}$ and X_{H_2O} is the molar fraction of H_2O. Some authors assume a different route (Eq. 34) for the formation of adsorbed atomic oxygen [376], [377]:

Table 19. C values for the ammonia synthesis rate equation

Catalyst	Temperature, °C				
	400	425	450	475	500
$Fe + Al_2O_3$	0.63	0.39	0.24	0.17	0.12
$Fe + Al_2O_3 + K_2O$	0.74	0.46	0.28	0.20	0.14

$$H_2O(g) + 3^* \rightleftharpoons 2\ H^* + O^* \tag{34}$$

where * denotes a surface site.

Recent reports have confirmed the equivalence of H_2O, CO, CO_2 and O_2 [378] with respect to their poisoning effect.

The experimentally determined effect of water vapor concentrations up to about 30 ppm on the activity of a commercial catalyst (BASF S 6–10) at 30 MPa is evident from Figure 25.

With continuing exposure oxygen compounds also cause irreversible damage to the catalyst activity that is causally linked with growth of the iron primary crystallite [375], [379]. This is probably one of the main causes of the decline in converter performance over the course of the catalyst operating life. This damage depends on the water-vapor partial pressure and is especially serious, in contrast to reversible poisoning, at high temperatures. In a pilot plant, Österreichische Stickstoffwerke (ÖSW), Linz, established that at 30 MPa and a water-vapor content of 250 ppm, for example, the production declined by about 15 % per month. For a carbon monoxide content of 5 ppm, they determined about a 4 – 5 % decrease in activity per year. The influence of the operating temperature is evident from the data. The performance of a catalyst operated at 570 °C is about 35 – 40 % under that of a catalyst charge operated at 520 °C. That is, the higher the temperature, the greater is the harmful effect of oxygen compounds [380]. Corresponding to the data, they established that above all, temperatures above 500 – 520 °C must be avoided in order to achieve a converter charge operating period of more than 2 – 3 years. If the temperature is kept at this level, generally recommended for modern plants, then even at CO concentrations of 20 ppm in the recycle loop gas, no serious deterioration of the catalyst performance is observed after a month of operation. With the highly purified synthesis gas of modern synthesis processes (with final gas purification by methanation the carbon monoxide level is lowered to below 5 ppm), operating periods of up to 14 years can be achieved for a converter charge without significant loss of activity (Fig. 26).

As already mentioned in Section 3.6.1.1, the concentration and combination of promoters affect the degree of irreversible damage. This must be considered in the choice of catalyst for a particular plant.

Sulfur, Phosphorus, and Arsenic Compounds. Sulfur, occasionally present in synthesis gases from coal or heavy fuel oil, is more tightly bound on iron catalysts than oxygen. For example, catalysts partially poisoned with hydrogen sulfide cannot be regenerated under the conditions of industrial ammonia synthesis. Compounds of phosphorus and arsenic are poisons but are not generally present in industrial synthesis gas. There are

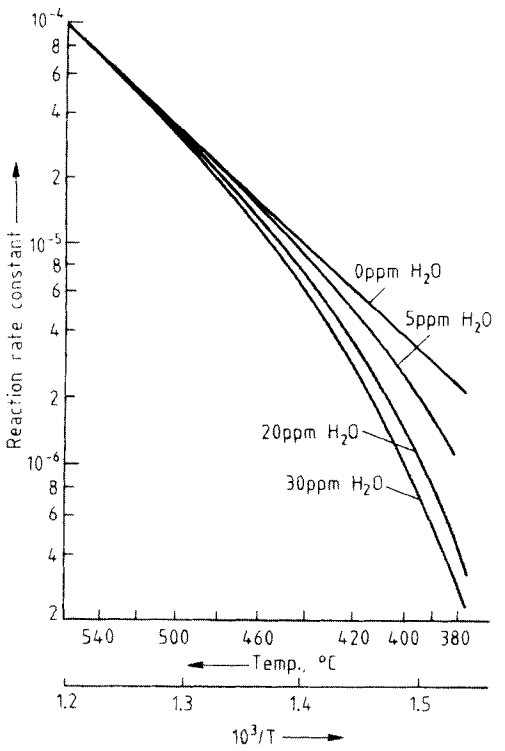

Figure 25. Reversible effect of increasing water vapor concentrations in the synthesis gas on the activity of industrial ammonia catalysts

indications that these permanent poisons exert the most detrimental effect when present as hydrogen compounds and are less harmful in higher oxidation states [381].

With regard to the sulfur bound on the catalyst surface, differences exist between the various types of ammonia catalysts, especially between those that contain alkali and alkaline earth metals and those that are free of them. Nonpromoted iron and catalysts activated only with alumina chemisorb S_2N_2 and thiophene. When treated with concentrations that lie below the equilibrium for the FeS bond, a maximum of 0.5 mg of sulfur per m^2 of inner surface or free iron surface is found; this corresponds to monomolecular coverage [382], [383]. The monolayer is also preserved on reduction with hydrogen at 620 °C, whereas FeS formed by treatment above 300 °C with high H_2S concentrations is reducible as far as the monolayer. For total poisoning, 0.16 – 0.25 mg S/m^2 is sufficient. Like oxygen, sulfur promotes recrystallization of the primary iron particle.

Under similar poisoning conditions, alkali- and alkaline earth-containing industrial catalysts adsorb more H_2S. In spite of this, however, in terms of activity, they are more stable toward the action of sulfur and are partially regenerable [383]. In a catalyst bed, most of the sulfur already has been taken up in the gas inlet layer. A catalyst sulfur content of several 100 ppm suffices to impair its activity [33].

In industrial plants, sulfur may reach the ammonia converter in various forms. In some plants, traces of H_2S and COS may not be removed in the upstream purification

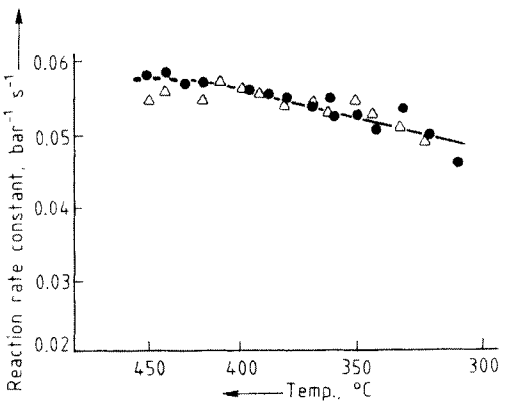

Figure 26. Activity of BASF ammonia catalyst S 6–10 in a commercial converter after 14 years of operation
• fresh catalyst; △ after 14 years operation

steps and so may enter the converter with the makeup gas. However, the sulfur contained in the compressor oil constitutes the main danger. On cracking the oil to lower molecular mass hydrocarbons, sulfur is freed as H_2S. It is therefore very important to use an oil with low sulfur content in ammonia plants, especially those still using reciprocating compressors. If after mixing with the recycle gas the make-up gas first passes through an ammonia condensation stage in which the H_2S and also to a certain extent COS are very effectively washed out by condensing ammonia, a sulfur content of the oil of 0.1 – 0.2 wt % ought to be sufficiently low. Otherwise, a value under 0.1 % is recommended [384]. In modern plants designed with centrifugal compressors and in which the sulfur content of the synthesis gas is extremely low because of very effective purification (about 0.5 – 1 μg S/m^3 (STP)), sulfur poisoning is of lesser importance than carbon monoxide and chlorine poisoning.

Chlorine compounds. The permanent poisoning effect of chlorine compounds is two orders of magnitude worse than that of oxygen compounds. Concentrations of about 0.1 ppm are viewed as the uppermost allowable limit in order not to affect adversely the life of ammonia catalysts [384]. The deactivation effect is based at least in part on the formation of alkali chlorides that are volatile at the upper synthesis temperatures.

Further information on catalyst poisoning is given in [374], [375].

3.6.2. Other Catalysts

3.6.2.1. General Aspects

For a long time efforts to improve the efficiency of industrial ammonia production concentrated on synthesis gas production, and major progress was achieved over the years. In ammonia synthesis itself considerable progress was made in converter design and recovery of the reaction enthalpie at high temperature, but there has been no substantial improvement in the catalyst since the 1920s. The standard commercial iron

catalyst still requires relatively high pressures (usually in excess of 130 bar), high temperatures (400–500 °C) and large reactor volumes (more than 100 m^3 for a capacity of 1800 t/d) to achieve good economics, although in a few cases a pressure as low as 80 bar has been used. From the vast amount of experimental and theoretical studies of the iron catalyst one can conclude that there is only limited potential for further improvement. Substantial energy savings would require lowering the synthesis pressure considerably, down to the synthesis gas production level, say. However, to compensate for the less favorable equilibrium situation much lower operating temperatures would be necessary, because otherwise too low an ammonia concentration would result, and additional energy would be needed for recovery, thus canceling the energy saving from synthesis gas compression. To reach this goal a synthesis catalyst with a volumetric efficiency some two orders of magnitude greater than magnetite would be necessary. Process studies show an energy saving potential of about 1 GJ/t NH_3 [385].

In the search for an alternative catalyst, most metals have been tested, either as primary components or as promoters. Much of this work was performed in the early, pioneering studies in the BASF laboratories [231], [232]. Most of the studies in the following years concentrated on the magnetite system in the sense of more fundamental and general catalytic research. Rising energy costs since the mid-1960s have given a new incentive to the search for other catalyst systems with improved performance. The first development which found commercial application was a cobalt-modified magnetite catalyst introduced in 1984 by ICI. With similar kinetic characteristics its volumetric activity is about twice that of the standard iron catalyst. The only other catalyst system which exhibits a promising potential for industrial application is based on ruthenium [172]. These new efforts to find improved catalysts could use methods and knowledge of modern surface science as developed on the example of the magnetite catalyst. Structural sensitivity and nature of the nitrogen adsorption and dissociation steps could serve as guidelines [173].

For the overall performance of potential catalysts in practical application additional factors, such as number of active sites, physical form, and porosity must also be taken into account. The classical commercial iron catalyst is an unsupported catalyst. First of all iron is a cheap material and secondly by the incorporation of alumina a surface area similar to that attained in highly dispersed supported catalysts can be obtained. Of course, for an expensive material such as the platinum group metals, the use of a support material is the only viable option. The properties of the supported catalyst will be influenced by several factors [172]

- Adequate surface of the carrier to achieve a reasonable metal loading.
- Dispersion stability by using a more active support with strong interaction between the support phase and the metal precursor. Too strong an interaction may cause difficulties in the metal reducing.
- Promoter localization with respect to metal sites and support sites.
- Gas transport effects will be governed by pore size, pore distribution, and tortuosity.

- Anion retention capability, which plays a role in the catalyst preparation by impregnation of a support with metal compound solutions.

3.6.2.2. Metals with Catalytic Potential

Materials that show significant ammonia synthesis activity can be divided into three categories according to their ability to form nitrides:

1) Platinum group metals: no stable nitrides (Ru, Os, Ir, Pt)
2) Metals forming nitrides unstable under reaction conditions (Mn, Fe, Co, Ni, Tc, Re)
3) Metals likely to be present as nitrides under synthesis conditions (groups 3–6 of the periodic table)

Of the platinum group metals only ruthenium and osmium show an activity superior to iron, though only in presence of alkali metal promoters, as may be seen from Table 20 [386].

Although osmium was the first active catalyst used by HABER in 1909 [387] in his laboratory-scale unit to demonstrate the technical viability of the high-pressure recycle process, this metal never became an industrial catalyst because of its limited availability and its dangerous properties. The interest of today therefore shifted to ruthenium. The most active ruthenium catalysts use a graphite support and alkali metal promotion, preferentially with rubidium or cesium [388], [389]. It is unlikely that the promoter is in metallic state as its high vapor pressure would probably lead to substantial losses under synthesis conditions. It is assumed that a charge transfer complex $M^+\cdots C^-$ is formed between the metal and the graphite. A major advantage of graphite is its ability to stabilize high loadings of alkali metals. A special limitation until recently was the chemical reactivity of carbon supports. In a typical ammonia synthesis environment with high hydrogen partial pressure, the catalyst may also catalyze the methanation of carbon, which would lead to destruction of the support. Indeed, this phenomenon has been observed [390], but it can be avoided by careful heat treatment of the support above 1500 °C [391]. With this modified carbon material lifetimes of at least six years are expected [386].

The group of metals forming low-stability or unstable nitrides includes Mn, Fe, Co, Ni, Tc and Re. As in the case of iron a clear structural sensitivity was found for rhenium but the role of promoters remains the subject of discussion. There are also indications of structure sensitivity for cobalt and nickel. It was attempted to improve the activity of the classical magnetite catalyst by alloying with nickel or cobalt. The only commercial catalyst is a cobalt containing magnetite [392].

Of the group of metals forming stable nitrides, only molybdenum is of some interest. Under synthesis conditions it is present as a nitride with some ammonia formation activity and structural sensitivity [393]. Molybdenum also seems to exhibit activity in biological nitrogen fixation [394] and is synthetically active at ambient conditions in the air-sensitive GLEMSER compounds [394].

Table 20. Ammonia synthesis activity of metals supported on carbon with potassium metal promotion (mL NH_3/mL catalyst, 573 K, 1283.13 mbar, H:N = 3:1

		Fe 0.72	Co 0.4	Ni 0.04
Mo 0.6		Ru 22.2	Rh 0.52	Pd 0
	Re 0.36	Os 5.6	Ir 0.68	Pt 0.008

The results of the intensive research in this field over the last decades demonstrate that, irrespective of the catalyst, the rate-determining step in the ammonia synthesis reaction is the dissociation of the nitrogen molecule and the catalyst effectivity is determined in the first instance by the activation energy of the dissociation reaction. The other common factor for the ammonia catalysis is the structure sensitivity of molecular nitrogen adsorption. Only if both conditions are favorable, and other factors such as hydrogen and ammonia inhibition do not play a major role, can a sufficient overall reaction rate be expected. The available data show that these conditions are fulfilled only for a limited number of metals: iron, ruthenium, and osmium. On account of its very strong ammonia inhibition rhenium is not an option. Extensive literature on non-iron catalysts is given in [172], [173]; kinetic investigations are reported in [173].

3.6.2.3. Commercial Ruthenium Catalysts

Since the early days of industrial ammonia synthesis only minor improvements have been achieved for the magnetite system: optimization of manufacturing procedures, promoter concentrations, and particle size to give somewhat higher activity and longer service life.

The most notable development for the magnetite system was the introduction of cobalt as an additional component by ICI in 1984 [395], [396]. The cobalt-enhanced catalyst formula was first used in an ammonia plant in Canada using ICI Catalco's AMV process (later also in other AMV license plants) and is also successfully applied in ICI's LCA plants in Severnside.

In 1979 BP disclosed to M.W. Kellogg a new catalyst composed of ruthenium on a graphite support [395], [397]. In October 1990, after a ten-year test program, Kellogg started the commercialization of the Kellogg Advanced Ammonia Process (KAAP) using this catalyst [397], which is claimed to be 10–20 times as active as the traditional iron catalyst. According to the patent [392] the new catalyst is prepared by subliming ruthenium-carbonyl [$Ru_3(CO)_{12}$] onto a carbon-containing support which is impregnated with rubidium nitrate. The catalyst has a considerably higher surface area than the conventional catalyst and, according to the patent example, it should contain 5 wt % Ru and 10 wt % Rb. Besides having a substantially higher volumetric activity, the promoted ruthenium catalyst works best at a lower than stoichoimetric H/N ratio of the feed gas as shown in Figure 27. It is also less susceptible to self-inhibition by NH_3 (Figure 28) and has excellent low-pressure activity. A diameter of 1.5–2.5 mm and a

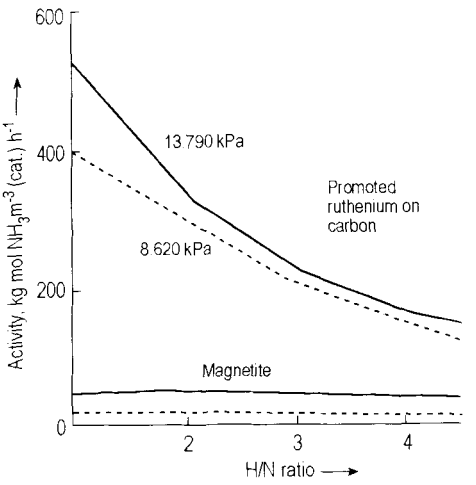

Figure 27. Effect of H/N ratio on activity of Ru and Fe_3O_4 catalysts [172]

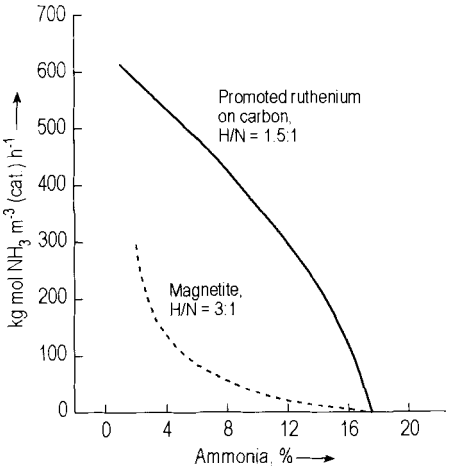

Figure 28. Ammonia inhibition of Ru and Fe_3O_4 catalysts [172]

lenght of about 6 – 7 mm are probably the dimensions of the particles of the commercial catalyst.

The potential for ruthenium to displace iron in new plants (several projects are in progress [398] of which two 1850 mtpd plants in Trinidad now have been successfully commissioned [1488]) will depend on whether the benefits of its use are sufficient to compensate the higher costs. In common with the iron catalyst it will also be poisoned by oxygen compounds. Even with some further potential improvements it seems unlikely to reach an activity level which is sufficiently high at low temperature to allow operation of the ammonia synthesis loop at the pressure level of the synthesis gas generation.

4. Process Steps of Ammonia Production

Today the term "ammonia synthesis" is increasingly used when referring to the total ammonia production process. Synthesis conditions are no longer viewed in isolation. Of course, they are an important consideration in the total process but can be determined properly only in relation to the total plant integration (see Chapter 5). A review of ammonia production technology up to 1974 is contained in [399], and [400] gives a description of the state of the art up to 1980; the United States patent literature in the field from 1972 to 1980 is covered in [401]. More modern and comprehensive reviews of ammonia production technology can be found in [402]–[404]. The journal *Nitrogen*, published by British Sulphur, presents an update of the state of the art from time to time. A valuable information soure is also the annual AIChE Ammonia safety symposium.

The complete process of industrial ammonia production may be subdivided into the following sections:

A) Synthesis gas production
   1) Feedstock pretreatment and gas generation
   2) Carbon monoxide conversion
   3) Gas purification
B) Compression
C) Synthesis

It has been already mentioned briefly, that compared to the synthesis section itself, where of course some progress has been made in converter design and optimization of heat recovery, the more fundamental changes over the years have occurred in synthesis gas preparation and gas compression. It is therefore appropriate to discuss the various methods for the synthesis gas generation, carbon monoxide shift conversion, and gas purification in some detail. Figure 29 shows schematically the options for the process steps for ammonia production.

4.1. Synthesis Gas Production

The goal is preparing a pure mixture of nitrogen and hydrogen in the stoichiometric ratio of 1:3. The raw materials are water, air, and a carbon-containing reducing medium, that, for its part, may contain hydrogen (natural gas, CH_4; naphtha, CH_2; petroleum, $\approx$ CH) and nitrogen; for example, natural gas from the Slochteren field in the Netherlands contains 14% nitrogen.

Usually only the carbon-containing materials and hydrogen from other sources are regarded as raw materials in the narrow sense because of the abundance of air, which

Figure 29. Options for generating and purifying ammonia synthesis gas

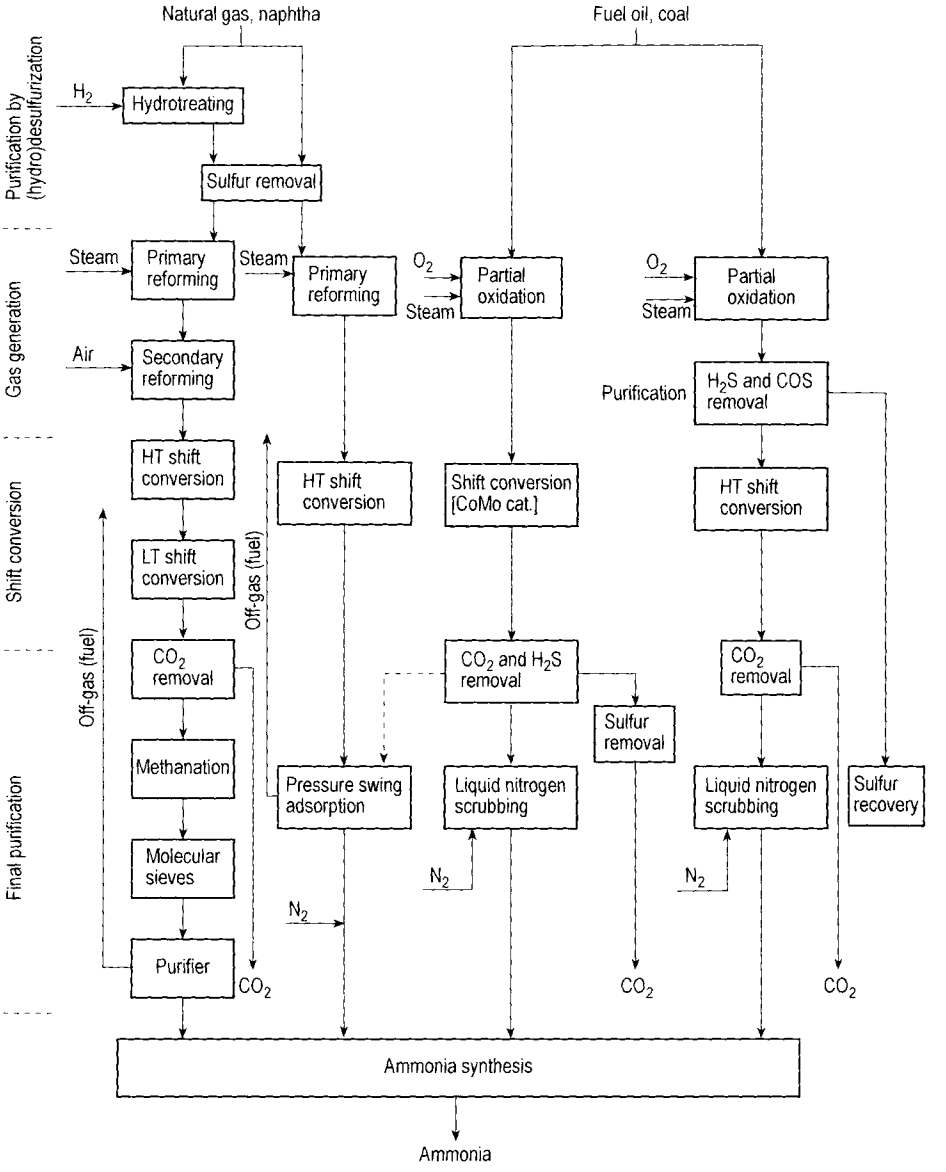

provides all of the nitrogen, and water, which generally supplies most of the hydrogen. The term feedstock is often applied to the total consumption of fossil fuel, although strictly speaking a distinction should be made between gasification feed and fuel for energy generation.

Certain raw materials for synthesis gas production that were once of primary importance currently are used only under special economic and geographical circumstances (e.g., China, where 66% of production is based on coal). These include solid

Table 21. Feedstock distribution of world ammonia production capacity

	1962		1972		1983		1998	
	10^3t N	%	10^3t N	%	10^3t N	%	10^3t N	%
Coke oven gas and coal	2800	18	4600	9	7200	8	16500	13
Natural gas	7800	50	32100	63	66850	74	96300	77
Naphtha	2050	13	10700	21	9050	10	7300	6
Other petroleum products	2950	19	3600	7	7200	8	4400	4
Total	**15600**	**100**	**51000**	**100**	**90300**	**100**	**122500**	**100**

Table 22. Relative ammonia plant investment and relative energy requirement for 1800 t/d NH_3

	Natural gas	Naphtha	Fuel oil	Coal
Relative investment	1.0	1.15	1.5	2.5
Relative specific energy requirement (based on lower heating values)	1.0	1.1	1.3	1.7

fuels, coke oven gas, and hydrogen produced by electrolysis. Reference [405] covers coke oven gas as a feedstock for ammonia synthesis and references [406]–[409] describe producing hydrogen by water electrolysis for ammonia production. If water electrolysis is used the energy requirement amounts to about 10 000 kWh/t NH_3.

Table 21 provides an overview of the raw material sources (apart from water and air) for world ammonia capacity.

Table 21 indicates that new ammonia plants are based almost exclusively on natural gas and naphtha. This trend is also expected to continue in the near future. Naturally, the regional distribution is diverse. In North America, for example, natural gas dominates, with 95 % of capacity. In the EU, 86 % of capacity is based on natural gas and 8 % on fuel oil [410].

The capital cost and the specific energy requirement (i.e., feed and fuel, and so the manufacturing cost) largely depend on the raw material employed [411], [412]. Table 22 shows the relative capital cost and the relative energy requirement for a plant with a capacity of 1800 t/d ammonia. For the natural gas based plant the current best value of 28 GJ/t NH_3 is used.

The chemical reaction of hydrocarbons, carbon, or coke with water, oxygen, air, or any combination of these is generally referred to as gasification. It yields a gas mixture made up of CO and H_2 in various proportions along with carbon dioxide and, where air is used, some nitrogen. Any carbon containing feedstock will undergo a reaction according to Equation (35) or (36) or both simultaneously.

$$[CH_x] + H_2O \rightleftharpoons CO + H_2 + x/2\ H_2 \qquad \Delta H > 0 \tag{35}$$

$$[CH_x] + 1/2\ O_2 \rightleftharpoons CO + x/2\ H_2 \qquad \Delta H < 0 \tag{36}$$

Light hydrocarbons ranging from natural gas (methane) to naphtha (max. C_{11}) undergo reaction with steam over a catalyst according to Equation (35) which is usually

called *steam reforming*. In the case of coal or coke, Equation (35) corresponds to the noncatalytic water gas process, which in its classical form is today only used in a number of plants in China and is otherwise only of historical interest. Corresponding to Equation (36), commonly known as *partial oxidation*, all carbon-containing feedstocks can be processed in a noncatalytic reaction with oxygen (together with some steam, which gives rise to a simultaneous reaction according to Eq. 35). An additional equilibrium reaction involved in any gasification process is the water gas shift reaction (37).

$$CO + H_2O \rightleftharpoons CO_2 + H_2 \qquad \Delta H^0_{298} = -41 \text{ kJ/mol} \tag{37}$$

Although reaction in the right hand direction is favored by lower temperatures it is responsible for the initial carbon content of the raw synthesis gas. To maximize the hydrogen yield, this reaction is carried out in a separate step over a different catalyst at a lower temperature than the preceding gasification step (Section 4.2).

From Equation (35) it can be seen that in the steam reforming variant the proportion of hydrogen supplied by the feedstock itself increases with its hydrogen content. It attains the theoretical maximum of 66% with methane. The hydrogen–oxygen bond energy in water is higher than the hydrogen–carbon bond energy in the hydrocarbon. The positive enthalpy per mole of hydrogen therefore decreases as the proportion of hydrogen contributed from the feedstock itself increases. Natural gas consists predominantly of methane and is therefore the most hydrogen-rich and energetically the best raw material for the steam-reforming route. In the partial-oxidation route less hydrogen is produced in the primary gasification step and the raw synthesis gas has a rather high CO content.

The raw gas composition is thus strongly influenced by the feedstock and the technology applied. But for the different feedstocks there are some constraints on the applicability of the various gas generation processes. The catalytic steam reforming technology can only be applied to light hydrocarbon feedstock (up to naphtha) but not for heavy hydrocarbons such as fuel oil or vacuum residue. These raw materials contain a substantial amount of sulfur and also minor quantities of heavy metals, which would poison the sensitive reforming catalyst. In addition cracking reactions will occur on the catalyst, depositing carbon, which not only blocks the catalyst pores but also restricts interparticle flow. Thus for heavy feedstocks the only choice is noncatalytic partial oxidation, which, however, is capable of processing any type of hydrocarbon feedstock. The various commercial coal gasification processes may also be classified as partial oxidations.

4.1.1. Steam Reforming

As the nickel-containing catalysts used in the reforming reaction are sensitive to poisons, any sulfur compounds present in the hydrocarbon feedstock have to be removed by hydrodesulfurization, generally with a combination of cobalt–molybdenum and zinc oxide catalysts [413]–[415]. (Eqs. 38, 39). In a few cases, especially with

a higher sulfur content in the feedstock, for example, in naphtha, nickel–molybdenum catalysts may also be used for the hydrodesulfurization step. Adsorption on activated carbon is an alternative when the feed is natural gas with a rather low sulfur content.

$$R\text{–}SH + H_2 \rightarrow RH + H_2S \quad (38)$$

$$H_2S + ZnO \rightarrow ZnS + H_2O \quad (39)$$

The general overall reaction for the steam reforming of hydrocarbons can be formulated as (40):

$$C_nH_{(2n+2)} + n\,H_2O \rightleftharpoons n\,CO + (2\,n + 1)\,H_2 \quad (40)$$

or more specifically for methane (Eq. 41), usually the major constituent of natural gas, as:

$$CH_4 + H_2O \rightleftharpoons CO + 3\,H_2 \qquad \Delta\,H^0_{298} = +\,206\ \text{kJ/mol} \quad (41)$$

Simultaneous with this equilibrium, the water gas shift reaction (Eq. 37) proceeds, and when this is included we arrive at the formal overall reaction (Eq. 42)

$$CH_4 + 2\,H_2O \rightleftharpoons CO_2 + 4\,H_2 \qquad \Delta\,H^0_{298} = +\,165\ \text{kJ/mol} \quad (42)$$

To introduce nitrogen to achieve the required stoichiometric hydrogen/nitrogen ratio for ammonia synthesis, the reforming reaction is split into two sections. In the first section, the *primary reformer*, the reaction proceeds in indirectly heated tubes filled with nickel-containing reforming catalyst and is controlled to achieve a partial conversion only (in a conventional reformer usually 65 % based on methane feed, leaving around 14 mol % methane in the effluent gas, dry basis). In the following secondary reformer — a refractory-lined vessel filled with nickel catalyst — the gas is mixed with a controlled amount of air introduced through a nozzle (burner). By combustion of a quantity of the gas the temperature is raised sufficiently (to about 1200 °C) that the endothermic reforming reaction is completed with the gas adiabatically passing the catalyst layer. In this way the outlet temperature is lowered to around 1000 °C, and a residual methane content of 0.5 % or lower (dry basis) is attained in conventional plants. Nitrogen already present in the natural gas tends to cause a reduced specific air ratio in the secondary reformer and a reduced secondary reformer temperature rise. Therefore, to maintain the same methane leak, the primary reformer exit temperature must be increased.

4.1.1.1. Thermodynamics, Operation, Pressure, Steam/Carbon Ratio

The steam reforming reaction of methane is endothermic and proceeds with an increase in volume. In Figures 30 and 31 [1487] the relationship between equilibrium methane concentration (a measure for the theoretical possible conversion) and temperature, steam-to-carbon ratio S/C, and reforming pressure are plotted for the range relevant for the reaction in the primary reformer.

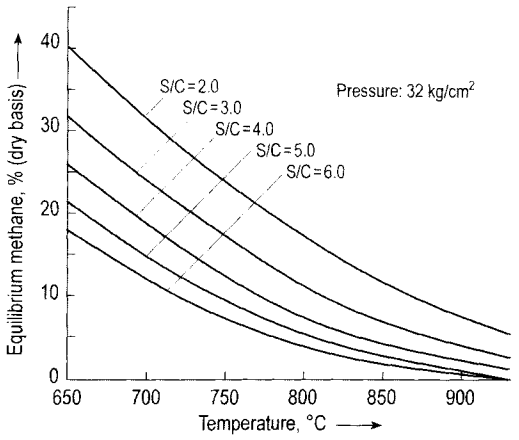

Figure 30. Methane equilibrium versus temperature at various S/C ratios

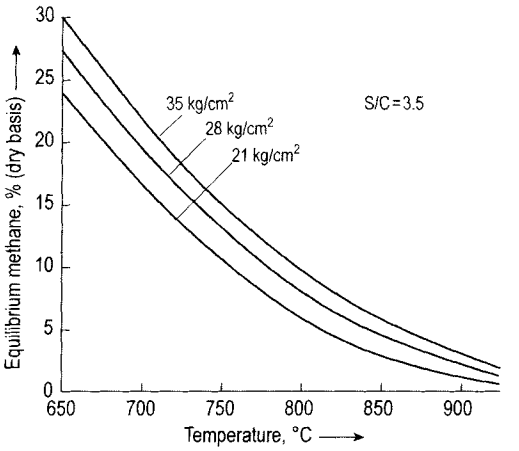

Figure 31. Methane equilibrium versus temperature at pressures

For the industrially interesting range, Equations (43–45) [416] may be used with reasonable approximation, altough they do not include a term for the small temperature dependence of the reaction enthalpy:

$$K_7 = \exp\left[\frac{-27.463}{T} + 30.707\right] \tag{43}$$

$$K_3 = \exp\left[\frac{+4.577}{T} - 4.33\right] < 600\,^{\circ}\mathrm{C} \tag{44}$$

$$K_3 = \exp\left[\frac{+4.084}{T} - 3.765\right] > 600\,^{\circ}\mathrm{C} \tag{45}$$

A table listing the thermodynamic equilibrium methane concentration in the outlet of the primary and secondary reformer over a wide range of operating pressures, outlet temperatures and S/C ratios can be found in [417] (see also [424]).

Because natural gas is usually under elevated pressure and the reforming reaction entails an increase in volume, significant savings in compression energy can be achieved if the process is performed under elevated pressure. But thermodynamically this is unfavorable: on account of the volume increase, an increase in pressure will reduce the conversion of methane. To compensate this, higher temperatures will become necessary (limited by reformer tube material). On the other hand, higher steam-to-carbon (S/C) ratio have a beneficial effect on the equilibrium methane concentration and could to some extent mitigate the negative influence of the increased pressure, but the penalty is a higher energy consumption.

There are additional reasons for applying a higher S/C ratio. First, it prevents carbon deposition on the catalyst, which may not only increase the pressure drop but also reduce the catalyst activity. As the rate of the endothermic reforming reaction is lowerded this way, it can result in local overheating of the reformer tubes (hot bands) and premature failure of the tube walls. Second it provides necessary steam for the shift conversion (Section 4.2). Third, it reduces the risk of carburization of tube material.

In principle carbon formation may occur via the following reactions (Eqs. 46 – 48):

Boudouard reaction:	$2\,CO \leftrightharpoons C + CO_2$	$\Delta H^0_{278} = -172.5$ kJ/mol	(46)
Methane cracking:	$CH_4 \leftrightharpoons C + 2\,H_2$	$\Delta H^0_{278} = +74.9$ kJ/mol	(47)
Carbon monoxide reduction:	$CO + H_2 \leftrightharpoons C + H_2O$	$\Delta H^0_{278} = -131.4$ kJ/mol	(48)

These reactions are reversible, and there is a dynamic equilibrium between carbon formation and removal. Under typical steam reforming conditions, reactions (46) and (48) are carbon – removing, whilst reaction (47) leads to carbon formation in the upper part of the tube [503]. With naphtha as steam reformer feed, irreversible pyrolysis (as in a steam cracker for ethylene production) with the sequence naphtha → olefins → polymers → coke will occur. The mechanism of carbon formation and the determination of the risk areas in the reformer operating conditions on the basis of relevant equilibrium data are discussed in some detail in various publications [362], [363], [418] – [420].

Modern natural gas based plants with a conventional primary reformer use a S/C ratio of around 3.0, compared to values of 3.5 – 4.0 in older installations. Lowerering the S/C ratio means energy saving, and regarding the primary reforming step, the minimum ratio should be theoretically only slightly over 1.0 to avoid cracking. Catalyst experts see the practical limits at 1.5 – 1.7 for methane steam reforming [421], [1487] and 2.2 for naphtha steam reforming. But to supply sufficient steam for the shift conversion step ist has to be at least 2.0 for stoichiometric reasons. An additional safety margin is advisable in case of operational problems with the S/C ratio control and to avoid hydrocarbon formation in the HT shift reaction (a problem which will be discussed later). So in practical operation for conventional reformers (high-duty re-

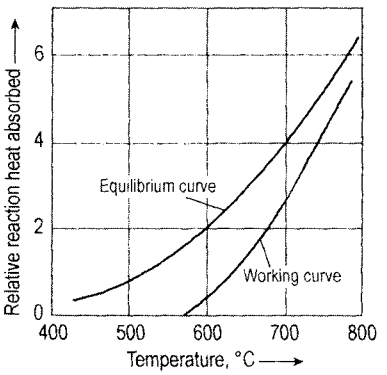

Figure 32. Equilibrium and working curves for reforming

formers) a value of about 3.0 is advisable, whereas in plants with reduced primary reforming (low-duty reformers; Section 4.1.1.6, Table 25) 2.7–2.8 may be sufficient.

4.1.1.2. Mechanisms and Kinetics of Steam Reforming

All steam reforming catalysts in the activated form contain metallic nickel as active component, but the composition and structure of the support and the nickel content differ considerably in the various commercial brands. Thus the theoretical picture is less uniform than for the ammonia synthesis reaction, and the number of scientific publications is much smaller. The literature on steam reforming kinetics published before 1993 is summarized by ROSTRUP-NIELSEN [362], and a more recent review is given by K. KOCHLOEFL [422]. There is a general agreement that the steam reforming reaction is first order with respect to methane, but for the other kinetic parameters the results from experimental investigations differ considerably for various catalysts and reaction conditions studied by a number of researchers.

It is rather difficult to relate data from industrial plants to laboratory experiments. To measure the intrinsic activities, a gradientless microreactor may be well suited, but to obtain kinetic data for the *extrinsic activity* of commercial-size catalyst particles useful for reformer layout, experiments in a pilot plant unit with fullsized reformer tubes are necessary. A numerical approach in which the experimental data are described by a closed analytical expression for the reaction rate is frequently used in reformer simulations. For example, it is possible to calculate the equilibrium gas composition for a given pressure and S/C ratio. Instead of plotting the change in the concentrations versus temperature, the corresponding enthalpy changes can be plotted. In this way we arrive at a equilibrium curve and a working curve, as shown in Figure 32.

As an example for an analytical expression, the formula given by MOE and GERHARD [423] is presented:

$$r = k_2 \left[K_3 p_{CH_4} p_{H_2O}^2 - p_{H_2}^4 p_{CO_2} \right] \tag{49}$$

with

$$k_2 = \exp\left[\frac{35000}{RT} - 7.912\right] \tag{50}$$

K_3 is the equilibrium constant for reaction (42), which is the product of the equilibrium constants for reactions (41) and (37) K_{41} K_{37}. For the ratio CO_2/CO the authors assume only a slight deviation from the equilibrium and use an empirical relation without a kinetic term: $CO_2/CO = f$ (CH_4 conversion, S/C ratio, K_{37}). Other kinetic expressions may be found in [362], [418], [422]. For the reaction mechanism [422] of steam reforming of methane, the following scheme (Eqs. 51–55) was proposed:

$$CH_4 + * \rightleftharpoons CH_2\text{–}* + H_2 \tag{51}$$
$$CH_2\text{–}* + H_2O \rightleftharpoons CO\text{–}* + 2\,H_2 \tag{52}$$
$$CO\text{–}* \rightleftharpoons CO + * \tag{53}$$
$$H_2O + * \rightleftharpoons O\text{–}* + H_2 \tag{54}$$
$$CO + O\text{–}* \rightleftharpoons CO_2 \tag{55}$$

From an interpretation of the kinetic measurements, it was assumed that the surface reaction (52) should be the rate-determining step. But the validity of this mechanism is questioned by some authors [362]. Based on extensive studies using nickel/magnesium/aluminium spinel catalyst, XU and FROMENT [1489] suggested a modification of the reaction scheme. According to this, H_2O reacts with surface Ni atoms to give adsorbed oxygen and gaseous hydrogen. Methane stepwise dissociatively adsorbed on Ni surface atoms, and the radicals formed in this way react with the adsorbed oxygen to finally yield gaseous CO and H_2.

In the extrinsic reaction rate, mass transfer plays a dominant role. The combined effect of the molecular diffusion of the reactants from the bulk gas through the gas film around a catalyst particle to the geometrical surface of the particle, and to some extent the Knudsen diffusion within the catalyst pores, are the limiting factors. As the intrinsic reaction is fast, the reactants will have reacted before they travel down the lenght of the pore. The effectivity of a steam reforming catalyst, that is, how much of the catalyst particle is utilized, varies with the reaction conditions and is only about 1 % at the exit. Because of this, the apparent activity increases with decreasing particle size, and the geometrical shape of the catalyst particle also has a distinct influence (Section 4.1.1.3).

Ethane, propane, and butane, usually present in smaller concentrations in addition to methane in most natural gases, react in the steam reforming in similar way, with the overall reaction corresponding to Equation (35). With higher hydrocarbons, as contained in naphtha, the reaction is more complex. Higher paraffins in naphtha feed will be first completely cracked down in a methane-forming reaction, which proceeds between 400 and 600 °C and could be described, for example, as follows (Eq. 56):

$$C_nH_{2n+2} + (n-1)/2\,H_2O \rightarrow (3n+1)/4\,CH_4 + (n-1)/4\,CO_2 \tag{56}$$

Table 23. Enthalpy of the naphtha/steam reaction for different reaction conditions

Temp., °C	S/C ratio	Pressure, bar	Stoichiometry	ΔH^0_{298} kJ/mol $CH_{2.2}$
450	2.0	31.5	$CH_{2.2} + H_2O \rightarrow 0.75\,CH_4 + 0.25\,CO_2 + 0.1\,H_2$	−41.7
750	3.0	28	$CH_{2.2} + 3\,H_2O$ $0.35\,CH_4 + 0.25\,CO + 0.4\,CO_2 + 1.45\,H_2 + 1.95\,H_2O$	+74.9
800	3.0	21	$CH_{2.2} + 3\,H_2O$ $0.2\,CH_4 + 0.4\,CO + 0.4\,CO_2 + 1.9\,H_2 + 1.8\,H_2O$	+102.6

Other equations, which contain CO and/or hydrogen as well, may be formulated, too. That a methanation reaction occurs is already obvious from the fact that the reaction product contains more methane than the naphtha feed and that the equilibrium conversion of the hydrocarbon in a direct reforming reaction according to equation (40) is lower than in reaction (56) at low temperature. The reaction of aromatic is principally similar but with higher risk of carbon formation.

$$C_nH_{2n+2} + n\,H_2O \rightarrow n\,CO + (2\,n+1)\,H_2 \qquad (40)$$

With rising temperature, reaction (40) becomes thermodynamically more favorable, for example, for *n*-heptane beyond about 620 °C [424]. The exothermic methanation reaction proceeds in the cooler entrance part of the reformer tubes, followed by the endothermic steam reforming reaction of the methane in the hotter part. Depending on the methane range and S/C ratio, the overall reaction of naphtha changes from exothermic (methanization) to endothermic (reforming to carbon oxides), as shown in Table 23 [425]:

The above reactions proceed also in the so-called rich-gas processes of British Gas and Lurgi/BASF, which convert naphtha with steam in autothermal reactions in a vessel filled with a special nickel-containing catalyst. It was formerly successfully used for town gas production from naphtha. This reaction may also used as pre-reformer ahead of a conventional tubular steam reforming furnace to convert higher hydrocarbons at low temperature and low S/C ratio into a methane reach gas which can than be reformed in the primary reformer with a standard methane reforming catalyst instead of an alkalized catalyst (Section 4.1.1.3.1).

For literature up to 1971, see also [426].

4.1.1.3. Reforming Catalysts

4.1.1.3.1. Primary Reformer Catalysts

In the tubular furnace of the steam reforming section, two elements are extremely important for performance; the catalyst activity and heat transfer through the walls of the reformer tubes, which strongly influence each other. Because of problems with both in the early days, catalyst makers blamed contractors for using excessive heat fluxes, which caused deterioration of the catalysts by sintering and chemical changes. For contractors and tube manufacturers, on the other hand, the culprit was the insufficient

thermal stability of the catalyst. Of course, the reality was more complex, and there were many and diverse causes for the problems experienced with both tubes and catalysts. There have been considerable improvements in both catalysts and in tube materials and manufacturing techniques over the years, and today problems and failures in this area are more operational than technological in this origin.

The active component of the primary reformer catalyst is nickel, which is finely dispersed over the support material as crystallites produced by reduction of nickel oxide. The nickel oxide content of unreduced catalyst is between 15 and 25 %.

A good primary reforming catalyst should meet the following requirements:

it should have the desired conversion of the hydrocarbon feed at the lowest possible tube wall temperature and the lowest possible pressure drop without forming carbon; have reasonable service life without deactivation (lifetime should at least be equal to turnaround intervals); withstand extraordinary conditions during start-up and shut-down; and, if possible, have the stability to withstand in situ regeneration procedures to eliminate the effects of incidental poisoning or carbon deposition. Today this profile can be largely fulfilled by all leading catalyst producers.

Two main factors influence catalyst activity: chemical composition and surface area. But of no less importance for the performance are the heat transfer characteristics, which are governed by the size and shape of the particles.

Support materials are α-alumina, calcium aluminate, and magnesia – alumina spinel, and different procedures are used in manufacturing. In one procedure, nickel is first precipitated, usually as its hydroxide, in the presence of a suitable dispersion component. After washing, drying, and calcining the oxide, the powder is mixed with an hydraulic cement, formed into particles and subjected to the appropriate treatment to give full hydraulic bonding of the cement. The nickel oxide is thus evenly dispersed throughout the lattice structure of the cement support.

The reduction process takes longer, and there is a greater degree of shrinkage than with the other type of catalyst, based on a prefabricated support. In this preparation procedure, the support pellets are impregnated with a nickel salt solution and dried, after which they are calcined to transform the nickel salt into the oxide. The surface area of the catalyst produced in this manner depends largely on the degree of firing of the support. With increasing temperature, the surface area decreases but the mechanical stability increases. Thus there is a trade-off between activity and strength. α-*Alumina* is now the predominant support for natural gas feedstocks in North America, but is increasingly used in other parts of the world, too. *Calcium aluminate* is still used worldwide on account of its natural alkalinity, which helps to suppress carbon deposition. It is therefore preferred for the manufacture of naphtha steam reforming catalysts. Catalysts intended for dealing with higher hydrocarbons are alkalized with potash – a development first introduced by ICI [427] – to avoid carbon formation (see Section 4.1.1.1) by cracking, which is acid-catalyzed (Eq. 57).

$$C_xH_y \rightarrow x\,C + y/2\,H_2 \qquad (57)$$

Alkalization suppresses acidic spots on the surface of the catalyst and also promotes the reactions (Section 4.1.1.1) which remove deposited carbon from the catalyst surface. It is also advisable when processing natural gas which contains C_{4+} hydrocarbons to fill the first third of the tube, where the highest heat flux occurs, with alkalized reforming catalyst.

Magnesium aluminate, the preferred support of one catalyst supplier, has a larger specific surface area. But this material must be calcined to a higher temperature during manufacture of the support particles to ensure it contains no free magnesium oxide, which would be hydrated to hydroxide at temperatures below 300 °C. This chemical change results in a volume increase, which would destroy the structure and impair the mechanical stability of the catalyst.

The various support materials have different effects on potential carbon formation. This seems to go in parallel with the Lewis/Brønsted acidity. The main commercially used catalyst supports can be ranked as follows in decreasing order of carbon forming tendency (and thus in decreasing order of the important minimum practical steam/carbon ratio): α-alumina > magnesium aluminate (spinel) > calcium aluminate > alkalized calcium aluminate [419].

Also important is the effect of the size and shape of the catalysts [428] on heat transfer and consequently performance. Unlike the most processes carried out under substantially adiabatic conditions, the endothermic steam reforming reaction in the tubes of the primary reformer has to be supplied continuously with heat as the gas passes through the catalyst. The strong dependency of the reaction rate on the surface temperature of the catalyst clearly underlines the need for efficient heat transfer over the whole length and crosssection of the catalyst. However, the catalyst material itself is a very poor conductor and does not transfer heat to any significant extent. Therefore, the main mechanism of heat transfer from the inner tube wall to the gas is convection, and its efficiency will depend on how well the gas flow is distributed in the catalyst bed. It is thus evident that the geometry of the catalyst particles is important.

To make full use of the enhanced activity attainable by increasing the internal surface area of the catalyst, the heat transfer characteristics (shape) have to be improved, too. Obviously both are strongly interrelated. If the catalyst of higher activity with an improved heat transfer characteristic is installed in a given reformer and the firing conditions are kept as before, the peak skin temperatures of the reformer tube will be reduced. If, on the other hand, the previous tube wall peak temperature is maintained, a higher throughput is possible. Figure 33 shows in a schematic manner the individual effects of surface and heat transfer characteristics.

Various catalyst shapes have been developed by the individual catalyst manufacturers and have progressively replaced Raschig rings, which themselves once displaced simple tablets. The shaped catalysts are applied especially in the high heatflux zone in the upper third of the tube; in the lower end of the tube there would be no significant difference between their performance and that of traditional sizes and shapes, apart from a certain reduction in the pressure drop. Examples are: a four-hole type (ICI

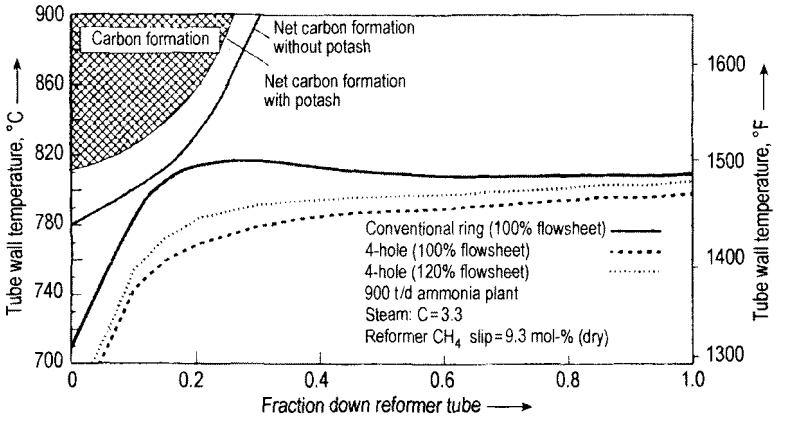

Figure 33. Shaped catalyst (ICI Katalco 4–Hole) in a top-fired primary reformer

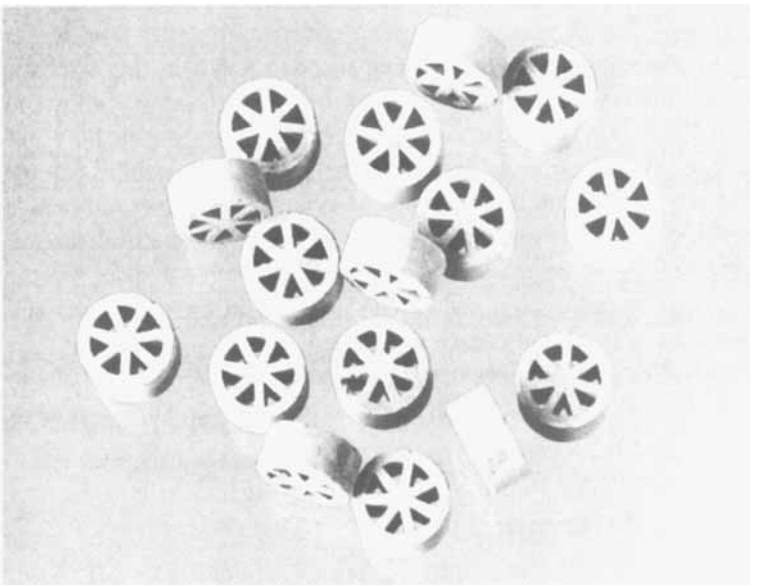

Figure 34. "Wagon Wheel" primary reforming catalyst (UCI)

Katalco), a six-shooter configuration (Topsøe), and a wagon-wheel shape (United Catalysts Inc.; Fig. 34).

Important in the catalyst loading procedure is to avoid breaking and also bridging, especially with the new forms. The latter occurs when catalysts particles, instead of packing down closely, become wedged together across the tube, leaving voids. This can lead to overheating of the reformer tubes, which may be viewed through the furnace box peep holes as hot spots or, in extreme cases, as hot bands on the tube skin. Special packing techniques have developed therefore, e.g., Unidense [429].

Catalyst makers also succeeded in minimizing the activity reducing effect of the potassium in the alkalized catalysts [430]. Pre-reduced primary reforming catalysts are now also marketed (ICI Katalco, Topsøe) [430], and splitloading of reformer tubes with more than one type of catalyst has now become very common. The benefitial effects concern pressure drop at increased plant load, carbon formation potential, catalyst activity, catalyst cost, and desired catalyst life. For example, a reformer tube may be loaded with 15 % alkali-free catalyst in pre-reduced form (top-section), 25 % unreduced alkali-promoted (middle section) and 60 % alkali-free unreduced catalyst (bottom section).

4.1.1.3.2. Secondary Reformer Catalyst

The secondary reforming catalyst was traditionally applied in the form of Raschig rings for the bulk and solid tables for the top layer. In comparison with primary reforming catalyst, the nickel content is lower (5 – 10 % vs. 15 – 25 %). This, along with higher sintering rates due to the higher temperatures, accounts for the lower activity, which is only 5 – 10 % of that of primary reforming catalyst. For some time it was thought that there would be no advantage in using shaped catalyst in this adiabatic type of reforming and that it would probably also not be stable enough to withstand the mechanical and thermal shock of starting and stopping the process air flow. But catalyst manufacturers have meanwhile increased the mechanical stability of the shaped catalysts to such an extent that, even in a secondary reformer, advantage can be taken of the higher activity resulting from the increased geometrical surface, allowing the catalyst volume to be reduced. This provides additional space for the gas – gas mixing zone above the catalyst bed (Section 4.1.1.5) in existing plants and avoids a costly modification in case of capacity increase.

Some contractors and catalyst vendors use target bricks instead of inert balls to protect the top layer of the catalyst, while others have no protection at all. The catalyst lifetime is usually in excess of six years.

4.1.1.4. Primary Reformer

This process unit consists of a multitude of parallel tubes loaded with the nickel catalyst (Section 4.1.1.3.1) in a furnace box in which the heat needed for the reaction is transferred to the tubes by radiation. The heat is generated in burners, generally gas-fired, in the furnace box. According to the disposition of the burners, primary reformers can be classified as top-fired, side fired, terraced-wall, or, less common, bottom-fired reformers. The furnace box is connected to a convection bank in which the heat content of the flue gas is used for various process duties, e.g., preheating of the process air for the secondary reformer, preheating of steam/hydrocarbon feed, steam superheating, and preheating of combustion air. Quite a number of variables have to be considered to arrive at an effective and reliable reformer design at reasonable cost. A special consideration is the lifetime of the expensive *reformer tubes*, made of highly

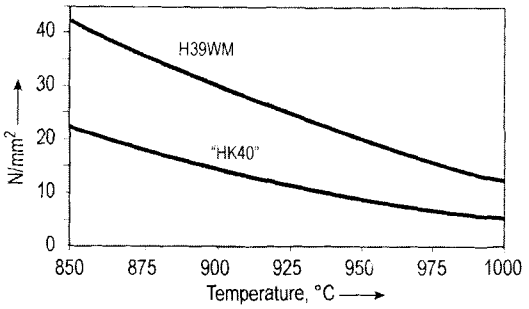

Figure 35. Mean 100 000-hour stress rupture values vs. temperature for HK 40 and micro alloy material.

alloyed chromium–nickel steel by centrifugal casting. A very important issue in this context is the *primary reformer* catalyst with respect to activity, service life, and heat transfer and pressure drop characteristics.

4.1.1.4.1. Reformer Tubes

Under the severe reaction conditions the tube material exhibits creep which finally leads to rupture. Thus, reformer tubes have limited service life. The time to rupture for a specific material depends on the tube-wall temperature and on the internal pressure. This limits the reforming pressure, which to save energy in synthesis-gas compression should be as high as possible. As the reforming reaction is endothermic and proceeds with a volume increase, the negatice effect of a pressure increase (lower conversion) has to be compensated by a higher reaction temperature and hence higher wall temperatures, but this is limited by the material. Another possibility for compensation is a higher steam surplus (steam/carbon ratio), but this is economically unfavorable. The furnace box usually accomodates 200–400 tubes (depending on plant capacity and reformer concept), 10–13 m long, with an inner diameter of 75–140 mm and a wall thickness of 11–18 mm.

The "creep rupture data" are derived from laboratory tests on material samples having a standardized geometrical form. The convenient way to express these data is to plot the stress versus the Larson–Miller parameter P:

$$P = T\,(\log t + K)\,1000 \tag{58}$$

Where T = material temperature, t = time to rupture, and K = a material-dependent constant.

Using these data the reformer tubes are usually designed for an expected lifetime of 100 000 h. For practical purposes plots of rupture stress versus temperature are used with the time to rupture as parameter, which in the example of Figure 35 is set as 100 000 hours lifetime.

The standard tube material for a long time was HK 40 (20 Ni/25Cr) but for replacements and new plants, HP modified (32–35Ni/23–27Cr stabilized with about 1.5% Nb) is being increasingly used on account of its superior high-temperature properties [431]. The high creep-resistance of this material is attributable to heat-stable

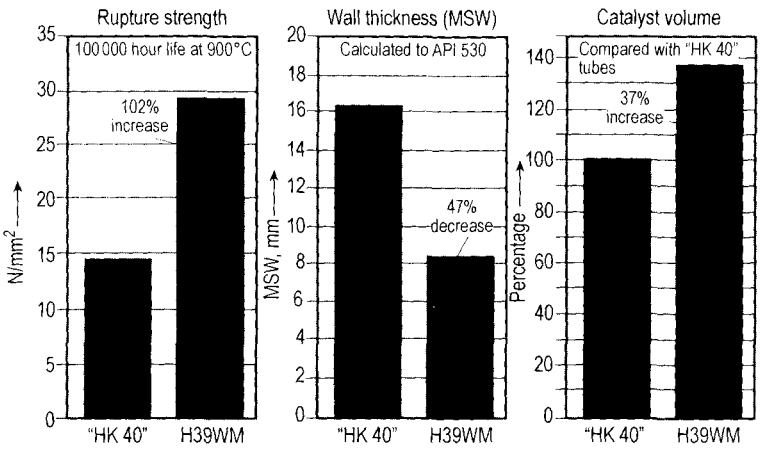

Figure 36. Benefits of Micro Alloy in reformer operation

complex chromium–niobium carbides. Generally the strength of these high-temperature alloys appears to be related to the low solubility of carbon in a highly-nickel matrix. This leads to crystallization of carbides on the grain boundaries. It is assumed that these carbides hinder the intergranular dislocations observed microscopically, which, macroscopically, translate to the well known phenomenon of creep. With HP modified, high-duty reformers with outlet pressures as high as 43 bar are in operation.

Recently a new-generation tube material has emerged, called Micro Alloy [1490]–[1493]. This contains not only niobium but also titanium and zirconium (or lanthanum), and has improved creep rupture strength still further. Table 24 shows the chemical composition of the tube materials.

The enhanced materials are equally useful in revamping older plants. Because they are inherently stronger, it is possible to retube the furnace with thinner tubes.

For the same outer diameter, the inner diameter and, therefore, the capacity of the tube can be increased. Thus more catalyst can be accomodated within a tube of a given outer diameter and, particularly when an optimized catalyst is used with improved packing and heat transfer properties, throughput is increased at (possibly) lower pressure drop than before retubing. Figure 36, demonstrates this by comparing HK 40 with Micro Alloy material.

4.1.1.4.2. Furnace Design and Layout

The layout of a primary reformer furnace is a complex task in which a number of parameters have to be well balanced. Two aspects have to be considered; the heat-consuming reaction of the hydrocarbon with the steam inside the tubes and the heat supply by radiation from the outside. The objective is to match both properly with respect to the desired conversion of the hydrocarbon at an economic steam/carbon

Table 24. Chemical composition of reformer tube alloys

Grade	Ni	Cr	Mn	Si	Nb	Ti/Zr	Mo	C	P	S
A 698 HK 40	19–22	23–27	≤ 1.5	0.5–2.0	-	-	≤ 0.5	0.35–0.45	≤ 0.04	≤ 0.04
HP modified	32–35	23–27	≤ 1.5	≤ 1.5	≤ 1.5	-		0.35–0.45	≤ 0.03	≤ 0.03
Micro Alloy	33–37	23–27	≤ 1.5	1.5–2.0	0.7–1.5	+	≤ 0.5	0.4–0.5	≤ 0.03	≤ 0.03

ratio and with a reasonable tube wall temperature profile. The progress of the reforming reaction along the tube, which determines the amount of heat needed at each location and the amount of radiation supplied from the outside, results in a specific tube wall temperature profile. For the purpose of determining the required creep rupture strength to achieve the selected lifetime, the peak temperature is used.

For example, general equations which define a two-dimensional heat transfer model are given in [432]. These were succesfully used in calculating, the temperature profiles of reactant temperature, outside tube wall temperature, and flue gas as a function of tube length. The progress of the reaction inside the tubes is described by selection of appropriate kinetic data for the catalyst used. As already mentioned, diagrams which give the enthalpy change of the reactants versus the feed as a function of temperature are used. These curves present the experimental data gained from a full-sized one-tube pilot plant in a useful form. They are especially suitable for the kinetics of naphtha steam reforming, which are difficult describe with closed mathematical expressions. The radiating heat flux around the tubes is not uniform around the tube circumference, and allowance has to be made in the calculations for the horizontal flux distribution. Calculations for top-fired reformers, for example, show that the outside tube rows absorb more heat than inner rows, which is compensated by allowing a higher mass flow in the outer rows. In the design the axial heat flux can be manipulated by varying the reformer configuration. The flux distribution around the individual tubes results from the furnace geometry (box dimension and row distance for example) and the ratio of tube diameter and pitch. Crucial factors in the design are also the internal heat transfer coefficient [433]–[436] and the pressure drop [437], [438].

Today contractors and licensors use sophisticated computerized mathematical models which take into account the many variables involved in the physical, chemical, geometrical and mechanical properties of the system. ICI, for example, was one of the first to develop a very versatile and effective model of the primary reformer. The program REFORM [361], [430], [439] can simulate all major types of reformers (see below): top-fired, side-fired, terraced-wall, concentric round configurations, the exchanger reformers (GHR, for example), and so on. The program is based on reaction kinetics, correlations with experimental heat transfer data, pressure drop functions, advanced furnace calculation methods, and a kinetic model of carbon formation [419], [439].

Furnace calculations are usually performed according to the method of RÖSLER [440] with numerical methods which allow a three-dimensional simulation. A furnace model in three dimensions takes into account, for example, the shielding effect by adjacent tubes, which may cause circumferential variations in the wall temperature of individual tubes. Another contributing factor to be modeled is the heat release pattern of the burner flames. Additional information on mathematical treatment of radiation is given in [441]–[443].

Usually the number, diameter, and length of the tubes are first tentatively chosen on basis of capacity and pressure drop considerations. These quantities are then optimized in an iterative procedure that adjusts all the interdependent design features. For

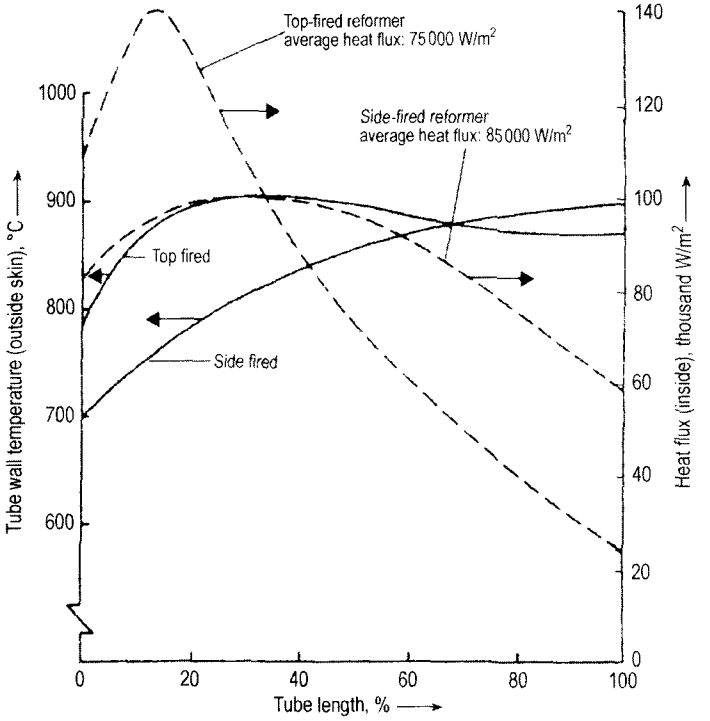

Figure 37. Tube wall temperature and heat flux profiles for top-fired and side-fired configurations.

example, in a top-fired furnace the distance between the rows has a strong influence on peak wall temperature and on the size of the furnace box and consequently on the investment cost. There is also a considerable effect of the tube pitch and tube diameter on the tube skin temperature. The same situation for heat flux was already mentioned above. Tube length is important for the radiant efficiency of the reformer box. On the other side of the optimization puzzle are the investment costs, mainly influenced by the reformer tube price and the size of the furnace box. Designing for a very high heat flux will reduce the dimensions and consequently the investment cost, but at the expense of operational reliability, whereas a more conservative furnace layout is more likely to assure a lengthy trouble-free operation. Ultimately, the design of an industrial tubular steam reformer is a compromise between economics and technical feasibility. As a rule of thumb for the interrelation of space velocity SV, average heatflux q_{av} and tube diameter d_t formula $q_{av} \cong d_t \cdot \mathrm{SV}$ is proposed in [444].

In many modern top-fired reformers the heat flux calculated for the inner tube wall surface is around 60 000 W/m^2, although in some designs it cam be as high as 75 000 W/m^2. The maximum heat flux may be 1.4 to 2 times higher. In side-fired and terraced-wall furnaces, where the mean fluxes are generally in the range of 60 000 – 85 000 W/m^2, the difference between mean and maximum flux is much smaller, as shown in Figure 37 [444].

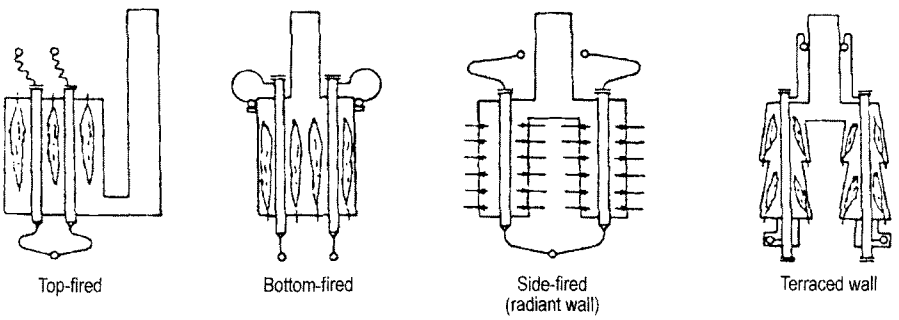

Figure 38. Primary reformer configurations.

Principally, a good design should reach the projected lifetime of 100 000 hours for the tubes, but this is only one side of the coin, the other being the actual operation of the furnace, which may not always be according to the design parameters. Influences which may shorten the service life are catalyst poisoning, loss of steam, thermal shock, overfiring in fast start-up procedures and condensation in hot tubes (e.g., water carry-over). Any loss of catalyst activity (poisoning) reduces the reaction rate and the heat absorption rate. The tube wall temperature in the affected part of the tube stabilizes at a higher level than originally designed. This leads to hot bands or hot spots, which can also result from improper catalyst loading, in which bridging of pellets leads to voids. A very important influence on actual tube life is thermal cycling, that is, how often the tubes are heated up and cooled down in combination with pressure changes. The cumulative effect of these cycles can be very damaging and leads to accelerated creep. Tubes with a thicker wall (e.g., 17 mm for 100 mm tubes) are less tolerant in this respect than those with thinner walls. The advanced tube alloys have reduced this problem to some extent. A good discussion of failure mechanisms and tube changing policy is given in [445].

4.1.1.4.3. Reformer Types, Burner Disposition, Mechanical Features

The arrangement of burnes is the criterium by which reformer designs are normally classified. The different possibilities are shown in Figure 38 [421].

Their thermal efficiency is not very different and in a top-fired furnace can be as high as 95 %. The enthalpy difference between inlet and exit, often referred to as reformer duty, is made up of the heat required to raise the temperature to the level at the tube exit and the enthalpy of the reforming reaction. In a typical tubular steam reforming furnace, about 50 % of the heat generated by combustion of fuel in the burners is transferred through the reformer tube walls and absorbed by the process gas (in a conventional ammonia plant primary reformer: 60 % for reaction, 40 % for temperature increase).

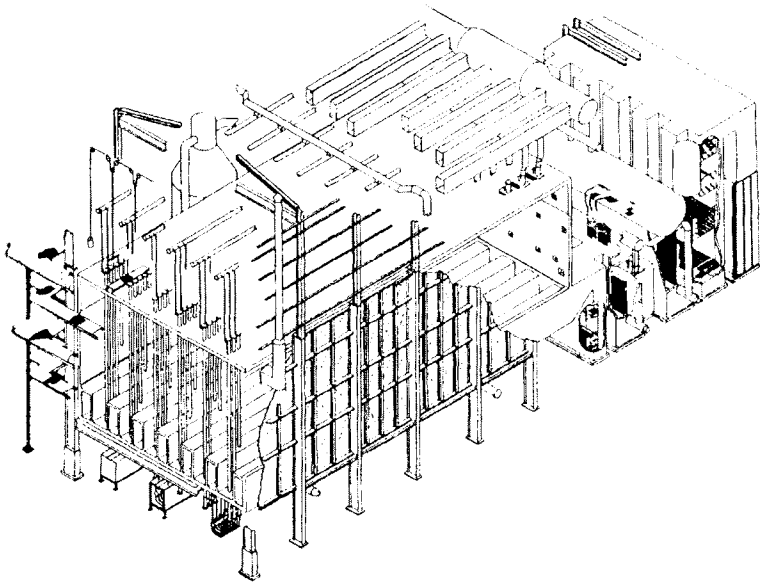

Figure 39. Example of a top-fired reformer

Top-fired reformers are preferred for large capacities. It is possible to accommodate 600 to 1000 tubes is one radiant box. Very large furnaces for methanol plants, in which there is mostly no secondary reformer and the furnace bears the whole reforming duty, have been built by various companies. Top-fired reformers in world-scale ammonia plants usually have between 300 and 400 tubes. The sytem has several advantages:

- Firing occurs only on one level, so the number of burners in relation to the number of tubes is smaller than in side-fired systems. This simplifies distribution piping for fuel gas and preheated combustion air, which is nowadays standard in all efficient plants.
- The radiation efficiency is higher than in other designs.
- The burners are located close to the "cold" inlet of the feed/steam mixture, which is where the strongest heating is needed.
- Less structural steel is needed.

However, the heat input is adjustable only to a limited degree. Figure 39 presents a sketch of a top-fired reformer [446].

In the **side-fired reformers** the burners are located in the wall, and the box accomodates one or two rows of tubes, which receive their heat mainly by radiation from the walls of the furnace box. This is claimed to provide a very uniform heat distribution, which may additionally be adjusted by control of the individual burners. The larger number of burners makes fuel and preheated combustion air distribution more complicated and more expensive. As the heigth and width of the reformer are fixed by the radiation geometry of the tubes and furnace box walls, it is only possible to

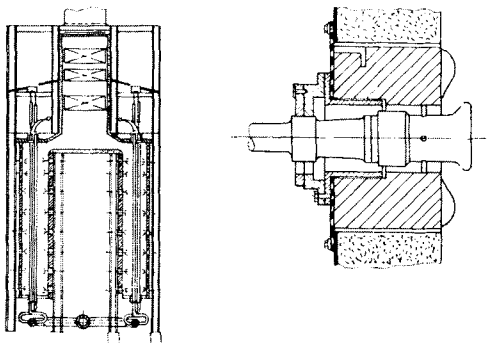

Figure 40. Example of a side-fired reformer. A) Left: Crosssection; B) Right: Radiation burner located in the side wall

extend the reformer lengthwise to accomodate more tubes. This limits it to 100 – 150 tubes, after which multiple radiant boxes becomes necessary. Therefore, this system seems to be more suited to smaller capacities or for low-severity reforming (reduced primary reformer) in a larger plant, as is the case in the Braun Purifier process or in the ICI AMV process. The maximum wall temperature is at the tube outlet, whereas the maximum heat flux is at relatively low temperature. The radiation efficiency is lower than in the top-fired system. It was mentioned [444] that the lower residence times in the flames of a side wall fired furnace could favor lower NO_x values in the flue gas. Figure 40 is an example for an side-fired reformer [426].

Bottom-fired furnaces are not very common in modern ammonia plants. They have a rather constant heat flux profile along the tube with high metal temperatures on the outlet side. Examples are the Exxon reformer and the old Chemico round furnaces.

The **terraced-wall type,** developed by Foster Wheeler may be regarded as an intermediate between the side-fired and bottom-fired tubes. The reformer has inclined walls with several terraces on which upward firing burners are installed. This unique burner positioning makes it possible to adjust the heat flux in each zone. Figure 41 is a schematic drawing of the Foster Wheeler terraced-wall furnace [426].

Apart from this principle question of choosing the reformer type, detailed mechanical design questions are important. The axial load of the weight of the tube and the catalyst has to be balanced by counterweights or spring hangers, designed to allow for the thermal expansion of the tubes. Proper design and adjustment is necessary to avoid tube bending during thermal expansion. For the connection to the feed headers flexible tube connections, commonly called "inlet pigtails", are used. For the connection to the outlet headers, contractors use different approaches. For example ICI, Jacobs (formerly Humphreys and Glasgow) and others use for their conventional furnaces a pigtail design, as shown in Figure 42.

Other designs use stiff connections between the tube outlet and the header. The *M. W. Kellogg reformer,* used in more than 140 reformers, uses the concept shown in Figure 43 [446]. The tubes of each row are welded to a horizontal header located inside the fire box between the flue gas tunnels. With equal numbers of tubes on both sides, a central riser connects the tube harp to the water-cooled transfer line on the top of the firebox. The tubes are suspended by spring hangers.

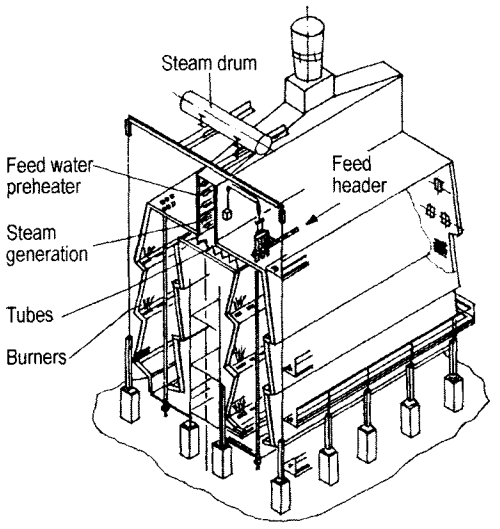

Figure 41. Example of a terraced-wall reformer (Foster Wheeler)

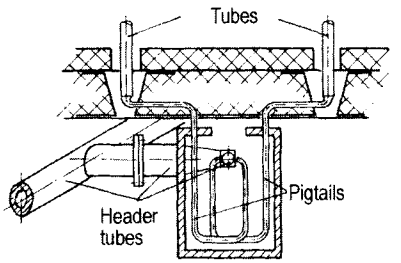

Figure 42. Reformer outlet pigtails [426]

In the *Uhde reformer* the tubes are rigidly connected to the header outside the fire box, as shown in Figure 44 [447]. Differences between the various outlet designs with respect to the amount of repair work (e.g., for isolation of a failed tube) are discussed in [404].

The skin temperature of lined connections, especially the transfer line between primary reformer and secondary reformer, have to be monitored to detect possible defects of the lining. In an extreme case such defects could lead to material overheating with dangerous consequences. Higher skin temperatures will also cause uncontrolled expansion stresses of these lines. A low silica content in the refractory material (and also in the reforming catalyst) is required to avoid plugging of downstream equipment by silica migration. This is especially important after the secondary reformer because of the higher process gas temperature. The refractory insulation, sometimes internally protected by a metallic shroud, is dimensioned to keep the skin temperature at 150–200 °C. With a diameter of around 1000 mm and a length of sometimes 25 m, these wall temperatures may lead to considerable expansions, which have to be mastered by appropriate flexibility of design (carefully selected fix points and bows), suspensions which allow sliding, and counterweights. For insulation of the fire box

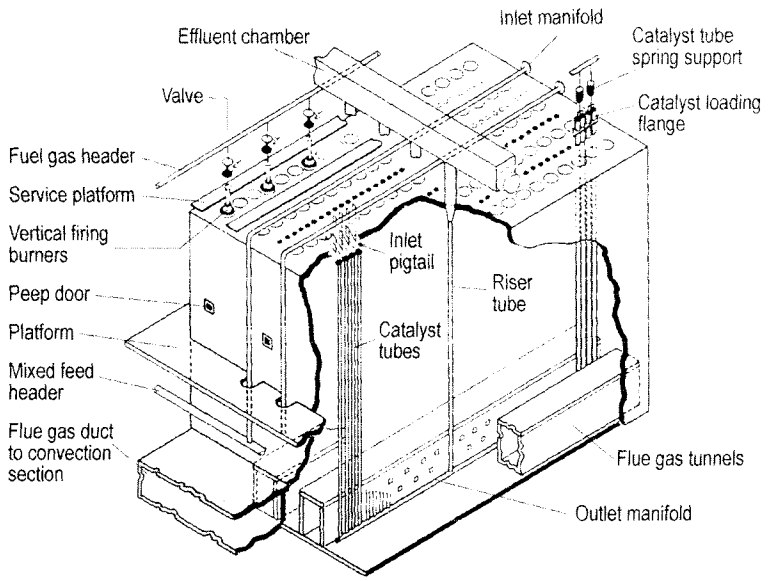

Figure 43. The Kellogg reformer

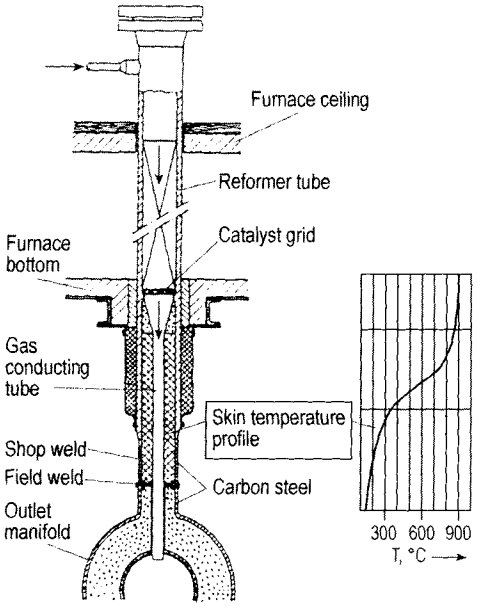

Figure 44. Reformer tube to manifold connection in the Uhde reformer

walls mostly heat-resistant bricks are used, but more recently ceramic mats are favored for this purpose as less labor is required to install them.

In top-fired reformers the hot flue gas – in most cases at a temperature of around 1000 °C – is withdrawn at the bottom of the reformer through tunnels (Figure 45) made

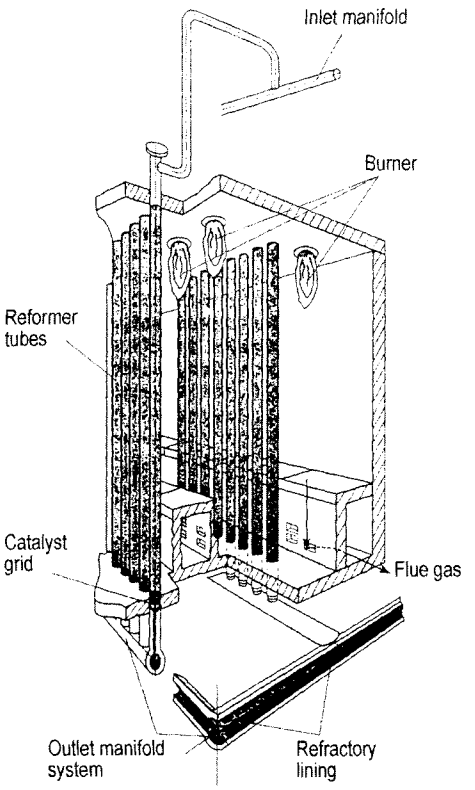

Figure 45. Example for the tunnels and transferline arrangement (Uhde reformer)

of brickwork. Proper dimensioning and positioning of the entrance openings to the tunnels is necessary to avoid an uneven flow profile in the furnace. In side-fired and terraced-wall reformers, the flue gas from the parallel radiant boxes is withdrawn at the top and fed to a common convection section.

The heat is used for the various process duties as shown in the example of Figure 46 (top-fired furnace).

4.1.1.5. Secondary Reformer

As already mentioned, in this process unit the nitrogen for ammonia synthesis is introduced and the reforming reaction is completed down to a very low methane content. Figure 47 shows the principal configuration of a secondary reformer.

Air compressed to the operating pressure is injected through a mixing device (burner) with high velocity (e.g., up to 100 m/s) into the hot effluent of the primary reformer, which is at lower velocity (around 15 m/s). The turbulence resulting from the differing velocities and densities of the gases effects the mixing process. As the process gas is above its auto-ignition temperature, ignition occurs as the two streams mix. Both

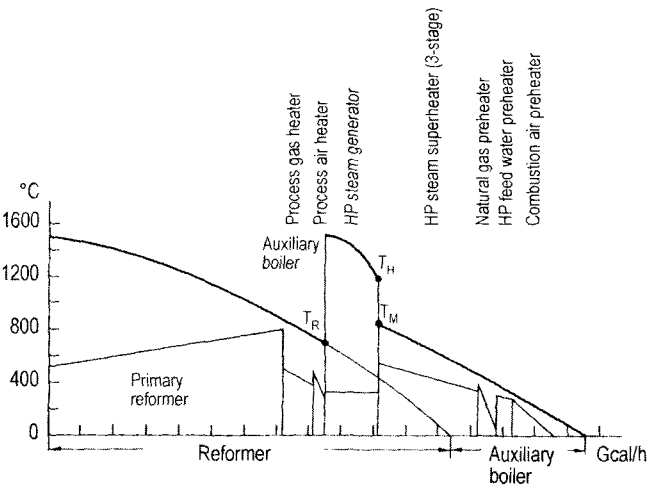

Figure 46. Example of the heat recovery in teh convection section (top-fired furnace, plant with auxiliary boiler)

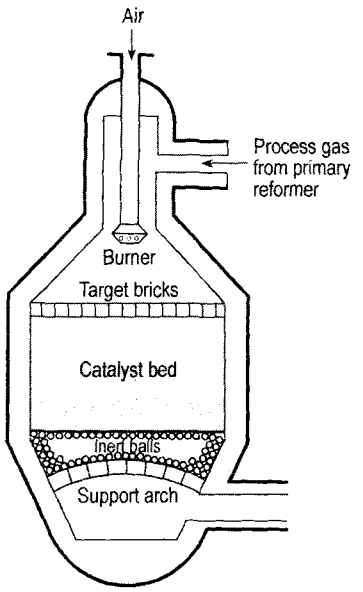

Figure 47. Typical secondary reformer [448]

the combustion section and the catalyst section determine overall performance of the reactor. In contrast to standard combustion process, fuel is in excess of the oxidant. Generally, only 20% of the process gas is burnt to heat the remaining 80% to the required temperature for the adiabatical reforming reaction on the catalyst. Essential point is to produce an evenly mixed gas stream for entry into the catalyst bed, and the combustion zone with its very high temperature should be suitably distant from the walls of the vessel; this is achieved by appropriate geometry of the burner and vessel. Catalyst activity and catalyst bed dimensions should be sufficient to attain a close approach to equilibrium.

In the last few years, licensors and contractors [444], [448]–[454], have made substantial efforts to develop improved designs for burners and combustion chambers. Worthy of mention are especially those which could cope with the more severe conditions that arise when using higher air-preheating temperatures or oxygen-enriched air, as in some designs. Even more extreme conditions exist in secondary reformers operated with pure oxygen instead of air, which are installed in some methanol and hydrogen plants.

Sucessful simulations have been performed with computerized fluid dynamics programs (CFD), based on the fundamental Navier–Stokes equations, with appropriate volume element grids and/or a finite elemet approach, and in some cases were backed up by isothermal physical modeling (hydraulic modeling) experiments [455]. Examples for the CFD software used are FLUENT (Fluent Inc.) [450] and CFDS-FLOW3D [456] and others, usually modified by the contractor or licensor [448] to adapt them to the conditions in a secondary reformer. Discussion of simulation with CFD can be found in [444], [448], [449].

4.1.1.6. Reduced Primary Reforming

The reformer furnace and flue gas duct are the dominaring structures in every steam reforming ammonia plant and represent about 25 % of the total investment cost. For this reason some modern concepts have reduced the size of the primary reformer by shifting part of the primary reformer duty to the secondary reformer. This is achieved by introducing more air into the secondary reformer, exceeding the quantity which is needed eventually to produce a 3:1 H_2:N_2 ratio in the synthesis makeup gas, and then rejecting the surplus of nitrogen at a subsequent process stage. An example for this approach is the Brown & Roots Braun Purifier Process in which the excess of nitrogen is removed together with methane and argon in a cyrogenic condensation system, called *Purifier*, downstream of the methanator. The *ICI AMV process* uses a similar principle and passes a nonstoichiometric synthesis gas (H_2:N_2 = 2.5:1) through the loop. The surplus is rejected in the hydrogen recovery stage by using a larger than normal purge-gas flow. The reduction in size of the reforming section can be considerable as may be seen from Table 25.

An incidental benefit of reducing the primary reformer load in this way is that the NO_x emission is reduced because less firing is required, which produces a lower flue gas quantity.

Some companies (for example, Jacobs, Foster–Wheeler, and Lurgi) have gone so far as to propose bypassing some of the natural gas around the primary reformer and feeding it straight to the secondary reformer, which then operates as a quasi-autothermal reformer.

Table 25. Primary reforming: Convential versus Reduced (low duty)

	Conventional	Reduced
Primary reformer		
Steam/carbon ratio	3.0	2.7
Exit temperature, °C	814	693
Outlet guage pressure, bar	39.5	30.1
Exit CH_4 content, mol % (dry basis)	13.2	29.4
Reforming heat duty, GJ/t NH_3	4.70	2.27
Relative catalyst volume %	100	80
Secondary reformer		
Process air inlet temperature °C	600	500
Exit temperature °C	1000	870
Exit CH_4 content, mol % (dry basis)	0.6	1.65
Ammonia plant		
Total energy consumption, GJ/NH_3	28	28

4.1.1.7. Pre-reforming

Another possibility to reduce the load of the tubular reformer is to install an upstream pre-reformer unit. This is actually an off-spring of the above-mentioned (Section 4.1.1.2) rich-gas (town gas) processes of British Gas [457], BASF/Lurgi [458]–[460], and Japan Gasoline [461]. This process has recently become the subject of renewed interest for increasing the capacity of existing natural-gas-based ammonia plants in which the primary reformer has been identified as bottleneck. Under the name pre-reforming, it is installed upstream of an existing tubular reformer [462]–[469]. The natural gas enters such a pre-reformer with a temperature of 530 °C instead of being fed to the primary reformer tubes at the same teamperature. A temperature drop of about 60–70 °C occurs in the catalyst bed due to the overall endothermic reaction. Medium-grade heat is used to reheat the exit gas to the correct primary reformer entrance temperature. This compensation heat may be derived from a variety of sources, including flue gas, process gas, or gas turbine exhaust. In the diagram in Figure 48 a pre-reforming arrangement is compared with a conventional configuration [470].

4.1.1.8. Heat-Exchange Reforming

The temperature of the flue gas from a traditional reformer is usually higher than 1000 °C, and the process gas at the outlet of the secondary reformer is also at around 1000 °C. From a thermodynamic point of view it is waste of exergy to use this high-level heat simply for raising steam and preheating process air for the secondary reformer. The boiling temperature in a 125 bar main boiler on the secondary reformer outlet is only 325 °C, and the process air is usually preheated in the reformer flue gas duct. A concept which completely avoids a fired primary reformer is the exchanger reformer, which with some simplification may be viewed as tubular heat exchanger with the

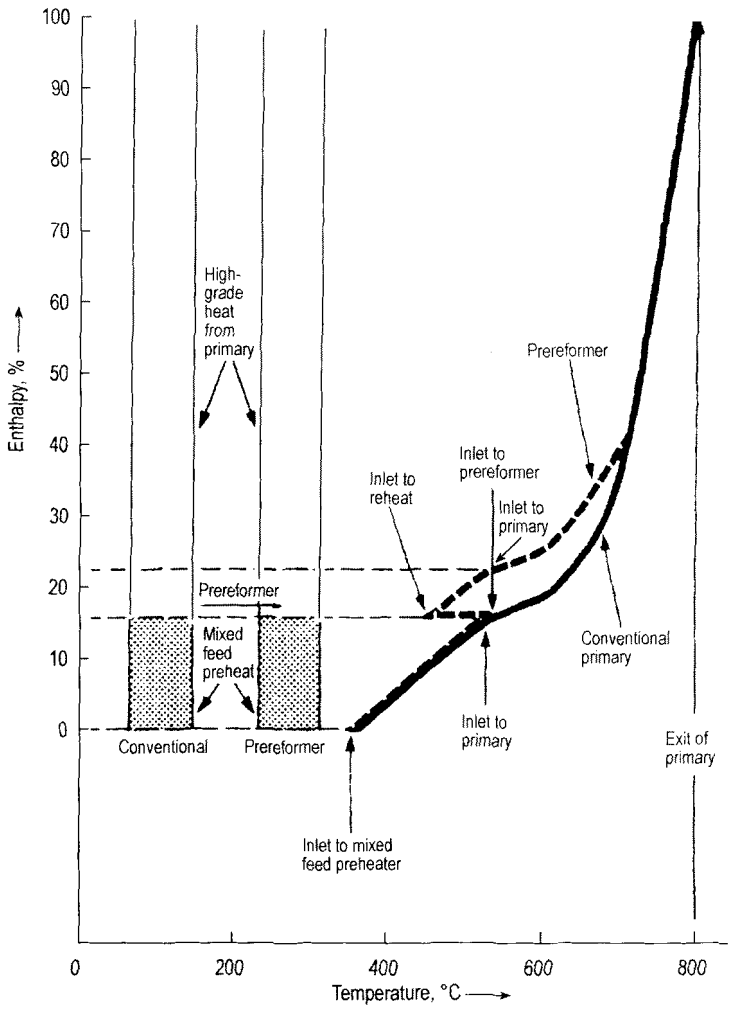

Figure 48. Pre-reforming versus conventional process configuration

catalyst inside the tubes, which are heated by the hot secondary reformer effluent flowing on the shellside.

In some designs the tubes may be open at the lower end, in which case the gas flow on the shell side consists of a mixture of the exit gases from the secondary reformer and from the reformer tubes. Commercially operating designs are the GHR of ICI [404], [471]–[474] and the KRES of M. W. Kellogg [398], [475]–[479].

In the ICI gas-heated reformer (GHR) (Figure 49) the reformer tubes consist of an outer scabbard tube with an open ended bayonet tube inside, and the annular space between the tubes is filled with the reforming catalyst. The steam/natural gas mixture enters the tubes via a double tube sheet and flows downwards through the catalyst, and the reformed gas leaves through the bayonet tubes. To enhance the heat transfer from

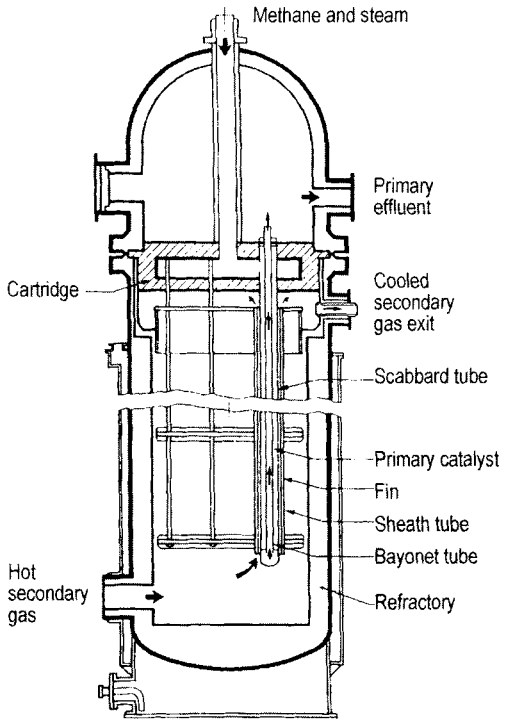

Figure 49. ICI gas-heated reformer (GHR)

the hotter secondary reformer outlet which flows on the shell side, the scabbard tubes are finned and surrounded by "sheath" tubes.

Quite recently ICI has come out with a modified design, the AGHR, with "A" standing for advanced. As shown in Figure 50, the bayonet tubes are replaced by normal tubes attached to a bottom tube sheet by a special seal that allows some expansion. In this way the delicate double tube sheet of the GHR is avoided. The seal which prevents leakage of methane-rich gas to the secondary reformer effluent flowing on the shell side has a unique design which is subject to patent applications of ICI. The AGHR will allow a single-line concept for world-scale plants whereas with the GHR several parallel units would be necessary in the case of large plants [404].

Because of the smaller size compared to a conventional fired reformer, considerable investment savings can be achieved. To close the heat balance between the exchanger reformer and secondary (autothermal) reformer, the latter has to take on a higher reforming duty, which may be achieved by using an over-stoichiometric amount of air or oxygen-enriched air. In some configurations, such as the KRES (Figure 51) concept of Kellogg, the exchanger reformer is partially bypassed, part of the feed (70 – 75 %) being fed directly into the autothermal reformer. The overall S/C ratio is 3.0 to 4.0 and the oxygen content in the enriched air is between 28 and 32 mol %. The mechanical design is relatively uncomplicated, and the pressure difference across the tube walls is only 3.4 bar (35 – 40 bar in a fired primary reformer). In contrast to the ICI GHR there is only one tube sheet and the tubes are open at the lower end, where the reformed gas

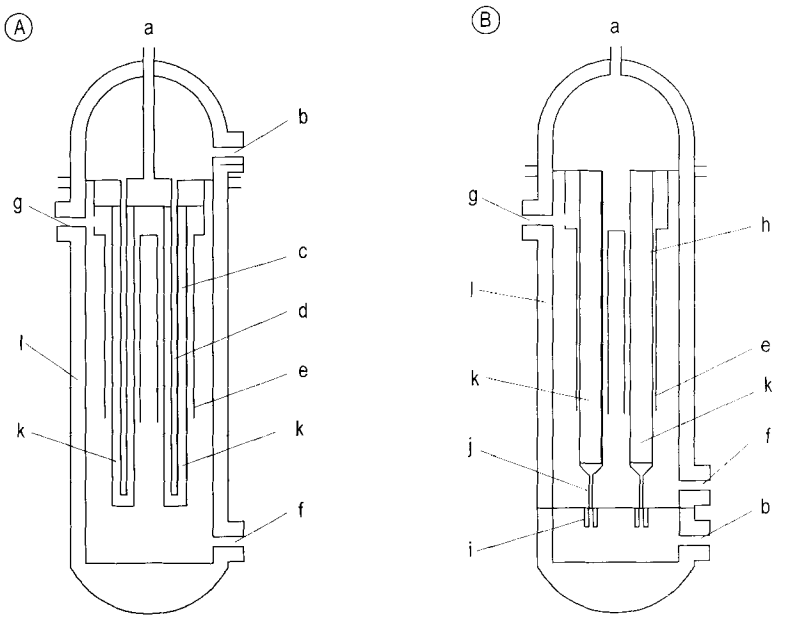

Figure 50. Comparison of GHR (A) with AGHR (B) a) Tubeside inlet; b) Tubeside outlet; c) Scabbard tube; d) Bayonet tube; e) Sheath tube; f) Shellside inlet; g) Shellside outlet; h) Catalyst tube; i) Seal; j) Tail pipe; k) Catalyst; l) Refractory lining

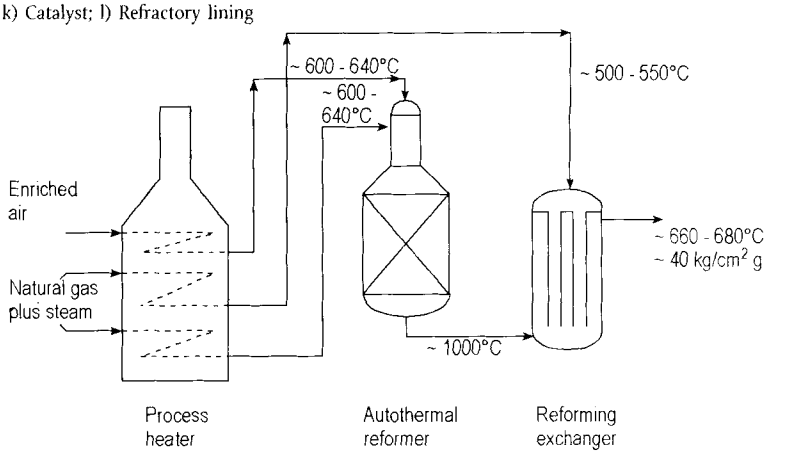

Figure 51. Kellogg reforming exchanger system (KRES) [404]

mixes with the hot effluent of the secondary reformer. The mixed gases flow upwards on the shell side, where baffles create a cross-flow to improve heat transfer. For mixing of the two gas streams, a multihole distributor is installed. Temperature and heat flux profiles for various process parameters of the KRES are shown in Figure 52.

Similar concepts are available from other licensors and contractors. Braun & Root, is offering the Tandem Reformer [480]–[483] a process developed and commercially

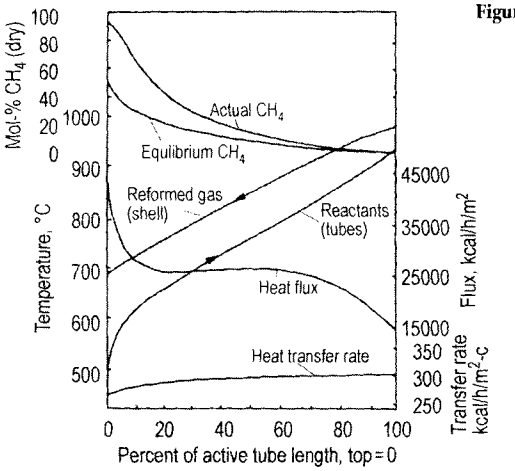

Figure 52. KRES temperature and heat flux profiles

tested in the former USSR in a hydrogen plant equivalent to a 400 t/d ammonia plant. Topsøe [404], [444], [483], [484] also has an exchanger reformer design.

A concept developed by Uhde goes a step further in this direction: exchanger reforming and subsequent noncatalytic partial oxidation, which provides the reaction heat, are accomodated in a single vessel. This combined autothermal reformer (CAR) design, shown in Figure 53, is operated at 17 bar in a demonstration unit producing 13 000 m^3/h of sythesis gas [485] – [488], [1485]. The steam/natural gas feed is passed through the reforming catalyst in the tubes, which are heated by the hot gas returning from the partial oxidation section below the tubes. The intensive mixing of the tube effluent with the oxygen or oxygen-enriched air in the partial oxidation zone (temperature about 1300 °C) is achieved by a vortex-type flow pattern. The residual methane content is governed by the amount of oxidant. For ammonia production all the feed will be passed through the reforming tubes; in other applications (methanol, oxo gas) a portion of feed can be fed directly to the oxidation chamber to attain a higher CO content.

4.1.1.9. Fully Autothermal Reforming

In the extreme case the whole reforming reaction could be performed without a tubular reformer by autothermal catalytic reforming in a design similar to a secondary reformer. In this case it would be necessary to use oxygen or oxygen-enriched air instead of air [402], [489] – [491], [1485].

Unlike the secondary reformer, which is fed with partially reformed gas, the autothermal reformer is fed directly with hydrocarbon feedstock. Because of the higher heat of reaction in the internal combustion (temperatures of 2000 °C and higher), the flow conditions, heat release characteristics and the risk of soot formation are very different from the situation in the normal secondary reformer, and special considerations in the

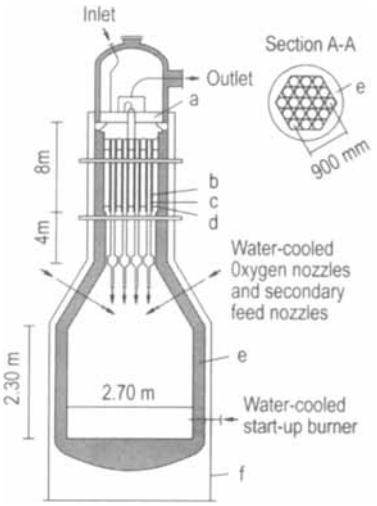

Figure 53. Uhde combined autothermal reformer (CAR)
a) Sandwich type tube sheet; b) Enveloping tube; c) Reformer tubes; d) Tube sheet; e) Refractory lining; f) Water jacket

design of burner and reactor are necessary. The burner must have excellent mixing characteristics which give a combustion zone with a turbulent diffusion flame, followed by a thermal zone in which homogeneous gas-phase reactions take place. In the following catalyst bed, a close approach to the thermodynamic equilibrium in the methane reforming reaction (Eq. 40) and the water gas shift reaction (Eq. 37) is attained. The combustion is a substoichiometric reaction with an overall oxygen/hydrocarbon ratio of 0.55 – 0.6.

Autothermal reforming of natural gas and also of naphtha at normal pressure was used in large scale in BASF in the early 1960s for the production of ammonia [492]. The catalyst beds consisted of three layers: a inert material on the top to prevent backflashing into the mixing chamber, a small intermediate layer consisting of a noble metal catalyst as starter, and a bottom layer of nickel catalyst for the reforming reaction. Two versions were in use, one of which was performed with a flame reaction in the empty space above the catalyst bed, while the other was used for naphtha. Feed and pre-mixed oxygen directly entered the catalyst bed, where the reaction was initiated in the noble catalyst layer.

4.1.1.10. Other Reforming Processes

The reaction heat in primary reforming is transferred continuously from the fire box through the tube walls to the reactants as the reaction proceeds. Running the reaction adiabatically in a bulk catalyst bed was formerly not thought to be technically feasible because in this case extremely high preheating temperatures of the steam/natural gas mixture would be necessary. But with the Regate process gas heater [493], [494] this should be possible. The Regate is similar to a steel works regenerator, exept that it operates on much shorter cycles of only 2 – 3 minutes. It is made up of refractory lined

vessels, each loaded with a heat-retaining mass and equipped with a burner. The vessels are operated alternately between combustion phase for re-heating and a heating phase for the feed gas, in which the heat-retaining mass cools down. The hot gas line to the process has no valves, and control of gas flow is effected automatically by valves on the inlet and flue gas lines. On account of the short cycle times, the temperature drop is only 40 °C in the phase in which the feed gas is heated. So far only pilot plant experience is available.

A unique steam reforming process [495]–[497] has been developed in Japan to the pilot-plant stage. It reportedly can operate without upstream desulfurization and should be able to gasify naphtha, crude oil, and atmospheric or vacuum residues.

For additional literature on steam reforming see [402]–[404], [426], [483], [491], [494], [498]–[503]; for steam reforming of naphtha [504]–[506]; for steam reforming catalysts [404], [507]–[509]; for reformer design [404], [510], [511].

4.1.2. Partial Oxidation

4.1.2.1. Chemistry of Partial Oxidation

Hydrocarbons or coal will react with an amount of oxygen insufficient for total combustion to CO_2 according to:

$$C_nH_m + n/2\ O_2 \longrightarrow n\ CO + m/2\ H_2 \quad (59)$$

$$C + 1/2\ O_2 \longrightarrow CO \qquad \Delta H^0_{298} = -110.6\ kJ/mol \quad (60)$$

For various reasons, in practical operation some steam must always be added, the quantity depending on feedstock and process configuration, so that the following reactions proceed in parallel:

$$C_nH_m + n\ H_2O \longrightarrow n\ CO + (n + m/2)\ H_2 \quad (40a)$$

$$C + H_2O\ (g) \longrightarrow CO + H_2 \qquad \Delta H^0_{298} = +131.4\ kJ/mol \quad (61)$$

Since in some processes with coal feedstock (e.g., the Lurgi Process) the reaction according to Equation (61) may proceed to a considerable extent, they are more often referred to as coal gasification rather than as partial oxidation, but this is just a matter of definition.

The reactions of the various hydrocarbons in partial oxidation processes are shown schematically in the following equations [512]–[515]. The reaction enthalpies listed (Eqs. 62–68) are not standard enthalpies, but assume 150 °C for the reactants and 1260 °C for the reaction product [512]:

Natural gas $CH_4 + \frac{1}{2}O_2 \rightarrow CO + 2H_2$ $\Delta H_{150/1260} = +71.2$ kJ/mol (62)

Naphtha $=CH_2 + \frac{1}{2}O_2 \rightarrow CO + H_2$ $\Delta H_{150/1260} = -16.7$ kJ/mol (63)

Heavy fuel oil $\equiv CH + \frac{1}{2}O_2 \rightarrow CO + \frac{1}{2}H_2$ $\Delta H_{150/1260} = -48.1$ kJ/mol (64)

In parallel also: $\equiv CH + H_2O \rightarrow CO_2 + \frac{3}{2}H_2$ $\Delta H_{150/1260} = +228.2$ kJ/mol (65)

$$CH_4 + 2\,O_2 \rightarrow CO_2 + 2\,H_2O \quad \Delta H_{150/1260} = -650\ \text{kJ/mol} \quad (66)$$

$$=CH_2 + \tfrac{3}{2}O_2 \rightarrow CO_2 + H_2O \quad \Delta H_{150/1260} = -510.8\ \text{kJ/mol} \quad (67)$$

$$\equiv CH + O_2 \rightarrow CO_2 + \tfrac{1}{2}H_2 \quad \Delta H_{150/1260} = -515\ \text{kJ/mol} \quad (68)$$

The extent to which the above reactions proceed is controlled by the oxygen feed to the partial oxidation generator.

Apart from minor amounts of nitrogen and slag-forming inorganic compounds, the feedstocks in these processes are composed of four elements: C, H, O, S, which are related by the following reactions (Eqs. 69–73) (from [512], reaction enthalpies at 1500 K) in the partial oxidation generator:

$$CO + \tfrac{1}{2}O_2 \leftrightharpoons CO_2 \quad \Delta H_{1227} = -280.5\ \text{kJ/mol} \quad (69)$$

$$CO + H_2O \leftrightharpoons CO_2 + H_2 \quad \Delta H_{1227} = -30.1\ \text{kJ/mol} \quad (70)$$

$$CH_4 + H_2O \leftrightharpoons CO + 3\,H_2 \quad \Delta H_{1227} = +227.3\ \text{kJ/mol} \quad (71)$$

$$CH_4 + \tfrac{1}{2}O_2 \leftrightharpoons CO + 2\,H_2 \quad \Delta H_{1260} = -23.0\ \text{kJ/mol} \quad (72)$$

$$CH_4 + CO_2 \leftrightharpoons 2\,CO + 2\,H_2 \quad \Delta H_{1260} = +257.5\ \text{kJ/mol} \quad (73)$$

Elemental carbon may react according to Equations (74–77) (from [512], reaction enthalpies at 1500 K):

$$C + H_2O \leftrightharpoons CO + H_2 \quad \Delta H_{1227} = +135.2\ \text{kJ/mol} \quad (74)$$

$$C + CO_2 \leftrightharpoons 2\,CO \quad \Delta H_{1227} = +165.4\ \text{kJ/mol} \quad (75)$$

$$C + 2\,H_2 \leftrightharpoons CH_4 \quad \Delta H_{1227} = -92.5\ \text{kJ/mol} \quad (76)$$

$$C + \tfrac{1}{2}O_2 \leftrightharpoons CO \quad \Delta H_{1227} = -115.1\ \text{kJ/mol} \quad (77)$$

At 1300 °C and complete conversion of the feedstock, the complex overall reaction in the partial oxidation process is strongly exothermic for any hydrocarbon, and steam has to be added to control the reaction temperature to prevent damage of the generator refractory material. Part of this steam forms additional hydrogen (Eqs. 40a, 61, 70); for this reason more hydrogen is formed in the partial oxidation processes than expected from Equations (62–64). The chemical nature of the feedstock has no influence on the result, as all organic structures are totally destroyed in the reaction; hence the composition depends only on the ratio of the elements C:H:O:S. An important condition for the partial oxidation process is to maintain an oxygen to carbon ratio above 1 (O/C > 1) otherwise significantly increased soot formation would occur.

At the reaction temperature of around 1300 °C a rather close approach to the equilibrium of various reactions is achieved. During cooling, the concentrations change on account of the temperature dependence of the equilibrium constants but due to rather rapid cooling rate in technical plants (quench or waste-heat boiler) the composition will become frozen at values corresponding to a temperature of about 900 °C.

Not much information is published on the kinetics of partial oxidation. The methane concentration is about 8 times higher than indicated by reaction (71), but as expected increasing pressure promotes methane formation. From a mere thermodynamical point of view no soot should be present at 1300 °C and O/C > 1. However, the raw sythesis gas contains more or less soot, depending on feedstock. Gasification of heavy oils fractions yields about 1–2% soot, but with methane the soot content is close to zero.

Soot-forming reactions can be the Boudouard reaction (Eq. 46) and CO reduction (Eq. 48) with hydrogen. At the reaction temperature the equilibrium is nearly completely shifted to the left-hand side; only at lower temperatures (< 1200 °C) does soot formation via these reactions become thermodynamically possible.

$$2\,CO \leftrightharpoons C + CO_2 \qquad \Delta H^0_{298} = -172{,}5\ \text{kJ/mol} \tag{46}$$

$$CO + H_2 \leftrightharpoons C + H_2O \qquad \Delta H^0_{298} = -131{,}4\ \text{kJ/mol} \tag{48}$$

Some authors assume that soot formation is only a result of thermal cracking of a portion of the hydrocarbon (Eq. 57), resulting at least partly from insufficient mixing of the reactants after the burner nozzle. Others relate it partially to the fact that Boudouard limit is reached during cooling down. Ash particles in the heavy oil fractions also seem to act as nuclei of condensation or catalysts (Ni) for soot formation [512], [513].

$$C_xH_y \rightarrow x\,C + y/2\,H_2 \tag{57}$$

In coal gasification processes (e.g., reaction with oxygen and steam countercurrently in a fixed bed or in a fluidized bed), exothermic combustion of carbon to carbon dioxide according to Equation (78):

$$C + O_2 \leftrightharpoons CO_2 \quad \Delta H^0_{298} = -393.8\ \text{kJ/mol} \tag{78}$$

followed by conversion to CO in the Boudouard reaction (Eq. 46). The carbon monoxide in turn may react with steam to produce either hydrogen and carbon dioxide (Eq. 70) or form methane and carbon dioxide (Eq. 71). The latter reaction is particularly promoted by higher gasification pressures. Carbon monoxide and hydrogen are also formed by direct endothermic carbon gasification with steam (Eq. 74). In the entrained flow processes (Texaco, Koppers–Totzek, and Shell) the reactions described overlap. The gas composition is determined by adjustment of the simultaneous equilibriums of the shift (Eq. 70), methane reforming (Eqs. 71, 73) and Boudouard reactions (Eq. 46).

4.1.2.2. Partial Oxidation of Hydrocarbons

For a long time the dominant processes were the Texaco Syngas Generation process (TSGP) and the Shell Gasification process (SGP). Quite recently Lurgi, which in the past was the leading contractor for the Shell process, has come out with an own partial oxidation process, named LurgiSVZ MPG process. Lurgi acquired technology for the MPG (multipurpose gasification) process from SVZ "Schwarze Pumpe" (Sekundärrohstoff-Verwertungszentum = secondary resource utilization center) and combined it with own developments [536].

In all three processes the reaction is performed in an empty pressure vessel lined with alumina. The reactants (oil and oxygen, along with a small amount of steam) are introduced through a nozzle at the top of the generator vessel. The nozzle consists of concentric pipes so that the reactants are fed separately and react only after mixing at the burner tip or in the space below. The temperature in the generator is between 1200

Table 26. Feedstock and raw-gas composition in partial oxidation (Texaco process, quench, 25 bar)

	Natural gas	Naphta	Heavy fuel oil	Tar (from bit coal)
Feedstock composition				
Approximate formula	$CH_{3.71}$	$CH_{2.31}$	$CH_{1.28}$	$CH_{0.75}$
C, wt%	73.40	83.8	87.2	88.1
H, wt%	22.76	16.2	9.9	5.7
O, wt%	0.76		0.8	4.4
N, wt%	3.08		0.7	0.9
S, wt%			1.4	0.8
Ash, wt%				0.1
Raw gas composition				
H_2, mol%	61.1	51.2	45.8	38.9
CO, mol%	35.0	45.3	47.5	54.3
CO_2, mol%	2.6	2.7	5.7	5.7
N_2, mol%	1.0	0.1	0.3	0.8
H_2S, mol%			0.3	0.2
CH_4, mol%	0.3	0.7	0.5	0.1
Soot, kg 1000 m^3 (STP)	-	1.8	10	6.1
Consumption [for 1000 m^3 (STP)]				
Feedstock, kg	262	297	323	356
Oxygen, m^3 (STP)	248	239	240	243
Steam, kg		74	148	186

and 1400 °C. About 2% of the hydrocarbon feed is transformed into soot, which is removed from the gas by water scrubbing. Depending on the process configuration the gas is either cooled by quenching or in a waste-heat boiler. The processes are rather similar; they mainly differ in the nozzle design, soot removal and recirculation, and process gas cooling. The reaction pressures may be as high as 80 bar; there are no mechanical or material limitations to raising the gasification pressure further, but with respect to the overall ammonia process this might be beyond the energy optimum because of the increasing energy demand for nitrogen and oxygen compression. Nevertheless, Texaco has successfully operated a pilot plant at 160 bar in California. Maximum raw gas generation capacity of a single generator corresponds to about 1000 t/d ammonia. Over 300 plants based on Shell and Texaco technology (for ammonia and other production facilities) have been built to date [514]. World-scale ammonia plants based on partial oxidation exist in Germany, India, China, and other countries [516], [517].

Partial oxidation has practically no restrictions regarding the nature of the hydrocarbon and the sulfur content. Natural gas, refinery gases, LPG, naphtha, heavy fuel, vacuum residue, visbreaker oil, asphalt, and tar can be used as feedstock. As the investment costs for partial oxidation are higher than for steam reforming, mainly because of the cyrogenic air separation, it is usually not a choice for the lighter hydrocarbons, but heavy feedstocks from fuel oil to asphalt, when favorably priced, can be a competitive option for various locations and circumstances. In some special cases, where the primary reformer is a bottleneck for a capacity increase, a small parallel partial oxidation unit based on natural gas could be installed, if a surplus of

Table 27. Partial oxidation of heavy fuel oil with and without CO_2 recirculation (Shell process)

	H_2O	CO_2
Generator feed		
Oil, kg	1	1
Steam, kg/kg feed	0.4	-
CO_2, kg/kg feed	-	1.2
Oxygen, m^3 (STP)	0.75	0.8
$CO + H_2$, m^3 (STP)	2.74	3.31
Raw gas (dry)		
H_2, mol%	46.1	29.3
CO, mol%	46.9	59.2
CO_2, mol%	4.3	8.8
VH_4, mol%	0.4	0.4
$N_2 + Ar$, mol%	1.4	1.5
$H_2S + COS$, mol%	0.9	0.8
Soot, H_2, wt% based on feed oil	2.6	2.6

oxygen is available at the production site. This possibility is in competition with other solutions, e.g., a parallel autothermal reformer (Section 4.1.1.9), or an UHDE CAR unit (Section 4.1.1.8). For processes other than ammonia production which require a sythesis gas with a high carbon monoxide content (methanol, oxo synthesis, production of carbon monoxide), partial oxidation can sometimes also be an economic possibility. How the gas composition can vary with the feedstock analysis may be seen from Table 26 [512], [518]. Increasing carbon content of the feedstock leads to higher CO concentrations in the raw gas. With recirculation of carbon dioxide to the gasifier, the CO content can be increased even further, as shown in Table 27 [512], [519]. Other parameters of influence are oxygen purity, operating pressure, and amount of steam added for reaction moderation.

Shell Gasification Process (SGP) [514], [520]–[523]. Preheated oxygen and the heavy oil fraction are introduced through a nozzle into an empty reactor vessel which is lined with high-alumina brickwork. The pressure shell is equipped with a special system to monitor the skin temperature for early detection of defects in the generator lining. Oil enters through the central tube of the burner nozzle. A high pressure drop of up to 80 bar is necessary to ensure sufficient atomization by the oxygen, which is fed through the annulus between the oil gun and the outer case of the burner nozzle. Steam is added as moderator for the reaction and to assist the atomization. The generator temperature is between 1200 and 1400 °C. The raw gas contains soot and ash. A waste heat boiler capable of producing 100-bar steam cools the gas down to about 340 °C. Figure 54 is a simplified flow sheet of the SGP [514].

After this the soot is removed from the product gas in two stages. About 95% is removed by direct water-spray (quench type), the remainder by countercurrent water-scrubbing in a packed column. Older units used a gas-oil fraction to extract the carbon from the aqueous soot suspension. The pebbles formed in this operation were separated with vibrating sieves and either re-mixed with the generator feed or separately

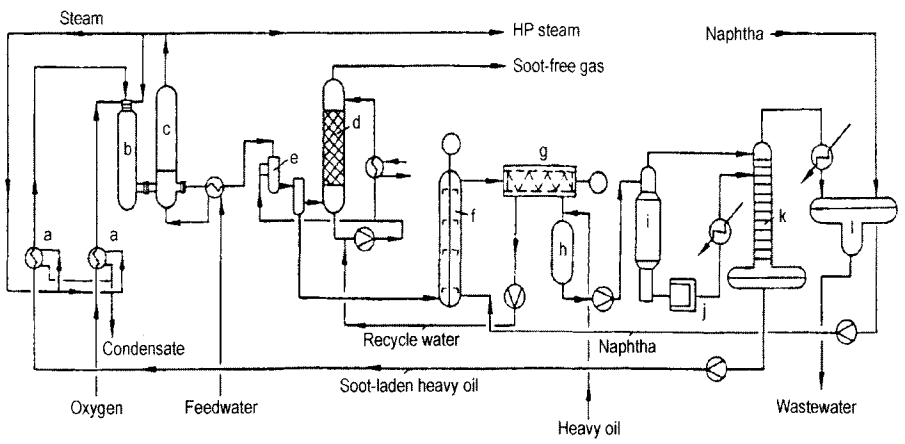

Figure 54. The Shell gasification process (SGP)
a) Preheater, b) Reactor, c) Waste heat boiler, d) Scrubber, e) Quench, f) Extractor, g) Vibrating screen, h) Flash tank, i) Soot-oil tank, j) Homogenizer, k) Naphtha stripper, l) Naphtha recycle tank

burnt in a steam boiler. A further development substituted the gas oil by naphtha, which on account of its high price was distilled off and recycled to the extraction stage before feeding the oil/pebble mixture to the generator. As a total recycle of the soot-free water would lead to ash built up in the soot-removal cycle, some wastewater run-down is necessary, which for environmental reasons requires nowadays an effective cleaning procedure [524] – [527]. Of special concern thereby is the removal of the heavy metals like nickel and vanadium. Stripping, floculation, chemicals addition and filtering operations were applied in a rather elaborate sequence. More recently, especially when using heavy feeds like visbreaker oil another technique for soot handling and water clean-up was developed. The carbon-water slurry is filtered off and the moist filter cake is subjected to a controlled oxidation in a multiple-hearth furnace. A vanadium concentrate (about 75 % V_2O_5) is obtained. The treatment of the run-down water is as described. From 1200 mtpd ammonia plant running on visbreaker oil, about 200 tons of vanadium can be recovered for metallurgical use [522]. Table 28 gives an example for the gas composition of an SGP plant (waste heat boiler) with an operating pressure of 55 bar.

Further information on the SGP is found in [528] – [531].

Texaco Syngas Generation Process (TSGP) [512] – [514], [518], [532] – [535], [537] – [542]. The burner nozzle is water cooled, but in contrast to the Shell Process oxygen is fed through the center pipe and oil through the outer annulus. This process, too, uses steam as moderator; the soot content in the raw gas is 1 – 2 % based on feed. The cooling of raw gas (about 1400 °C) is effected either by direct quenching with water from the soot water cycle or by a waste heat boiler (Section 4.6) as shown in Figure 55 [532].

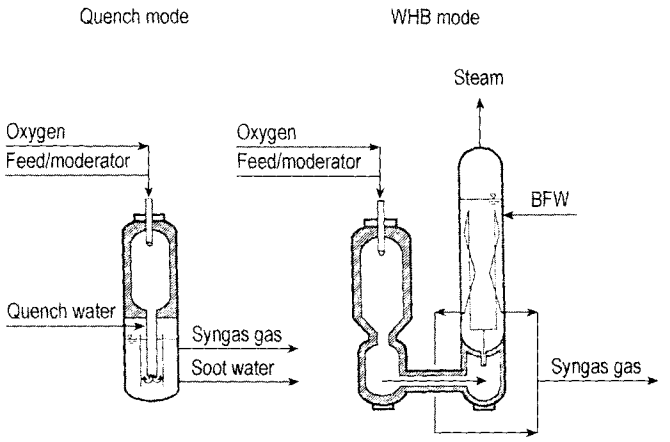

Figure 55. Raw gas cooling in the Texaco Syngas Generation Process

Table 28. Example of Shell gasification at 55 bar [513]

Heavy fuel oil, wt%		Oxygen, mol%		Raw gas (dry), mol%	
C	84.6			CO	46.3
				CO_2	4.7
				CH_4	0.5
H	11.3			H_2	46.3
S	3.5			H_2S	0.8
N	0.4	N_2	2.0	N_2	0.6
		Ar	3.0	Ar	0.8
O	0.13	O_2	95.0		
Ash	0.07				

With the Texaco process the quench mode is preferred for ammonia production as it offers some advantage by providing directly the major part of the steam needed in the subsequent carbon monoxide shift conversion. As can be seen in Figure 56 the quench is followed by two-step sootscrubbing, consisting of a venturi-scrubber and a subsequent packed column for countercurrent scrubbing. The soot can be extracted from the water with naphtha, because of its more lipophilic surface properties. The soot–naphtha suspension is separated in a settler from the nearly carbon-free "grey-water", which is recycled to the quench and scrubbing section. The soot–naphtha phase is mixed with feed oil, after which the naphtha is distilled of in a stripping column and returned to the soot-extraction step.

To prevent accumulation of ash and slag in the water circuit, some water is discharged continuously. In a combined chemical and physical treatment sulfides, cyanides and suspended solids (ash) are removed. A concentrated sludge has to be filtered off and disposed of. The run-off water from the filters is stripped of ammonia and after pH-adjustment sent to a biological treatment unit. Uhde [532] has developed an alternative route for soot treatment in which the soot is filtered off and subjected to combustion, and the filtered water is recycled to the quench and scrubbing circuits. Let down water is treated as described above. This soot treatment technique avoids not

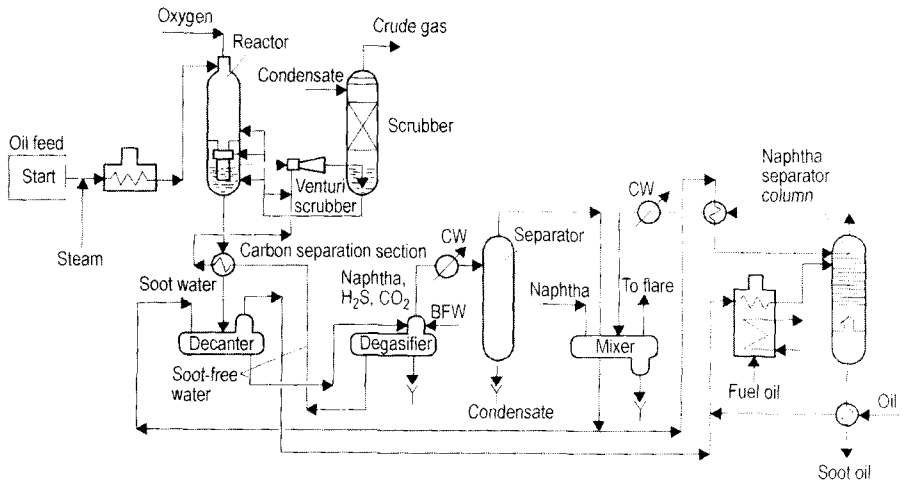

Figure 56. Soot removal in the Texaco Process

only the energy consuming and costly naphtha extraction step but also has advantages when processing oils with high vanadium content.

A typical gas composition (dry basis, mol%) produced from heavy fuel oil at 88 bar (quench type) [513] is CO 48.3, H_2 44.6, CO_2 4.6, CH_4 0.5, N_2 0.6, Ar 0.8 (introduced with the oxygen), H_2S 0.6, COS 300 ppm. (Feedstock (wt%): C 85.7, H 10.73, S 2.65, N+ash 0.6, O 0.32: oxygen purity 95.0 mol%).

A recent development is the Uhde [532] three-stream burner with an adjustable tip. A portion of the of oxygen enters through the center nozzle, the remainder through the outer annulus, the oil is fed through the inner annulus. The center oxygen nozzle also accommodates the preheat burner. This combi-burner concept avoids the change from preheat burner to process burner in the start-up phase, a cumbersome procedure necessary when using the traditional two-stream Texaco burner. As tested in a demonstration plant the carbon conversion could be increased to better than 99.6%, which means a reduction soot formation by a factor better than 5.

LurgiSVZ MPG Process [536]. The process is offered in two versions which differ in synthesis gas cooling: quench or boiler mode. Burner and reactor are essentially the same for both versions. For ammonia, the quench mode ist preferred because the quenchend synthesis gas saturated with water has the right temperature level to be fed directly to a dirty shift catalyst. Gasification pressure can be as high as 100 bar. The special burner design (multiple nozzle concept) is the main reason for high feedstock flexibility, it also accepts different non-mixible feeds without choking and can even handle slurries with particles in the mm-range. The oxidant (O_2, enriched air) is mixed with steam as moderator prior to feeding it to the burner. Burner and reactor are tuned

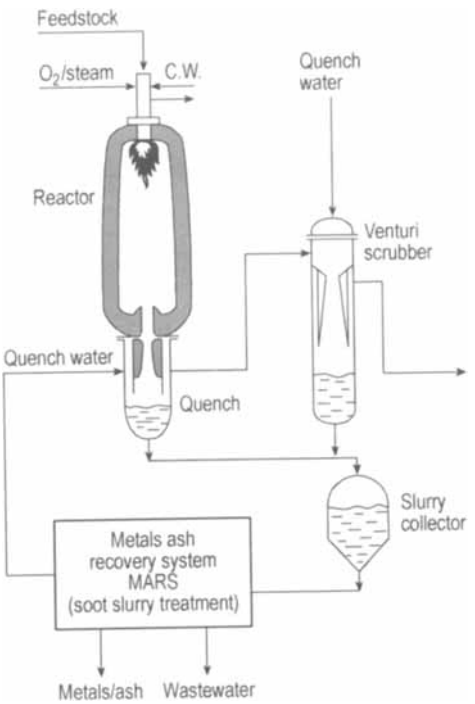

Figure 57. LurgiSVZ MPG (quench version)

by fluid dynamic simulation for optimum performance. The burner management system includes a sophisticated safeguarding system as well as a logic for fully automatic start-up.

For the quench cooling, water from the soot removal section ist injected radially into a quench ring. At the bottom of the separator part, soot slurry mixed with ash (in case of low-ash feed) is withdrawn. When processing high ash feedstock, molten slag is formed which flows down the refractory wall into the quench where it is blast-cooled into glassy spheres (1–2 mm in diameter), which collect at the quench separator bottom and are drawn off via a slag lock-hopper. Figure 57 shows the MPG quench version.

The raw gas from the partial oxidation contains soot, about 0.8 wt% of the hydrocarbon feed. Soot particles together with ash are removed mainly in the venturi scrubber downstream of the quench. The soot slurry from quench and venturi is sent to the metals ash recovery system (MARS) Figure 58. First the soot slurry is flashed to atmospheric pressure and then filtered, leaving a filter cake with about 80 % residual moisture. The filter cake is subjected to a controlled combustion in a multiple hearth furnace. Under the conditions applied, a metal oxide concentrate containing 75 wt% of vanadium, together with some nickel and iron, is obtained which can be sold to metal reclaimers. The MARS ist practically autothermal as the heat of combustion is sufficient to evaporate the moisture of the filter cake.

The filter water from the MARS is recycled to quench and venturi. Surplus of water, formed the gasification step has to be rejected. It is fed to a stripper to remove traces of

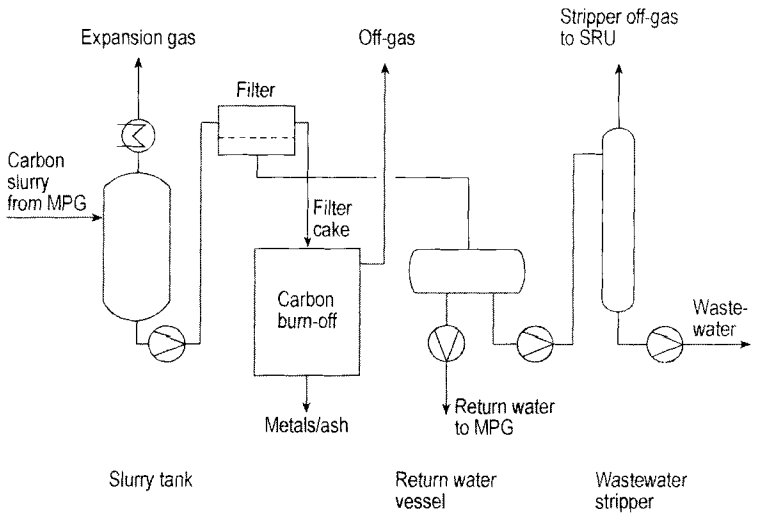

Figure 58. Metals ash recovery sytem in the LurgiSVZ process

ammonia, hydrogen cyanide and hydrogen sulfide, with the off-gas sent to a Claus unit with tailgas treatment. After this the stripped water which still contains traces of NH_3, HCN and H_2S and metals ist subjected to a flocculation and sedimentation procedure and finally purified in a biological wastewater treatment unit.

Ash and soot removal in the waste heat boiler version ist slightly different, the MARS is identical.

4.1.2.3. Partial Oxidation of Coal (Coal Gasification Processes)

As in any gasification of coal the exothermic reaction of carbon with oxygen to CO (60) and CO_2 (Eq. 78) and the endothermic reaction with water (Eq. 61) run in parallel in different extent it seems to be often a mere semantic question whether to classify a process as a partial oxidation or to use just the more general expression of coal gasification. Bouduard equilibrium (Eq. 46), water gas shift equilibrium (Eq. 37) and methane formation equilibrium (Eq. 71) are additional determinants

$$C + 1/2\ O_2 \rightleftharpoons CO \qquad \Delta H^0_{298} = -110.6\ \text{kJ/mol} \qquad (60)$$

$$C + O_2 \rightleftharpoons CO_2 \qquad \Delta H^0_{298} = -393.8\ \text{kJ/mol} \qquad (78)$$

$$C + H_2O(g) \rightleftharpoons CO + H_2 \qquad \Delta H^0_{298} = +131.4\ \text{kJ/mol} \qquad (61)$$

Historically the water gas process was used for ammonia production. Coke was reacted intermittently with air and steam in a fixed bed. The heat provided by the exothermic reaction of coal and air in the "blow phase" is stored in the fixed bed and provides the heat needed for the endothermic reaction of carbon with steam in the "run

Table 29. Coal gasification processes in commercial operation. Suitable feedstocks

	Pressure, bar	Temp., * °C	Anthracite	Bituminous coal	Lignite	Ash > 30 %
Lurgi (dry)	20–100	300–600	+/++	+/++	++	yes
British Gas/ Lurgi	20–70	450	+/++	++	-/+	no
Winkler/HTW	1–10	1050	+	+	++	yes
Koppers/Totzek		1800	+	++	++	no
Shell	20–40	1500	+	++	++	no
Texaco	20–40	1350	+	++	-	no
Dow	10–20	1000–1450	+	++	-	no

* At gasifier outlet.

phase" (Chapter 2). This old atmospheric pressure process is still used with some improvements in number of smaller ammonia plants (30 000–80 000 t/year) in China but elsewhere no longer in operation [543].

Coal gasification processes [544]–[547] in commercial operation are shown in Table 29 [545].

So far only the Koppers–Totzek, Texaco and Lurgi gasifiers, and probably the Winkler process in some smaller installations, have been used in ammonia plants, but the successful demonstration of the Shell process in other applications make it a potential candidate for ammonia production, too. Additional processes in different stages of technical development are the HTW and the Dow process. Information on the status and the development in the gasification of coal can be obtained from [541], [545], [548]–[554].

The **Koppers–Totzek Process** [555]–[560] used in several ammonia plants in China, India, and South Africa, operates practically at atmospheric pressure. Figure 59 is a simplified sketch of the gasifier.

Dry coal dust is fed to the two (sometimes four) burners of the gasifier. Oxygen, together with a small amount of steam, is introduced immediately at the head of the burners, and the mixture enters the reaction zone with high velocity. Core flame temperature may be as high as 2000 °C. The residence time is less than 1 s and the gas leaving the top of the reactor vessel is at 1500–1600 °C. The hot gas is cooled in a waste-heat boiler, followed by a water scrubber to remove carbon and ash traces from the raw gas and to effect further cooling. The soot water suspension is fed to a settler, and water and carbon slurry are separately recycled to the process. Liquid slag is withdrawn from the reactor bottom. Any surplus of water has to be cleaned prior to discharge. The combustion chamber has a refractory lining and, in addition, a water jacket for cooling. The process can handle bituminous coal and lignite, the maximum gas capacity of one generator is about 50 000 m^3/h. Typical gas composition (mol%) is CO_2 8–12, CO 59–62, H_2 26–29.

To overcome the disadvantage of atmospheric pressure operation, a version was developed capable of operating at 25–30 bar. This **PRENFLOW** (pressurized entrained flow) process [561], [562] is being tested in a 48 t/d pilot plant.

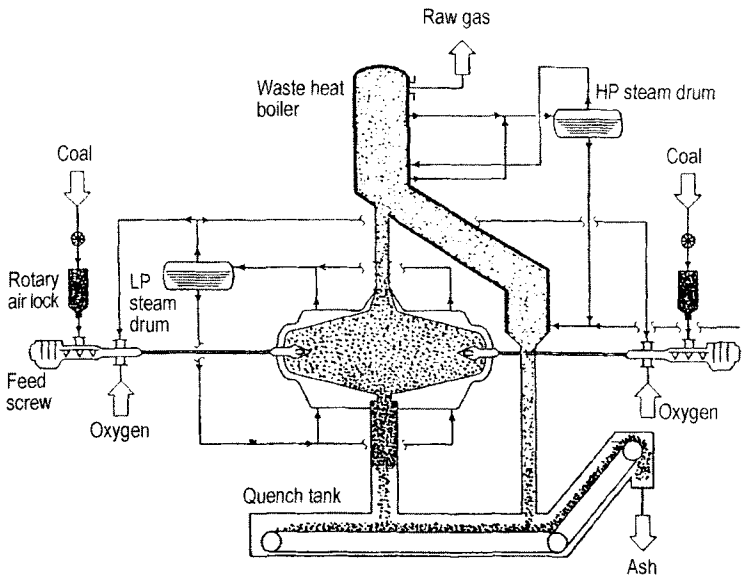

Figure 59. Koppers–Totzeck gasifier

A new concept of a atmospheric pressure gasification that has been presented recently [563] is the **Advanced Coal Gasification Process (ACGP)**, developed by AECI Engineering, Kynoch Ltd, and Babcock Wilson. Similar to the Koppers–Totzek, it is an entrained flow process. Pulverized coal and oxygen are injected near the base of the gasifier through eight burners by a proprietary feed technique that applies a special pump capable of injecting the coal dust directly instead of using a lock-hopper screw device as in the traditional Koppers–Totzek process. The gasifier is a slender column with a square cross section, which is lined with highly heat resistant material in the combustion area. The upper part is made of finned tubes which are welded together and have a watercirculation by thermosyphon action. So far no commercial installation has been constructed but it is claimed that one unit is capable to produce the ammonia synthesis gas for 750 t/d of ammonia The developers believe that the low investment costs resulting from the rather simple mechanical design could economically off-set the energetic disadvantage of the pressure-less gasification.

The **Texaco Coal Gasification Process** [545], [564]–[571] is rather similar to the Texaco partial oxidation process for heavy hydrocarbons. An aqueous slurry containing 60–70% coal is fed by reciprocating pumps to the generator at a pressure of 20–40 bar. For ammonia and hydrogen production, quench cooling is applied, whereas for CO-rich synthesis gas (e.g., methanol, oxo-procces) the waste heat boiler version is recommended. Waste-heat boiler, quencher, and carbon scrubber are especially adapted to deal with the ash and slag introduced with the bituminous coal feed. Carbon is removed from the soot water in a settler system, the slurry is recycled to the process.

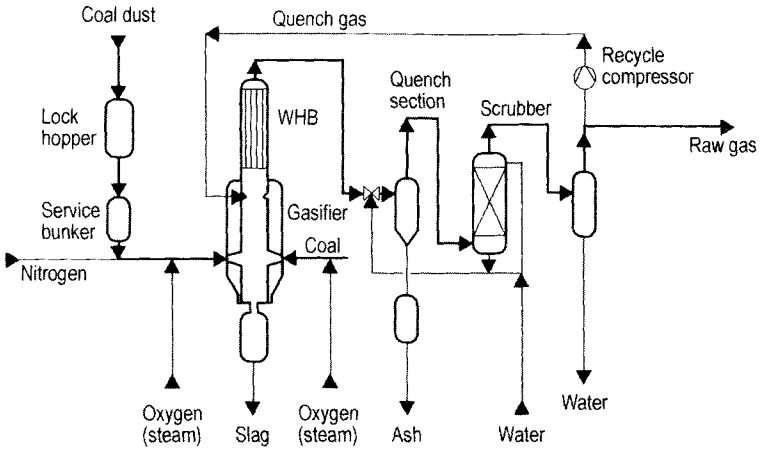

Figure 60. Shell coal gasification process (SCGP)

In its coal gasification process [545], [572]–[577] **Shell** has completely departed from the concept of its process for partial oxidation of heavy hydrocarbons. With reversed flow pattern in the gasifier (from bottom to top), dry coal dust is introduced via lock hoppers into the reactor vessel operating at 20–40 bar. The reactor vessel is refractory-lined and scrubbing with water in a venturi jet and a packed column is used to remove the particulates from the raw gas. Much development was dedicated to the liquid-slag withdrawal system and the nitrogen-aided coal-feeding system. A scheme of the process is presented in Figure 60 [545].

The **Lurgi Dry Gasifier** [545], [578]–[584] performs the reaction in a moving bed, usually operating at 25–30 bar. Figure 61 shows the principle of this gasifier. Crushed coal with a particle size of 4–40 mm enters the top of the gasifier through a lock hopper and is evenly distributed over the cross section of the coal bed surface by a distribution disk equipped with scraper arms. Ash with only 1% of residual carbon is removed at the bottom of the gasifier by a revolving grid with slots through which steam and oxygen are introduced. The temperature in the lower section of the bed is around 1000 °C, and at the top where the raw gas exits about 600 °C. As a result of this lower temperature the raw gas has an increased content of impurities such as tars, phenols, and some higher hydrocarbons. In addition the methane content is relatively high (up to 10–15%), so that purification and conditioning of the raw gas is a rather elaborate task [547]. The process actually can use any sort of coal and can handle ash contents higher than 30%. The **British Gas/Lurgi Slagging Gasifier** [545], [580], [585] operates without a grate with withdrawal of the liquid slag.

The classic **Winkler gasifier**, which operates at atmospheric pressure, is today still in use in some smaller plants (e.g., in China). In a further development **(HTW process)** by Rheinbraun it has been tested in a demonstration plant with lignite at 10 bar [586], [587].

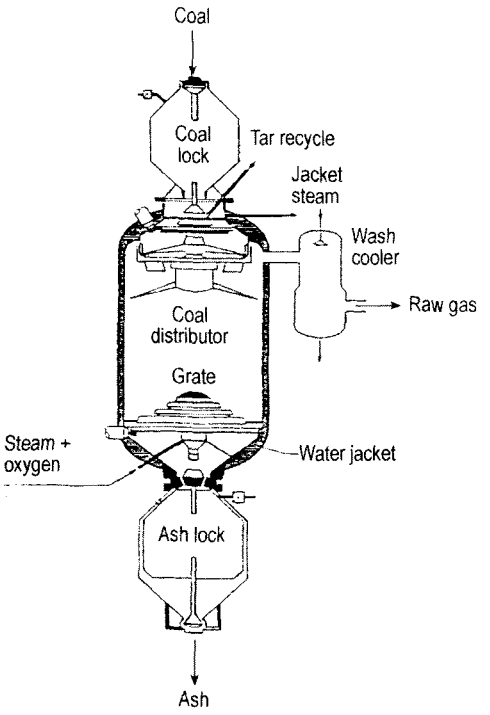

Figure 61. Lurgi dry bottom gasifier

4.1.3. Alternative Routes for Supply of Synthetic Gas

Hydrogen-containing byproduct gases or waste gases from other processes (examples are given in Table 30) can principally be used for ammonia production. The methods for recovering pure hydrogen from these gases are largely identical with those described in the Sections 4.2 and 4.3. In addition cryogenic processes such as condensation or methane wash may be applied [588]. In the past, ammonia plants based on coke-oven gas had some importance, but their present share of world capacity is lower than 3 %, and other byproduct gases contribute less than 0.5 %.

Ammonia plants based on **water electrolysis** for hydrogen production contribute less than 0.5 % to world production and are a very uneconomic option. One metric ton of ammonia requires theoretically 1976 m^3 H_2 (STP). As conventional alkaline water electrolysis has an electric energy consumption of 4.6 MWh/1000 m^3 H_2 (STP) [589], the hydrogen supply for the ammonia plant corresponds to 9.1 MW [589]. With the theoretical heat equivalent of 3600 kJ/kWh (hydroelectric power supply assumed) the hydrogen production for 1 t NH_3 consumes 32.7 GJ. When generating the electric power from fossil feedstocks a conversion factor of 10 900 kJ/kWh has to be used to give a figure of 99 GJ, which is more than three times the total energy consumption of a modern natural-gas-based ammonia plant. In addition to the above-mentioned

Table 30. Examples of hydrogen-rich gases [588]

	Pressure, bar	% H_2	% CO
Refinery sector			
Catalytic reformer	18–20	70–90	
Hydrocracker HP vents	42–140	70–90	
Hydrotreater vents	14–56	65–85	
Chemical and other industry			
Ethylene off-gas	10	90–95	
Acetylen off-gas	10	50–55	27
Styrene off-gas	18–32	80–90	
Coke oven gas	0.5	60–64	5

figures, energy for air separation to yield the stoichiometric nitrogen requirement (about 80 kWh/t NH_3) and for compression is required (about 700 kWh/t NH_3). Application of pressure (6–200 bar) has no significant influence on the power consumption of the electrolysis. The total energy needed for electrochemical decomposition of water decreases only slightly with increasing temperature, but the reversible part of energy requirement (ΔF), which has to be supplied as electric energy, decreases considerably (3 kWh /m^3 (STP) at 800–900 °C) H_2 [590], which means that an increasing amount of the total energy could be supplied as heat, but this definitely would not improve the competiveness. High-temperature electrolysis is still in the development stage.

In addition the investment cost for conventional water electrolysis is rather high, about 1 000 DM/kW_{el} in 1989. This would give a total investment for a world-size plant capacity 1 200 t/d of ammonia, which is about 2.5 times the value of a natural-gas-based steam reforming ammonia plant [590].

4.2. Carbon Monoxide Shift Conversion

As ammonia synthesis needs only nitrogen and hydrogen, all carbon oxides must be removed from the raw synthesis gas of the gasification process. Depending on feedstock and process technology, this gas contains 10–50 % carbon monoxide and also varying amounts of carbon dioxide. In the water gas shift reaction, traditionally known as carbon monoxide shift conversion, the carbon monoxide serves as reducing agent for water to yield hydrogen and carbon dioxide. In this way not only is the carbon monoxide converted to readily removable carbon dioxide but also additional hydrogen is produced:

$$CO + H_2O \leftrightharpoons CO_2 + H_2 \quad \Delta H^0_{298} = -41.2 \text{ kJ/mol} \tag{37}$$

As no volume change is associated with this reaction, it is practically independent of pressure, but as an exothermic process, it is favored by lower temperatures, which shift the equilibrium to the right-hand side. Even with a low excess of steam in the gas, the equilibrium concentrations of CO are low; for example, 0.2 vol % at 220 °C and

0.12 vol% at 200 °C for a steam/gas ratio of 0.4. The temperature dependence of the equilibrium constant K_p as defined by Equation (79) is given in the Equation (80) [591].

$$K_p = f_{CO_2} f_{H_2} / f_{CO} f_{H_2O} \quad (79)$$

$$1/K_p = \exp 13.148 - 5639.5/T - 1.077 \ln T - 5.44 \times 10^{-4} - 1.125 \times 10^{-7} T^2 + 49170/T^2 \quad (80)$$

The variation of the heat of reaction may be calculated with following formula [592]:

$$\Delta H = -47.617 + 1.302 \times 10^{-2} T - 0.126 \times 10^{-5} T^2 + 0.791 \times 10^{3} T^{-1} \text{ kJ/mol} \quad (81)$$

To keep the temperature low the heat of reaction must be removed in an appropriate way, and to achieve a sufficient reaction rate effective catalysts have to be applied. The process is therefore performed in steps, with intermediate heat removal between the individual catalyst beds, in which the reaction runs adiabatically. Recently, quasi-isothermal reactors have been developed in which cooling tubes run though the catalyst layers.

As the process configuration and catalysts are to some extent different for steam reforming and partial oxidation, they are treated separately here.

4.2.1. Shift Conversion in Steam Reforming Plants

In the traditional plant concept, the gas from the secondary reformer, cooled by recovering the waste heat for raising and superheating steam, enters the high-temperature shift (HTS) reactor loaded with an iron – chromium catalyst at 320 – 350 °C. After a temperature increase of around 50 – 70 °C (depending on initial CO concentration) and with a residual CO content of around 3% the gas is then cooled to 200 – 210 °C for the low-temperature shift (LTS), which is carried out on a copper – zinc – alumina catalyst in a downstream reaction vessel and achieves a carbon monoxide concentration of 0.1 – 0.3 vol%.

4.2.1.1. High-Temperature Shift Conversion (HTS)

4.2.1.1.1. High-Temperature Shift Catalyst

In the unreduced state the HTS catalyst is iron(III) oxide (Fe_2O_3) containing additionally 5 – 10% chromic oxide (Cr_2O_3). During operation, it is reduced more or less stoichiometrically to the composition of magnetite (Fe_3O_4) [593] – [595]. The catalyst is active in the temperature range of 300 – 500 °C. Steam surplus is not only necessary for thermodynamic reasons but also to suppress undesirable side reactions. Decreasing the steam surplus lowers the oxygen to carbon ratio in the HTS to such an extent that the

atmosphere can reduce magnetite partially to metallic iron. In addition the Boudouard reaction can occur under these conditions. The resulting carbon is deposited within the catalyst particles causing their disintegration, and iron carbides will be formed, which are effective Fischer – Tropsch catalysts that lead to the formation of some methane and higher hydrocarbons [404], [596], [597]. The minimum steam surplus depends on the CO/CO_2 ratio, lower values allowing lower steam surplus. Thus in conventional plant operation at 32 – 35 bar with CO/CO_2 of 1.65 – 2.13, an S/C ratio in the primary reformer of around 3.0 seemed to be the minimum with respect to the HT shift, whereas for concepts with reduced primary reforming and a CO/CO_2 ratio of 1.2 (the Braun process, for example) an S/C ratio of 2.8 was sufficient. Newly introduced HTS catalysts with additional copper promotion (e.g. 3 %) suppress this side reaction [598] and are therefore less sensitive to lower steam-to-gas ratios. The presence of MgO and ZnO should also effect some reduction of methane formation [599] – [602]. A review of catalyst research, surface science investigations and relevant literature is given in [603]. The function of Cr_2O_3 is mainly to prevent the sintering of the iron oxide, which leads to a reduction of surface area. But attempts to substitute Cr by Ce or Zr [604] – [607] (because in commercial Fe/Cr catalysts a minor amount of the chromium is still present as Cr^{6+} [603]) resulted in a lower activity of these Cr-free catalysts.

In the production of the HTS catalyst, mixed iron(III)hydroxide and chromium(III)-hydroxide are precipitated from an aqueous solution of ferrous sulfate and chromic acid by addition of sodium hydroxide solution while agitating with air to perform the oxidation of Fe^{II} to Fe^{III} and injecting steam for temperature adjustment. The oxide slurry is washed in alternating agitating and settler operations (to achieve a very low residual sulfur content). The washed hydroxides are spray-dried and the resulting powder is granulated with an additive which serves as lubricant and binder and than pressed into tablets of the required size 6 × 6 mm, 9 × 5 m, 9 × 9 mm are standard, but other dimensions are possible, too). Some manufactures use iron nitrate instead of iron sulfate as raw material. The BET surface area of commercial Fe – Cr HT shift catalysts is between 30 and 80 m^2/g, depending on Cr_2O_3 content and calcining temperature [608]. The space velocities in commercial HT reactors are today approximately 3500 – 4500 h^{-1}.

The classical HTS iron catalyst is resistant against sulfur compounds, but this is of greater importance in partial oxidation processes and less for the practically sulfur-free steam reforming gas.

4.2.1.1.2. Reaction Mechanism and Kinetics

The reaction kinetics were studied by many researchers with sometimes different or contradictory results. Reviews are found in [592], [602], [603], [609]. A reason for this is that often diffusional effects were not eliminated, and therefore no real intrinsic reaction rates were obtained [610], [611]. In industrial practice equations are required for dimensioning reaction vessels and catalyst. The mathematical expressions used for this purpose are for the most part not based on theoretical assumptions and research

results; they are rather just a quantitative modeling of laboratory measurements and can usually be extrapolated only to a limited extent beyond the range of the measurement conditions. Correlation with measurements in industrial units and allowance for activity decline with operating time and inclusions of safety margins led to useful mathematical expressions for design purposes. An early example is a rate equation given by LAUPICHLER [612], but its accuracy was not very satisfactory. A better approach to reality is achieved by an expression developed by MOE [631]. Another equation was developed on the basis of a theoretical assumption of a stepwise reaction on the catalyst surface, assuming the reaction of CO to be rate-determining and equilibrium conditions for the other steps involved. Assuming that the relevant equilibrium constants are very small and that there are no diffusional limitations, an equation of the following form can be derived (82) [609]:

$$r = kP\,[\mathrm{CO}]\left[1 - \frac{[\mathrm{CO_2}]\,[\mathrm{H_2}]}{K_\mathrm{p}\,[\mathrm{CO}]\,[\mathrm{H_2O}]}\right] \tag{82}$$

To make allowance for mass transport restrictions, the equation can be modified by including a term containing the diffusion coefficient of CO. For operating pressures between 10 and 50 bar, when the reaction rate is controlled by bulk diffusion, Equation (83) can be applied:

$$r = k_\mathrm{H} P^{1/2}\,[\mathrm{CO}]\left[1 - \frac{[\mathrm{CO_2}]\,[H_2]}{K_p\,[\mathrm{CO}]\,[\mathrm{H_2O}]}\right] \tag{83}$$

The same equation was derived empirically from the experimental observations, indicating that the forward rate with respect to CO is first order and with respect to water zero order and that the forward reaction rate is proportional to the square root of the total pressure between 10 and 50 bar ($p^{0.60}$ for 1 – 10 bar; some authors report a maximum reaction rate between 11 and 30 bar [613], [614]). BOHLBRO [613] proposed a power law type rate expression (Eq. 84) which fitted well his experimental data covering a wide range of conditions, diffusion-free and diffusion-controlled, atmospheric and elevated pressure, with commercial catalysts of various particle sizes.

$$r = k\,(p_\mathrm{CO})^l\,(p_{\mathrm{H_2O}})^m\,(p_{\mathrm{CO_2}})^n\,(p_{\mathrm{H_2}})^q\,(1-\beta) \tag{84}$$
$$\beta = p_{\mathrm{CO_2}}\,p_{\mathrm{H_2}}/K\;p_\mathrm{CO}\,p_{\mathrm{H_2O}}$$

Virtual activation energies of 114.6 to 59.8 kJ/mol were found, depending on catalyst particle size. CHINCHEN [612] found for the intrinsic reaction measured on an ICI catalyst the real activation energy to be 129.4 kJ/mol.

Two reaction mechanisms were proposed [602]: a) the catalyst acts as a simple adsorbent on which the reactants react on the surface (Langmuir – Hinshelwood type); b) the active catalyst sites are successively oxidized and reduced by the adsorbed reactants (Rideal – Eley type). Evaluation of the vast amount of experimental material leads to the conclusion that the HT shift (and also the LT shift) proceeds via mechanism (b), which schematically may be formulated as shown in Figure 62.

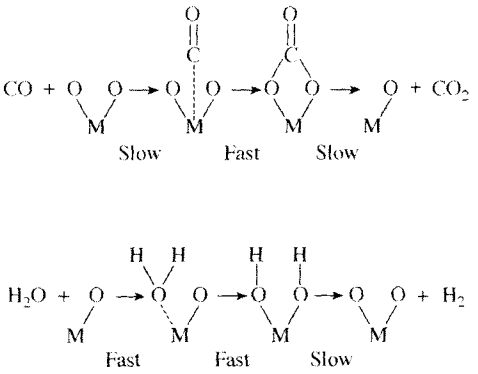

Figure 62. Oxidation–reduction mechanism of the HT shift conversion

To calculate the amount of catalyst for a particular case, mass and heat balance have to be considered; they can be described by two differential equations: one gives the differential CO conversion for a differential mass of catalyst, and the other the associated differential temperature increase. As analytical integration is not possible, numerical methods have to be used for which today a number of computer programs are available with which the calculations can be performed on a powerful PC in the case of shift conversion. Thus the elaborate stepwise and graphical evaluation by hand [592], [609] is history. For the reaction rate r in these equations one of the kinetic expressions discussed above (for example, Eq. 83) together with the function of the temperature dependence of the rate constant has to be used.

Following practical rules of thumb [592] are useful for choosing the operation conditions: Equilibrium approach should be 10 – 20 °C at a converter outlet temperature of $\leq$ 450 °C; maximum catalyst temperature should not exceed 550 °C; adiabatic temperature rise for 1 % CO (wet basis) converted: 10.6 °C at 500 °C, 11.0 °C at 400 °C, 11.6 °C at 225 °C; inlet temperatures for HTS below 330 °C are uneconomical.

4.2.1.2. Low-Temperature Shift Conversion (LTS)

The classical iron–chromium catalyst exhibits a sufficient activity only above temperatures of 320–360 °C. The introduction of the new copper–zinc based low-temperature shift catalyst in 1963 [615], made it possible to take advantage of the lower equilibrium CO concentrations at temperatures around 200 °C, shown for various steam/gas ratios in Figure 63. As can be seen from the diagram, a rather low CO concentration even at very low steam/gas ratios should be attainable with a sufficiently active LTS catalyst. In combination with methanation (Section 4.3.2.1.) it was possible to replace the energy consuming copper liquid scrubbing stage, which was used in old plants to remove the comparatively high residual CO content (around 3 %) after the HTS.

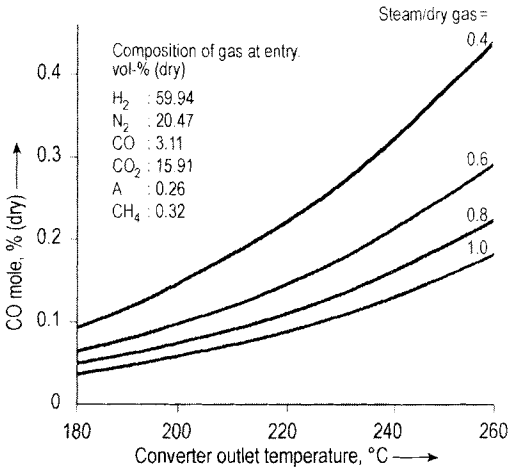

Figure 63. Equilibrium CO concentrations in LTS

4.2.1.2.1. Low-Temperature Shift Catalyst

The LTS catalyst, supplied in pellets like the HTS catalyst, consists of 40–55% copper oxide, 20–30% zinc oxide, the balance being alumina. The catalyst properties are influenced far more by the formulation and manufacturing procedure [616] than by its chemical composition. It makes a great difference whether the individually prepared components are just mixed physically as oxides or are incorporated by co-precipitation. The latter procedure assures a rather fine distribution of the copper oxide crystals, which are well separated from each other by zinc oxide and even smaller alumina crystals. This retards sintering of the copper cristallites in the reduced catalyst during prolonged operation [617], [618]. The co-precipitation step of the catalyst manufacturing sequence has to be very carefully controlled with respect to temperature, pH, and agitation to achieve the desired result. Commercial pellet sizes range from 6.4 × 3.2 mm to 3.5 × 3 mm; the surface area is around 60–120 m^2/g, and the pore volume 0.35–0.45 ml/g.

The copper oxide is reduced in situ with hydrogen and a carrier gas (usually nitrogen) to form the fine copper crystallites of about 10^{-6} cm on which the activity depends.

Sulfur, usually present as H_2S, has to be below 0.1 ppm, but even with such low concentrations, the catalyst is slowly poisoned. The ZnO adsorbs the sulfur and it finally transforms into bulk ZnS. When the ZnO is exhausted in a given layer of the catalyst, the H_2S causes deactivation of the copper by sintering. The poisoning process moves through the catalyst as a relatively sharp front and can be seen in the change of the catalyst temperature profile over time [619], [620] (Figure 64).

The LTS catalyst is protected by a guard bed, formerly loaded with ZnO, but nowadays usually with LTS catalyst [621]. Changing the guard bed more frequently prolongs the service life of the main LTS catalyst bed. Without a guard bed the lifetime is normally 2–4 years, depending on gas quality. With an upstream guard bed,

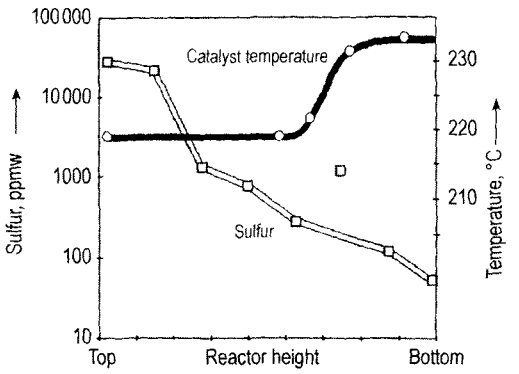

Figure 64. Sulfur and temperature profile for used LTS catalyst

changed at appropriate intervals the life time of the main bed can be extended to 6 – 10 years [499]. Traces of chlorine compounds [622], which may be introduced with the natural gas or more often with the process air to the secondary reformer, may also deactivate the LTS catalyst by accelerating the sintering of the copper particles. Unlike sulfur poisoning, chlorine is more diffusely distributed over the whole catalyst bed by migration as volatile zinc and copper chlorides. A chlorine guard catalyst for installation upstream of the LTS is offered by catalyst vendors.

As chemical composition and formulation of the LTS catalyst are very similar to methanol production catalysts, small quantities of methanol are formed and found in the process condensate after cooling the LTS effluent. In a consecutive reaction, amines (mainly methylamine) are formed from the methanol and traces of ammonia originating from the secondary reformer and the HTS. These pollutants are removed from the process condensate by steam stripping and ion exchange. Byproduct formation is higher with fresh catalyst and declines with operating time. New catalyst types with increased activity and higher selectivity have reduced the problem. The tendency for methanol formation increases with decreasing steam/gas ratio [623].

4.2.1.2.2. Reaction Mechanism and Kinetics

Compared to the HT shift reaction fewer publications exists on the reaction kinetics of LT shift reaction. Studies made before 1979 may be found in [602]. A rather simple power law (Eq. 85), for example [624] fitted well measurements between 200 and 250 °C, but the weak point is that the exponents are temperature dependent. An expression of the Langmuir – Hinshelwood-type, published in [625], includes additionally the influence of H_2 and CO_2 concentration on the reaction rate.

$$r = k\,(p_{CO})^{l}\,(p_{H_2O})^{m};$$
$$200\ °C:\ l = 0.45,\ m = 0.07;\ 250\ °C:\ l = 1.07,\ m = 0.55 \qquad (85)$$

A more complex formula (Eq. 86), used for evaluation of catalyst volume, is described in [592]:

$$\frac{d\,(G\,[CO_2])}{dV} = \frac{A}{T}\,\frac{k_l\,[CO]\,[H_2O]^{1/2}\,(1 - K/K_p)}{1/p + k_a\,[CO] + k_b\,[CO_2]} \tag{86}$$

k_l, k_a, k_b temperature dependent functions, G g mols/sec wet gas, V catalyst volume, A constant, $K = (CO_2)\,(H_2)/(CO)\,(H_2O)$, K_p equilibrium constant, P total pressure.

For comparison of the activity of commercial shift catalysts, sometimes the so-called K_w *value* is found in the literature. This term, introduced by K. ATWOOD is defined for shift reactions as follows [626]:

$$K_w = SV_w \log[(CO_{in} - CO_{eq})/(CO_{out} - CO_{eq})] \tag{86a}$$

The index w refers to wet gas.

For the LT shift an oxidation reduction mechanism has been discussed which is similar to that proposed for the HT shift, but this concept is not unquestioned and the presently available experimental material provides no convincing evidence.

4.2.1.3. Intermediate-Temperature Shift (ITS)

A relatively new process concept is the intermediate temperature shift [627], [628], which performs the reaction in a single step. The catalyst is based on a copper–zinc–alumina formulation and optimized for operating in a wider temperature range (200–350 °C) than the standard LTS catalyst (190–275 °C). The reaction heat can be removed by use of a tube-cooled reactor raising steam or heating water for gas saturation to supply process steam in the reforming section (Linde LAC, ICI Catalco LCA). In a new plant using the spiral-wound Linde reactor [629], a methane slip of only 0.7 mol% (dry basis) is achieved. Further purification is performed by PSA. Generally the shift conversion reactors have an axial gas flow pattern, but recently radial gas flow configurations have been chosen in some instances. The lower gas velocities result in reduced pressure drop, which saves compression energy and allows the use of smaller catalyst tablets (3 × 3 mm or 2 × 2 mm), which because of the higher activity can achieve a lower CO leakage. In a 1000 t/d plant without hydrogen recovery the ammonia production would be increased by 10 t/d. Ammonia Casale has patented radial flow designs for both HTS and LTS. In a recent revamp the pressure drop was reduced from 0.55 to 0.35 bar in the HTS and from 0.55 to 0.22 in the LTS. The CO leakage from the LTS could lowered to 0.11% from 0.25% [628].

Additional literature on shift conversion in steam reforming plants can be found in [402], [404], [498], [499], [630]–[638].

In some ammonia process schemes operating without a secondary reformer and applying pressure swing adsorption (PSA) for further purification (KTI PARC), only a HTS is used.

4.2.2. Shift Conversion in Partial Oxidation Plants

The raw synthesis gases from partial oxidation of heavy hydrocarbons and coal differ mainly in two aspects from that produced from light hydrocarbons by steam reforming. First, depending on the feedstock composition, the gas may contain a rather high amount of sulfur compounds (mainly H_2S with smaller quantities of COS); second, the CO content is much higher, in some cases in excess of 50 %. The sulfur compounds (Section 4.3.1.4) can be removed ahead of the shift conversion to give a sulfur-free gas suitable for the classical iron HTS catalyst. In another process variant the sulfur compounds are removed after shift conversion at lower concentration because of dilution by CO_2. The standard iron catalyst can tolerate only a limited amount of sulfur compounds. With a sulfur concentration in the feed >100 ppm sulfur will be stored as iron sulfide (Eq. 87):

$$Fe_3O_4 + 3\,H_2S + H_2 \rightleftharpoons 3\,FeS + 4\,H_2O \qquad (87)$$

FeS also catalyzes the shift reaction, but its activity is only half that of Fe_3O_4 [592]–[594]. In principle the catalyst can tolerate up to 500 or 1000 ppm H_2S, but with a considerable loss of mechanical strength, which is additionally affected by other contaminants in the gas, such as soot and traces of formic acid. For this reason the *so-called dirty shift catalyst* is used in this case, which was originally introduced by BASF [639]. This cobalt–molybdenum–alumina catalyst [603], [630], [640]–[644] is present under reaction conditions in sulfidized form and requires for its performance a sulfur content in the gas in excess of 1 g S/m^3. Reaction temperatures are between 230 and 500 °C. COS is not hydrolyzed on dirty shift catalysts, but may be removed in the subsequent sour-gas removal stage using the Rectisol process. Separate hydrolysis on alumina based catalysts is possible at temperatures below 200 °C [603].

In later developments aditionally potassium carbonate promotion of the dirty shift catalysts was introduced [645], [646] which increased the activity at low temperatures to achieve CO values sufficiently low to use a methanation step after CO_2 removal. But according to [647] it is also possible to achieve such low CO concentrations with nonalkalized dirty shift catalyst as shown in Figure 65.

The vertical lines represent different sulfur concentrations together with the temperatures at which the catalyst begins to lose sulfur to the gas. In the example of Figure 65, the gas must have a sulfur content higher than 550 ppm to keep the catalyst in the sulfided state at the outlet of the first bed.

Equations to describe reaction rate measurements on dirty shift catalyst are given in [648], [649].

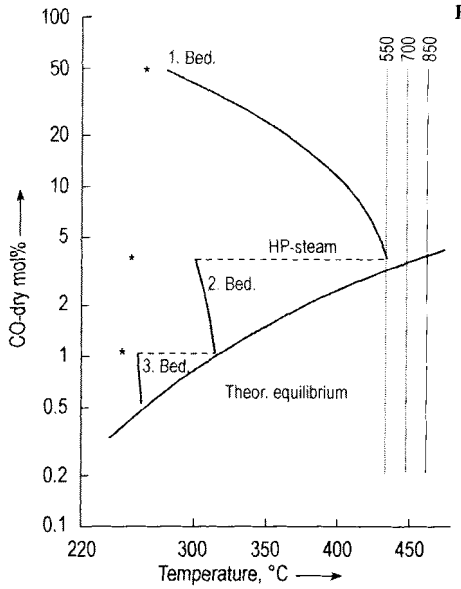

Figure 65. Dirty shift conversion on BASF catalyst K 8-11

Irrespective of the catalyst type used, the high initial carbon monoxide concentrations mean that the reaction must generally be performed in steps, with intermediate cooling. But it has also been reported that the CO content can be reduced from 50 to 0.8 % in a single step in a large hydrogen plant by using a quasi-isothermal reactor (e.g., the Linde spiral-wound reactor).

4.3. Gas Purification

In further purification, carbon dioxide, residual carbon monoxide, and sulfur compounds (only present in the synthesis gas from partial oxidation) have to be removed as they are not only a useless ballast but above all poisons for the ammonia synthesis catalyst.

The raw synthesis gas produced by steam reforming of natural gas and light hydrocarbon feedstocks is free of sulfur. Any sulfur contained in the feedstock has to be removed of upstream of gasification to avoid poisoning of the sensitive reforming catalysts. This is usually performed by hydrodesulfurization and adsorption of the H_2S by ZnO. As this is an essential part of the steam reforming process, it was already treated in Section 4.1.1.

In partial oxidation processes there is no prior treatment of the feedstock and the total sulfur contained in the coal or hydrocarbon feed is converted in the gasification to H_2S and a smaller amount of COS. As H_2S is soluble in the same solvents which can be used for CO_2 removal, selective absorption and/or desorption is a special problem

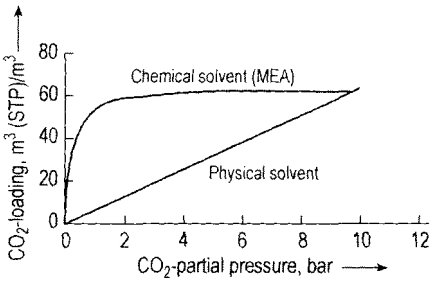

Figure 66. CO_2 loading characteristics of various solvents

encountered in partial oxidation of sulfur containing feedstocks. Therefore removal of the sour gases, as CO_2 and H_2S are frequently called, and the subsequent recovery of sulfur will be treated in a separate section.

4.3.1. CO_2 Removal

The standard method is to scrub the CO_2-containing synthesis gas under pressure with a solvent capable of dissolving carbon dioxide in sufficient quantity and at sufficient rate, usually in countercurrent in a column equipped with trays or packings. The CO_2-laden solvent is flashed, often in steps, to around atmospheric pressure, and the spent scrubbing liquid is subsequently heated and regenerated in a stripping column before being recycled to the pressurized absorption column. In the early days of ammonia production water, often river water, served as solvent in a once-through process without regeneration and recycling.

Today a variety of solvents are used and they can be categorized as physical or chemical solvents. In the physical solvents the carbon dioxide dissolves without forming a chemical compound, and this allows recovery simply by flashing. In the chemical solvents the carbon dioxide becomes fixed as a chemical compound, which needs heat for its decomposition. At low carbon dioxide partial pressures, the chemical solvents absorb substantially more carbon dioxide than the physical solvents; at higher partial pressures the physical solvents (according to Henry's law, the loading is approximately proportional to the CO_2 partial pressure) have a higher loading capacity than the chemical solvents, for which the solubility approaches a saturation value. Figure 66 shows the loading characteristic for various solvents.

Chemical solvents are best suited to scrubbing gases that have a relative low CO_2 partial pressure, whereas the physical solvents are more suitable for higher CO_2 contents in the raw gas. As both sour gases, CO_2 and H_2S, have good solubility in the applied solvents, special process configurations are required for partial oxidation gases to recover separately a pure CO_2 fraction and an H_2S-rich fraction suitable for sulfur disposal.

Chemical solvents are aqueous solutions of potassium carbonate or alkanolamines containing additional activators to enhance mass transfer and, in some cases, inhibitors to limit or prevent corrosion processes. Primary and secondary amines, for example, monoethanolamine (MEA) and diethanolamine (DEA), exhibit a high mass-transfer rate for carbon dioxide but have a high energy demand for regeneration. For this reason tertiary amines are commonly used today, for example, methyldiethanolamine together with an activator. Triethanolamine does not achieve the required final CO_2 concentration, and in the few cases where it was used it was followed by additional scrubbing with monoethanolamine (MEA). The **solvents with physical absorption** characteristics are various poly-glycol ether mixtures, *N*-methyl pyrrolidone, methanol, propylene carbonate, and sulfolan with additives. Table 31 (from [650], supplemented and modified) lists the various solvents and their properties.

Over the years considerable progress has been achieved in improving the efficiency of the carbon dioxide removal systems. The first generation of single-train steam reforming ammonia plants used MEA and consumed about 5.8 GJ/t NH_3, which was about 41% of the total energy consumption. Table 32 demonstrates the progress made in energy consumption.

The first progress was made by addition of corrosion inhibitors (e.g., Amine Guard introduced by Union Carbide) [651]–[655], which allow a higher loading of the solvent. The energy consumption of the modern systems, as shown in the last two lines of Table 32 depends largely on process configuration and required final purity, which may range from 50 to 1000 ppm in the purified gas. There is also a trade-off between energy consumption and investment costs.

4.3.1.1. Process Configuration

Usually packed towers are used for absorption and regeneration. Column diameters and height of the packings in connection with the required circulation rate of the solvent and the heat needed for regeneration can be varied over a considerable range to meet the process conditions of the individual ammonia plant. Packed height requirement is calculated according to the concept of height of transfer units and number of transfer units using mass-transfer rate expressions and absorption equlibrium data from laboratory and pilot plant measurements with the relevant type of packing material (geometry). Heat effects associated with the gas absorption have to be considered, too, and will complicate the calculation. As flooding represents the maximum capacity condition for a packed column it is used as design basis for the column cross section. In addition the pressure drop has to be evaluated. Standard procedures and data on packing characteristics are found in [656]. Compared to the widely used Pall rings newer packing forms such as Cascade mini rings, Metal Intalox, Tellerettes and others, are more effective and will allow to reduce absorber dimensions. Ceramic packings are no longer used in newer plants because they can loose their mechanical strength after some time of operation as the result of being leached by the solvent.

Table 31. Solvents used for CO_2 removal

	Chemical absorption processes			Physical absorption processes				
	Alkanolamine processes		Hot poptash processes	Selexol	Fluor solvent	Purisol	Rectisol	Sulfinol D
	MEA	aMDEA	Selexol	Fluor solvent	Purisol	Rectisol	Sulfinol D	
CO_2 p.press. inlet	low mod	mod high	mod high	mod high	high	high	high	high
CO_2 outlet, ppm	50	50 (any)	< 500	< 1000	1%	< 1000	< 10	< 1000?
Corrosion inhibitor	yes	no	yes	no	no	no	no	no
Solovent losses	yes	no	no	no	no	no	yes	yes
Absorber temp. °C	40–60	60–70	90	−5	−3	amb.	< −30	25–85
Hot regeneration	yes	small amount	yes	no	no	no	no	yes
Dew point raw gas	sat'd	sat'd	sat'd	−5	−3	−5	−5	10
Solution reclaimer	yes	no	no	no	no	no	no	yes
Regeneration gas	no	no	no	air	air	N_2	no	no

Table 32. Heat requirements for regeneration in CO_2 removal systems [404], [651]

Process	Heat requirement, kJ/mol CO_2
MEA (without Amine Guard)	209
MEA (with Amine Guard III)	116
Benfield hot potash (1-stage)[a]	88
BASF aMEAD process (1-stage)[a]	73
Benfield LoHeat	28–35
BASF aMEAD process (2-stage)[b]	28–30

[a] Single-stage regeneration. [b] Two-stage regeneration.

Another risk is breakage which may occur in plant upsets. For example rapid depressurization could lift the packing. For this reason the material of modern packings is either steel (often stainless steel because of potential erosion/corrosion) or polypropylene. In some processes the variation of the promoter concentration may be a variable in the optimization puzzle, too.

The number and pressure level of the intermediate flashing stages are determined by tolerable synthesis gas losses and the CO_2 specification. In most cases a higher or lower proportion of the CO_2-laden solution is regenerated simply by flashing, and only a fraction of the total solvent circulation is regenerated by stripping. With increasing chemical character of the solvent the stripping duty increases, and in the old MEA CO_2-removal systems all CO_2 had to be recovered in this way, needing a high consumption of low pressure steam.

The flashed solvent, containing a CO_2 load corresponding to the CO_2 partial pressure (semi-lean solution), is returned to first stage of the scrubber; the stripped lean solution is fed to the top of the second stage and its residual CO_2 content determines the achievable purity in the treated gas.

An important issue is the proper design of the distributors for the solvent and an adequate liquid holdup in the pump sump to balance fluctuation in the liquid flow sometimes caused by foaming. Foaming may require addition of suitable antifoaming agents. To reduce the mechanical energy demand the laden solution is depressurized over a hydraulic turbine mounted on the pump shaft. In processes which need addition of inhibitors to prevent corrosion, careful control of inhibitor concentration is required.

4.3.1.2. Chemical Absorption Systems

4.3.1.2.1. Hot Potash Systems

The commercial hot potash systems differ in the type of activator used to increase the reaction rate between the CO_2 and the solvent. The activators enhance mass transfer and thus influence not only the regeneration energy demand (circulation rate of the solvent) but also the equipment dimensions. The following activators are used: in Benfield [657]–[660] and Carsol [661], [662] processes ethanolamines; in the Giammarco Vetrocoke process glycine (originally arsenic oxide) [663]–[666]; in the Catacarb system [667], [668] amine borate; in the Exxon Flexsorb HP process [669], [670] a sterically hindered amine; in the Carbosolvan process [671], [672] sulfosolvan B. New activators named ACT-1 (UOP) [673], [674] and LRS-10 [675], [676] (British Gas) have been introduced recently. All hot potash systems need corrosion inhibitors the concentration of which must carefully to be monitored.

Benfield LoHeat System (UOP) [677]. The high thermal efficiency of this two-stage adsorption process using lean and semi-lean solvent is achieved by recompression of the flash steam with an injector or a mechanical vapor compressor. UOP has also developed a number of other process configurations [404], [669], [678]–[680]. The diethanolamine promoter enhances the mass transfer by carbamate formation (Eqs. 88–90) [681]:

$$R_2NH + CO_2 \rightleftharpoons R_2NCOOH \quad (88)$$

$$R_2NCOOH + K_2CO_3 + H_2O \rightleftharpoons 2\,KHCO_3 + R_2NH \quad (89)$$

Overall reaction:

$$K_2CO_3 + CO_2 + H_2O \rightleftharpoons 2\,KHCO_3 \quad (90)$$

Optimum CO_2 absorption is achieved if the concentration of K_2CO_3 is about twice of the concentration of $KHCO_3$. UOP defines a so-called conversion factor $F_c = 1 - \{[K_2CO_3]/([K_2CO_3] + 0.69\,[KHCO_3])\}$ which should be 0.25–0.30. The $KHCO_3$ content should be kept under control for another reason: it is less soluble than K_2CO_3 and could precipitate if the concentration becomes too high. Precipitated bicarbonate peels off the passivation layer, and problems may arise by formation of a slurry composed of bicarbonate, vanadium, and iron. Normally the vanadium of the corrosion inhibitor oxidizes the iron on the metal's surface ($V^{5+} + Fe^{2+} \rightleftharpoons V^{4+} + Fe^{3+}$). The resultant Fe_3O_4 produces a tight, coherent film on the steel surface, thus preventing any corrosion as long as it remains intact. Figure 67 is a simplified flowsheet of the Benfield LoHeat CO_2 removal process [404].

Recently UOP has introduced a new activator, called ACT-1 [673] which is claimed to reduce CO_2 levels in the absorber exit gas in existing plants and should reduce the solvent circulation rate as well. For new installations the enhanced mass transfer achieved with the new activator translates into smaller towers and therefore to investment capital savings. The activator is an amine compound, but speculations on its nature are still going on.

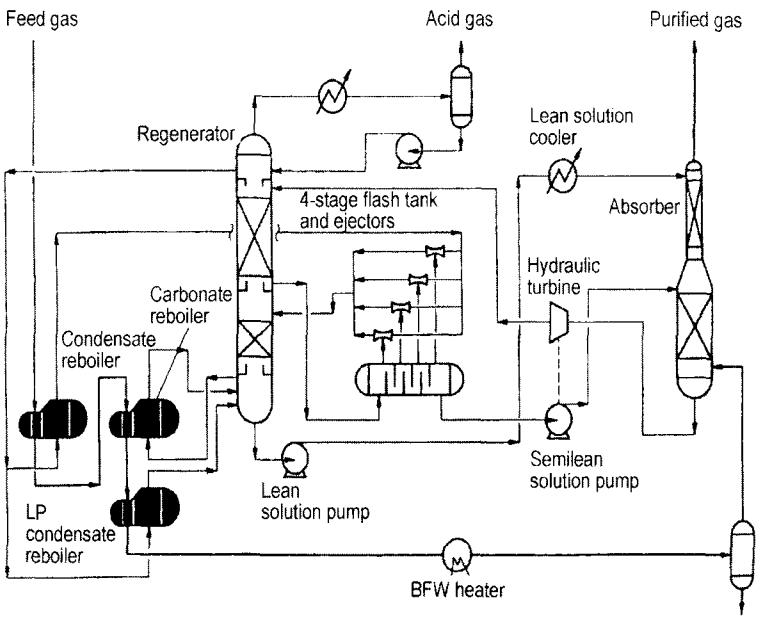

Figure 67. Benfield LoHeat CO_2 removal process.

Catacarb Process [667], [681], [682]. This process was introduced about 30 years ago. A modified potassium salt solution is used, containing various stable and non toxic catalysts and corrosion inhibitors. The process is very versatile and allows the process and mechanical configuration to be tailored to a wide range of CO_2 partial pressures. Figure 68 showes a Catacarb single-stage low heat design.

Giammarco – Vetrocoke process [663] – [666], [681], [683]. This process was developed in the 1950s and is suitable for carbon dioxide absorption as well as for treating hydrogen sulfide gases. Among the several tested and used activators arsenic trioxide proved to be the most efficient (an increase of efficiency a the factor of 10 – 12 compared to non promoted potash). It also acted as a corrosion inhibitor. Arsenic-promoted Giammarco – Vetrocoke systems were used in quite a number of ammonia plants. Because of its toxicity and for environmental reasons the arsenic was later replaced by glycine in a concentation of 30 – 50 g/L with vanadium compounds added as corrosion inhibitor. A two-stage process with intermediate flash and lean and semi-lean solution circle is normally used.

LRS 10 of British Gas [675], [676], [681]. This new activator combination for hot potash systems was commercially introduced in 1988 and since then used in 30 plants which include ammonia, LNG, hydrogen and vinyl acetate. A corrosion inhibitor is still used in the absorption solution.

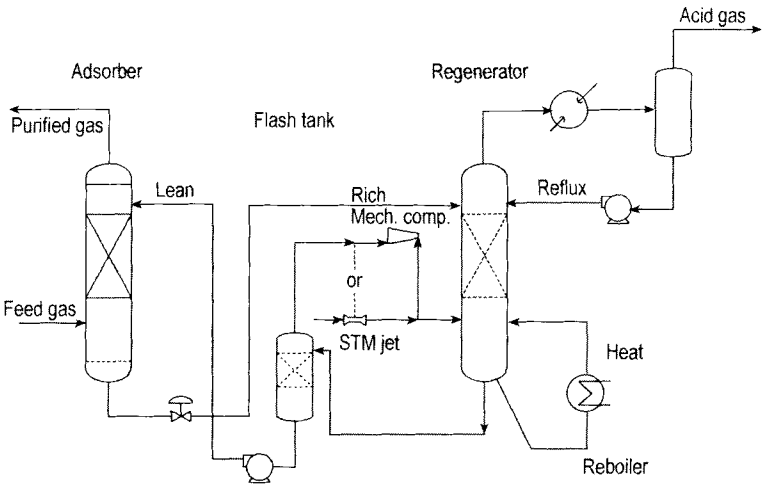

Figure 68. Catacarb single stage low heat design.

Exxon's Flexsorb process [669], [670] uses a sterically hindered amine as an effective promoter of a hot potash system. A lower energy requirement and less solution makeup than in other processes are claimed. So far it has been successfully used in several large plants.

Other hot potash processes offered are the **Carbosolvan process** [671] and the **SPIC process** [681].

4.3.1.2.2. Ethanolamine-Based Systems

MEA Process. Some organic compounds of the group of ethanolamines with the general formula $R_nN(C_2H_5OH)_{3-n}$ where R is H or an aliphatic group, have been successfully used as aqueous solutions in CO_2-removal systems. Very important was for a long time monoethanolamine (MEA), which was introduced in 1943 for the purification of ammonia synthesis gas. It actually was the first solvent to substitute water scrubbing and it remained for a long time, until the less energy consuming MDEA and hot potash processes were developed. In fact practically all of the 600 to 1000 t/d single-train ammonia plants used this solvent for CO_2 removal. The chief merits of MEA was that a rather low residual carbon dioxide content in the treated gas could be achieved in a very simple and inexpensive process configuration, but admittedly at the expense of very high energy consumption in form of low-level steam for solvent regeneration. But energy (natural gas consumption) was not a matter of concern in those days. The basic disadvantage of the system was that the carbamate formed in the absorption solution (depending on CO_2 loading and MEA concentration in water) is extremely corrosive. On account of this corrosion problem, in early MEA units it was not possible to use MEA solution containing more than 20%. Union Carbide intro-

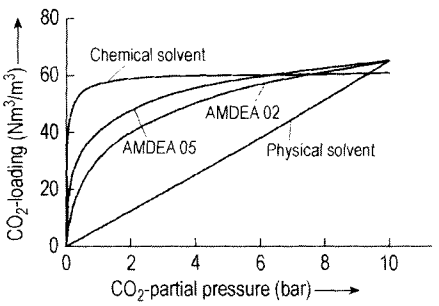

Figure 69. CO_2-loading capacity of various solvents

duced a corrosion inhibitor, named *Amine Guard* by which dramatically reduced corrosion and the MEA concentration could be raised to 30%, resulting in higher CO_2 loading of the solvent. As can be drawn from Table 32, the energy saving achieved thereby was considerable. Today there are worldwide quite a number of MEA units still in operation, which are increasingly being revamped to more efficient processes, e.g. aMDEA. For new installations the MEA technology has become obsolete.

A leading process today is the **BASF Activated MDEA process (aMDEA).** [684]–[690]. The process uses an aqueous solution of the tertiary amine methyldiethanolamine (MDEA) with a special amine activator. No corrosion inhibitors are necessary, and unlike MEA no solvent degradation is observed, so recovery installations are not required. Owing to the low vapor pressure of MDEA and the activator, there are no losses of the active solvent components. The carbon dioxide binds much less strongly to MDEA than to MEA, and the solvent character is more like a hybrid between a strong chemical and a purely physical solvent. On account of the relative weak binding forces, a substantial amount of carbon dioxide can be recovered simply by flashing to low pressure, and only a small amount has to be recovered by stripping. The process is very versatile: increasing the activator concentration shifts the character of the solvent more to the chemical side and vice versa, as illustrated by Figure 69. For example, highly activated MDEA 06 has a more chemical solvent behavior with high efficiency in absorption, but a more energy intensive regeneration, ideal for low-investment configurations and best suited revamps in which only the solvent is swapped. On the other hand, weakly promoted MDEA 01, with moderate adsorption efficiency and low energy requirement, is an excellent choice for purification of natural gas with high CO_2 partial pressure.

The possible process configurations include a wide rage of two- and single-stage designs, the latter allowing old MEA units to be revamped [689], [691]–[693] simply by swapping the solvent without changing the process equipment. Figure 70 gives a standard two-stage configuration normally used in modern low-energy ammonia plants. Table 33 gives examples of aMDEA process options.

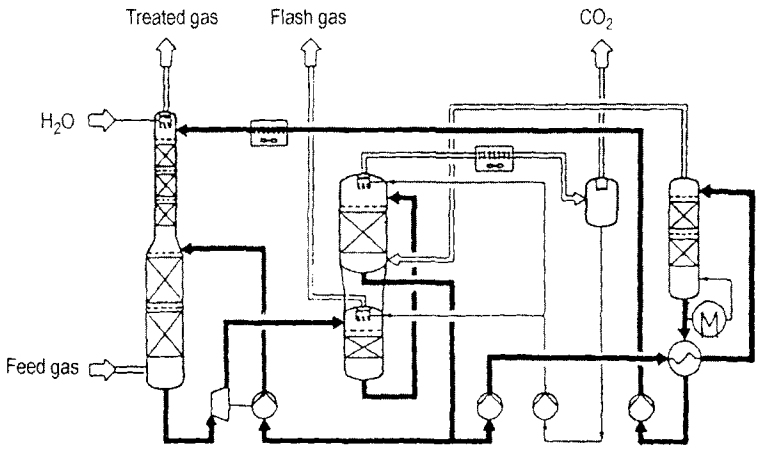

Figure 70. BASF aMDEA Process (Standard two-stage configuration)

Table 33. Examples of aMDEA process options in steam reforming ammonia plants:

	aMDEA 02 (two-stage)	aMDEA 03 (two-stage)	aMDEA 03 (one-stage)
Feed gas	100	100	100
CO_2 in feed, vol%	18	18	18
CO_2 in lean gas, vol%	0.1	0.1	0.1
Solvent circulation	102	100	43
(lean/semi-lean)	(12/88)	(12/88)	-
Packing height	180	100	52
(lean/semi-lean)	(47/53)	52/48	-
Reboiler duty	98	100	250
Specific energy, MJ/kmol CO_2	28.5	28	73

4.3.1.3. Physical Absorption Solvents

Selexol Process (UOP) [667], [694]–[703]. This process, originally developed by Allied Chemical and now marketed by UOP, uses polyethylene glycol dimethyl ether as solvent, which is stable, noncorrosive, not very volatile, but has a rather high capacity to absorb water. For this reason a relatively dry raw gas (dew point –5 °C) is required, which is achieved by chilling. The solvent is also suited for application in partial oxidation processes, as the solubility of H_2S is 8 times higher than that of CO_2, which allows the recovery of a pure CO_2 fraction and also a fraction rich in H_2S for producing elemental sulfur in a Claus plant, which will be described in more detail in the following section. To achieve a high CO_2 recovery rate, which is important when ammonia is to be converted to the maximum possible extent to urea, a 3-stage flash is used as shown in Figure 71. In the first step the solution is depressurized to an intermediate pressure to flash the less soluble gases. To minimize the CO_2 loss the flash gases are recompressed and recycled to the absorption column. The next flash drum is at about atmospheric pressure in which the medium-pressure solvent is flashed and more than 70% of the CO_2 is released. Then follows a vacuum flash in a third vessel,

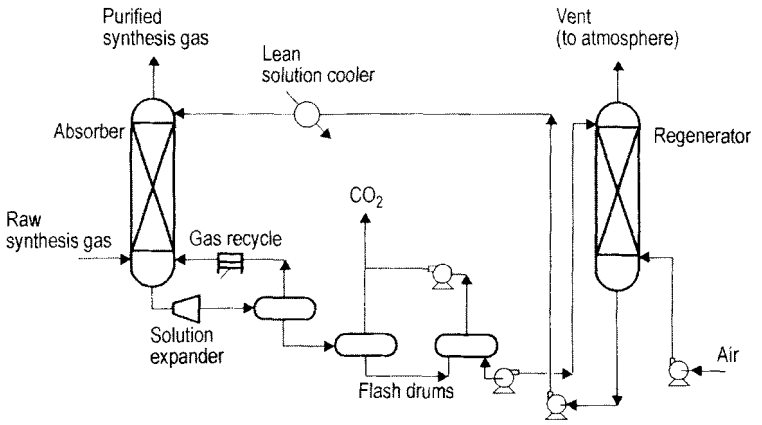

Figure 71. Selexol R: physical CO_2 absorption process (steam reforming gas)

after which the last traces of CO_2 are stripped out with air in a packed column. To avoid any loss of carbon – besides the small amount which goes with the lean gas to the methanation – the stripping air may be added to the process air of the secondary reformer. Practically no heat is required for regeneration, but for comparison with processes requiring regeneration heat, the mechanical power needed should be included.

The **Sepasolv MPE process (BASF)** [667], [685] is similar and uses polyethylene glycol methyl isopropyl ether. No commercial plants are in operation so far.

The **Fluor Solvent Process** [704]–[706], [708] is based on propylene carbonate, which has good chemical stability when used with sulfur-free gases, but is less suited for sulfur-containing gases in partial oxidation plants. The process configuration used for ammonia plants is similar to that of the Selexol plant, using several flash stages, and final air or nitrogen stripping for CO_2 recovery and solvent regeneration. Only a few commercial installations are known.

The physical solvents *methanol* (Rectisol process), *sulfolane* (Sulfinol Process) and *N-methylpyrrolidone* (Purisol) are preferentially used in the treatment of partial oxidation gases and will be described separately in the following section.

4.3.1.4. Sour Gas Removal in Partial Oxidation Processes

Raw synthesis gas produced by partial oxidation has a carbon dioxide partial pressure between 10 and 30 bar, depending mainly on feedstock and gasification pressure. In the lower half of this partial pressure range chemical solvents based on tertiary amines (e.g., MDEA) might be suitable in some cases, but at higher values physical solvents become increasingly preferable. In addition the presence of sulfur compounds, mainly H_2S along with a minor quantity of COS, introduces some complications for CO_2 removal from partial oxidation gases. Since the sour gases are both

soluble in the solvents and a separate recovery in the regeneration stage is only partially possible (only pure CO_2 can be obtained along with a CO_2 fraction more or less rich in H_2S), two principal plant flow sheets are possible. In one, a first scrubbing stage, which removes the sulfur compounds, is positioned upstream of the shift conversion. The second stage, removing pure CO_2, is located downstream of the shift reactors. This concept reduces the effort required to receive a highly concentrated H_2S fraction suitable for further processing in a **Claus** plant [709], [710] or a sulfuric acid plant. For systems which can not produce a CO_2 fraction with a H_2S concentration suitable for these gas-phase oxidations alternatively a liquid oxidation of the H_2S, e.g., the Stratford–Holmes process, could be applied for sulfur recovery. In another arrangement, which removes the sour gases after shift conversion and has to operate over dirty shift catalyst (see Section 4.2.2), the H_2S is diluted by a large amount of CO_2. This makes it even more difficult to design the regeneration step for producing a H_2S-rich fraction for downstream processing and a pure CO_2 fraction for urea or other uses.

The **Rectisol process** [667], [707], [711]–[715] seems to be the prime choice in partial oxidation plants. The process, invented by Lurgi and developed further by Linde, operates with chilled methanol, a cheap and readily available solvent, in which carbon dioxide, hydrogen sulfide and carbonyl sulfide (COS) are readily soluble at low operating temperatures of below –30 °C. The Henry absorption coefficient for H_2S is about six times higher than for CO_2.

The Rectisol process is very versatile and allows a number of different configurations. When used with the Shell partial oxidation process (Figure 54) a first scrubbing stage, which removes the sulfur compounds — and the of course the relatively low CO_2 content — from the gas is positioned upstream of the shift conversion. The second stage, removing the high amount of carbon dioxide formed in the shift conversion, is located downstream of the shift reactors. A different arrangement, used in the quench version of the Texaco partial oxidation process, has both seperation steps after the shift conversion, as shown in Figure 72.

After separation of the surplus steam as process condensate, the shifted gas is cooled in an ammonia chiller followed by additional condensate separation. The gas then passes the hydrogen sulfide absorber, where it is scrubbed with sulfur-free methanol pre-laden with CO_2. Next it enters the carbon dioxide absorber, where its carbon dioxide content is removed in different sections: in the top section, through which it passes last, it is washed with practically pure methanol from the hot regeneration stage. Additional sections use flash-regenerated methanol, and interstage cooling is provided to remove the absorption heat. Hydrogen sulfide enrichment in the hot regeneration stage is achieved by a special design involving a combination of flashing and reabsorption.

The applicability of the **Selexol process** for partial oxidation gases [568] was already mentioned. With high H_2S concentrations in the raw synthesis gas a H_2S rich fraction can be separated and fed to a Claus plant for production of elemental sulfur. At lower H_2S concentrations a liquid-phase oxidation has to be applied. As shown in the example of Figure 73, two H_2S-containing CO_2 streams are treated in separate

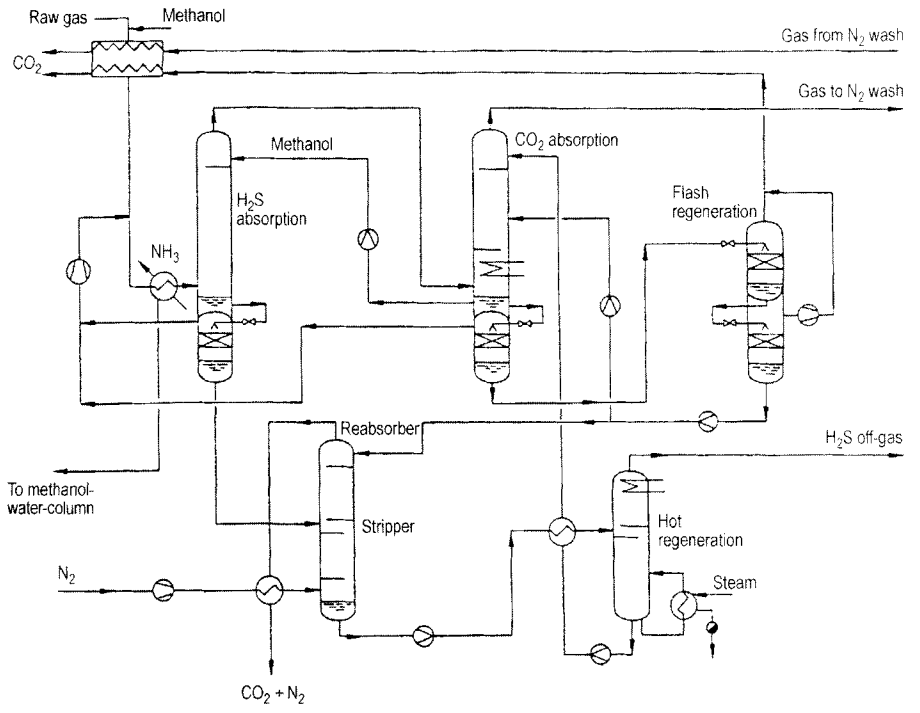

Figure 72. Rectisol sour gas removal used in Texaco Gasification process (quench type)

Stratford-Holmes liquid-phase oxidizers [716] which have a common regeneration to yield solid sulfur, which is filtered off. A COS hydrolysis stage has to be installed upstream of the sour gas scrubbing unit as Selexol does not remove this sulfur compound. The Stratford system uses a solution of vanadium salts in a higher oxidation state, which will oxidize the hydrogen sulfide to elemental sulfur. The carbon dioxide stream from low-pressure flashing contains, for example 0.8% H_2S and is purified down to 5 ppmv followed by a zinc oxide absorption to bring the content down to 0.1 ppmv, suitable for downstream processing (e.g., urea production). The other fraction from vacuum flashing and the stripper has a H_2S concentration of 4% (the example is based on a Texaco coal gasification gas). The tail gas from this oxidizer contains less than 160 ppmv H_2S and a smaller amount of COS as the hydrolysis step cannot remove it completely. The reduced vanadium salts are re-oxidized with air.

The **Lurgi Purisol process** [663], [717], [718], [726] uses *N*-methylpyrrolidone (NMP) as solvent and can be operated at ambient temperature or, with inclusion of a refrigeration unit, at temperatures down to −15 °C. The H_2S/CO_2 selectivity is superior to Selexol, permitting the production of a rich Claus gas with about 50% H_2S even at relatively low concentration of hydrogen sulfide in the raw gas. The solubility of COS is only 20% of that of H_2S, but it is largely hydrolyzed by the NMP. Preferred operating pressure is 45 to 85 bar. The process can, of course, be

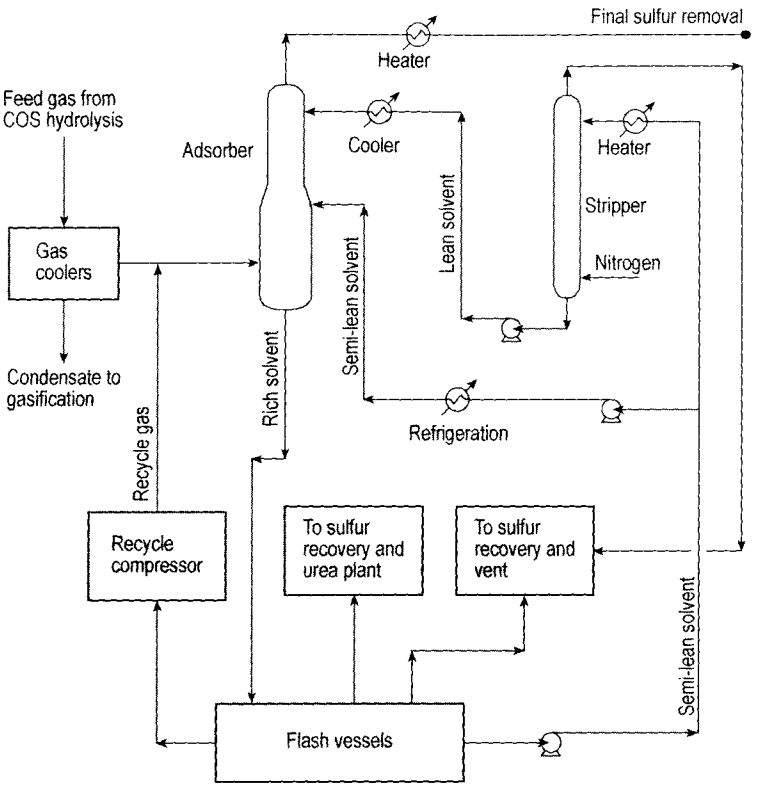

Figure 73. Selexol acid gas removal (partial oxidation gas)

applied in steam reforming plants, too, but in this case the raw gas (25 – 30 bar) is compressed after the LT shift to higher pressure before being fed to the Purisol absorber. Similar to Selexol, vacuum flashing and air stripping are used for solvent regeneration to achieve values below 1000 ppm CO_2 in the lean gas.

The **Sulfinol process** [719] – [722] cannot strictly be classified as a physical solvent process, as the solvent is a mixture of sulfolane (tetrahydrothiophene 1,1-dioxide), DIPA (diisopropanolamine), and water in a ratio of about 45 : 40 : 10. Sulfolane is a true physical solvent, whereas the DIPA is a chemically acting component. To achieve a higher CO_2/H_2S selectivity, DIPA may be substituted by MDEA (methyldiethanolamine) in the M-Sulfinol process. In partial oxidation process a concept with two separate Sulfinol units is preferred: the first ahead of the shift conversion (gas composition for example CO_2 5.4 vol %, H_2S 0.5 vol %), and the second one for recovery of sulfur-free CO_2after the shift conversion (feed gas for example CO_2 33 vol %, H_2S 0 vol %).

Surveys and additonal literature on the CO_2-removal processes are found in [723] – [734]; a theoretical analysis is given in [734].

4.3.2. Final Purification

After bulk removal of the carbon oxides has been accomplished by shift reaction and CO_2 removal, the typical synthesis gas in steam reforming ammonia plants still contains 0.2 – 0.5 vol % CO and 0.005 – 0.2 vol % CO_2. In partial oxidations the residual CO content after the shift conversion is usually higher, around 1.5 – 2.5 %. These compounds and any water present have to be removed down to a very low ppm level, as all oxygen-containing substances are poisons for the ammonia synthesis catalyst [735].

4.3.2.1. Methanation

Copper liquor scrubbing [737], for carbon monoxide removal, commonly employed in early plants has become obsolete and is now operated in only a few installations. Not only does it have a high energy demand, but it is also environmentally undesirable because of copper-containing wastewater. The choice today is methanation, which is by far the simplest method to reduce the concentrations of the carbon oxides well below 10 ppm and is widely used in steam reforming plants. It is actually the reverse reaction of steam reforming of methane:

$$CO + 3\,H_2 \rightleftharpoons CH_4 + H_2O\,(g) \quad \Delta H^0_{298} = -206\ \text{kJ/mol} \tag{91}$$

and

$$CO_2 + 4\,H_2 \rightleftharpoons CH_4 + 2\,H_2O\ (g) \quad \Delta H = -165\ \text{kJ/mol} \tag{92}$$

The advantages of simplicity and low cost more than outweigh the disadvantages of hydrogen consumption and production of additional inerts in the makeup gas to the synthesis loop.

The reaction is carried out over a supported nickel catalyst at a pressure of 25 – 35 bar in this section of the steam reforming plant and at a temperature of 250 – 350 °C. The required catalyst volume is relatively small. Under conditions where the reaction is limited by the intrinsic reaction rate, methanation activity is directly related to the nickel metal surface area formed on catalyst reduction. The function of the support is to provide a matrix on which the nickel crystallites can be finely dispersed and which also prevents sintering during prolonged operation. To achieve optimum size of the crystallites, in commercial methanation catalysts the nickel is normally incorporated by co-precipitation rather than by impregnation. To achieve a good balance between reducibility and sintering resistance, additional promoters are used. Nickel content is usually between 20 and 40 % [738]. Precious metals, especially ruthenium, have excellent methanation activity at very low temperatures (150 – 175 °C), but under conditions used in steam reforming plants they are no more effective than the standard nickel catalysts. Measurements showed that the methanation of CO_2 is slower than that of CO. A kinetic relation is given in Equation (93):

$$SV = \frac{k_{CO}\,P^{0.5}}{\log_{10}(CO_{in}/CO_{out})} \approx \frac{C\,k_{CO}\,P^{0.5}}{\log_{10}(CO_{2in}/CO_{2out})} \tag{93}$$

SV = space velocity, h^{-1}, P = pressure in psi absolute, k_{CO} = reaction rate for CO, C = constant ≈ 0.5.

If a breakthrough of carbon monoxide from the low-temperature shift or carbon dioxide from the absorption system occurs, the intensely exothermic methanation reaction can reach temperatures exceeding 500 °C very quickly [739]. For example, 1 % CO_2 breakthrough leads to an adiabatic temperature rise of 60 °C; 1 % CO increases the temperature by 74 °C [738]. Controls should be installed and other security measures taken to avoid these high temperatures because the catalyst may be damaged or the maximum allowable operating temperature of the pressure vessel wall exceeded. Catalysts containing nickel must not be exposed to gases containing CO at temperatures below 200 °C because of the risk of nickel carbonyl formation. $Ni(CO)_4$ is an extreme toxic substance, stable at low temperatures. Nitrogen blanketing of the methanator is advised in shut down operations [736].

Methanation as final purification for the raw gas from partial oxidation was proposed by Topsøe [739]. In this case the shift conversion is carried out in two stages with a special sulfur-tolerant shift catalyst followed by removal of hydrogen sulfide and carbon dioxide in an acid gas removal unit. Because of the potential danger of a sulfur break-through causing poisoning, the normal copper – zinc – alumina catalyst is usually not applied, which is surprising as the same risk exists in partial oxidation based methanol plants for the similarly composed methanol catalyst.

4.3.2.2. Selectoxo Process

The Selectoxo process (Engelhard) reduces the hydrogen consumption of the methanation system, as well as the inert gas content of the purified synthesis gas fed to the synthesis loop. After low-temperature shift conversion, the cooled raw gas is mixed with the stoichiometric quantity of air or oxygen needed to convert the carbon monoxide to carbon dioxide. The mixture is then passed through a precious-metal catalyst at 40 – 135 °C to accomplish this selective oxidation [740] – [743]. The carbon dioxide formed by the Selectoxo reaction adds only slightly to the load on the downstream carbon dioxide absorption system.

4.3.2.3. Methanolation

Methanolation [744], [745] has been proposed for partially replacing methanation. It converts the residual carbon oxides to methanol, preferably at higher pressure in an intermediate stage of synthesis gas compression. Methanol is removed from the gas by water scrubbing. The methanol may be recycled to the steam reformer feed or recovered as product. As full conversion of the carbon oxides is not achieved, a clean up methanation unit must follow the methanolation section.

4.3.2.4. Dryers

It is energetically advantageous to add the purified synthesis gas at a point in the synthesis loop where it can flow directly to the synthesis converter (see Section 4.5.1). For this reason water and traces of carbon dioxide must be removed from the makeup gas downstream of methanation. This is accomplished by passing the makeup gas through molecular sieve adsorbers, which can be positioned on the suction side or in an intermediate-pressure stage of the synthesis gas compressor.

4.3.2.5. Cyrogenic Methods

4.3.2.5.1. Braun Purifier Process

Cyrogenic methods are usually used for final purification of partial oxidation gases, but may be also incorporated in steam reforming plants. A prominent example for the application in a steam reforming concept is the Braun Purifier process [746]–[753].

The purifier is a cryogenic unit placed downstream of the methanator and its duty is to remove the nitrogen surplus introduced by the excess of air used in the secondary reformer of the Braun ammonia process (Sections 4.1.1.6 and 5.1.4.2). Additionally the inert level in the synthesis loop is reduced through this unit because methane is completely and argon is partially removed from the makeup gas. Another advantage of the process is that it separates the front-end and the synthesis loop, permitting the H/N ratio in the synthesis loop to be set independent of the secondary reformer. The purifier is a relatively simple unit composed of feed/effluent exchanger, a rectifier column with an integrated condenser and turbo-expander. At –185 °C methane and argon are washed out. The cooling energy is supplied by expansion of the raw gas over the turbo-expander (pressure loss about 2 bar) and expanding the removed waste gas to the pressure level of the reformer fuel.

4.3.2.5.2. Liquid Nitrogen Wash

Normally, for the partial oxidation processes, only a high-temperature shift conversion is used. This results in a carbon monoxide content of the gas after shift conversion of 3 vol % or sometimes somewhat higher. Liquid nitrogen wash [754]–[756] delivers a gas to the synthesis loop that is free of all impurities, including inert gases and is also the means for adding some or all of the nitrogen required for synthesis.

The nitrogen is liquefied in a refrigeration cycle by compression, cooling, and expansion. It flows to the top of a wash column, where it countercurrently contacts precooled synthesis gas from which most of the methane and hydrocarbons have been condensed. All of the cold equipment is installed in an insulated "cold box." The wash column temperature is about –190 °C. Liquid nitrogen wash systems are in operation at pressures up to 8 MPa corresponding to the highest gasification pressures. Careful surveillance of the inlet gases is required. As water and carbon dioxide in the inlet gas

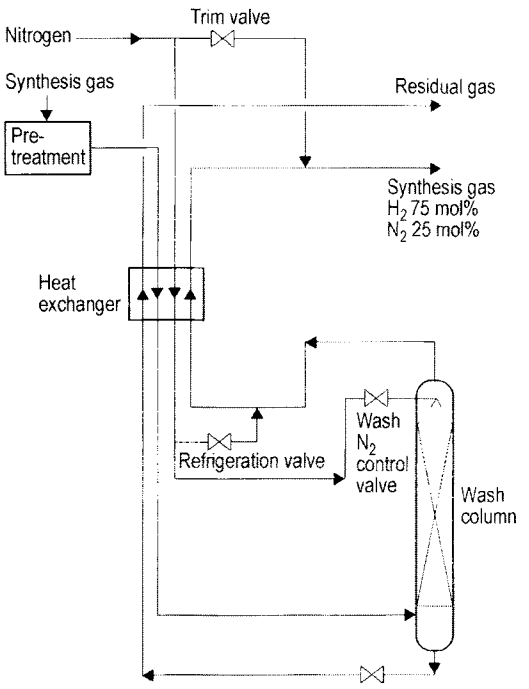

Figure 74: Liquid nitrogen wash

will freeze, causing operating difficulties, removal of these impurities down to a very low level is required. Traces of nitric oxide (NO) may react with olefinic hydrocarbons, causing explosions [757], [758].

Normally, an air separation plant is installed in conjunction with liquid nitrogen wash for economy in operation. In modern plants, the air separation and the nitrogen wash frequently are closely integrated with one another so that economies can be realized in the refrigeration system. Figure 74 is a simplified flow diagram of a liquid nitrogen wash.

4.3.2.6. Pressure Swing Adsorption

This process is actually more than a process just for final purification. It can be used to replace the LT shift conversion, carbon dioxide removal, methanation, and even the secondary reformer as well [404], [728], [759]–[762]. It uses molecular sieves as adsorbents in a series of vessels operated in a staggered cyclic mode changing between an adsorption phase and various stages of regeneration. The regeneration of the loaded adsorbent is achieved by stepwise depressurization and by using the gas from this operation to flush other adsorbers at a different pressure level in the regeneration cycle. The hydrogen recovery may be as high as 90 % depending on the number of adsorbers in one line, which may be as high as 10. Very high purity can be obtained, with about 50 ppm argon and less than 10 ppm of other impurities.

The process scheme for the ammonia plant may consist of production of pure hydrogen followed by separate addition of pure nitrogen from an air separation unit [763]–[765]. In a special version the nitrogen can be added in the PSA unit itself to increase hydrogen recovery [766]–[769]. In some processes it may also remove the excess nitrogen introduced with the process air fed to the secondary reformer, e.g. the LCA Process of ICI (Section 5.1.4.3). Since this technology has proven its reliability in rather large hydrogen plants for refineries it is now also used for world-scale ammonia plants, e.g., the Linde LAC process (Section 5.1.4.4).

4.4. Compression

4.4.1. Reciprocating Compressors

Up to the mid-1960s reciprocating compressors were used to compress the synthesis gas to the level of the synthesis loop, which was around 300 bar in the majority of the plants at that time. Higher pressures were used in a few installations, for example, in Claude and Casale units. Prior to about 1950 gas generation processes and shift conversion operated at essentially atmospheric pressure. The gas was first compressed to the level of the CO_2 removal section (usually 25 bar) and afterwards to around 300 bar for final purification (at that time usually copper liquor scrubbing) and synthesis. Reciprocating compressors with as many as seven stages in linear arrangement with intermediate cooling were used, whereby the CO_2 removal section was usually installed between the 3rd and 4th stages. Machines with a suction volume up to 15 000 m^3 (STP) for the first stage were not uncommon. Huge flywheels were designed as the rotors of synchronous motors (ca. 125 rpm) with two crankshafts on both sides connected over crossheads with the piston rod for the horizontally arranged stages. In some instances gas engines were used as drivers.

The rapid technical progress in the hydrocarbon based technologies of steam reforming and partial oxidation made it possible to generate the synthesis gas at a pressure level sufficient for the CO_2 removal operation. As gasification proceeds with a considerable volume increase and feedstocks such as natural gas are usually already available under pressure at battery limits, considerable savings in compression energy are achieved in this way.

Along with the introduction of pressure gasification, horizontally balanced compressors in which the cylinders are in parallel configuration on both sides of a common crankshaft became the preferred design. In these machines a good dynamic balance can readily be achieved, higher speeds are possible and also the use of asynchronous motors is possible. The low height of the arrangement has less severe requirements for foundations, allows simpler piping connections and facilitates maintenance. When gas engine drivers (two-stroke type) were used instead of electric motors, some designs applied a common crankshaft for the piston rods of the gas machine cylinders and

compressor cylinders. In a very few cases steam turbines with special speed reduction gears have been used. In smaller plants, the various compression services, e.g., natural gas, process air, and synthesis gas compression, were apportioned among the crankshaft throws in such a manner that a single compressor can perform all compression duties [770]. Further information on reciprocating compressors is given in [771] – [774].

4.4.2. Centrifugal Compressors

One of the most important features of the energy integrated single-stream steam reforming ammonia plant pioneered by M. W. Kellogg in 1963 was the use of centrifugal compressors for the compression duties of synthesis gas and recycle, process air, and refrigeration. From this time onwards application of centrifugal compressors became standard practice in most ammonia plants irrespective of the synthesis gas generation technology. The fundamental advantage of these machines are low investment (single machines even for very large capacities) and maintenance cost, less frequent shutdowns for preventive maintenance, and high reliability (low failure rate) [775]. In most cases the centrifugal compressors in ammonia plants are directly driven by steam turbines. This avoids the losses associated with generation and transmission of electric power. For this reason the overall efficiency of a plant with steam-driven centrifugal compressors is superior, although the centrifugal compressors are inherently less efficient than reciprocating units. A further advantage is that centrifugal compressors require only a fraction of the space needed for reciprocating compressors.

Manufacturing capabilities limit the minimum possible passage width (today about 2.8 mm) at the outer circumference of a centrifugal compressor impeller and this imposes a limit on the minimum effective gas volume leaving the last impeller. Unless the total volumetric gas flow has a reasonable relationship to the passage width of the last impeller and the pressure ratio, excessive pressure losses would occur within the passage and in the diffusers between the impellers, rendering the machine extremely ineffective. The first single-train ammonia plants with a capacity of 550 – 600 t/d had to lower the synthesis pressure to 145 – 150 bar to meet the required minimum gas flow condition. Today, with improved manufacturing techniques, the minimum gas flow from the last wheel is 350 m^3 for synthesis gas with a molecular mass of about 9 and an efficiency of around 75 %. This corresponds to a capacity of 400 t/d at 145 bar. As newer synthesis catalysts allow a pressure of 80 bar in the synthesis loop (ICI's LCA Process, Kellogg's KAAP) a centrifugal compressor could be used down to 220 t/d. Of course, for today's world-scale capacities of 1200 – 1800 t/d these technical limitations have no influence on the synthesis pressure, which even for plants with 1800 t/d is between 155 and 190 bar [402], [404], [776] – [778].

The tensile strength of the steels normally used to manufacture the compressor impellers allow a maximum wheel tip speed of about 330 m/s, which limits the pressure increase attainable by each impeller. A pressure increase, for example, from

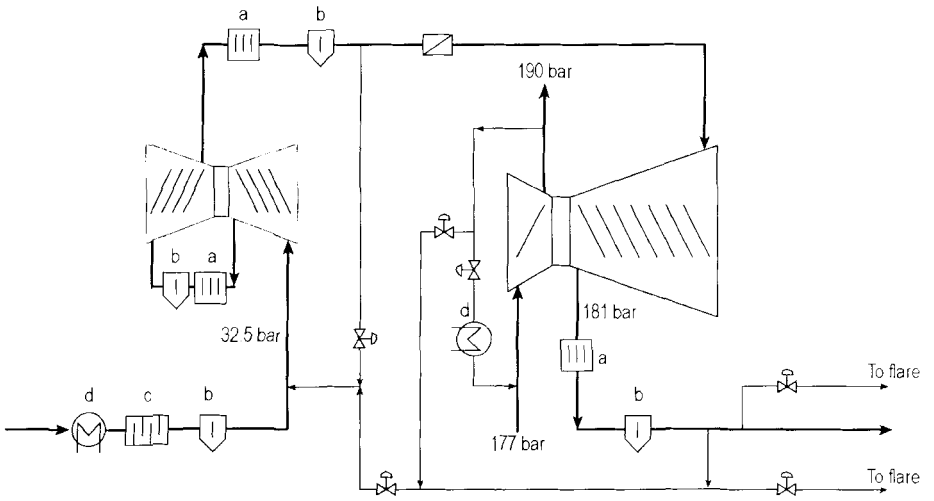

Figure 75. Centrifugal compressor for make-up and recycle gas compression of an ammonia plant (courtesy of Uhde)
a) Air cooler; b) Separator; c) Silencer; d) Water cooler

25 to 200 bar would require 18 – 20 impellers. However, a compressor shaft must have sufficient rigidity to avoid excessive vibration, and this limits the possible length such that a compressor shaft cannot accommodate more than eight or nine impellers. It is therefore necessary to arrange several compressor casings in series, with compression ratios from 1.8 to 3.2.

To overcome the pressure drop (5 – 20 bar) in the synthesis loop re-compression of the recycle gas is required. In practically all modern ammonia plants, the shaft of the final casing also bears the impeller for the compression of the recycle gas. Depending on synthesis configuration, mixing of make-up gas and recycle can be performed inside the casing or outside (three or four-nozzle arrangement; Fig. 77).

In older plants which used a reciprocating compressor for the recycle, a recycle cylinder was often mounted together with the other cylinders on the reciprocating frame. Sometimes special rotary compressors, so-called mole pumps were also used, with the unique feature that compressor and electric driver were completely enclosed in a common high-pressure shell. In old Casale plants, the makeup gas was introduced into the high pressure recycle loop and acted as the driving fluid of an injector which compressed the recycle gas.

Today modern plant concepts for world-scale capacity plants tend to limit the number of compressor casings to two. Figure 75 shows an example of the synthesis gas compressor of a large ammonia plant.

Geared or metal diaphragm couplings are used to connect the shafts of the individual casings (two in Figure 75). These flexible couplings prevent possible compressor damage resulting from slight misalignment and shaft displacement.

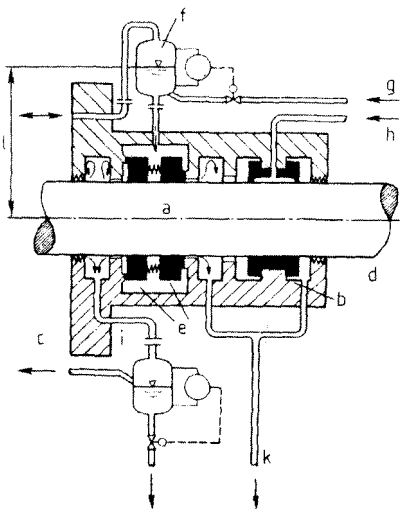

Figure 76. Liquid film shaft seal with cylindrical bushing for a high-pressure centrifugal compressor
a) Shaft; b) Bearing; c) Pressure side; d) Ambient side; e) Floating seal rings; f) Seal oil surge vessel; g) Seal oil; h) Lube oil; i) Drain to gas – oil separator; k) Drain to lube oil tank; l) Elevation for seal oil head

Sealing of the rotating shaft against the atmosphere is an important and demanding task. The high pressures and the high rotational speeds involved do not allow mechanical contact shaft seals. Usually, liquid-film shaft seals with cylindrical bushings (floating rings) are applied [779]. In this concept, an oil film between the shaft and a floating ring, capable of rotation, provides the actual sealing. The floating ring is usually sealed to the compressor casing by O-rings. Seal oil flows between both halves of the floating ring. Part of the oil returns to the reservoir, while the remainder flows against the gas pressure into a small chamber from which, together with a small quantity of gas, it is withdrawn through a reduction valve. Figure 76 is a schematic diagram of a liquid film shaft seal.

The seal oil pressure in the floating ring cavity must always be slightly higher than the gas pressure within the casing which is provided by static height difference of the oil level in the elevated oil buffer vessel. In this way normally no oil should enter into the synthesis gas. As the labyrinth section on the pressure side is connected with the suction side through an equalizing line, it is necessary to seal the compressor shaft towards the atmosphere only at suction pressure level.

Often, seal oil supply is combined with the lubricating oil system, with oil reservoir, filters and (in part) pumps in common.

Bearings. The high rotational speeds and the relatively large masses of the compressor rotors place high demands on the performance of the bearings. This is especially true for the thrust bearings, which must withstand high thrust forces. The minimum clearances necessary at the labyrinths and the impellers allow practically zero wear. Any wear resulting in friction could lead instantly to severe damage. For these reasons, in addition to measuring bearing temperatures, the axial position of the rotor and the radial vibrational deflections are continuously monitored by sensors. An increased vibrational amplitude is often an early indication of mechanical faults, such as rotor imbalance, bearing damage, occurrence of friction, or misalignment.

Dry (oil-less) gas seals represent an interesting concept for centrifugal compressors. Development dates back to 1969 and the first commercial application was in a natural-gas compressor in 1973. Since then they have been widely used in off-shore service [780]–[782]. Only recently have they gained acceptance in the ammonia industry, where several compressors for synthesis gas and refrigeration duty equipped with dry seals have been successfully placed in service. Nitrogen is used as an inert fluid for the seal, which is achieved at the radial interface of rotating and stationary rings. During operation the seal is not completely tight; some of the seal gas flows back to the suction side to be re-compressed, and a small amount from the suction side may go to the atmospheric side and is sent to the flare on account of its content of combustibles. During stops, when the shaft is not rotating, the seal ring is pressed tight against the seat by means of a spring and the differential gas pressure. Dry gas seals in combination with oil-lubricated bearings (dry/wet) have the advantage that a much smaller oil system is required and that there is no contact between oil and gas, which eliminates an emission source.

Magnetic Bearings. A new development, already in commercial service, but so far not used in ammonia plants, is magnetic bearings [780], [783]. Magnetic bearings promise a wider temperature range, are less prone to wear, are less prone to developing vibrations due to imbalance and require less maintenance. A combination of magnetic bearings and dry seals (dry/dry) could totally eliminate the oil system.

Integrated geared centrifugal compressors developed by DEMAG and GHH are a new development which might become of interest for plants of smaller capacity operating at lower pressure. The driver (e.g., a steam turbine) drives a common gear to which the individual compression stages are connected. Each stage has a single impeller which runs with very high speed, for example, 25 000 rpm or higher. Compressors with three or four stages are in operation, for example, a methanol synthesis compressor for 75 000 m^3/h and a pressure of 75 bar. It is likely that this concept can be extended to a final pressure of 120 bar with ammonia synthesis gas.

Compressor control is achieved basically by controlling the rotational speed of the driver, in modern plants often with the help of a distributed control system (DCS). If the volumetric flows through the machine at start-up or during reduced load operation deviate too far from the design values, it is necessary to re-circulate gas through individual stages or through the whole machine. Otherwise the compressor can enter a state of pulsating flow, called surge, which could cause damage. Anti-surge control (minimum by-pass control, kickback control) is designed to prevent this condition, as well as to minimize the incidence and degree of uneconomical re-circulation. A point of discussion is sometimes the minimum load at which the compressor can run without kickback, which means without loss of efficiency. Usually a load of 75 % is possible, and with special impeller design, the value may be lowered to 70 % but with a slight sacrifice of full-load efficiency.

Other compression duties in the plants, such as process air in steam reforming plants and air, and oxygen, and nitrogen compression in partial oxidation plants, are

also performed by centrifugal compressors. Also for the ammonia compression in the refrigeration section centrifugal compressors are normally in service. In some cases screw compressors have been used for this duty on account of their good efficiency and load flexibility, which is of interest in plants where the ammonia product is split between direct users at the site and cold storage in changing ratios.

Criteria for compressor selection and economic comparisons are discussed in [784]–[792]. Additional information is given in [793]–[806]. Operational problems, mechanical failures, repair and maintenance are described in a number of papers presented at the annual AIChE Ammonia Safety Symposia.

4.4.3. Compressor Drivers

Steam turbines. In modern plants the centrifugal synthesis gas compressors, including recycle, are almost exclusively driven by a steam turbines. These are generally extraction turbines with a condensing section. Steam is extracted at suitable pressure levels (e.g. 45–55 bar) to provide, for example, the process steam in steam reforming plants, and for other drivers, e.g., air compressor, ammonia compressor, boiler feed water pumps, and blowers.

As failures and breakdowns of these large rotary machines could lead to long and expensive repairs and to a corresponding loss of production it is advisable to keep the essential spare parts, for example, spare rotors, in stock. In older steam turbines, sometimes blade failures occurred, but this is no longer a problem due to improved blade design and shroud bands, which are standard today.

Gas turbines have also been used as drivers for compressors in ammonia plants. The exhaust may be used for steam production, for preheating duties, or as combustion air in the primary reformer [804], [807]–[811].

4.5. Ammonia Synthesis

Under the conditions practical for an industrial process ammonia formation from hydrogen and nitrogen (Eq. 94)

$$N_2 + 3\,H_2 \rightleftharpoons 2\,NH_3 \quad \Delta H = -92.44\ \text{kJ/mol} \tag{94}$$

is limited by the unfavorable position of the thermodynamic equilibrium, so that only partial conversion of the synthesis gas (25–35 %) can be attained on its passage through the catalyst. Ammonia is separated from the unreacted gas by condensation, which requires relatively low temperatures for reasonable efficiency. The unconverted gas is supplemented with fresh synthesis gas and recycled to the converter. The concentration of the inert gases (methane and argon) in the synthesis loop is controlled by withdrawing a small continuous purge gas stream. These basic features together

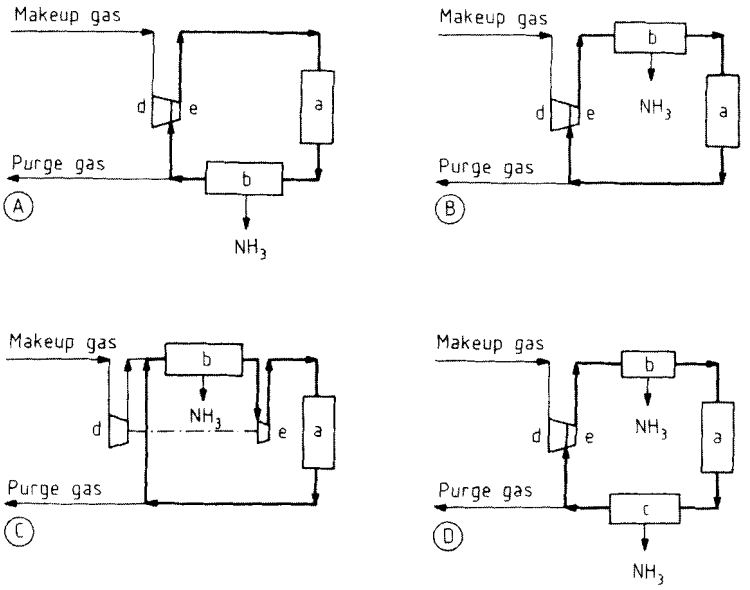

Figure 77. Schematic flow diagrams of typical ammonia synthesis loops
A) Synthesis loop for pure and dry makeup gas; B) Product recovery after recycle compression; C) Product recovery before recycle compression (four-nozzle compressor design); D) Two stages of product condensation
a) Ammonia converter with heat exchangers; b) Ammonia recovery by chilling and condensation; c) Ammonia recovery by condensation at ambient temperature; d) Synthesis gas compressor; e) Recycle compressor

with the properties of the synthesis catalyst and mechanical restrictions govern the design of the ammonia synthesis converter and the layout of the synthesis loop. Evaluation criteria are energy consumption, investment and reliability.

4.5.1. Synthesis Loop Configurations

A number of different configurations are possible for the synthesis loop. They can be classified according to the location of ammonia condensation and the point at which the makeup gas is introduced. Figure 77 shows the principal possibilities.

If the makeup gas is absolutely free of catalyst poisons, such as water and carbon dioxide (for example, after molecular sieve drying or liquid nitrogen wash), it can be fed directly to the synthesis converter (Fig. 77 A). After the gas leaves the synthesis converter, ammonia is condensed by cooling and the recycle gas is referred to the recycle compressor. This represents the most favorable arrangement from a minimum energy point of view. It results in the lowest ammonia content at the entrance to the converter and the highest ammonia concentration for condensation.

When the makeup gas contains water or carbon dioxide, advantage is taken of the fact that these materials are absorbed completely by condensing ammonia. This requires the condensation stage to be located partially or wholly between the makeup gas supply point and the converter. This arrangement has the disadvantage that the

ammonia concentration for condensation is reduced by dilution with the makeup gas. Also, at equal condensing temperature, a higher ammonia concentration exists at the inlet to the converter. Figure 92 B shows the simplest such configuration. An additional drawback of this arrangement is that all the ammonia produced must be compressed with the recycle gas in the recycle compressor.

The scheme shown in Figure 92 C, the frequently used "four-nozzle compressor", avoids this waste of energy. With this arrangement, recycle compression follows directly after condensing and separating the ammonia. In this configuration, it is possible to cool the recycle gas using cooling water or air immediately before admixing the makeup gas (i.e., before diluting the recycle gas) and thereby to reduce the energy expenditure for refrigerated cooling.

Splitting the cooling step for ammonia condensation also offers advantages when the recycle gas is compressed together with the makeup gas. This applies especially at synthesis pressures above about 25 MPa (250 bar). At these pressures, a greater portion of the ammonia formed can be liquefied by cooling with cooling water or air (see Fig. 92 D).

When ammonia-containing recycle gas and carbon dioxide containing makeup gas mix together under certain conditions of concentration and temperature, precipitation of solid ammonium carbamate can result.

In recent years, also as a retrofit in existing plants, molecular sieve drying of makeup gas has increasingly been applied in order to realize the energy-saving arrangement of the synthesis loop corresponding to Figure 92 A.

4.5.2. Formation of Ammonia in the Converter

The central part of the synthesis system is the converter, in which the conversion of synthesis gas to ammonia takes place. Converter performance is determined by the reaction rate, which depends on the operating variables. The effect of these parameters is discussed briefly in the following (see also Section 4.5.7).

With increasing pressure, ammonia formation increases (Fig. 78). This results not only from the more favorable equilibrium situation for the reaction, but also from the effect on the reaction rate itself. In industrial practice, there are plants that operate at about 8 MPa (80 bar), but there are also those that operate at more than 40 MPa (400 bar). Today, plants are built mainly for synthesis pressures of 150 – 250 bar. Typical operating parameters for modern synthesis loops with different pressures are listed in Table 34.

Converter performance decreases with increasing inert gas content (Fig. 79). The usual range is 0 – 15 vol %. For a secondary loop based on purge gas, it can be 30 % or more (see Section 4.5.6).

Converter performance also diminishes (Fig. 80) with increasing oxygen content of the synthesis gas. Today, a level of 10 ppm in the makeup gas, corresponding to about 3 ppm in the converter inlet gas, is usually, not exceeded (see also Section 3.6.1.5).

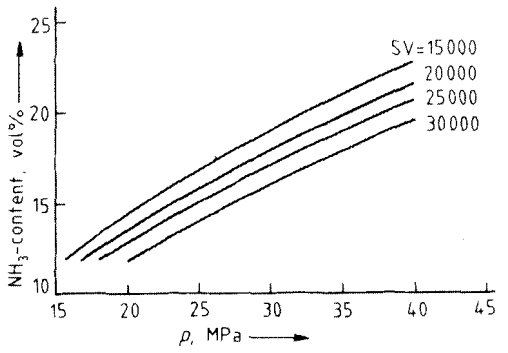

Figure 78. Performance for a four-bed quench converter as a function of operating pressure with space velocity (per hour) as parameter; 10% inerts in the inlet synthesis gas

Table 34. Typical operating parameters for modern synthesis loops at 140 and 220 bar (1000 t/d NH_3) [402, p. 226]

Parameters	Inlet pressure, bar	
	140	220
Inlet flow, Nm^3/h	500 000	407 000
Inlet NH_3 conc., mol%	4.1	3.8
Outlet NH_3 conc., mol%	17.1	19.9
Inlet inert conc., mol%	8.0	12.0
NH_3 separator temperature, °C	−5	−5
Relative catalyst volume	1	0.6

In contrast to the above-mentioned variables, the dependence of the converter performance on the H_2/N_2 ratio shows a true maximum (Fig. 81). The optimum conversion at high space velocity [SV = m^3 (STP) gas $h^{-1} \cdot m^{-3}$ catalyst] lies close to an H_2/N_2 ratio of 2 and approaches 3 at low space velocities. The reason is that equilibrium plays a greater role at low space velocities and has a maximum at a ratio of 3, except for small corrections [33] with regard to the behavior of real gases. Usually, the ratio is adjusted to 3, because in most plants, conversions near equilibrium are attained.

In practice, space velocities vary from about 12 000 h^{-1} at about 15 MPa (150 bar) to about 35 000 h^{-1} at about 80 MPa (800 bar). Usually, with increasing space velocity, the ammonia concentration in the effluent synthesis gas from a given converter does indeed go down (Figs. 78, 79, 81). However, the operating point normally chosen means that the increase in gas flow rate more than compensates for the reduced ammonia concentration. Thus, a still higher ammonia production rate is achieved. Plant operation often takes advantage of these phenomena. For example, this characteristic can be used to maintain ammonia production rate when the synthesis catalyst ages and its activity declines. Increasing converter flow rate and declining synthesis catalyst activity can reach a point, even with careful control, where the reaction "blows out" and production ceases. This occurs when the heat of reaction is no longer sufficient to provide the temperatures necessary for operation of the feed–effluent heat exchanger. The heat exchanger then fails to heat the cold converter feed gas to the required reaction "ignition" temperature. Achieving maximum ammonia production requires operating in the neighborhood of this "blow out" point, in turn requiring very

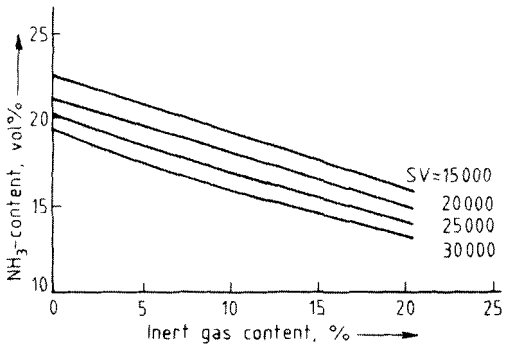

Figure 79. Performance of a converter as a function of inlet inert gas (CH_4 and Ar) content with space velocity (per hour) as parameter, inlet NH_3 content is 3.5 %; 30 MPa pressure; catalyst particle size is 6 – 10 mm

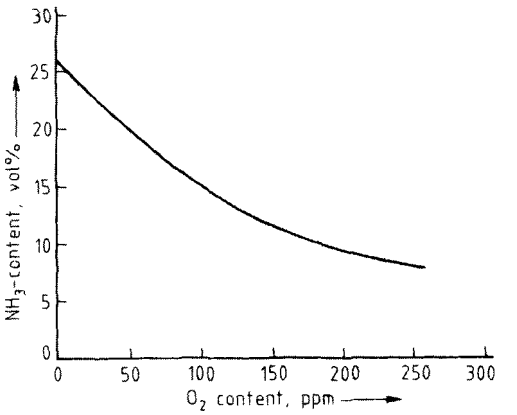

Figure 80. Performance of a converter as a function of oxygen content (all oxygen-containing impurities) in the inlet synthesis gas

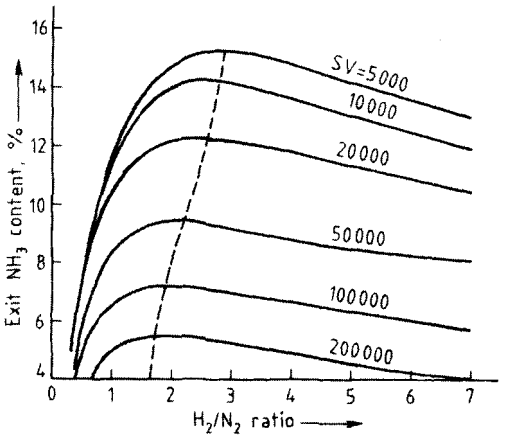

Figure 81. Ammonia conversion as a function of hydrogen/nitrogen ratios in the inlet synthesis gas with space velocity (per hour) as parameter; 9.7 MPa pressure [811]

careful control [812] – [814]. If the synthesis converter is to be operated in this region, then it is advisable to oversize the converter feed – effluent heat exchanger system to attain a higher degree of control stability.

Converter Design. Design of ammonia synthesis reactors is not just the calculation of the required catalyst volume; other parameters have to be considered, too, and for

some of them optimum values have to be found. This raises the question of the definition of optimum. In the early days with more strict material and fabrication-related limitations the converters were usually designed for minimum high-pressure volume, and this meant maximum use of the catalyst. Today the objective is to optimize the heat recovery (at the highest possible level) and to minimize the investment for the total synthesis loop.

The ammonia converter is a demanding engineering and chemical engineering task. To calculate the parameters for the design, including dimensions and number of catalyst beds, temperature profiles, gas compositions, and pressure drop, a suitable mathematical model is required.

Two differential equations describe mathematically the steady-state behavior of the reactor section of a converter. The first models the concentration – position relationship for transformation of the reactants to products, i.e., the reaction kinetic equation (Section 3.5). The second handles the temperature – position behavior of the reacting synthesis gas, the catalyst, and the vessel internals. The form of the latter is characteristic of the type of converter. The temperature profile depends not only on the rate of reaction heat evolution but also on the method and nature of the system for removing heat from the catalyst bed or beds. Additional equations describe the behavior of the separate feed – effluent heat exchanger system [815] – [819]. General information on converter calculations are given in [183], [818] – [820]. Computer programs and applications can be found in [821] – [825]. For a discussion of modeling of different converter types, see [815] – [819], [825], [826]. Models for multibed quench converters are described in [825] – [832]. Tubular reactors are treated in [833] – [840]. The individual effects of the operational parameters are evaluated in [33], [253], [840].

The reaction temperature profile is of particular importance because the reaction rate responds vigorously to temperature changes. Figure 82 plots lines of constant reaction rate illustrating its dependence on temperature and ammonia concentration in the reacting synthesis gas. The line for zero reaction rate corresponds to the temperature – concentration dependence of the chemical equilibrium. From Figure 82 it is apparent that there is a definite temperature at which the rate of reaction reaches a maximum for any given ammonia concentration. Curve (a) represents the temperature – concentration locus of maximum reaction rates. To maintain maximum reaction rate, the temperature must decrease as ammonia concentration increases.

If the objective in design or operation were optimizing catalyst utilization, then Figure 82 shows that the converter temperature – composition profile should follow curve (a), which corresponds to maximum reaction rate at all points. It is also obvious that in reality this "ideal" temperature – concentration profile cannot be achieved. For example, a synthesis gas with about 3 % ammonia concentration entering the converter cannot be heated to the "ideal" temperature by heat exchange because the very high temperature required does not exist in the converter system. To reach the "ideal" temperature, the first portion of the catalyst must initially operate adiabatically. Consideration of the service life of the catalyst requires that this maximum initial temperature not exceed that recommended by the manufacturer, usually 530 °C (cf. Section

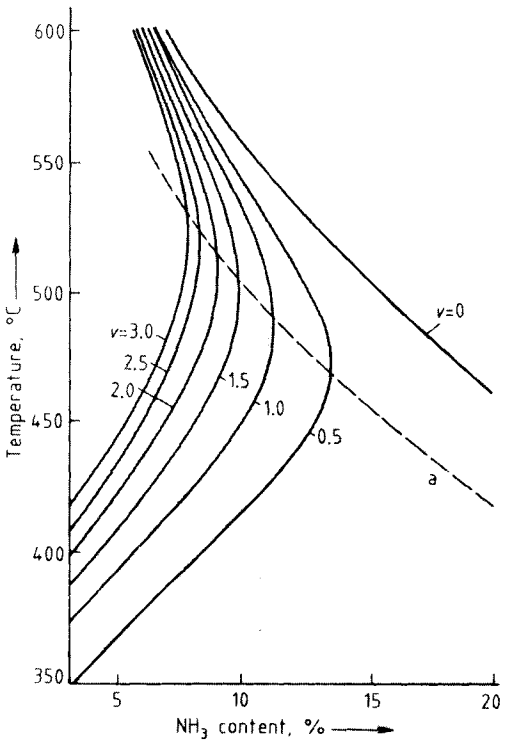

Figure 82. Nitrogen reaction rate r in m^3 $NH_3/(m^3$ catalyst · s) as a function of temperature and ammonia concentration at 20 MPa pressure and 11 vol% inerts in the inlet synthesis gas
a) locus of temperatures resulting in maximum reaction rate at a given ammonia concentration

3.6.1.4). Following this initial adiabatic temperature rise, it is possible to minimize the required catalyst volume by cooling the reacting synthesis gas such that, as ammonia formation progresses, the temperature follows curve (a). In the days when converters were designed to operate at very high pressures and temperatures and before the advent of improved construction materials, the converter design represented a real limitation on plant capacity. To maximize converter output and plant capacity to achieve the most favorable overall manufacturing cost, it was necessary to optimize catalyst utilization. A converter temperature–concentration profile was often compared to the "ideal" for optimum usage of high-pressure vessel and catalyst volumes [841], [842].

4.5.3. Commercial Ammonia Converters

4.5.3.1. Principal Converter Configurations

Commercial converters can be classified into two main groups:

1) Internally cooled with cooling tubes running through the catalyst bed or with catalyst inside the tubes and the cooling medium on the shell side. The cooling

medium is mostly the reactor feed gas, which can flow counter- or cocurrently to the gas flow in the synthesis catalyst volume (*tube-cooled converters*).

2) The catalyst volume is divided into several beds in which the reaction proceeds adiabatically. Between the individual catalyst beds heat is removed by injection of colder synthesis gas (*quench converters*) or by indirect cooling with synthesis gas or via boiler feed water heating or raising steam (*indirectly cooled multibed converters*).

The gas flow can have an axial, cross-flow or radial flow pattern. The different cooling methods can be combined in the same converter.

The severe conditions of high pressure, high temperature, and high hydrogen partial pressures place strict requirements on the construction materials and design for both groups. For example, almost all converters consist of an outer pressure vessel containing a separate inner vessel housing the catalyst and other internals, such as gas distributors and heat exchangers. Relatively cool converter feed gas flows through the annular space between the outer pressure shell and the internal "basket". This shields the outer shell from the high-temperature "basket", permitting use of comparatively low-alloy chromium–molybdenum steels for its construction. Often, part of the converter feed–effluent heat-exchange system surface is placed within the converter pressure shell. By this means, the nozzle penetration through the pressure shell for the converter effluent gas is also maintained at relatively low temperature. Today, this latter feature is not always necessary; the state of the art in converter construction materials now allows design of exit nozzles for the maximum anticipated temperatures, i.e., up to about 530 °C. References [843] and [844] review some literature on ammonia converters.

4.5.3.2. Tube-Cooled Converters

To remove the heat evolved in the synthesis reaction, the converters have cooling tubes in the catalyst beds. With these tubes, the heat is transferred to the converter feed gas to heat it to the reaction ignition temperature or to an external cooling medium. The known designs for such converters are suited only for small production capacities and therefore currently of limited interest. When designed to utilize the heat of reaction for heating the converter feed gas, such converters have the further disadvantage that temperature control is sluggish and temperature oscillations dampen out very slowly, if at all, a phenomenon called "hunting".

Countercurrent Design. Typical of such converters is the countercurrent design of the *Tennessee Valley Authority (TVA)* [812], [838], [842], [845]–[850]. Part of the feed gas to this unit enters the converter at the top and flows down through the annular space between the pressure shell and the basket. The main gas flow enters the converter at the bottom and joins the shell cooling gas. The mixture is heated to about 200 °C in an internal exchanger located beneath the catalyst bed. The gas then enters the cooling tubes that run through the catalyst bed (Fig. 83 A). There it absorbs the heat released in the reaction and reaches the required reaction ignition temperature of

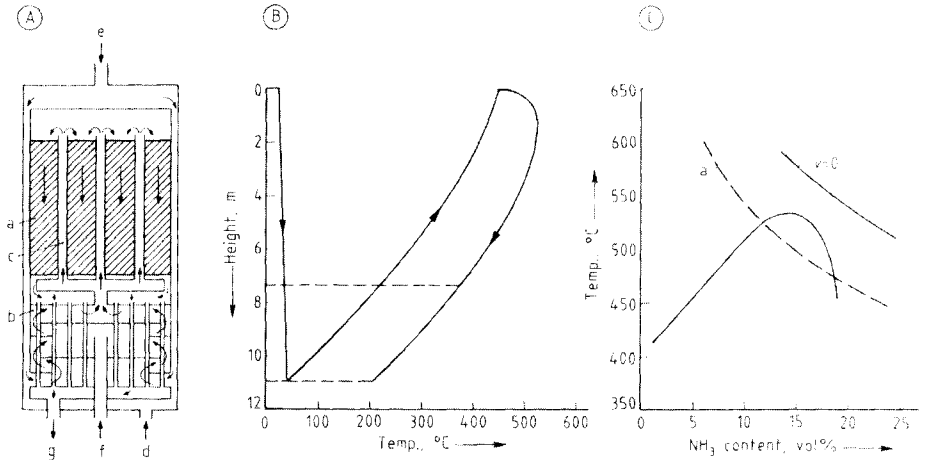

Figure 83. Countercurrent tube-cooled converter (TVA converter) [842]
A) Converter layout; a) Catalyst; b) Heat exchanger; c) Cooling tubes; d) Main gas inlet; e) Vessel wall cooling gas inlet; f) Temperature control gas (cold-shot) inlet; g) Gas exit
B) Gas temperature profile through the converter; C) Ammonia concentration versus temperature (cf. Fig. 82)

about 400 °C. The reaction begins almost adiabatically in the catalyst bed. As the reacting gas temperature rises, the temperature difference between the reacting gas and the cooling tubes increases, resulting in increasing heat removal (Fig. 83 B). As the reacting gas reaches the bottom of the catalyst bed, the rate of reaction begins to decrease sufficiently, because of high ammonia concentration, that cooling predominates and the temperature of the reacting gas begins to fall. Figure 83 C shows the converter temperature–concentration profile. The reaction temperature at first somewhat exceeds that for maximum reaction rate but eventually falls below curve (a). Cold converter feed gas can be admitted at a point within the internal heat exchanger to control both the total system and reaction temperature profiles through bypassing. *Casale* has employed a similar converter design concept [851].

Other tube-cooled converters with countercurrent flow are the *Mont Cenis reactor* [848], [852], [856], the original *Haber–Bosch reactors* [854], the *Claude converter* [856], [857], and the older Fauser design [852]. These converters were all used in relatively small plants and are now obsolete.

An interesting rebirth of the countercurrent principle is the new *ICI tube-cooled converter* used in the LCA process.

Recently a rather unique concept was developed by a *Fast Engineering Ltd.* in Russia [859]. The catalyst bed of the radial flow reactor is subdivided by cooling elements into several sections in a spiral-like configuration, as shown in Figure 84. In a revamp operation the existing converter of a 600 t/d ammonia plant in the Cherkassy production complex was equipped with a new basket having the innovative design filled with

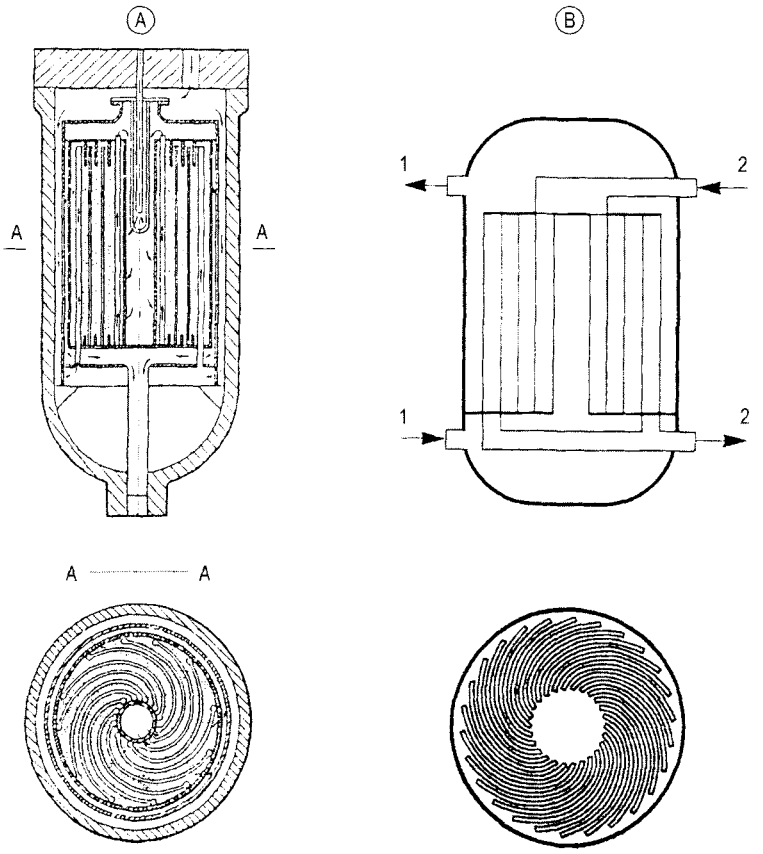

Figure 84. Tube cooled ammonia converter (Fast Engineering)

3 mm catalysts particles. The performance was in full agreement with the calculated characteristics of process kinetics, hydrodynamics, and heat transfer.

Cocurrent Design. The *Nitrogen Engineering Corporation (NEC) converter* applies cocurrent flow by means of bayonet tubes [842], [845], [847]–[849], [860]–[864]. This design places maximum heat-exchange temperature difference and thus thus maximum cooling performance at the catalyst bed inlet, the point of maximum reaction rate, and therefore maximum heat evolution. The intent is to obtain closer approach to curve (a) (cf. Fig. 85 C). Figure 85 A shows the general arrangement of the converter, catalyst bed, and heat exchanger; Figure 85 B, the temperature profile of the system. Chemico, a derivative of NEC, continued to apply such converters with only slight changes [852].

The converter of the Japanese Consulting Institute [867], [1495] combines a catalyst bed with co-current cooling tubes and adiabatic beds (Section 4.5.3.3). An older Uhde design uses U-tubes for cooling a single bed, having co-current and counter-current flow [853].

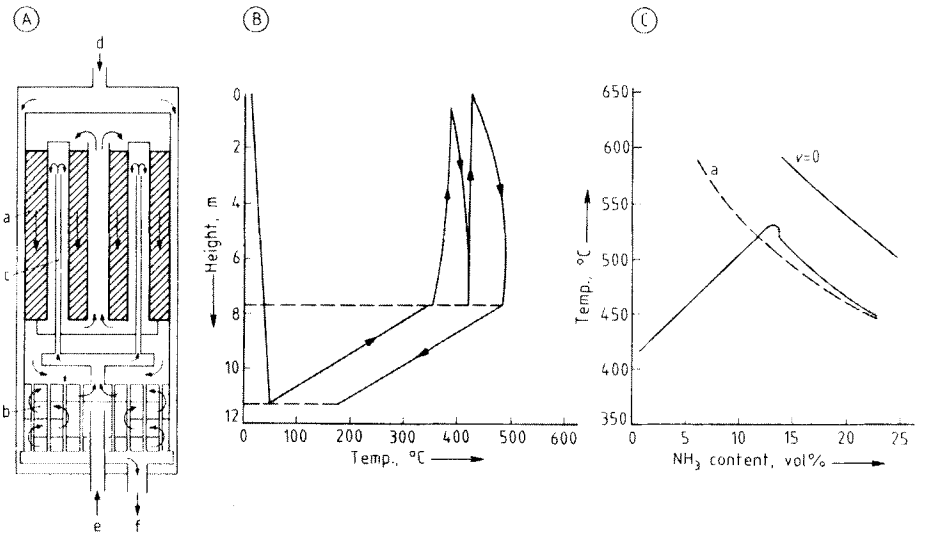

Figure 85. Cocurrent-flow tube-cooled converter [842]
A) Converter; a) Catalyst; b) Heat exchanger; c) Cooling tubes; d) Gas inlet; e) Temperature control gas (cold-shot) inlet; f) Gas exit
B) Gas temperature profile through the converter;
C) Ammonia concentration versus temperature (cf. Fig. 82)

4.5.3.3. Multibed Converters

Multibed Converters with Direct Cooling (Quench Converters). In quench converters cooling is effected by injection of cooler, unconverted synthesis gas (cold shot) between the catalyst beds. The catalyst beds may be separated by grids designed as mixing devices for main gas flow and cold shot, or be just defined by the location of cold gas injection tubes as for example in the ICI lozenge converter.

In this type of converter only a fraction of the recycle gas enters the first catalyst layer at about 400 °C. The catalyst volume of the bed is chosen so that the gas leaves it at ca. 500 °C (catalyst suppliers specify a maximum catalyst temperature of 530 °C). Before it enters the next catalyst bed, the gas is "quenched" by injection of cooler (125–200 °C) recycle gas. The same is done in subsequent beds. In this way the reaction profile describes a zig-zag path around the maximum reaction rate line. A schematic drawing of a quench converter together with its temperature/location and temperature/ammonia concentration profiles is presented in Figure 86.

A disadvantage is that not all of the recycle gas passes over the entire catalyst volume so that considerable ammonia formation occurs at higher ammonia concentration and therefore at lower reaction rate. Therefore a higher catalyst volume is needed compared to an indirectly cooled multibed converter. However, no extra space is required for interbed heat exchangers, so that the total volume of the high-pressure vessel will remain about the same as that for the indirectly cooled variant [865].

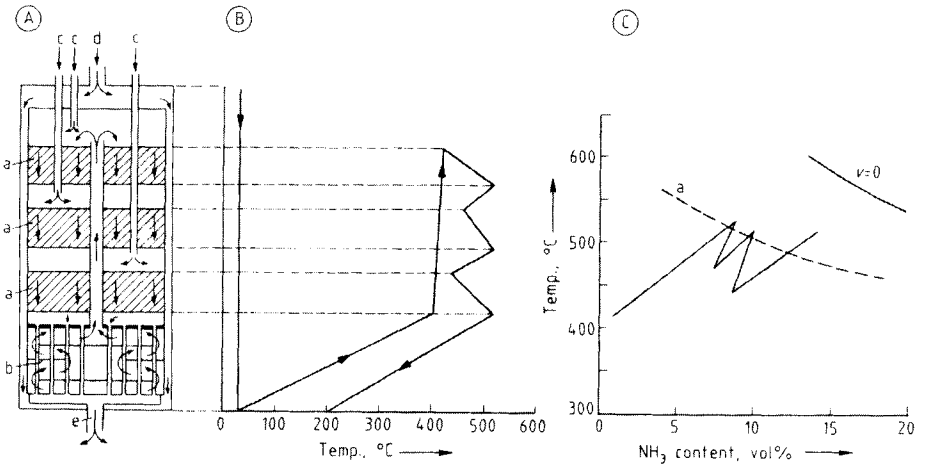

Figure 86. Multibed converter with quench cooling [864]
A) Converter; a) Catalyst; b) Heat exchanger; c) Quench gas inlets; d) Gas inlet; e) Gas exit
B) Gas temperature profile through the converter;
C) Ammonia concentration versus temperature (cf. Fig. 82)

As the quench concept was well suited to large capacity converters it had a triumphant success in the early generation of large single-train ammonia plants constructed in the 1960s and 1970s. Mechanical simplicity and very good temperature control contributed to the widespread acceptance. For example, M. W. Kellogg alone has installed more than 100 of its quench converters. Though being increasingly replaced by the indirect-cooling concept by revamp or substitution they are still extensively used. Descriptions of earlier designs of *Kellogg, BASF, and Uhde* can be found in [843]–[845], [866], [867].

The most important example is the *M. W. Kellogg three- or four-bed converter* [844], [868]–[870] (Figure 87). In this design, the catalyst "basket" is not easily removable from the pressure vessel. The catalyst can be changed by draining it at the bottom of the converter through "downcomers" that connect all catalyst beds with one another. The converter feed–effluent exchanger, attached to the top head, is designed for disassembly.

Other designs were used by *BASF* [844], *Casale* [844], *Chemico, Grand Paroisse* [843], *ICI* [867], *Uhde* [844], and others.

An interesting variant in this group is the *ICI lozenge converter* [280], [851], [868]. This design (Fig. 88) has a single catalyst bed that is divided into several zones (usually four) by quench gas distributors, through which colder recycle gas is injected evenly across the whole cross section of the catalyst bed. For this reason it is justifiable to classify this converter as a multibed type. The distributors consist of banks of transverse sparge pipes which deliver gas at regular intervals along their length. The spargers are in a void space within horizontal mesh-covered structures, whose cross section is lozenge shaped so that the catalyst particles can flow freely past them during loading and unloading. A special version of this reactor concept is the opposed flow

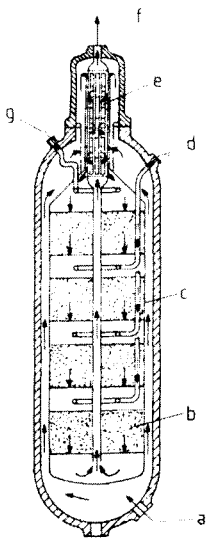

Figure 87. Kellogg four-bed vertical quench converter
a) Gas inlet; b) Catalyst bed; c) Basket; d) Quench; e) Interchanger; f) Gas outlet; g) Bypass

design [871], [872], suggested for very large capacities. In this configuration the converted gas is collected and withdrawn from the middle of the catalyst bed, with down-flow in the upper half and up-flow in the lower half of the catalyst bed. The uninterrupted catalyst bed is maintained in the opposed-flow converter. A design similar to that of ICI with direct injection of the quench gas into the single catalyst bed has been proposed by *Chemico* [873].

Converters with axial flow face a general problem: with increasing capacity the depth of the catalyst beds must be increased because for technical and economic reasons it is not possible to increase the bed diameter, and thus the pressure vessel diameter, above a certain limit. To compensate for the increasing pressure drop conventional axial flow converters have to use relatively large catalyst particles, which have the disadvantage of lower activity compared to smaller particles mainly on account of diffusion restriction. *Radial gas flow* in the converter avoids this dilemma, and with this concept it is possible to design converters for very large capacities without excessive diameters and with low pressure drop, even with small catalyst particle size. The advantages of radial flow are discussed in [874]–[877]. Radial flow has been also applied in tube-cooled converters [878]. The first radial flow converter introduced commercially and then widely used was the *Topsøe S 100 converter* [844], [852], [868], [879]–[884], which has two catalyst layers with a catalyst particle size of 1.5–3 mm. Figure 89 shows a schematic of the converter [402].

The major part of the gas enters the vessel at the top and flows down as shell cooling gas. It then passes through the feed–effluent heat exchanger and flows upwards through a central pipe to the first catalyst bed, which is traversed from the inside to the outside. After the effluent from the first bed has been quenched with cooler recycle gas, it enters the second bed and passes through it in the inward direction. The cold gas enters through the bottom of the vessel and is mixed with the inlet gas to the first bed for temperature control.

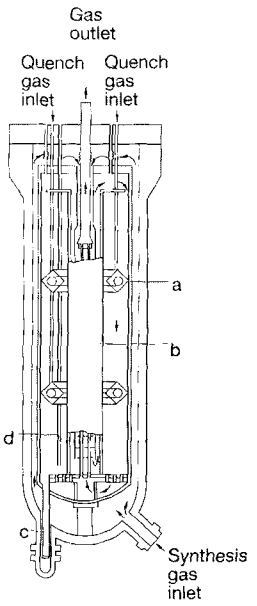

Figure 88. ICI lozenge converter
a) Quench gas distributors; b) Heat exchanger; c) Catalyst discharge nozzle; d) Tube for thermocouples

Radial flow quench converters have also been used by *Chemoproject* [885], *Österreichische Stickstoffwerke* [886], and *Lummus* [887].

Axial–radial flow pattern was introduced by Ammonia Casale. Converters with strictly radial gas flow require mechanical sealing of the top of each catalyst bed and dead catalyst volume with little or no flow to avoid bypassing of the catalyst. In the Casale concept there is no need for a dead catalyst zone as the annular catalyst bed is left open at the top to permit a portion of the gas to flow axially through the catalyst. The remainder of the gas flows radially through the bulk of the catalyst bed. As shown in Figure 90 this is achieved by leaving the upper part of the catalyst cartridge at outlet side unperforated so that gas entering from the top is forced to undergo partially axial flow.

Crossflow was chosen as a different approach by M. W. Kellogg in their horizontal quench converter to obtain low pressure drop even with small catalyst particles [843], [880], [881], [888]–[890]. The catalyst beds are arranged side by side in a removable cartridge which can be removed for catalyst loading and unloading through a full-bore closure of the horizontal pressure shell. As the cartridge is equipped with wheels it can be moved in and out on tracks, thus needing no crane. The gas flows vertically from the top to the bottom. The temperature difference between the top and the bottom requires special design measures to prevent uneven circumferential warming of the pressure shell and to avoid bending.

Multibed Converters with Indirect Cooling. In converters of this type cooling between the individual beds is effected by indirect heat exchange with a cooling medium, which may be cooler synthesis gas and/or boiler feed water heating and steam raising. The heat exchanger may be installed together with the catalyst beds

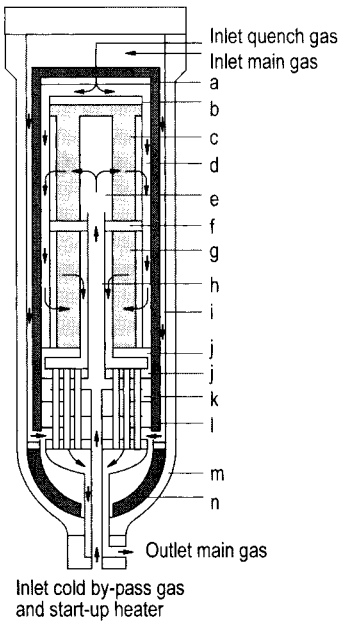

Figure 89: Haldor Topsøe S100 converter
a) Outer internal lid; b) Inner internal lid; c) First catalyst chamber; d) Inner annular space; e) Perforated center tube; f) Catalyst support plate 1; g) Second catalyst chamber; h) Transfer tube; i) Outer annular space; j) Catalyst support plate 2; k) Heat exchanger; l) Refractory fiber; m) Pressure shell; n) Refractory cement

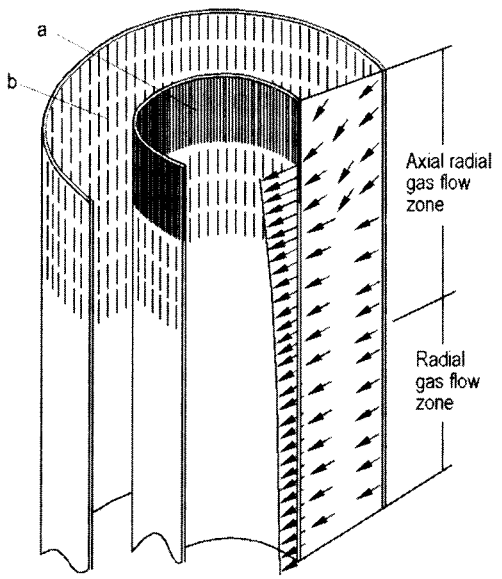

Figure 90. Ammonia Casale axial–radial flow pattern
a) Unperforated wall; b) Perforated wall

inside one pressure shell, but an attractive alternative, especially for large capacities, is to accommodate the individual catalyst beds in separate vessels and use separate heat exchangers. This approach is especially suitable when using the reaction heat for raising high-pressure steam. The indirect cooling principle is applied today in most large new ammonia plants, and also in revamps an increasing number of quench converters are modified to the indirect cooling mode. Figure 91 shows a schematic of

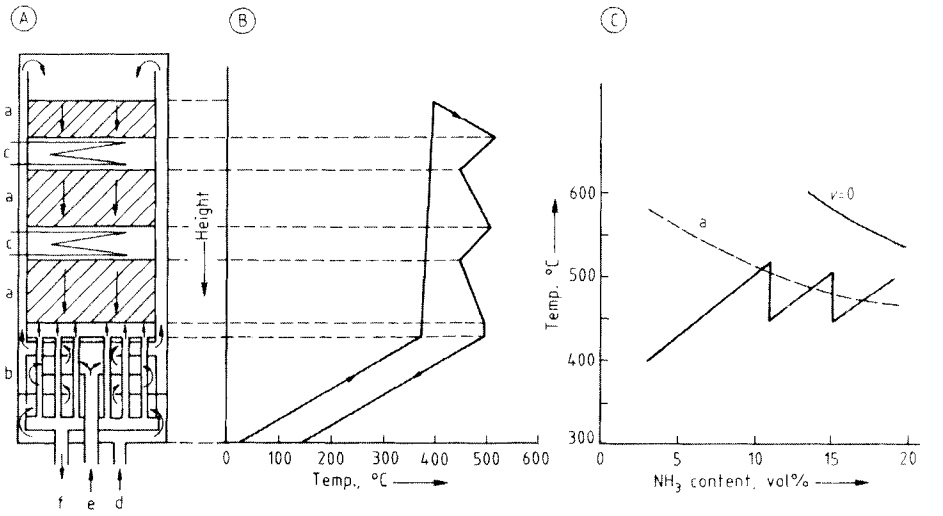

Figure 91. Multibed converter with indirect cooling
A) Converter; a) Catalyst; b) Heat exchanger; c) Cooling section; d) Gas inlet; e) Temperature control gas (cold-shot) inlet; f) Gas exit
B) Gas temperature profile through the converter;
C) Ammonia concentration versus temperature (cf. Fig. 82)

the principle together with temperature/location and temperature/ammonia concentration profile.

Converters with indirect cooling have been known since the early days of ammonia production, for example, the *Fauser–Montecatini reactor* [843], [844], [848], [867], [891]–[893]. In this converter, tube coils between catalyst beds transfer the reaction heat to a closed hot water cycle under pressure, operating by natural draft. The hot water releases the absorbed heat in an external steam boiler generating about 0.8 t of steam per tonne of ammonia at about 45 bar (ca. 250 °C).

In the well-known *Uhde–Chemie Linz converter* with three catalyst beds – described in various versions [841], [843], [844], [868], [894]–[897] – the indirect cooling is provided by converter feed gas. Feed gas enters at the top, passes down the annulus between basket and shell to cool the pressure wall, flows through the shell side of the lower feed–effluent heat exchanger, and then via the center pipe and interbed exchangers to the top of the first catalyst bed. The gas passes downwards through the catalyst beds and the tube side of the interbed exchangers and the lower heat exchanger to leave the reactor vessel. For trimming purposes a quench is foreseen.

Further development of the radial flow concept used in the quench converter Topsøe Series 100 has led to the successful launch of the *Topsøe Series 200* converter [623], [874], [898]–[904] designed for indirect cooling. Two versions are shown in Figure 92, with and without a lower internal heat exchanger. A "cold shot" ahead of the first catalyst bed is installed for temperature adjustment. In the converter without a lower

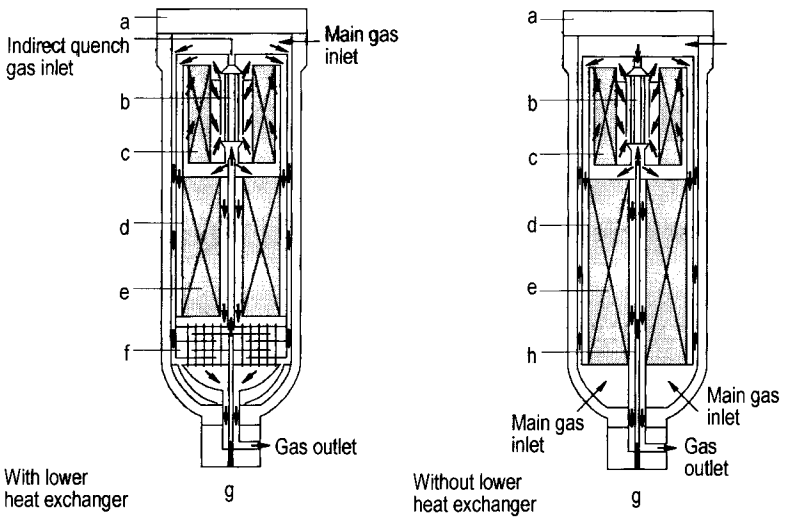

Figure 92. Topsøe Series 200 converter
a) Pressure shell; b) Interbed heat exchanger; c) 1st Catalyst bed; d) Annulus around catalyst bed; e) 2nd Catalyst bed; f) Lower heat exchanger; g) Cold bypass; h) Cold bypass pipe

exchanger the feed gas enters at the bottom and flows as pressure wall cooling gas to the top of the converter. After passing the centrally installed interbed exchanger on the tube side, the gas is mixed with cold gas for temperature adjustment and passes through the first catalyst bed radially from the outside to the inside. The exit gas flows through the shell side of the interbed exchanger before it enters the second bed, which is crossed in the same direction as the first one. Recently the *Topsøe Series 300 Converter*, which contains three catalyst beds and two central interbed exchangers in a single pressure shell has been commercialized.

Casale [905]–[910] has also successfully commercialized converters based on the axial–radial flow concept with indirect cooling.

Kellogg has re-engineered its *horizontal cross-flow* quench converter for *indirect cooling* [843], [888], [911]–[913] (Fig. 93). As in the quench version the pressure shell has a full-bore closure to remove the catalyst cartridge for loading and unloading. The reactor contains two catalyst beds, with the second one split into two parallel sections. Reactor feed gas passing between cartridge and shell is used to keep the pressure wall cool, and an inlet –outlet heat exchanger is located between first and second bed. A cold shot is installed for adjusting the inlet temperature of the first catalyst bed. A horizontal design with indirect cooling is also proposed in [914].

In the *C. F. Braun (today Brown & Root)* ammonia synthesis concept [915]–[920], separate vessels were used for the two catalyst beds of the original version. The feed–effluent heat exchanger was located between the first and second reactor vessel, and the second catalyst vessel was followed by a waste-heat boiler for high pressure steam. This basic concept was already introduced in the heyday of the quench converters and prior to the first energy crisis. Today Brown and Root uses three catalyst

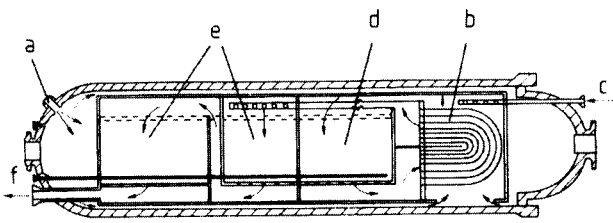

Figure 93. Kellogg horizontal intercooled ammonia converter
a) Inlet; b) Interbed heat exchanger; c) Bypass; d) Bed 1; e) Bed 2; f) Outlet

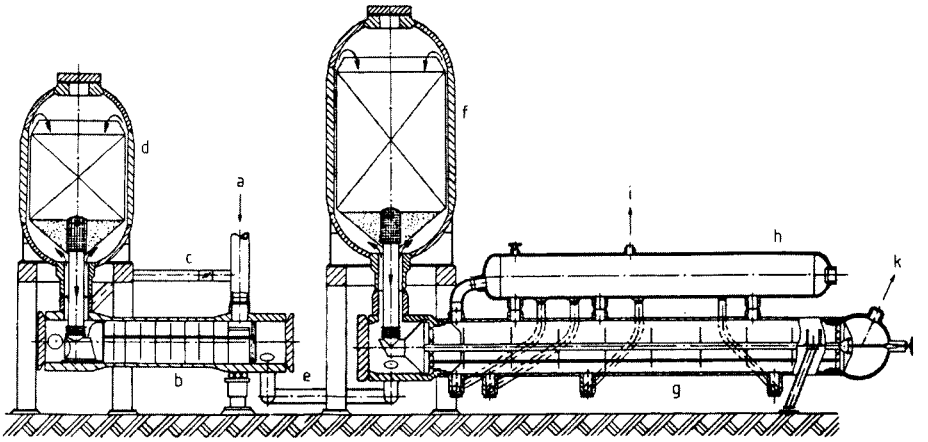

Figure 94: C. F. Braun converters with interbed heat exchanger and waste heat boiler
a) Gas inlet; b) Feed – first bed effluent exchanger; c) Bypass for temperature control; d) First bed; e) Line to second bed; f) Second bed; g) Waste heat boiler (Borsig); h) Steam drum; i) Steam outlet; k) Gas outlet

vessels [921] – [924] with boilers after the second and the third. The gas flow is axial and the mechanical design rather simple. Contrary to most converter designs, in which the pressure shell is kept below 250 °C by means of insulation or by flushing with cooler gas, the pressure vessel wall of the C. F. Braun reactors is at 400 °C, which is possible with modern steels in compliance with the Nelson diagram (see Chapter 8). Figure 94 shows the two-bed version of the C. F. Braun converter system.

To withstand the high outlet temperature level (450 – 500 °C) needed for the high-pressure boilers, a special design is employed to keep the outlet nozzle cool. Brown & Root has devised a good solution by direct coupling the boilers and the exchanger to the converter.

Uhde has used three catalyst beds for capacities up to 1800 t/d (Figure 99). The first two are accommodated in a single pressure vessel together with an inlet – outlet exchanger. Then a waste heat boiler generating high-pressure steam cools the gas before it enters the second vessel containing the third bed, which discharges through a second external high-pressure boiler. The gas flow is in radial mode in all three catalyst beds.

Topsøe has now introduced a hot-wall converter with only one catalyst bed and no internal heat-exchange equipment, similar to Brown & Root, but with radial flow. Three of these converters can be combined with an external heat exchanger and two

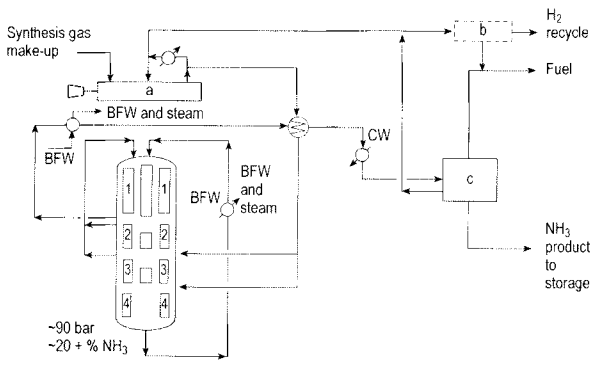

Figure 95. Kellogg advanced ammonia process (KAAP)
a) Compressor; b) PGRU; c) Refrigeration

high-pressure boilers to give an arrangement as described for Brown & Root. This *Topsøe Series 50 converter*, can also be combined with the Series 200 reactor and two external high-pressure boilers to attain the configuration as described for Uhde (Topsøe Series 250).

Kellogg has developed for its ruthenium catalyst based *KAAP ammonia process* [404], [478] a special converter design. Four radial flow beds are accommodated in a single pressure shell with intermediate heat exchangers after the first, second and third bed. The first bed is loaded with conventional iron catalyst, the following ones with the new ruthenium catalyst. Figure 95 is a simplified sketch of the converter and the synthesis loop of the KAAP for a new plant. For revamps Kellogg has also proposed a two-bed version completely loaded with ruthenium catalyst to be placed downstream of a conventional converter [398].

Optimizing the Temperatur Profile and Bed Dimensions in Multibed Converters is an important design aspect. With closer approach to equilibrium, the volume of catalyst required in the individual beds increases, requiring greater total catalyst volume and appropriate changes in the catalyst bed dimensions. The literature has frequently treated the problem of optimizing both the distribution of catalyst volume between a given number of beds and the bed inlet temperatures [815], [817], [842], [925] – [928]. Reference [929] examines optimizing the temperature profile in a given four-bed quench converter. For additional literature, refer to Section 4.5.2.

4.5.4. Waste-Heat Utilization and Cooling

The reaction heat of ammonia synthesis is 46.22 kJ/mol at STP, which corresponds to 2.72 GJ/t NH_3. Utilization of this heat at the highest possible temperature for generating high-pressure steam is a major contribution to the high total energy efficiency of modern ammonia plants [930]. Early converters, operating at about 300 bar, equipped with a lower heat exchanger for raising the inlet temperature for the (first) catalyst bed to the ignition temperature (ca. 400 °C) , received the converter feed at about ambient temperature and therefore had outlet temperatures of ca. 250 °C (ca. 15.5 °C per mol % of ammonia formed).

Initially there was practically no heat recovery, and nearly the total heat content of the gas down to ambient temperature and thus the reaction heat was transferred to cooling water. Subsequently plants were modified to use this heat to some extent, but the low temperature level allowed only boiler feed water heating and generation of low-pressure steam (ca. 20 bar). In some instances, water circulation was installed to use this heat in other plants or production steps. As for any type of converter the outlet temperature rises with increasing inlet temperature (ΔT is determined by the degree of conversion), in further developments an additional heat exchanger for converter feed versus the converted gas was installed, downstream of the above-mentioned heat recovery. In this way the temperature level at which heat could be recovered was increased, ultimately to the point where the inlet temperature to waste-heat recovery is equal to the outlet temperature of the last catalyst bed. In practice this corresponds to moving the lower heat exchanger (which in multibed converters exchanges feed to the first catalyst bed against effluent from the last bed) partially or completely to a position outside of the converter and downstream of the waste-heat recovery installation. In this way the waste heat downstream of the synthesis converter in modern plants is available in the temperature range around 480 to 290 °C. The steam pressure, formerly 100 bar, has now been raised to 125 bar, which means that the gas can be cooled in the boiler to ca. 350 °C; the remaining recoverable heat is used for boiler feed water heating.

The trend followed in newer plants is to increase conversion per pass with the result of higher ammonia outlet concentrations and lower outlet temperatures from the last bed. However, as optimum energy efficiency of the whole ammonia plant requires maximum high-pressure steam generation, part of the heat must be recovered before the reaction is completed in the reactor system. This can be accomplished [900], [901], [930], [931] by using three catalyst beds in separate pressure vessels with boilers after the second and the third vessel and an inlet–outlet heat exchanger for the first catalyst bed.

Advanced ammonia concepts produce as much as 1.5 t of high-pressure steam per tonne of ammonia, which correspond roughly to 90% of the standard reaction enthalpy. Figure 96 is a temperature–enthalpy diagram for a converter system corresponding to the original C. F. Braun arrangement. High-pressure steam (113 bar, 320 °C) is generated in this example after the second catalyst bed.

Appropriate design of waste-heat boilers is described in Section 4.6.

4.5.5. Ammonia Recovery from the Synthesis Loop

In all commercial plants ammonia is recovered from the synthesis loop by cooling the synthesis gas to condense the ammonia under synthesis pressure. The liquid ammonia product is separated from the gas, which is recycled. Arrangement and location of the ammonia separator(s), recirculation compression, addition of makeup gas and extraction of purge gas are discussed in Section 4.5.1 (see also Figure 77).

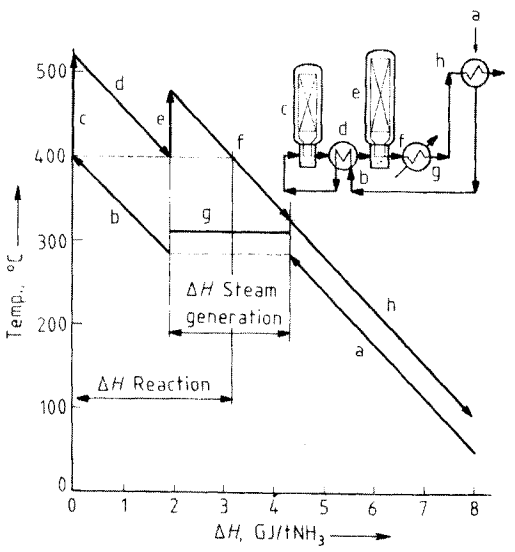

Figure 96. Temperature versus enthalpy diagram for a two-bed system with steam generation
a) Heating in main feed effluent exchanger; b) Further heating in feed – first bed effluent exchanger; c) Temperature rise in first bed; d) Cooling in feed – first bed effluent exchanger; e) Temperature rise in second bed; f) Cooling by steam generation; g) Temperature level of waste heat boiler; h) Cooling in main feed effluent exchanger

In high-pressure synthesis loops (> 450 bar) cooling by water and or air is sufficient to obtain the required low residual ammonia concentration in the gas. In more modern plants, which operate at moderate pressures, this cooling has to be supplemented by refrigeration, for which a mechanical ammonia refrigeration cycle, with one or more temperature levels is generally used. Refrigeration down to – 25 °C is used, which with inclusion of the necessary temperature difference in the chiller requires ammonia evaporation at about atmospheric pressure. The amount of ammonia vaporized (and consequently reliquefied by compression and water or air cooling) can be substantial. At a loop pressure in the range 100 to 150 bar the quantity of reliquefied ammonia may be twice the ammonia product flow.

The liquid ammonia of the high-pressure separator is flashed to about 20 bar, whereby the majority of the dissolved gases are released in the let-down vessel. This gas is normally used as a fuel, preferably after removal of ammonia vapor to avoid NO_x formation in the combustion furnace.

The ammonia from the let-down vessel may be sent directly to downstream users or flashed further to atmospheric pressure for storage in a cold tank. All ammonia vapors removed from flash gases and from purge gas by water scrubbing can be recovered as pure liquid product by distillation if there is no direct use for the aqueous ammonia.

Absorption refrigeration with aqueous ammonia instead of a mechanical refrigeration system [932] – [937] did not find widespread application.

Although ammonia condensation was already used in HABER's lab-scale ammonia plant and in early pilot plants of BOSCH, the first commercial units of BASF used ammonia absorption in water to remove the product from the cool synthesis loop gas, because various technical problems were encountered with refrigeration at that time. It was only in 1926 that ammonia condensation was introduced in the Haber – Bosch

plants. In the early 1920s LUIGI CASALE successfully used condensation for his first plant. Water cooling was sufficient on account of the very high synthesis pressure.

Recovery of ammonia by water scrubbing offers the advantage of achieving a very low residual ammonia content, but the drawback is that the whole recycle gas has to be dried afterwards and in addition distillation of aqueous ammonia is necessary to yield liquid ammonia. Nevertheless the scrubbing route was again proposed for a synthesis loop to be operated under extremely low pressure (around 40 bar) [938]. Snam Progetti [280], [939], [940] has proposed removing the ammonia from the loop gas at ambient temperature down to 0.5 mol% by absorption in dilute aqueous ammonia.

The extent to which the ammonia concentration in the gas can deviate from that expected for ideal behavior can be seen from Tables 4 and 5 (Section 3.1). For example, at 30 °C the ammonia vapor pressure according to Table 4 is 1.167 bar, corresponding to 5.84 mol% at the total pressure of 20 bar. In contrast, Table 5 gives the ammonia concentration in a 1/3 nitrogen/hydrogen mixture at 20 bar total pressure as 9.8 mol%.

Ammonia recovery by adsorption on solids has been also proposed [1498], [1499].

4.5.6. Inert-Gas and Purge-Gas Management

Apart from nitrogen and hydrogen, the fresh make-up gas supplied to the synthesis loop usually contains small quantities of inert gases. These include methane (from gas generation), argon (from the process air), and helium (from the natural gas). Because they are inert , they tend to concentrate in the synthesis loop and must be removed to maintain the loop material balance. A portion of the inert gases dissolves in the liquid produced in the ammonia separator. Solubility data are found in Section 3.1. Table 6 gives the solubilities for 3/1 hydrogen/nitrogen mixtures and can be used as a rough approximation. Figure 4 gives vapor–liquid equilibrium ratios for use in making precise calculations of the dissolved quantities of inerts. If the synthesis gas pressure is high, for example, 300 bar), and the inert gas concentration in the synthesis loop make-up gas low enough, for example, under 0.2 vol% [941], then dissolution in the product ammonia suffices to remove the inerts from the synthesis loop.

With a higher inert gas content in the make-up gas this method is not applicable, because the required partial pressure of the inert gas at equilibrium in the loop gas would become so high that a synthesis under moderate pressure would be virtually impossible. So, in addition to removal as dissolved gases (flash gas), inerts have also to be removed from the gas phase by withdrawing a small purge-gas stream from the loop. At the same time expensive synthesis gas is also lost from the loop, unfortunately associated with the loss of valuable hydrogen and nitrogen, which lowers the ammonia yield. Therefore, determining the appropriate inert gas concentration requires a precise economic calculation.

A high inert gas level has various drawbacks. It decreases the specific converter performance by reducing the hydrogen and nitrogen partial pressures. The gas recycle

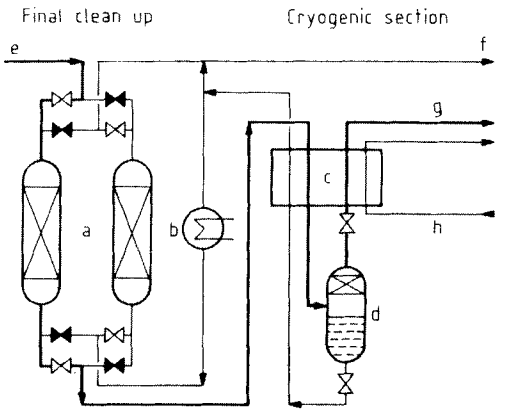

Figure 97. Simplified flow diagram of cryogenic hydrogen recovery unit
a) Molecular sieve adsorbers; b) Heater; c) Plate-fin exchanger; d) Separator; e) Ammonia-free purge gas; f) Fuel gas to reformer burners; g) Hydrogen product to syngas compressor; h) NH_3 refrigerant

flow is increased by the amount of inert gas. Piping and equipment must correspondingly be increased in size, and the associated power consumption for recycle gas increases. Moreover, there is an unfavorable effect on condensation of the ammonia product. Because of the dilution, less ammonia can be condensed from the recycle synthesis gas by less expensive air or water cooling or higher temperature level refrigeration.

There are several possibilities for reducing the losses associated with the purge gas. The most capital-intensive method consists of feeding the purge gas to a second synthesis loop operating at a slightly lower pressure [942], [943]. As this loop can operate at a very high inert level (40 % or more), only a very small final purge stream is necessary and no recompression is needed. Up to 75 % of the hydrogen from the first-loop purge stream can be recovered. This system has the advantage that nitrogen is also recovered, but it is too expensive for use in modern plants and revamps. For this reason other methods have been developed.

4.5.6.1. Hydrogen Recovery by Cyrogenic Units [944]

Ammonia is first removed from the purge gas by cooling or in a water wash operating at 7.5 MPa (75 bar). Molecular sieve adsorbers then eliminate moisture and traces of ammonia (Fig. 97). The dry, ammonia-free purge gas from the adsorbers next enters the cold box. Heat exchange with cold product hydrogen fraction and with gas rejected to fuel cools the purge gas to a temperature of about −188 °C. Partial condensation liquefies methane and argon as well as some of the nitrogen and helium. These are removed in a separator, leaving a hydrogen-rich gas.

The liquid flows through a control valve, reducing its pressure, and into a brazed aluminum (plate-fin or core-type) heat exchanger. The hydrogen-rich gas also flows into the same exchanger (in separate passages) where the vaporizing liquid and the hydrogen are warmed by cooling the entering purge gas. Liquid ammonia from the ammonia plant may be used to provide additional refrigeration, especially at plant startup.

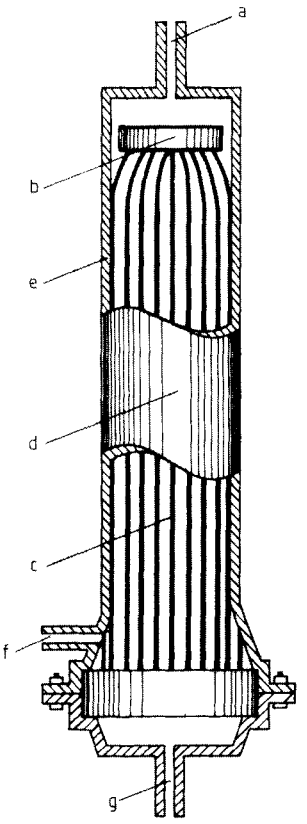

Figure 98. Gas separator module
a) Nonpermeate gas outlet; b) Fiber bundle plug; c) Hollow fiber; d) Separator (length, diameter, and number of separators determined by ammonia process); e) Coated carbon steel shell; f) Feed stream of mixed gases; g) Permeate gas outlet

The warm hydrogen-rich gas flows back to the suction side of the second stage of the synthesis gas compressor (6.5–7 MPa). About 90–95% of the hydrogen and 30% of the nitrogen in the purge gas can be recovered.

The remaining gas, with a high concentration of inerts, serves as fuel for the primary reformer. After heating in a preheater, a portion serves to regenerate the molecular sieves and then likewise flows to reformer fuel.

Cryogenic hydrogen recovery units are supplied by firms such as *Costain Engineering (formerly Petrocarbon Development)* [945]–[955], *Linde* [956], and *L'Air Liquide*, among others. Reference [957] reports on the changes in operating conditions of an ammonia plant resulting from the operation of a cryogenic hydrogen recovery unit.

4.5.6.2. Hydrogen Recovery by Membrane Separation

Monsanto has developed a new separator system known as Prism. The process uses selective gas permeation through membranes to separate gases. This principle has been applied to separating hydrogen from other gases [958]–[961]. The membranes are hollow fibers with diameters of about 0.5 mm. The fiber is a composite membrane consisting of an asymmetric polymer substrate and a polymer coating. The design of a

single separator module (length, 3 – 6 m; diameter, 0.1 – 0.2 m) resembles a shell and tube heat exchanger. A bundle with many thousands of hollow fibers is sealed at one end and embedded in a tube sheet at the other. The entire bundle is encased in a vertical shell (Fig. 98).

The purge gas is water scrubbed at 135 – 145 bar, reducing the ammonia concentration to less than 200 ppm. The scrubbed purge gas is heated to 35 °C and sent directly to the Prism separators. Trace concentrations of ammonia and water vapor in the gas stream pose no problem to the membrane. Therefore, a dryer system is not required.

The gas stream enters the separator on the shell side, i.e., the outside of the hollow fibers. Hydrogen permeates through the wall of the fibers. Hydrogen-rich permeate gas flows down the bore of the fiber and through the tube sheet and is delivered at the bottom of the separator. The remaining (nonpermeating) gases, nitrogen, methane, and argon, are concentrated on the shell side, recovered through the top and pass to the next separator module. Several separators operate in series. The rate of permeation decreases across a bank of separators as the hydrogen partial pressure differential across the membrane approaches zero. Therefore, a second bank of separators with lower pressure on the tube side is used to increase the hydrogen recovery. Of the recovered hydrogen, 40 – 70% leaves the first bank of separators at 70 bar and is returned to the second-stage suction of the synthesis gas compressor. In the second bank, permeate hydrogen is recovered at 25 – 28 bar and returned to the first-stage suction of the syngas compressor. Overall hydrogen recovery is 90 – 95%. The remaining nonpermeate gas stream normally flows to primary reformer fuel.

The main advantages of the Prism separator system are simplicity, ease of operation, and low maintenance. Reference [962] compares membrane and cryogenic separation units for a large ammonia plant.

For further literature on gas separation by membranes, see [963] – [969].

Membrane technology is also offered by other licensors; an example is the *Polysep Membrane System of UOP* [970]. In addition to the systems based on hollow fibers, membrane modules have been developed in which the membrane is in the form of a sheet wrapped around a perforated center tube using spacers to separate the layers. The raw gas flows in axial direction in the high pressure spacer and the permeate is withdrawn in the low pressure spacer. Such a module, for example, is marketed under the name *Separex* [971], [972].

4.5.6.3. Hydrogen Recovery by Pressure Swing Adsorption

Pressure swing adsorption (PSA) on zeolite molecular sieves (see Section 4.3.2.6) may be also used for hydrogen recovery from purge gas [761]. The process, originally developed by Union Carbide under the name HYSIV, is now marketed as *Polybed PSA by UOP* [970], [973], [974]. PSA technology is also offered by *Linde* and other companies. If required, the process also offers the possibility to supply pure hydrogen from

the purge gas for other uses. PSA units usually operate at adsorption pressures of 20–30 bar and achieve recovery rates higher than 82% for hydrogen and 20% for nitrogen. Carbon-based *adsorbents* for pressure swing adsorption have also been investigated [973], [974] and a process developed by *Bergbau-Forschung* [975] is offered by Costain.

4.5.6.4. Hydrogen Recovery with Mixed Metal Hydrides

A proprietary hydrogen separation process utilizing the reversible and selective adsorption capability of mixed metal hydrides has been proposed. The hydride, forming compounds, such as $LaNi_5$, FeTi, or Mg_2Cu, are in the form of ballasted pellets. The ballast material serves as a heat sink to store the heat of adsorption. Subsequently, this is used to supply the heat of desorption. The ballast also is the binder for the pellets, preventing attrition. Each type of metal hydride is susceptible to certain contaminants. Therefore, selection of the metal hydride must be based on the analysis of the gas to be treated. No ammonia removal step is required upstream of the unit. The system yields 99 mol% hydrogen product at a recovery efficiency of 90–93% [972], [976], [977]. No large commercial installations are known to be in operation at this time.

4.5.6.5. Argon Recovery from Ammonia Purge Gas

The waste gas from hydrogen recovery plants is more highly enriched in argon than the purge gas. If potential markets for argon exist, then it may be possible to supplement the hydrogen recovery plant with one for recovering argon. Cryogenic argon recovery from ammonia purge gas is discussed in [978]–[980]. Typical argon recoveries are in excess of 90%, with a purity of 99.999%.

4.5.7. Influence of Pressure and Other Variables of the Synthesis Loop

The influences of individual parameters can be summarized as given in [981]:

- Pressure: increasing pressure will increase conversion due to higher reaction rate and more favorable ammonia equilibrium.
- Inlet temperature: there are two opposed effects as increasing temperature enhances reaction rate but decreases the adiabatic equilibrium concentration.
- Space velocity: increasing the space velocity normally lowers the outlet ammonia concentration, but increases total ammonia production.
- Inert level: increasing the inert level lowers the reaction rate for kinetic and thermodynamic reasons (Section 3.5).

- Hydrogen/nitrogen ratio: a true maximum reaction rate for a certain H/N ratio; at lower temperatures the maximum lies at lower H/N ratios (Section 3.5). Position of the maximum also depends on the space velocity values (Section 4.5.2).
- Recycle rate: at constant pressure and production rate, the consequence of higher recycle rate is a lower ammonia concentration. In this case the difference to the equilibrium concentration and thus the reaction rate increases with the result that less catalyst is required. However, the temperature level for waste heat recovery decreases and with lower temperature differences, larger heat exchanger surface areas become necessary and the cross sections of piping and equipment have to be enlarged on account of the higher gas flow.
- Separator temperature: together with pressure and location of make-up gas addition, the temperature of the ammonia separator determines the ammonia concentration at the converter inlet. A lower temperature means lower ammonia concentration, which translates into either a lower catalyst volume or a higher conversion.
- Catalyst particle size (Section 3.6.1.2): smaller catalyst particles give higher conversion because of lower diffusion restrictions (higher pore efficiency)

The question of the best synthesis pressure is rather difficult and extremely dependent on optimization parameters such as feedstock price, required return on investment, and site requirements. In principle it is possible to calculate the minimum amount of mechanical work needed in the synthesis loop. If plots of kilowatt hours versus synthesis pressure for makeup gas compression, recycle, and refrigeration are superimposed the result will be a minimum, for which a value of 155 bar is reported in [982], [983]. The result is strongly dependent on assumed boundary conditions, and other studies came to higher values in the range 180 – 220 bar. However, such diagrams should be interpreted with care. First, this type of plot is strongly influenced by the catalyst activity, and thus by any factors that affect it, such as grain size and minimum possible temperature for the first bed, and especially the equilibrium temperature of the last bed [984]. Second, this approach considers only the mechanical energy and ignores completely the recovered energy of reaction, its energy level, and its impact on the energy balance of the complete ammonia plant. Third, the temperature attainable at a given site by air or water cooling will affect the refrigeration duty. And fourth, the type of front end can profoundly alter the result. The front-end pressure determines the suction pressure of the synthesis gas machine. In a plant based on partial oxidation with an operating pressure of 80 bar, less than half as much energy is needed to compress the makeup gas to 180 bar, for example, as in a steam reforming plant with a suction pressure of only 25 bar.

Thus the problem of choosing the best synthesis pressure is complex because not only does the entire energy balance have to be examined, but also the mechanical design and the associated investment costs. For an actual project, the costs for energy (i.e., the feedstock) have to be weighed against investment. With the exception of some processes which used extremely high pressures (Casale, Claude) a pressure of around 300 bar was common for the old multi-stream plants operated with reciprocating

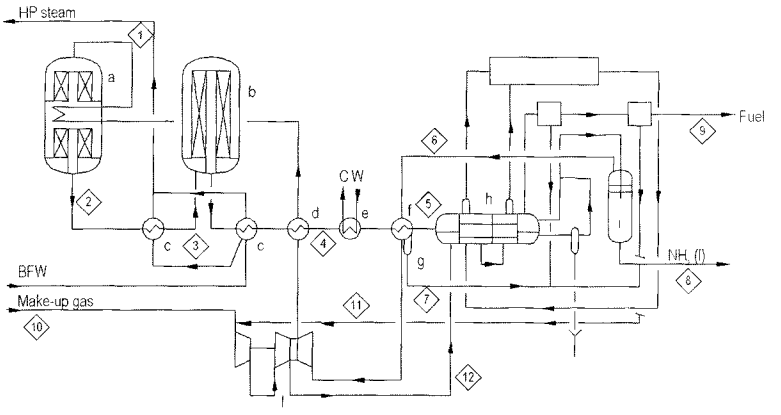

No.	Flow rate,	T, °C	p, MPa	Gas composition, mol%					Production of NH_3
	kmol/h			N_2	H_2	CH_4	Ar	NH_3	liquid, t/h
1	28344	295	18.80	23.53	61.20	8.20	2.89	4.18	
2	25368	469	18.48	20.43	50.79	9.15	3.23	16.40	
3	25368	401	18.38	20.43	50.79	9.15	3.23	16.40	
4	24672	336	18.26	19.60	47.99	9.43	3.31	19.67	
5	21613	21	18.02	22.33	54.71	10.67	3.78	8.51	
6	28344	0	17.88	23.54	61.20	8.20	2.88	4.18	
7	3060	21	18.02	0.30	0.55	0.50	0.09	98.55	51.36
8	3678	20	2.50	0.02	0.03	0.12	0.01	99.82	62.51
9	320	38	0.25	46.55	21.72	24.34	7.21	0.18	0.01
10	7667	35	3.23	25.89	72.73	1.07	0.31	0.00	
11	374	38	3.25	5.22	90.20	2.86	1.72	0.00	
12	8041	35	18.20	24.93	73.54	1.16	0.37	0.00	

Figure 99. Example of a synthesis loop for 1500 t/d NH_3 (Krupp–Uhde)
a) Converter with two radial beds and internal heat exchange; b) Converter with one radial bed; c) Waste heat recovery; d) Heat exchanger; e) Water cooling; f) Heat exchanger; g) No. 1 separator; h) Refrigerated cooling; i) No. 2 separator; j) NH_3 recovery; k) H_2 recovery

compressors. The centrifugal compressor is one of the most important features of single-train ammonia plants. The first of these plants, with a capacity of 600 t/d, were built in the mid-1960s and the maximum attainable synthesis pressure was restricted to ca. 150 bar by technical limitations of the centrifugal compressor, which needed a minimum gas flow (see also Section 4.4). Of course, at current plant sizes of 1200–1800 t/d this constraint is no longer of importance. These plants usually operate in the pressure range of 170–190 bar and it is a confirmation of the argumentation presented above that the different pressures are not reflected in the overall energy consumption of the complete ammonia plant. Analysis of the effects of various parameters on the energy consumption of the synthesis loop are also reported in [900], [901]. At constant equilibrium temperature for the effluent from the last bed (constant ammonia concentration) energy consumption of the loop was found to be almost independent of pressure in the range of 80–220 bar [984].

4.5.8. Example of an Industrial Synthesis Loop

Figure 99 is an example of modern ammonia synthesis loop (Krupp–Uhde) with a two-vessel converter system and three indirectly cooled catalyst beds producing 1500 t/d NH_3 at 188 bar.

The gas enters the converter (a) at 295 °C and is subsequently heated in the internal heat exchanger to 390 °C before it enters the first catalyst layer. The outlet gas from the first layer then passes through the aforementioned heat exchanger and enters the second bed, after which the gas leaves the converter with 469 °C and passes a waste heat boiler generating 125 bar steam. The inlet gas of the second vessel, which accommodates the third catalyst bed, has a temperature of 401 °C and the outlet enters a further waste heat boiler generating 125 bar steam.

4.6. Waste-Heat Boilers for High-Pressure Steam Generation

Though high pressure steam generation in waste heat boilers [404], [985] does not represent a separate process step comparable to those described in the preceding sections, a special section seems to be appropriate because of its great influence on efficiency and reliability of the plants. The operating conditions are more severe than those normally encountered in power plants; on account of the high pressure on both sides, the heat transfer rates and thus the thermal stresses induced are much higher.

After the secondary reformer of steam reforming plants the gas has to be brought down from around 1000 °C to about 350 °C for the HT shift. In earlier-generation plants two boilers were usually installed in series, with a bypass around the second to control the inlet temperature for the HTS. Common practice for a long time was to use a water-tube design. A famous example is the Kellogg bayonet-tube boiler, applied in more than 100 plants. Because of size limitations two parallel units were installed. For sufficient natural water circulation these boilers needed a steam drum at a rather high elevation and a considerable number of downcomers (feed water) and risers (steam/water mixture).

In contrast, fire-tube boilers are much better suited for natural circulation and the steam drum can sit in piggyback-fashion, right on top of the boiler. This makes it possible to provide each boiler with its own separate steam drum, which allows greater flexibility in the plot plan. But it took some time before this boiler type was accepted in ammonia plants as the stress pattern is more complex and less predictable than in water-tube boilers.

In a fire-tube boiler, the inlet tube sheet and the tube sheet welds are exposed to the extreme temperature of the reformed gas, which creates rather large temperature gradients and therefore high expansive stress. A positive feature of the fire-tube design, however, is that debris in feed water (mainly magnetite particles spalling from the water-side surface of the tubes) can collect at the bottom of the horizontally-mounted

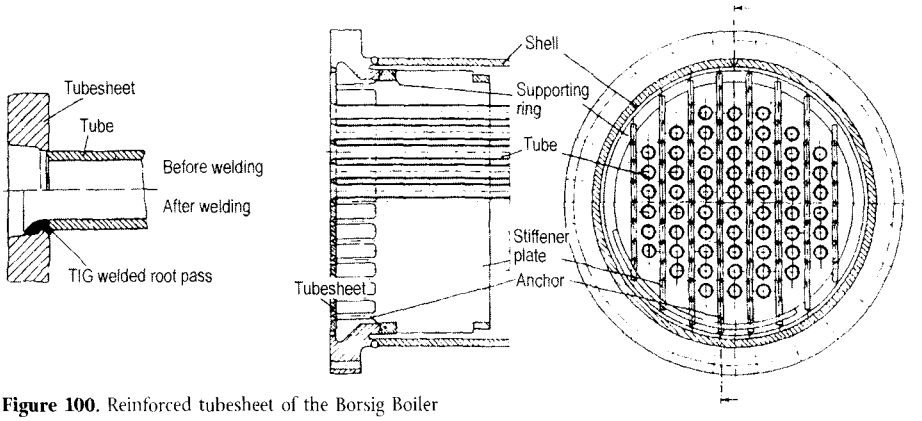

Figure 100. Reinforced tubesheet of the Borsig Boiler

vessel without creating difficulties and are removed easily by blow down. Water-tube boilers, especially bayonet-types, are very sensitive in this respect, since the deposits may collect in the lowest and most intensively heated part of the tube. In an extreme case of scaling, this may restrict the water flow to the point where boiling occurs irregularly (film boiling). The risk is overheating and tube failure.

The key factor which allowed the use of fire-tube boilers after the secondary reformer was the development of thin-tube-sheet designs. Thick tube sheets in this kind of service are too rigid and have too big a temperature gradient, and the resultant high stress on the tube-to-tubesheet welds can lead to cracks. The inherent flexibility of thin tube sheets assists in dispersing stresses and reduces the risk of fatigue failure of the tube-to-tubesheet welds and tubesheet-to-shell welds. In all that various designs using this concept, the tubesheet is only 25 – 30 mm thick. The hot inlet channel and the tubesheet are shielded by a refractory layer, and the tube inlets are protected by ferrules.

In the *Uhde* [986], [987] and *Steinmüller* [989] concept the tubesheet is anchored to and supported by the tubes to withstand the differential pressure, which imposes some restriction on the tube length. *Babcock-Borsig's* [988], [990], [991] tubesheet is reinforced by stiffening plates on the back side (Figure 100). Both solutions have full-penetration tube-to-tubesheet welds for the tubes to prevent crevice corrosion. *Struthers* [992] reduces stress by making the tubesheet-to-shell connection flexible.

The synthesis loop boiler on the exit of the converter is also a very important piece of equipment. In some modern plants not equipped with an auxiliary boiler it supplies nearly half of the total steam generation. It may generate as much as 1.5 t of steam per tonne of ammonia, equivalent to about 90 % of the reaction heat. Fire-tube versions have been also used, including Babcock–Borsig's thin-tubesheet design. But compared to the secondary reformer service, where the gas pressure is lower than the steam pressure, the conditions and stress patterns are different. In the synthesis loop boiler the opposite is the case, with the result that the tubes are subjected to longitudinal compression instead of being under tension. Several failures in this application have been reported [993], and there was some discussion of whether this type of boiler is the best solution for the synthesis loop waste-heat duty.

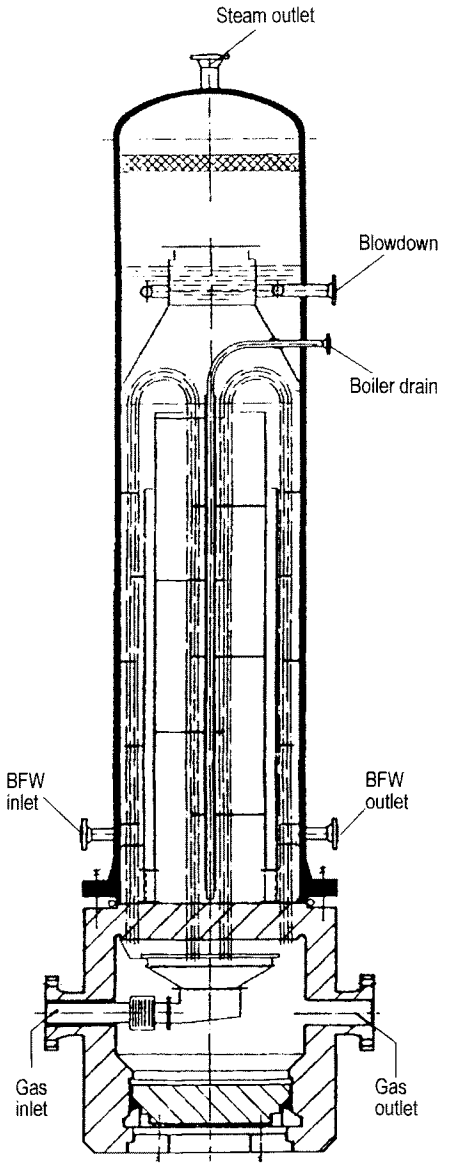

Figure 101. U-tube synthesis loop boiler

More generally accepted now are thick-tubesheet concepts in various configurations. Proven U-type designs are available from *Uhde* [931], *Balcke-Dürr* [994], [995], [997], *Kellogg* [996] and *Babcock-Borsig* [991]. A special advantage is that the tube bundle, being rigidly mounted at the end only, is essentially free of stress. The main tubesheet is protected in various ways against damage by the hot gas. The principle is shown in Figure 101. A variation offered by Uhde for use as first first boiler in the synthesis loop has cooling channels in the tube sheet fed by incoming boiler feed water.

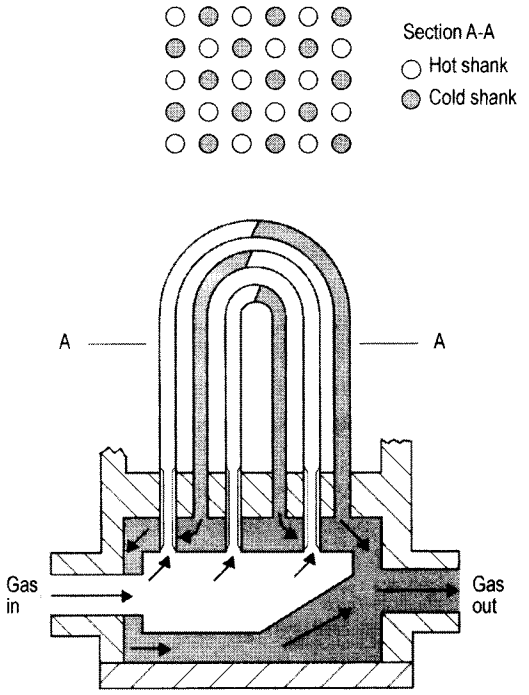

Figure 102: Babcock – Borsig's hot/cold synthesis loop boiler

An interesting approach is *Babcock – Borsig's Hot/Cold Tubesheet* [998]. The hot and cold ends of the tubes are arranged alternately, so that a hot shank is always next to a cold shank and vice versa (Figure 102). The advantage is that the tubesheet and the hot end tube wall temperature inside the tubesheet can be kept below 380 °C, which avoids nitriding and allows ferritic ferrules to be used. The entire tubesheet surface is shielded additionally by the cooled gas exiting from the cold ends of boiler tubes.

Another very successful design is the *horizontal synthesis loop waste*-heat boiler of *Balcke-Dürr AG* [999]. This boiler is a straight-tube design with thick tubesheets on both ends. A particular feature is the welding of the tubes to the 6 mm Inconel cladding of the tubesheet. This weld is mainly for sealing purposes; the mechanical tube-to-tubesheet joint which accomodates the stress is provided by hydraulic expansion of the tubes over the entire thickness of the tubesheet [1000], [1001]. The hydraulic expansion provides redundant gas-tightness.

Waste-heat boilers in partial oxidation plants, which cool the exit gas of the generator from 1400 °C to around 350 °C, face additional difficulties. The gas contains soot and probably some fly ash particles. Very high gas velocities and appropriate design are necessary to prevent any deposition on the heat exchange surfaces and to reduce the danger of attrition as well. A special design (L. u. C. Steinmüller GmbH) for use with Texaco gasifications is shown in Figure 103 [1002]. Good circulation rate on the water side helps to stand the high heat flux (700 kJ m^{-2} s^{-1}) in the entrance nozzles to the

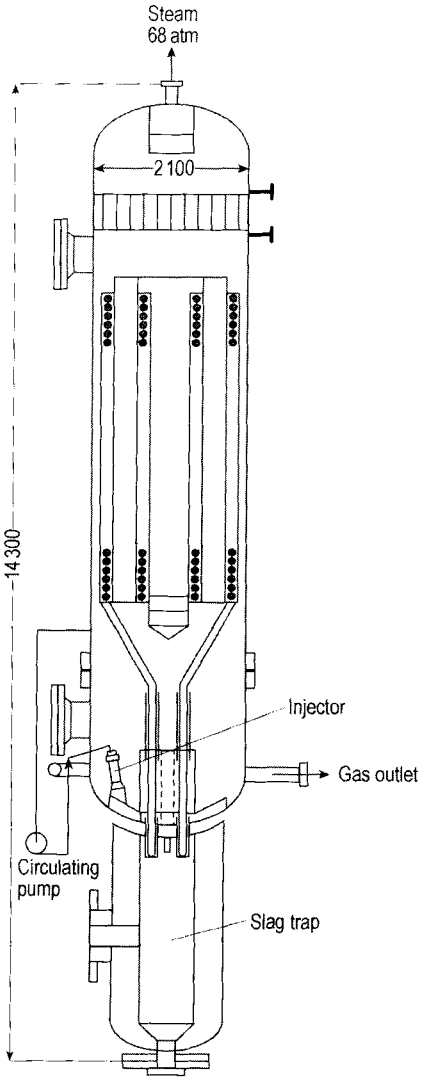

Figure 103. Waste-heat boiler for Texaco gasification

spiral-wound tubes. The Shell process uses also proprietary designs (Fasel-Lentjes) [1003].

Additional information on waste-heat boilers is found in [895], [929], [930], [1004].

5. Complete Ammonia Production Plants

The previous sections mainly considered the individual process steps involved in the production of ammonia and the progress made in recent years. The way in which these process components are combined with respect to mass and energy flow has a major influence on efficiency and reliability. Apart from the feedstock, many of the differences between various commercial ammonia processes lie in the way in which the process elements are integrated. Formerly the term ammonia technology referred mostly to "ammonia synthesis technology" (catalyst, converters, and synthesis loop), whereas today it is interpreted as the complete series of industrial operations leading from the primary feedstock to the final product ammonia.

The major determinant for process configuration is the type of feedstock, which largely governs the mode of gas generation and purification. The other important factor is the plant capacity, which, together with consumption and costs of feedstock and energy, is decisive for the production economics. An important development was the concept of single-train plants, first introduced for steam reforming based production by M. W. Kellogg in 1963 with a capacity of 600 t/d. Before then maximum capacities had mostly been about 400 t/d, with several parallel trains in the synthesis gas preparation stage and the synthesis loop. Today world-scale plants have capacities of 1200 – 1500 t/d, and some have 1800 t/d. The lowest capital cost and energy consumption result when steam reforming of natural gas is used. In addition site requirements can influence the layout considerably. In contrast to a stand-alone plant, ammonia production at a developed industrial site may import and/or export steam and power, which affects the total energy consumption.

With the exception of the Koppers – Totzek coal gasification process, which operates at near atmospheric pressure, all modern gasification processes operate at elevated pressure. Steam reforming of light hydrocarbons at 30 – 40 bar and partial oxidation of heavy hydrocarbons at 40 – 90 bar are generally used.

5.1. Steam Reforming Ammonia Plants

5.1.1. The Basic Concept of Single-Train Plants

The innovative single-train concept was a technical and an economical breakthrough and triggered a tremendous increase in world ammonia capacity. No parallel lines, even for high capacity, and a highly efficient use of energy, with process steps in surplus supplying those in deficit, were the main features. Figure 104 shows a block flow diagram and the gas temperature profile for a steam reforming ammonia plant.

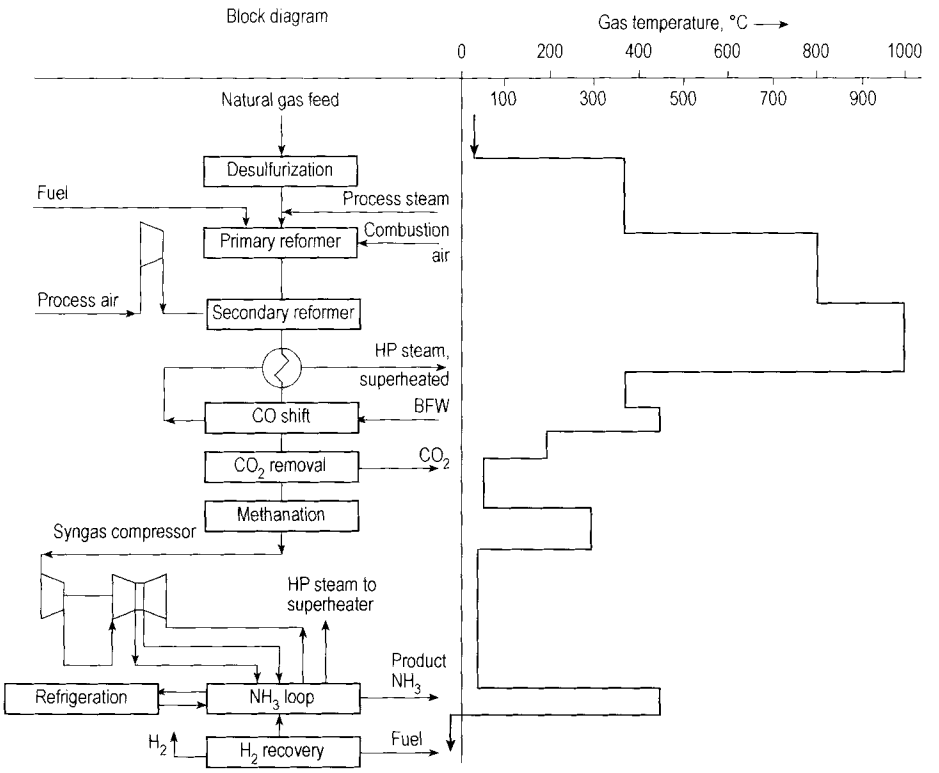

Figure 104. Block diagram and gas temperature profile for a steam reforming ammonia plant

High level surplus energy is available from the flue gas of the reformer and the process gas streams of various sections, while heat is needed, for example, for the process steam for the reforming reaction and in the solvent regenerator of the carbon dioxide removal system. Because considerable mechanical energy is needed to drive compressors, pumps, and blowers, it was most appropriate to use steam turbine drives, since sufficient steam could be generated from the waste heat. As the level was high enough to raise high-pressure steam (100 bar) it was possible to use the process steam first to generate mechanical energy in the synthesis gas compressor turbine before extracting it at the pressure level of the primary reformer. Table 35 lists all significant energy sources and sinks within the process.

The earlier plants operated at deficit, and needed an auxiliary boiler, which was integrated in the flue gas duct. Auxiliary burners in tunnels or flue gas duet were additionally used in some instances. This situation was partially caused by inadequate waste heat recovery and low efficiency in some energy consumers. Typically, the furnace flue gas was discharged in the stack at rather high temperature because there was no air preheating and too much of the reaction heat in the synthesis loop was rejected to the cooling media (water or air). In addition, efficiency of the mechanical drivers was low and the heat demand for regenerating the solvent from the CO_2 removal unit (at

Table 35. Main energy sources and sinks in the steam reforming ammonia process

Process section	Origin	Contribution
Reforming	primary reforming duty	demand
	flue gas	surplus
	process gas	surplus
Shift conversion	heat of reaction	surplus
CO_2 removal	heat of solvent regeneration	demand
Methanation	heat of reaction	surplus
Synthesis	heat of reaction	surplus
Machinery	drivers	demand
Unavoidable loss	stack and general	demand
Balance	auxiliary boiler or import	deficit
	export	surplus

that time aqueous MEA) was high. Maximum use was made of direct steam turbine drive, not only for the major machines such as synthesis gas, process air, and refrigeration, but even for relatively small pumps and blowers. The outcome was a rather complex steam system. Even after substitution of the smaller turbines by electric motors in more recent installations, the steam system in the modern plant is still a complex system as shown in Figure 106. Ammonia plant steam systems and steam generation are described in [402], [404], [985], [1004] – [1006].

The first generation of the single-train steam reforming plants is discussed in [426], [1007] – [1012], and the required catalysts are reviewed in [633], [1013] – [1014]. A survey of the development of the steam reforming concept through 1972 can be found in [1015]. Other references which cover the development of the steam reforming before the introduction of the single-train concept (1940 to 1960) can be found in [402 p. 276].

The new plant concept had a triumphant success story. By 1969, 30 new Kellogg large single-train plants with capacities of 1000 t/d or more were in operation, and other contractors were offering similar concepts.

The decrease in energy consumption compared to the older technology was dramatic, and with the low gas prices at that time it is understandable that greater emphasis was placed on low investment cost, although there was a considerable potential for further reducing the energy consumption.

With the advent of the single-train steam reforming plants, it became standard for licensors and engineering contractors to express the total net energy consumption per tonne of ammonia in terms of the lower heating value of the feedstock used. The total net energy consumption is the difference between all energy imports (mainly feedstock) and all energy exports (mostly steam and/or electric power) expressed as lower heating values, whereby electric power is converted with an efficiency of 25 – 30 % and steam is accounted for with its caloric value.

Table 36. Development of the net energy consumption of natural gas based steam reforming ammonia plants (real plant data) in GJ/t NH_3

Year	1966	1973	1977	1980	1991
Plant	A	B	C	D	E
Feed	23.90	23.32	23.48	23.36	22.65
Fuel, reformer	13.00	9.21	7.35	5.56	5.90
Fuel, auxiliary boiler	2.60	5.02	3.06	1.17	
Export					0.55
Total	39.50	37.55	33.89	30.18	28.00

5.1.2. Further Development

The significant changes in energy prices from 1973 onwards were a strong challenge to process licensors, engineering contractors and plant owners to obtain better energy efficiency. The overall energy consumption was reduced from around 45 GJ/t NH_3 for the first large single-train units to less than 29 GJ/t NH_3 (Table 36).

Energy saving modifications are described in [1016] – [1025], [1027], [1029] – [1031]. Some of the most important improvements compared to the first generation of plants are discussed below.

Feedstock Purification. In feedstock purification, mainly desulfurization, adsorption on active carbon was replaced by catalytic hydrogenation over cobalt – molybdenum or nickel – molybdenum catalyst, followed by absorption of the H_2S on ZnO pellets with formation of ZnS. By itself this measure has no direct influence on the energy consumption but is a prerequisite for other energy saving measures, especially in reforming and shift conversion.

Reforming Section. In the reforming section energy savings were achieved by several, often interrelated, measures, of which the most important are the following:

- Reduction of the flue gas stack temperature to reduce heat losses to the atmosphere [623]
- Avoiding excessive heat loss by better insulation of the reformer furnace
- Introduction of combustion air preheating [1028]
- Preheating the reformer fuel
- Increased preheat temperatures for feed, process steam and process air
- Increased operating pressure (made possible by using improved alloys for the reformer tubes and improved catalysts)
- Lowering of the steam to carbon ratio [1032]
- Shifting some reformer duty from primary to secondary reformer with the use of excess air [753], [1033] or oxygen-enriched air [1034] in the secondary reformer, including the possibility of partially bypassing the primary reformer [1035], [1124]

- Installing a prereformer or rich-gas step is another possibility to reduce primary reformer duty and stack temperature of the flue gas [462]–[470], especially in LPG- and naphtha-based plants

A more recent development that breaks away from the usual plant configuration is to replace the traditional fired primary reformer with an exchanger reformer which uses the heat of the effluent of the secondary reformer [471]–[478], [1036], [1037]. Also other applications have been reported in which flue gas [1038] heat from the fired reformer is used to perform a part of the reforming.

Shift Conversion. Improved LT shift catalysts can operate at lower temperatures to achieve a very low residual CO content and low byproduct formation. A new generation of HT shift catalysts largely avoids hydrocarbon formation by Fischer–Tropsch reaction at low vapor partial pressure, thus allowing lower steam to carbon ratio in the reforming section (see Section 4.2.1.1.1).

Carbon Dioxide Removal Section. In the carbon dioxide removal section the first generation of single-train plants often used MEA with a rather high demand of low-grade heat for solvent regeneration. With additives such as UCAR Amine Guard [651], [655], solvent circulation could be reduced, saving heat and mechanical energy. Much greater reduction of energy consumption was achieved with new solvents and processes, for example BASF aMDEA or Benfield LoHeat. Other hot potash systems (Giammarco Vetrocoke, Catacarb) and physical solvents (Selexol) were introduced (Section 4.3.1).

Final makeup gas purification was improved by removing the water and carbon dioxide traces to a very low level by using molecular sieves. Some concepts included cryogenic processes with the benefit of additional removal of methane and argon.

Ammonia Synthesis Section. In the ammonia synthesis section conversion was increased by improved converter designs (see Section 4.5.3), larger catalyst volumes, and to some extent with improved catalysts. The main advances in converter design were the use of indirect cooling instead of quenching, which allowed the recovery of reaction heat as high pressure steam. Radial or crossflow pattern for the synthesis gas instead of axial flow was introduced. All modern plants include installations for hydrogen recovery (cryogenic, membrane, or PSA technology; see Section 4.5.6).

Machinery. Developments in compressor and turbine manufacturing have led to higher efficiencies.

- Gas turbine drive for a compressor and/or an electric generator combined with the use of the hot exhaust as combustion air for the primary reformer or raising steam (combined cycle) [804], [807]–[810], [1038].
- Employing electric motors instead of condensation turbines [1039].

- Application of liquid and gas expansion turbines can recover mechanical work (e.g., let-down of the CO_2-laden solvent, liquid ammonia, purge and fuel gas).

Steam system and waste heat recovery were improved by the following measures: increased pressure and superheating temperature of high-pressure steam; providing a part of the process steam by natural gas feed saturation [651], [1033], [1040]–[1042]; inclusion of a steam superheater downstream of the secondary reformer [985], [1043].

Process Control and Process Optimization. Progress in instrumentation and computer technology has led to increased use of advanced control systems and computerized plant optimization. Advanced control systems [1044]–[1053] allow operating parameters to be kept constant in spite of variations in external factors such as feedstock composition or ambient or cooling water temperatures. These systems may be operated in open loop fashion (set values changed manually by the operator) or in closed fashion (set points automatically adjusted to optimum values by using a computer model with input of operational and economic data). Also plant simulation [1054]–[1058] is possible by using extensive computer models of complete plants. These models can simulate in real time the dynamic response to changes in operating parameters, plant upsets, etc. Such systems are used for off-line optimization studies and for operator training [1058], [1059].

The above list, by no means complete, is also a survey of options for plant revamps (Chapter 6).

Many of these elements are strongly interrelated with each other and may affect different sections of the plant concept. It is thus a demanding engineering task to arrive at an optimum plant concept, which can only defined by the conditions set by the feedstock price, the site influences, and the economic premises of the customer. An evaluation of the individual merits of the described measures in terms of investment and operational cost in a generalized form is not possible and can be done only from case to case in real project studies.

To illustrate the forgoing discussion of the concept of the single-train steam reforming plant, Figure 105 presents a modern low-energy ammonia plant with flow sheet and process streams (UHDE process).

Figure 106 shows a simplified diagram of the steam system. Even in such an advanced plant the quantity of steam generated from waste heat is as much as 3.4 times the weight of ammonia produced.

5.1.3. Minimum Energy Requirement for Steam Reforming Process

The energy saving measures described in Section 5.1.2 have considerably reduced the demand side (e.g., CO_2 removal, higher reforming pressure, lower steam to carbon ratio, etc.). On the supply side, the available energy has been increased by greater heat

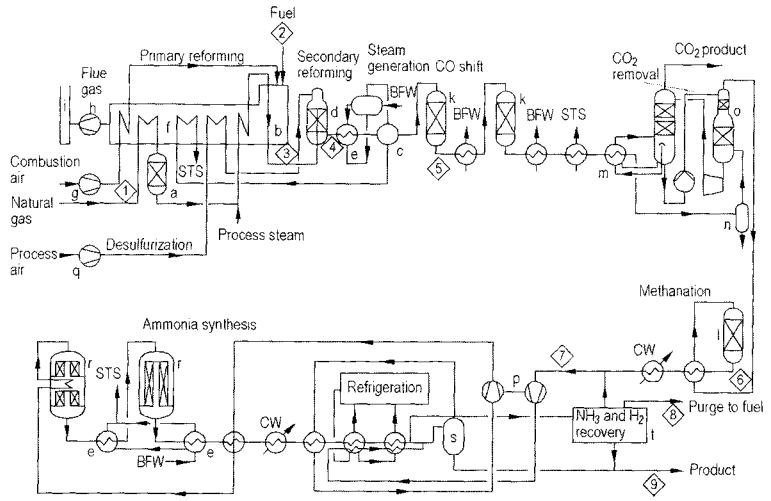

	1	2	3	4	5	6	7	8	9
CH_4, mol%	91.24	91.24	14.13	0.60	0.53	0.65	1.16	24.34	0.12
C_nH_m, mol%	5.80	5.80							
CO_2, mol%	1.94	1.94	10.11	7.38	18.14	0.01			
CO, mol%			9.91	13.53	0.33	0.40			
Ar, mol%				0.28	0.25	0.30	0.37	7.21	0.01
H_2, mol%			65.52	54.57	59.85	73.08	73.54	21.72	0.03
N_2, mol%	1.02	1.02	0.33	23.64	20.90	25.56	24.93	46.55	0.02
NH_3, mol%								0.18	99.82
Dry gas, kmol/h	1713.7	534.43	5296.4	8414.2	9520.7	7764.0	8041.4	319.9	3676.6
H_2O, kmol/h			3520.6	4086.1	2979.6	22.8	13.3	0.2	0.9
Total, kg/h	30213	9422	121183	199555	199555	70084	71004	6496	62626
p, MPa	5.00	0.25	3.95	3.90	3.61	3.43	3.23	0.25	2.50
T, °C	25	25	808	976	229	50	35	38	20

Figure 105. Modern integrated single-train ammonia plant based on steam reforming of natural gas (Uhde process)
a) Sulfur removal; b) Primary reformer; c) Steam superheater; d) Secondary reformer; e) Waste heat boiler; f) Convection section; g) Forced draft fan; h) Induced draft fan; i) Stack; k) HT and LT shift converters; l) Methanator; m) CO_2 removal solvent boiler; n) Process condensate separator; o) CO_2 absorber; p) Synthesis gas compressor; q) Process air compressor; r) Ammonia converter; s) High-pressure ammonia separator; t) Ammonia and hydrogen recovery from purge and flash gas

recovery. The combined effects on both sides have pushed the energy balance into surplus. Because there is no longer an auxiliary boiler which can be turned down to bring the energy situation into perfect balance, the overall savings usually could not be translated into further actual reduction of the gross energy input to the plant (mainly natural gas). In some cases this situation can be used advantageously. If the possibility exists to export a substantial amount of steam, it can be economically favorable (depending on feedstock price and value assigned to the steam) to deliberately increase the steam export by using additional fuel, because the net energy consumption of the plant is simultaneously reduced (Table 37).

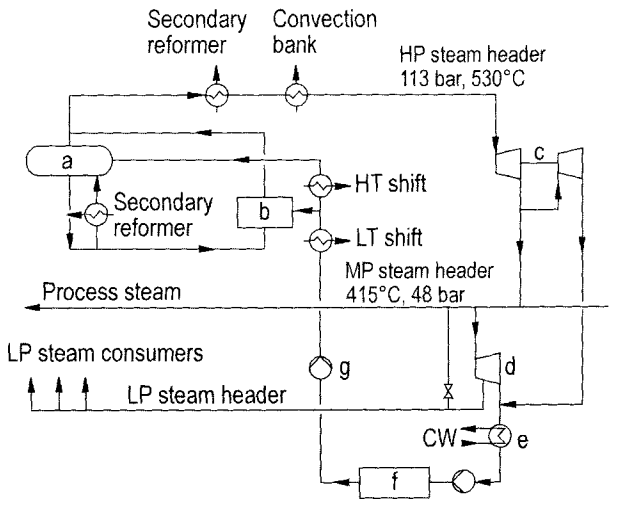

Figure 106. Steam system of a modern steam reforming
a) Steam drum, 125 bar; b) NH_3 loop; c) Turbine for syngas compressor; d) Turbine for process air compressor and alternator; e) Surface condenser; f) Condensate treatment; g) BFW pump

Table 37. Increase of plant efficiency by steam export (GJ/t NH_3)

	Plant		Difference
	A	B	
Natural gas	27.1	32.6	+ 5.5
Electric power	1.1	1.1	
Steam export		- 6.4	- 6.4
Total energy	28.2	27.3	- 0.9

A reduction in gross energy demand, that is, a lower natural gas input to the plant, can only be achieved by reducing fuel consumption, because the actual feedstock requirement is determined by the stoichiometry. So the only way is to decrease the firing in the primary reformer, which means the extent of reaction there is reduced. This can be done by shifting some of the reforming duty to the secondary reformer with surplus air or oxygen-enriched air, although this makes an additional step for the removal of surplus nitrogen necessary. A more radical step in this direction is total elimination of the fired primary reformer by using exchanger reformers like the ICI GHR and the Kellogg KRES.

Based on pure methane, it is possible to formulate a stoichiometric equation (95) for ammonia production by steam reforming:

$$CH_4 + \underbrace{0.3035\,O_2 + 1.131\,N_2}_{1.4345\ \text{air}} + 1.393\,H_2O \longrightarrow CO_2 + 2.262\,NH_3 \qquad (95)$$

$\Delta H = -86$ kJ/mol and $\Delta F = -101$ kJ/mol at 25 °C

From a mere thermodynamic point of view, in an ideal engine or fuel cell, heat and power should be obtainable from this reaction. Since real processes show a high degree of irreversibility, a considerable amount of energy is necessary to produce ammonia from methane, air and water. The stoichometric quantity of methane derived from the

Table 38. Specific energy requirement for ammonia production compared to the theoretical minimum

	GJ/t NH_3 (LHV)	% theory
Classical Haber–Bosch (coke)	80–90	(338–431)
Reforming, 0.5–10 bar (1953–55)	47–53	225–254
Reforming, 30–35 bar (1965–75)	33–45	139–215
Low energy concepts (1975–84)	29–33	139–158
Modern concepts (since 1991)	$\leq$ 28	134
Stoichiometric CH_4 demand	20.9	= 100

above reaction is 583 m^3 per tonne of ammonia, corresponding to 20.9 GJ/t NH_3 (LHV), which with some justification could be taken as minimum value. If full recovery of the reaction heat is assumed, then the minimum would be the lower heating value of ammonia, which is 18.6 GJ/t NH_3. Table 38 compares the specific energy requirement for ammonia production by steam reforming with the theoretical minimum.

Comparison of energy consumption figures without precise knowledge of design and evaluation criteria can be misleading. First of all the state of the ammonia product should be noted. Relative to the delivery of liquid ammonia to battery limits at ambient temperature, the production of 3 bar ammonia vapor at the same temperature would save 0.6 GJ/t NH_3, while delivery as liquid at – 33 °C would need an extra 0.3 GJ/t NH_3. The temperature of the available cooling medium has a considerable influence. Increasing the cooling water temperature from 20 to 30 °C increases energy consumption by 0.7 GJ/t NH_3. A detailed energy balance, listing all imports and exports, together with the caloric conversion factors used for steam and power is needed for a fair comparison of plants. The beneficial effect of energy export to the net energy consumption is discussed above. Gas composition is also of some importance. Nitrogen content is marginally beneficial: 10 mol% nitrogen leads to a saving of about 0.1 GJ/t NH_3, whereas a content of 10 mol% carbon dioxide would add 0.2 GJ/t NH_3 to the total consumption value [1060].

Energy requirements and energy saving possibilities are also discussed in [1016], [1018], [1025]–[1031].

The energy consumption figures discussed so far represent a thermodynamic analysis based on the first law of thermodynamics. The combination of the first and second laws of thermodynamics leads to the concept of ideal work, also called exergy. This concept can also be used to evaluate the efficiency of ammonia plants. Excellent studies using this approach are presented in [1061], [1062]. Table 39 [1061] compares the two methods. The analysis in Table 39 was based on pure methane, cooling water at 30 °C (both with required pressure at battery limits), steam/carbon ratio 2.5, synthesis at 140 bar in an indirectly cooled radial converter.

Almost 70% of the exergy loss in the process occurs in the reforming section and in steam generation. From conventional first law analysis it can be seen that almost all of the losses are transferred to the cooling water. As the analysis assumes water in liquid

Table 39. Energy analysis of a low energy ammonia plant (GJ/t NH_3)

	HHV	LHV	Exergy
Input			
Natural gas consumption			
Reformer feed	24.66	22.27	23.28
Reformer fuel	7.49	6.78	7.08
Auxiliary boiler fuel	0.34	0.29	0.33
Total consumption	32.49	29.34	30.69
Losses			
Reforming	0.38	0.38	1.94
Steam generation	0.33	0.33	2.39
Shift, CO_2 removal, methanation	1.30	1.30	0.67
Synthesis	1.70	1.70	1.55
Turbines and compressors	6.50	6.50	0.54
Others (including stack	1.30	0.68	0.46
Total losses	11.51	10.89	10.55
NH_3 product	20.98	17.12	20.14
Efficiency, %	64.60	58.40	65.60

state, the LHV analyses in Table 39 is not completely balanced. For a perfect balance the heat of evaporation of water (as a fictive heating value) would have to be included.

5.1.4. Commercial Steam Reforming Ammonia Plants

Especially with ammonia processes based on steam reforming technology it has become a habit to differentiate between processes from various licensors and engineering contractors. This is not so much the case for partial oxidation plants (see Section 5.2). Strong competition together with increased plant sizes and the associated financial commitment has reduced the number of licensors and engineering contractors to a few companies capable of offering world-scale plants, often on a lump-sum turnkey basis. In some cases these companies sub-license their processes and special engineering know-how to competent engineering companies possessing no knowledge of their own in the ammonia field. There are also several smaller companies with specific and sometimes proprietary know-how which specialize in revamps of existing plants or small plant concepts.

In the following, each of the commercially most important processes is discussed in some detail and a shorter description of economically less important processes is given. The process configuration offered and finally constructed by a given contractor may vary considerably from case to case, depending on economic and site conditions and the clients' wishes. Thus plants from the same contractor and vintage often differ considerably. It is possible to categorize steam reforming plants according to their configuration in the reforming section:

1) Advanced conventional processes with high duty primary reforming and stoichiometric process air in the secondary reformer
2) Processes with reduced primary reformer firing and surplus process air
3) Processes without a fired primary reformer (exchanger reformer)
4) Processes without a secondary reformer using nitrogen from an air separation plant

In principle the amount of flue gas emitted should be related to the extent of fired primary reforming, but generalizations are questionable, because sometimes the plant layout, as dictated by site requirements, may considerably change the picture for the specific flue gas value.

5.1.4.1. Advanced Conventional Processes

Kellogg Low-Energy Ammonia Process [1031], [1063]–[1070]. The Kellogg process is along traditional lines, operating with steam/carbon ratio of about 3.3 and stoichiometric amount of process air and low methane slip from the secondary reformer. The synthesis pressure depends on plant size and is between 140 and 180 bar. Temperatures of the mixed feed entering the primary reformer and of the process air entering the secondary reformer are raised to the maximum extent possible with today's metallurgy. This allows reformer firing to be reduced and, conversely, the reforming pressure to be increased to some extent to save compression costs. An important contribution comes from Kellogg's proprietary cross-flow horizontal converter, which operates with catalyst of small particle size, low inlet ammonia concentration, and high conversion. Low-energy carbon removal systems (Benfield LoHeat, aMDEA, Selexol) contribute to the energy optimization.

When possibilities to export steam or power are limited, part of the secondary reformer waste heat is used, in addition to steam generation, for steam superheating, a feature in common with other modern concepts. Proprietary items in addition to the horizontal converter are the traditional Kellogg reformer, transfer line and secondary reformer arrangement, waste-heat boiler, and unitized chiller in the refrigeration section.

According to Kellogg 27.9 GJ/t NH_3 can be achieved in a natural gas based plant with minimum energy export, but with export of larger quantities of steam this value could probably be brought down to about 27 GJ/t NH_3. Figure 107 shows a simplified flowsheet of the process [1069] with Selexol CO_2 removal unit.

Haldor Topsøe Process. In addition to technology supply, Haldor Topsøe also produces the full catalyst range needed in ammonia plants. The energy consumption of a basically classic plant configuration has been reduced considerably by applying systematic analysis and process engineering. Descriptions and operational experience are given in [464], [623], [1028], [1071]–[1082].

Topsøe offers two process versions. The first operates at steam/carbon ratio of 3.3 and with rather high residual methane content from the secondary reformer. Shift

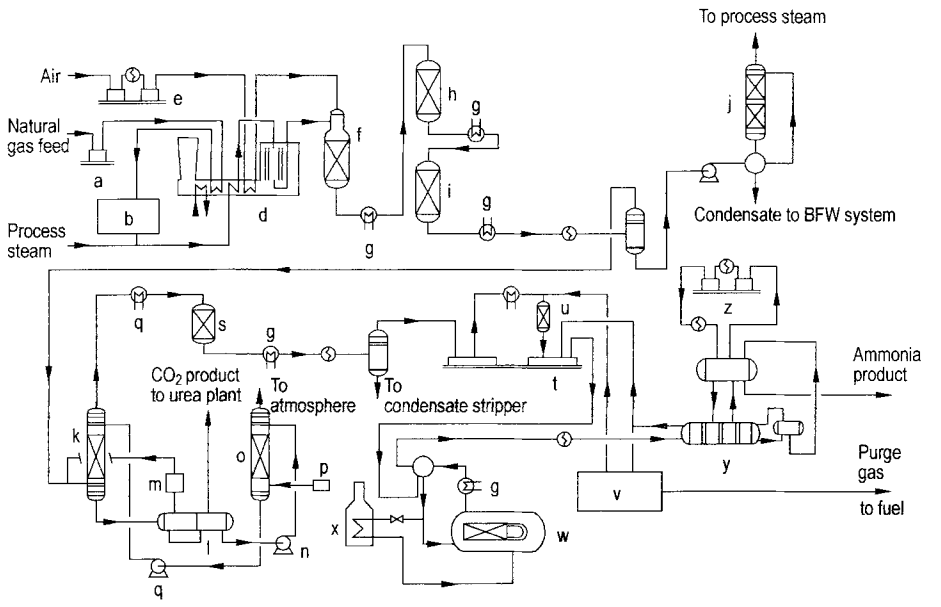

Figure 107. M. W. Kellogg's low energy process
a) Feed gas compressor; b) Desulfurization; d) Primary reformer; e) Air compressor; f) Secondary reformer; g) Heat recovery; h) High temperature shift converter; i) Low temperature shift converter; j) Condensate stripper; k) CO_2 absorber; l) CO_2 flash drum; m) Recycle compressor; n) Semi-lean Pump; o) Stripper (other options are, e.g., Benfield or BASF aMDEA); p) Stripper air blower; q) CO_2 lean pump; r) Methanator feed preheater; s) Methanator; t) Synthesis gas compressor; u) Dryer; v) Purge gas H_2 recovery; w) Ammonia converter; x) Start-up heater; y) Refrigeration exchanger; z) Refrigeration compressor

conversion is conventional, the Benfield or Vetrokoke process is used for carbon dioxide removal, and the synthesis pressure depends on plant size ranging between 140 and 220 bar when the proprietary Topsøe two-bed radial converter S 200 is used. A simplified flowsheet is presented in Figure 108.

An actual plant has reported a consumption of 29.2 GI/tNH [1080].

The second version has a S/C ratio of 2.5 and shift conversion with medium- and low-temperature catalysts, both copper-based. For CO_2 removal Selexol or aMDEA is chosen. The synthesis is performed at 140 bar with a Topsøe two-bed S 200 radial converter, followed by a single-bed radial S 50 converter (S 250 configuration). After the converters, high-pressure steam is generated. An additional proprietary item is the side-fired reformer.

For this most energy-efficient concept, so far not been demonstrated in an industrial installation, a figure of 27.9 GI/tNH_3 is claimed for a stand-alone plant [1079].

Krupp–Uhde Process. Uhde (now Krupp–Uhde), in the ammonia business since 1928, markets a low-energy ammonia plant with classic process sequence and catalysts [1083]–[1090]. High plant reliability at competitive overall costs was a major objective.

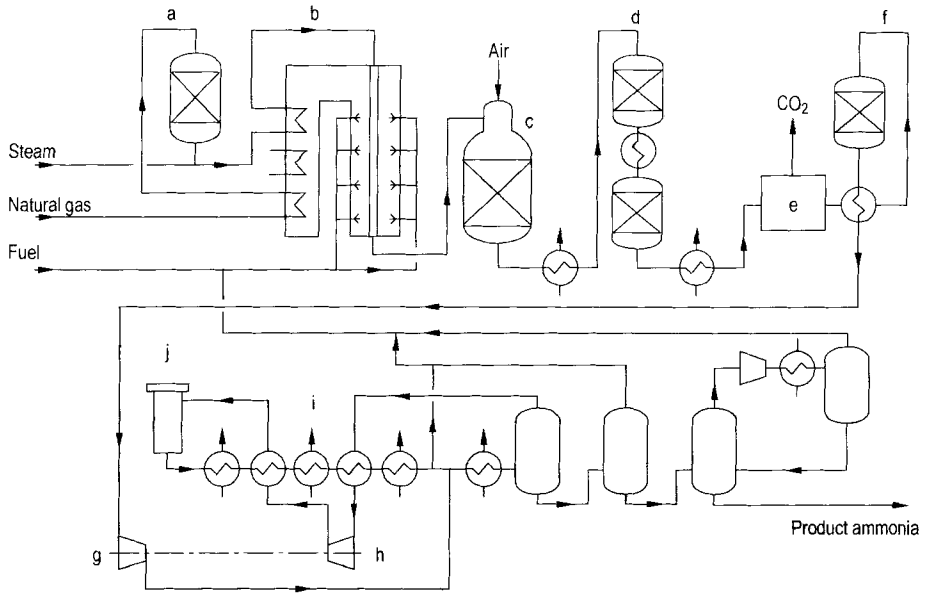

Figure 108. Haldor Topsøe's low energy process
a) Desulfurization; b) Primary reformer; c) Secondary reformer; d) Shift conversion; e) CO_2 removal; f) Methanation; g) Main compressor; h) Recycle compressor; i) Heat recovery; j) Converter

A process flow diagram together with the main process streams is presented in Figure 105.

Key features are the high reforming pressure (up to 41 bar) to save compression energy, use of Uhde's proprietary reformer design [1084] with rigid connection of the reformer tubes to the outlet header, also well proven in many installations for hydrogen and methanol service. Steam to carbon ratio is around 3 and methane slip from the secondary reformer is about 0.6 mol % (dry basis). The temperature of the mixed feed was raised to 580 °C and that of the process air to 600 °C. Shift conversion and methanation have a standard configuration, and for CO_2 removal BASF's aMDEA process is preferred, with the possibility of other process options, too. Synthesis is performed at about 180 bar in Uhde's proprietary converter concept with two catalyst beds in the first pressure vessel and the third catalyst bed in the second vessel.

After each converter vessel high pressure steam (125 – 130 bar, up to 1.5 t/t NH_3) is generated (Uhde also offers its own boiler design in cooperation with an experienced boiler maker). Heat exchange between inlet and outlet of the first bed is performed in the first vessel, and gas flow in all beds is radial. When only a minimum of energy export (steam or power) is possible, the process heat from the secondary reformer outlet is partly used to raise high-pressure steam, and partly for superheating high-pressure steam. Refrigeration uses screw compressors with high operational flexibility and efficiency.

Achieved net energy consumption is about 28 GJ/t NH_3 and UHDE's engineers expect values of below 27 GJ/t NH_3 when a gas turbine and large steam export is included [1088].

LEAD Process (Humphreys & Glasgow, now Jacobs) [940], [1091]. The LEAD process is a highly optimized conventional approach with synthesis at 125 bar and two converter vessels, the first of which contains two catalyst beds with axial-flow quenching, while the second has a third bed with small particle size catalyst and radial flow. A consumption of 29.3 GJ/t NH_3 is claimed.

Exxon Chemical Process. The Exxon Chemical process [1092], [1093] was specifically designed for the company's own site in Canada and so far not built for third parties. It uses a proprietary bottom-fired primary reformer furnace and a proprietary hot potash carbon dioxide removal system with a sterically hindered amine activator. Synthesis loop and converter are licensed by Haldor Topsøe A/S. Synthesis is carried out at 140 bar in a Topsøe S-200 converter and total energy consumption is reported to be 29 GJ/t NH_3.

Fluor Process. The Fluor process [280], [934], [940], [1094] uses the proprietary propylene carbonate based CO_2 removal system with adsorption refrigeration using low level heat downstream of the low-temperature shift. Methanation and CO_2 removal are placed between the compression stages and thus operate at higher pressure. With a value of 32 GJ/t NH_3 [934] this is not really a low-energy concept.

Lummus Process. For the Lummus process schemes [280], [940], [1095]–[1097] a consumption of 29.6 [941] to 33.5 GJ/t NH_3 [1099] is quoted. In the synthesis section either an axial flow quench converter or a radial flow converter with indirect cooling is used. CO_2 removal is performed with a physical solvent, and there are no special features compared to other conventional process configurations.

Integrating the ammonia and urea process into a single train was proposed by **Snamprogetti** to reduce investment and operating costs [1099] (see also Chapter 7).

5.1.4.2. Processes with Reduced Primary Reformer Firing

Braun Purifier Process [753], [940], [1100]–[1110]. Characteristic of the low-energy Braun purifier process (originally C. F. Braun, later Brown & Root, now M. W. Kellogg) is the reduced primary reformer duty, which is achieved by shifting a proportion of the reforming reaction to the secondary reformer by using about 150 % of the stoichiometric air flow. The excess nitrogen introduced in this way is removed after the methanation step in a cryogenic unit known as a purifier [1105], which also removes the methane and part of the argon. The result is a purer synthesis gas

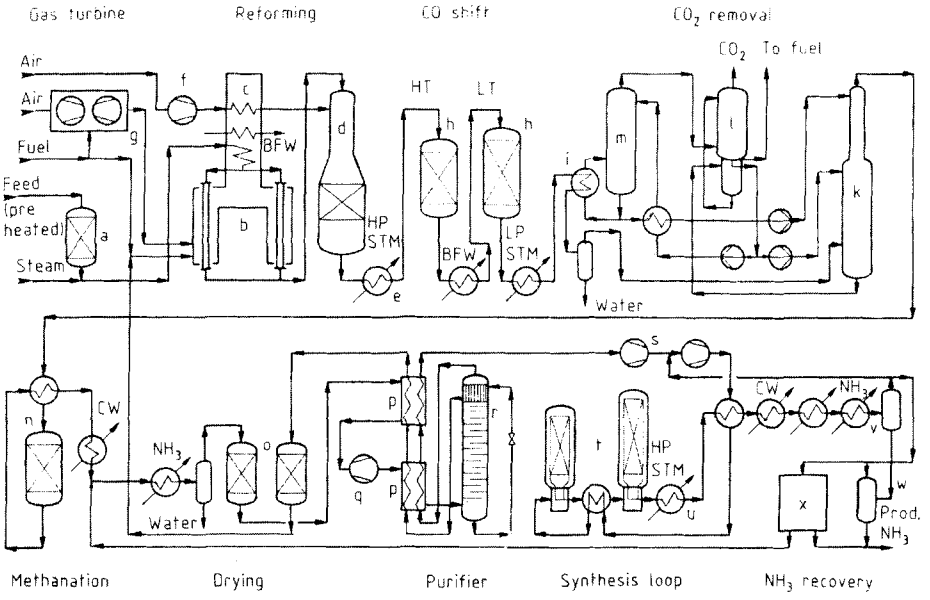

Figure 109. The Braun purifier ammonia process
a) Sulfur removal; b) Primary reformer; c) Convection section; d) Secondary reformer; e) Waste heat boiler; f) Process air compressor; g) Gas turbine; h) High- and low-temperature shift converters; i) CO_2 removal solvent reboiler; k) CO_2 absorber; l) CO_2 desorber; m) CO_2 stripper; n) Methanator; o) Driers; p) Purifier heat exchanger; q) Expansion turbine; r) Purifier column; s) Synthesis gas compressor; t) Synthesis converters; u) Waste heat boiler; v) High-pressure ammonia separator; w) Ammonia letdown vessel; x) Ammonia recovery from purge gas

compared to conventional processes, and only minimal purge from the loop is required. A typical flow diagram of this process is shown in Figure 109.

Synthesis is carried out in the proprietary Braun adiabatic hot-wall converter vessels (Figure 94). Each catalyst bed (of which three are now used in newer plants [1104]) is accommodated in a separate vessel with an inlet–outlet heat exchanger after the first and high-pressure steam boilers after the following. The smaller furnace produces less flue gas and consequently less waste heat, which makes it easier to design a balanced plant with no energy export. The lower reforming temperature allows a reduction of the steam/carbon ratio to about 2.75 without adverse effects on the HT shift, because of the less reductive character of the raw gas on account of its higher CO_2 content. In energy balanced plants, the use of waste heat in the secondary reformer effluent is split between steam raising and steam superheating.

The concept shows great flexibility [1106] for design options. It is possible, for example, to aim for minimal natural gas consumption, even at the cost of importing some electric power. On the other hand, it is possible to improve the overall efficiency further by exporting a greater amount of energy. In this latter case it is advantageous to incorporate a gas turbine to drive the process air compressor. The hot exhaust (about 500 °C) of the turbine contains 16–17 mol% of oxygen and can serve as preheated combustion air of the primary reformer. In addition it is possible to include an electric generator to cover the plant demand and export the surplus. The Braun & Root process

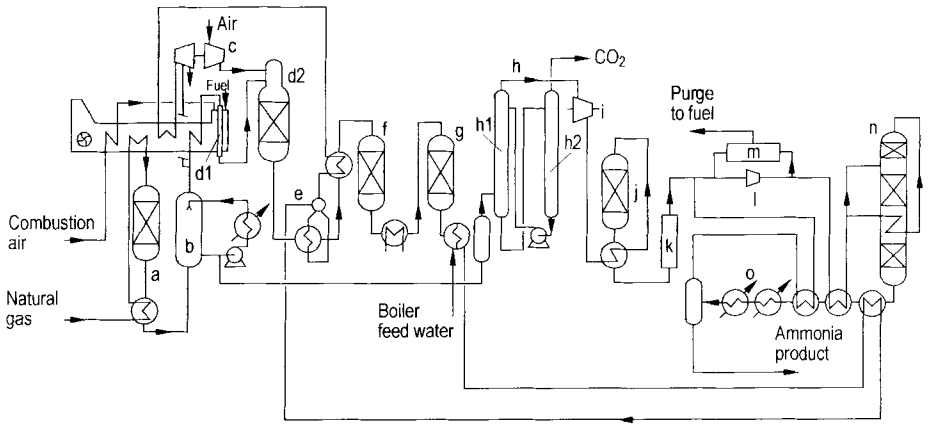

Figure 110. ICI AMV process
a) Desulfurization; b) Natural gas saturation; c) Process air compression; d1) Primary reformer; d2) Secondary Reformer; e) Boiler; f) High temperature shift; g) Low temperature shift; h) Selexol CO_2 removal; h1) CO_2 absorber; h2) Regenerator; i) Single stage compression; j) Methanation; k) Cooling and drying; l) Circulator; m) Hydrogen recovery; n) Ammonia converter; o) Refrigeration system

can attain 28 GJ/t NH_3 in a balanced plant, but with steam export and realization of the available improvement possibilities a value of 27 GJ/t NH_3 seems feasible.

ICI AMV Process. The ICI AMV process [1034], [1083], [1111]–[1122], also operates with reduced primary reforming (steam/carbon ratio 2.8) and a surplus of process air in the secondary reformer, which has a methane leakage of around 1 %. The nitrogen surplus is allowed to enter the synthesis loop, which operates at the very low pressure of 90 bar with an unusually large catalyst volume, the catalyst being a cobalt-enhanced version of the classical iron catalyst. The prototype was commissioned 1985 at Nitrogen Products (formerly CIL) in Canada, followed by additional plants in China. A flow sheet is shown in Figure 110.

In the Canadian plant, only the air compressor is driven by a steam turbine, which receives the total steam generated in the plant and has an electric generator on the same shaft. All other consumers, including synthesis gas compressor, are driven by electric motors. Separate machines are used for makeup gas and recycle compression. The makeup gas compressor is located upstream of the methanator to make use of the compression heat to warm up the cold gas coming from the Selexol carbon dioxide scrubber.

A further key feature is that about half of the process steam is supplied by feed gas saturation. The synthesis converter is a three-bed design with quench between the first two beds and an exchanger after the second bed to raise the gas temperature of the feed to the first bed. Excess nitrogen and inerts (methane and argon) are removed by taking a purge gas stream from the circulator delivery and treating it in a cryogenic unit operating at loop pressure. The recovered hydrogen is returned to the circulator suction. Demonstrated efficiency is 28.5 GJ/t NH_3.

Foster Wheeler AM2 Process. The Foster Wheeler AM2 process [1035], [1123], also belongs to the group of processes that shift load from the primary to the secondary reformer, but differs from the preceding concepts in that only 20–50 % of the total feedstock is treated in the tubular primary reformer. The remaining feed is directly sent to the secondary (autothermal) reformer which operates with a high surplus of process air (up to 200 %) and a rather high methane slip of 2.75 % (dry basis). After conventional shift, further purification is performed by Selexol CO_2 removal, methanation, and molecular sieve drying. A cryogenic unit operating at synthesis pressure rejects the nitrogen surplus from the loop. An energy consumption of 29.3 GJ/t NH_3 is claimed.

Humphreys & Glasgow BYAS Process. The Humphreys & Glasgow (now Jacobs) BYAS process [1113], [1124], [1125] resembles the above-described processes in its principal process features: a considerable proportion of the feed is sent directly to the secondary reformer, bypassing the fired primary reformer; use of excess air in the secondary reformer; installation of a cryogenic unit as last step of make-up gas production to remove excess nitrogen, residual methane, and the majority of the argon. As a consequence the inert level in the loop can be kept rather low, with only a small withdrawal of purge gas. An energy consumption as low as 28.7 GJ/t NH_3 is claimed [1126]. The process is especially suited for revamps, where it allows plant capacity to be increased.

Jacobs Plus Ammonia Technology [1127] is especially tailored for small capacities in the 300 to 450 t/d range, with a load shift from primary to secondary reformer and use of excess process air. To produce a stoichiometric synthesis gas the surplus nitrogen has to be rejected in the final purification. This is done in a PSA unit, which receives the purge gas and part of the synthesis gas taken ahead of the methanation step. All nitrogen, methane, residual carbon oxides, and argon are adsorbed to give a stream of pure hydrogen. Hydrogen and the remainder of the synthesis gas downstream of methanation are mixed to achieve a 3:1 H_2:N_2 gas composition, with a lower inerts content than the synthesis gas after methanation. The consumption figure reported for a totally energy-balanced plant is 28.8 GJ/t NH_3, and with substantial steam export a value of 26.8 GJ/t NH_3 is claimed.

Montedison Low-Pressure Process. The Montedison low-pressure process [940], [1036], [1128], [1129] involves a split flow to two primary reformers. About 65 % of the feed–steam mixture flows conventionally through the radiant tubes of a fired primary reformer followed by a secondary reformer. The balance of the feed–steam mixture passes through the tubes of a vertical exchanger reformer. This exchanger reformer has a tube sheet for the catalyst tubes at the mixed feed inlet. There is no tube sheet at the bottom of the tubes, where the reformed gas mixes directly with the secondary reformer effluent. The combined streams flow on the shell side to heat the reformer tubes in a manner similar to that described for the M. W. Kellogg KRES reformer, see Sections 4.1.1.8 and 5.1.4.3). The process air flow is stoichiometric. Synthesis is performed at 60 bar in a proprietary three-bed indirectly cooled converter with am-

monia separation by water, from which ammonia is then recovered by distillation using low-grade heat. Other process steps are conventional. As driver of the process air compressor the installation of a gas turbine is suggested with use of the hot exhaust as preheated combustion air for the fired primary reformer. For this process, which has been tested in a 50 bar pilot plant, an energy consumption of 28.1 GJ/t NH_3 is claimed [1036].

Kellogg's LEAP Process. In the late 1970s Kellogg [280], [938], [940], [1130] proposed a process which extends the basic idea of the concept described above even further. The flow of the preheated gas stream mixture is split into three streams, with 47% through catalyst tubes in the radiant section of the fired primary reformer, 12% through catalyst tubes in the convection section, and 41% through the tubes of an exchanger reformer heated by the effluent of a secondary reformer. It was intended to operate the ammonia synthesis at the pressure of the front end by using no synthesis gas compression or only a small booster. An enormous quantity of the classical ammonia synthesis catalyst would have been necessary, and for recovery of the ammonia from the loop a water wash with subsequent distillation was suggested, using low-level heat in an integrated absorption refrigerator. A consumption below 28 GJ/t NH_3 was calculated.

In the **GIAP concept** [1133] 46% of the feed is reformed in a traditional fired reformer and 54% in an exchanger reformer, heated by the effluent of the secondary reformer. The parallel operation avoids the need for air separation to provide oxygen-enriched air for the secondary reformer. In case of availability of oxygen at the site, the fired reformer may be eliminated and the whole reforming job is performed in the exchanger reformer/secondary reformer combination. A conventional HT and LT shift conversion is used, followed by an MDEA CO_2-removal unit. For final purification PSA is applied; there is no methanation step. The synthesis is performed at a pressure level of 72–80 bar using conventional ammonia catalyst in three identical blocks consisting of a reactor, a boiler, and an economizer. Ammonia is condensed at –10 and –27 °C. An overall consumption of 27.7 GJ/t NH_3 is claimed.

5.1.4.3. Processes without a Fired Reformer (Exchanger Reformer)

ICI LCA Process. The ICI LCA process [1131]–[1136] was a radical breakaway from the design philosophy of the highly integrated large plant used successfully for the previous 25 years. Figure 111 shows a diagram of the so-called core unit which includes only the sections essential for ammonia production (up to 450 t/d). A separate utility section, shown in Figure 112, supplies refrigeration, steam, electricity, includes cooling and water-demineralization system, and, if needed, recovers pure carbon dioxide. Both figures show the configuration of the first two plants built at Severnside (UK) with a capacity of 450 t/d each.

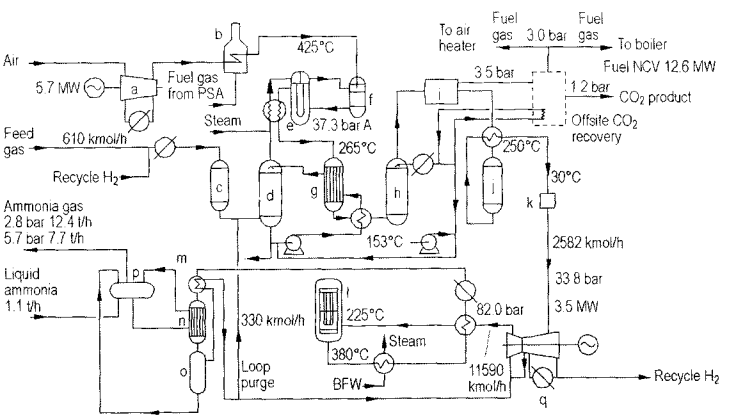

Figure 111. ICI LCA process (core unit)
a) Process air compressor; b) Start-up air heater; c) Hydrodesulfurization; d) Saturator; e) GHR; f) Secondary reformer; g) Shift converter; h) Desaturator; i) PSA system; j) Methanator; k) Gas dryer; l) Ammonia converter; m) Two-stage flash cooling (one stage shown); n) Chiller; o) Catchpot; p) Flash vessel q) Synthesis gas compressor.

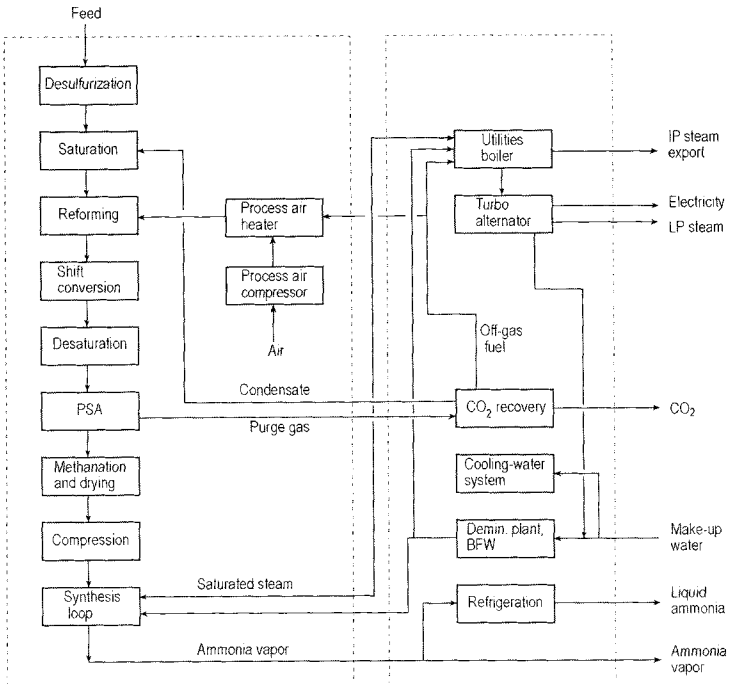

Figure 112. Arrangement of core units and utility section

Feed gas is purified in a hydrodesulfurization unit operating at lower than usual temperatures and passes through a saturator to supply a part of the process steam, while the balance is injected as steam. Heated in an inlet–outlet exchanger to 425 °C

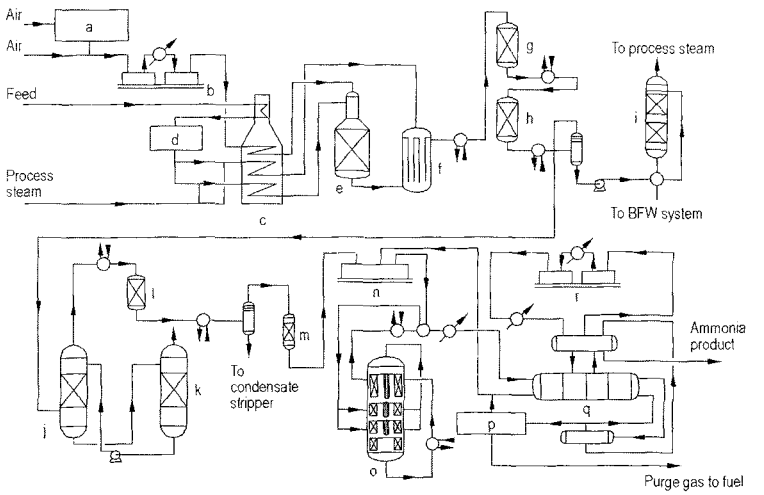

Figure 113. Kellogg's Ammonia 2000 process (integrated KRES/KAAP process)
a) Air separation unit; b) Air compressor; c) Process heater; d) Sulfur removal; e) Autothermal reformer; f) Reforming exchanger; g) HTS; h) LTS; i) Condensate stripper; j) CO_2 absorber; k) CO_2 stripper; l) Methanator; m) Dryer; n) Synthesis gas compressor; o) KAAP ammonia converter; p) Purge gas recovery unit; q) Refrigeration exchanger; r) Refrigeration compressor

the mixed feed enters the ICI gas heated reformer (GHR) [471]–[473] at 41 bar, passing to the secondary reformer at 715 °C. The shell side entrance temperature of the GHR (secondary reformer exit) is 970 °C, falling to 540 °C at the exit of the GHR. Methane levels at the GHR exit and the secondary reformer are 25% and 0.67% respectively (dry basis). Overall steam to carbon ratio is 2.5–2.7. The gas, cooled to 265 °C in the inlet/outlet exchanger, enters a single-stage shift conversion reactor with a special copper–zinc–alumina-based catalyst that operates in quasi-isothermal fashion and is equipped with cooling tubes in which hot water circulates, whereby the absorbed heat is used for feed gas saturation, as described above. CO_2 removal and further purification is effected by a PSA system, followed by methanation and drying.

Synthesis operates at 82 bar in a proprietary tubular converter loaded with a cobalt-enhanced formulation of the classical iron catalyst. Purge gas is recycled to the PSA unit, and pure CO_2 is recovered from the PSA waste gas by an aMDEA wash. Very little steam (60 bar) is generated in the synthesis loop and from waste gases and some natural gas in the utility boiler in the utility section, and all drivers are electric.

The original intention was to design an ammonia plant which can compete with modern large capacity plants in consumption and specific investment, and, by means of lower energy integration, to achieve greater flexibility for start-up and reduced-load operation, needing minimum staffing. The basic plant features (GHR, isothermal shift, and synthesis) can in principle be applied to larger capacities. The flow sheet energy consumption is 29.3 GJ/t NH_3.

Kellogg Ammonia 2000 Process [398], [476]–[478]. Kellogg has combined its KAAP synthesis loop (see Sections 4.5.2 and 4.5.3) with its KRES exchanger reformer/autothermal reformer combination (see Section 4.1.1.8) in Ammonia 2000, an optimized integrated concept for green-field plants, intended for use in world-scale single-train plants in the 1800 t/d range. Figure 113 presents a simplified flow diagram.

Desulfurized gas is mixed with steam and then split into two streams in approximate ratio 2:1. These are separately heated in a fired heater. The smaller of the two enters the exchanger reformer at 550–550 °C, while the remainder is passed directly to the autothermal reformer at 600–640 °C. The exchanger reformer and the autothermal reformer use conventional nickel-based primary and secondary reforming catalysts, respectively. To satisfy both the stoichiometry and the heat balance, the autothermal reformer is fed with enriched air (30% O_2). The required heat for the endothermic reaction in the tubes of the exchanger reformer comes from the gases on the shell side, comprising a mixture of the effluent from the autothermal reformer and the gas emerging from the tubes. The shell side gas leaves the vessel at 40 bar.

Synthesis proceeds at about 90 bar in a four-bed radial-flow converter (hot-wall design) with interbed exchangers. The first bed is charged with conventional iron-based catalyst for bulk conversion and the others with Kellogg's high activity ruthenium-based catalyst, allowing an exit ammonia concentration in excess of 20% to be obtained. The other process steps are more along traditional lines. The overall energy consumption claimed for this process can be as low as 27.2 GJ/t NH_3.

The LCA and Ammonia 2000 processes are environmentally favorable because atmospheric emissions of both nitrogen oxides and carbon dioxide are dramatically reduced as there is no reforming furnace.

Chiyoda Process [1137]. In this process the traditional fired primary reformer is also replaced by an exchanger reformer and the heat balance requires excess air in the secondary reformer with the consequence of a cryogenic unit as final step in the make-up gas preparation to remove the surplus of nitrogen. Additionally, gas turbines are proposed as drivers for the process air compressor and synthesis gas compressor with the hot exhaust being used for steam generation and feed gas preheating.

5.1.4.4. Processes without a Secondary Reformer (Nitrogen from Air Separation)

KTI PARC Process. The KTI PARC ammonia process [651], [1138]–[1144] uses the following process elements: air separation unit, classical primary reformer at 29 bar, standard HT shift, power generation in a Rankine cycle with CFC to generate electric power (optional), carbon dioxide removal (optional, only when pure CO_2 product is required), PSA, nitrogen addition, synthesis loop. In this concept four sections of the classical process sequence (secondary reforming, LT shift, CO_2 removal, methanation) can be replaced by the fully automatic high-efficiency PSA system, which has a proprietary configuration (UOP) in which nitrogen flushing enhances hydrogen recovery. The overall efficiency ranges from 29.3 to 31.8 GJ/t NH_3.

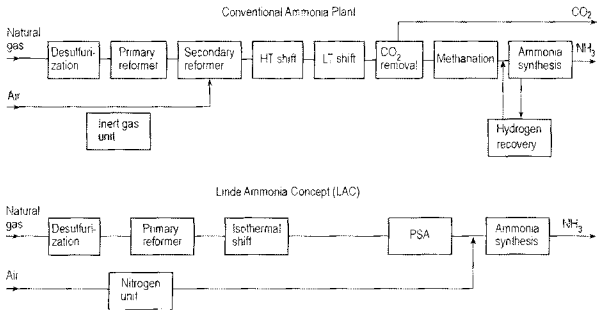

Figure 114. Comparison of Linde LAC process with a conventional process

Linde LAC Process. The recently announced Linde LAC process [1145]–[1149] consists essentially of a hydrogen plant with only a PSA unit to purify the synthesis gas, a standard cryogenic nitrogen unit, and an ammonia synthesis loop. In principle it is similar to the PARC process, but designed for world-scale capacities. A 1350 t/d plant is presently under construction. Figure 114 compares the LAC process to a conventional one. If pure CO_2 is needed, it can be recovered by scrubbing the off-gas from the PSA unit at low pressure or, probably with better energy efficiency, by installing the CO_2 removal unit directly in the synthesis gas train ahead of the PSA system. The synthesis converter and loop are based on ICI and Casale know-how. According to Linde the process should consume about 28.5 GJ/t NH_3 or, with inclusion of pure CO_2 recovery, 29.3 GJ/t NH_3.

Humphreys & Glasgow MDF Process (now Jacobs) [280], [1097], [1098], [1151]–[1153]. This concept has a configuration similar to the Linde LAC process. Energy consumption with inclusion of pure CO_2 recovery (which is optional) is 32.8 GJ/t NH_3.

5.2. Ammonia Plants based on Partial Oxidation

5.2.1. Ammonia Plants based on Heavy Hydrocarbons

Although partial oxidation processes can gasify any hydrocarbon feedstock, on account of its higher energy consumption and investment costs, commercial use of this technology is restricted to the processing of higher hydrocarbons, which can contain as much as 7% sulfur. Where natural gas is unavailable or the heavy feedstock can be obtained at a competitive price, this gasification technology can be an economic choice.

There are two commercially proven partial oxidation routes for heavy feedstocks: the Shell process and the Texaco process. Recently Lurgi has come out with an own partial oxidation variant, named LurgiSVZ MPG Process (Section 4.1.2.2). In contrast to the steam reforming, for which most contractors have their own proprietary technology for the individual process steps, the engineering firms which offer ammonia plants based on heavy hydrocarbons have often to rely for the individual process stages on different licensors. Lurgi, for example, has built very large capacity ammonia plants that use Shell's gasification process, its own proprietary version of the Rectisol process, Linde's air separation and liquid nitrogen wash, and Topsøe's technology for synthesis converter and loop.

Independent, experienced engineering companies, not directly active in ammonia plant design may be used as general contractors to coordinate a number of subcontractors supplying the different technologies required. This is in line with the fact that the degree of energy integration is usually lower than in steam reforming technology, because in absence of a large fired furnace, there is no large amount of flue gas and consequently less waste heat is available. Therefore, a separate auxiliary boiler is normally included to provide steam for mechanical energy and power generation. Nevertheless, some optimization has successfully reduced the overall energy consumption, for which in older installations values of around 38 GJ/t NH_3 were reported. In recent commercial bids, values as low as 33.5 GJ/t NH_3 have been quoted.

The arguments presented above suggest describing the two principal routes, Shell and Texaco, which differ in the gasification process, rather than listing all individual contractor design approaches. Figure 115 shows the classical sequence of process steps for both cases.

Processes Using Shell Gasification (e.g., Lurgi) [521]–[531]. A cryogenic air separation plant provides oxygen for the gasification and the nitrogen for the liquid nitrogen wash and for supplying the stoichiometric amount for the synthesis of ammonia. Oil enters the alumina-lined gasification vessel through a central jet in the burner nozzle. A substantial pressure drop is needed to ensure atomization of the oil and proper mixing with oxygen, fed through the annulus between the jet and the outer case of the burner nozzle. The temperature in the gasification vessel (generator) is between 1200 and 1400 °C, and the pressure between 35 and 65 bar.

The hot gas contains soot, formed because of insufficient mixing of the reactants, and fly ash. A waste-heat boiler, a proprietary item of the Shell process, raises 100 bar steam and cools the gas to 340 °C. Soot is removed from the raw gas in a two-stage water wash. Older installation used an elaborate technique to remove the soot from the water by extraction with naphtha and light oil to form soot pellets which could be burnt or recycled to the feed oil. In newer installations the carbon–water slurry is filtered off in automatic filters, and the moist filter cake is subjected to a controlled oxidation in a multiple-hearth furnace.

A selective Rectisol unit with methanol of about – 30 °C as solvent is used to remove H_2S and COS (together with some CO_2) to less than 0.1 %. The removed sulfur-rich

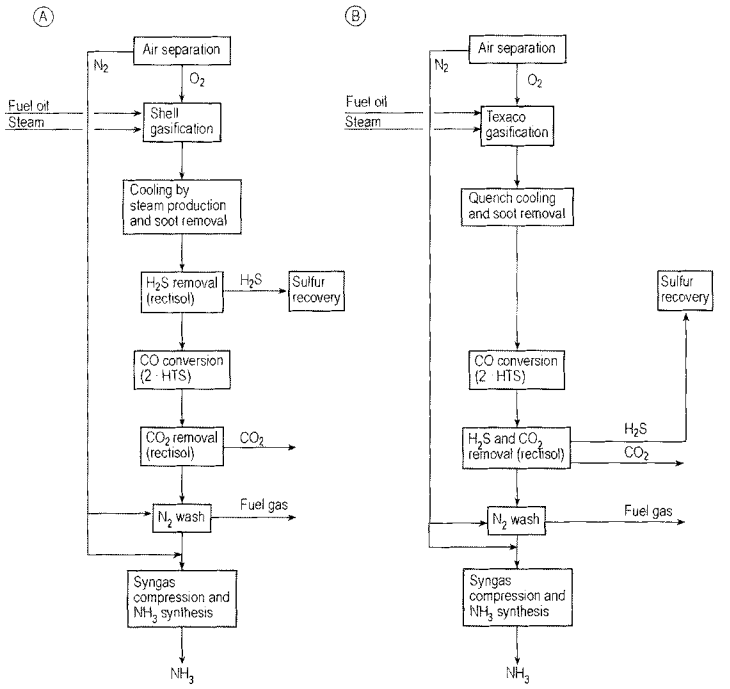

Figure 115. Flow diagrams of ammonia production from fuel oil or heavy residues by the Shell (A) and the Texaco (B) process (standard configuration)

fraction is sent to a Claus plant for recovery of elemental sulfur or converted to sulfuric acid. The gas is heated subsequently by heat exchange, supplied with steam in a saturator, and then fed to shift conversion, which proceeds stepwise with intermediate heat removal. The gas is cooled by a direct water cooler, and the hot water is recycled to the saturator.

A second Rectisol wash stage follows to remove CO_2 by absorption at – 65 °C in methanol, which is regenerated by flashing and stripping. Molecular sieve adsorption then removes residual traces of methanol and CO_2. To remove residual CO a liquid nitrogen wash is applied for final purification with the advantage of also lowering the argon content in the makeup gas, which is adjusted by nitrogen addition to the stoichiometric ratio $N_2:H_2 = 1:3$. Converter and synthesis loop configuration depend on the licensor chosen. Plant descriptions are given in [1154]–[1157].

Processes Using Texaco Gasification (e.g., Foster Wheeler, Linde, Uhde). Temperatures in the generator are similar to those in the Shell process; units with operating pressures up to 90 bar are in operation [513], [532], [533], [537], [540]–[542]. Some modern installations (e.g., Linde) use pumps for liquid oxygen instead of oxygen compressors. In contrast to the Shell arrangement, oxygen enters the gasifier through the central nozzle of the burner, and oil is fed through the annular space between central nozzle and outer burner tube. Instead of a waste-heat boiler a direct water

quench is applied for cooling the raw synthesis gas, which is subsequently scrubbed first in a Venturi scrubber and then in a packed tower to remove the soot. Texaco also offers a version operating with a waste-heat boiler instead of a water quench. Although this is preferable when producing CO-rich synthesis gases (e.g., methanol or oxogas), quench is thought to be more economical when hydrogen-rich gases are manufactured. Soot recovery from the water is performed by extraction with naphtha. The soot–naphtha suspension is mixed with feed oil, and the naphtha is distilled off and recycled to the extraction stage. The shift reaction uses a cobalt–molybdenum–alumina catalyst [630], [640]–[643] which is not only sulfur-tolerant but also requires a minimum sulfur content in the gas for proper performance. The conversion is subdivided into stages with intermediate cooling by raising steam. The following Rectisol process has a somewhat more elaborate configuration than the version used in the Shell route. The large amount of carbon dioxide formed in shift conversion lowers the H_2S concentration in the sour gas, and for this reason a special concentration step is required for methanol regeneration to obtain pure CO_2 and a fraction sufficiently rich in H_2S for a Claus plant or a sulfuric acid plant. The remaining process steps are identical with the Shell route. Figure 116 gives an example of a Linde flow diagram. Descriptions of plants using the Texaco process can be found in [630], [1158].

Topsøe Process. A concept using enriched air instead of pure oxygen and methanation instead of a liquid nitrogen wash was proposed by Topsøe [1159], [1160]. A Shell gasifier with a waste-heat boiler or a Texaco generator with a quench are equally well suited to this process. After soot removal, shift conversion is performed on a sulfur-tolerant catalyst in several beds with intermediate cooling, leaving a residual CO content of 0.6 mol%. An appropriate process (Rectisol or amine based) removes the sour gases H_2S, COS, and CO_2, and this is followed by methanation. Makeup gas drying, compression, and synthesis loop have no special features. The anticipated energy consumption is 34.8 GJ/t NH_3. A basically similar synthesis gas preparation, but based on gasification with pure oxygen, is already used in large commercial plant in Japan [1161].

Foster Wheeler Air Partial Oxidation process [1035], [1162] is a proposed modification of the Texaco gasification process. It is intended to operate at 70 bar with highly preheated air (815 °C) instead of pure oxygen. The synthesis gas purification train comprises soot scrubbing followed by shift conversion, acid gas removal (for example Selexol), and methanation. The gas is dried and finally fed to a cryogenic unit, which removes the surplus nitrogen by condensation together with methane, argon, and residual carbon monoxide. The rejected nitrogen is heated and expanded in a turbine, which helps to drive the air compressor.

A major aspect in the design concept is the separation of nitrogen and oxygen. A conventional air separation plant is based on the fractional distillation of oxygen and nitrogen, which differ in boiling point by only 13 °C. In the cryogenic unit for the Foster Wheeler process a lesser quantity of nitrogen is separated from hydrogen with a

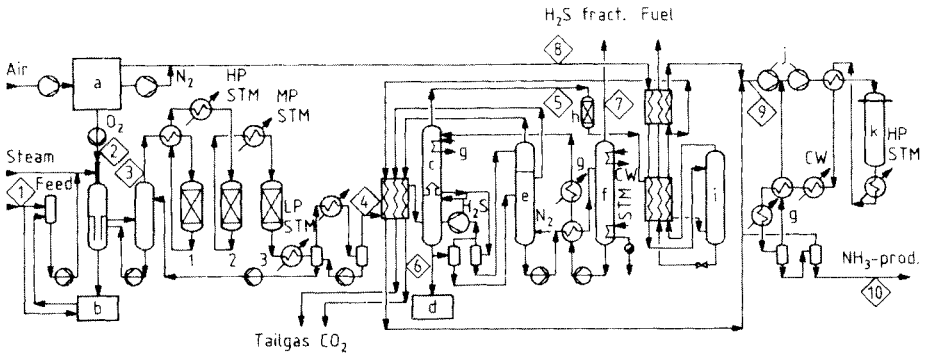

① Feed: heavy fuel oil

m = 44 t/h
p = 0.4 MPa
t = 90 °C

Composition, wt%

C	84.6
H	10.0
O	0.4
N	0.4
S	4.5
Ash	0.1

② Oxygen

m = 49.6 t/h
p = 9.0 MPa
t = 150 °C

Purity

O_2 = 98.5 vol%

balance: Ar and N_2

⑩ Ammonia

m = 56.25 t/h
p = 2.5 MPa
t = 11 °C

		③	④	⑤	⑥	⑦	⑧	⑨
H_2	vol%	43.0	60.8	96.3	0.9	0.1	–	75.00
CO	vol%	47.7	1.5	2.3	0.1	–	–	–
CO_2	vol%	6.9	35.8	–	98.8	67.4	–	–
N_2	vol%	0.1	0.1	0.2	0.1	2.5	100.00	25.00
CH_4	vol%	0.8	0.5	0.8	0.1	–	–	–
Ar	vol%	0.4	0.3	0.4	0.0	–	–	–
H_2S + COS	vol%	1.1	0.8	–	–	30.0	–	–
H_2O	vol%		0.2	–	–	–	–	–
kmol/h		5680	8250	5200	1800	200	1750	6650
p	MPa	8.37	7.65	7.30	0.15	0.25	7.4	7.1
t	°C	255	45	−63	−15	15	15	10

Figure 116. Ammonia production based on heavy fuel oil (Linde flow scheme with Texaco gasification)
a) Air separation unit; b) Soot extraction; c) CO_2 absorption; d) Methanol/H_2O distillation; e) Stripper; f) Hot regenerator; g) Refrigerant; h) Dryer; i) Liquid N_2 scrubber; j) Syngas compressor; k) NH_3 reactor
Material Balance

much higher boiling point difference (57 °C). According to Foster Wheeler this leads to considerable saving in capital investment and energy consumption compared to the traditional approach using pure oxygen from an air separation plant and a liquid nitrogen wash for gas purification. A figure of 35.6 – 37.6 GJ/t NH_3 is claimed for heavy oil feedstock and 31.4 – 32.7 for natural gas as feedstock. A similar variant also using air instead of pure oxygen is offered by *Humphreys & Glasgow* (now Jacobs) [1163].

5.2.2. Ammonia Plants Using Coal as Feedstock

In the early days the entire ammonia industry was based on coal feedstock. Today coal or coke (including coke oven gas) is no longer of major economic importance. In 1990, for example, only 13.5 % of the world ammonia capacity was based on this raw material [410]. Apart from a few plants operating in India and South Africa, the majority of coal-based ammonia plants is found in China. Commercially proven coal gasification processes are Lurgi (dry gasifier), British Gas/Lurgi (slagging gasifier), Winkler/HTW, Koppers–Totzek, Shell, Texaco, and Dow [544]–[546]. So far the Koppers–Totzek, Texaco, and Lurgi processes have commercial importance for ammonia production [548]–[554]. Pressureless Winkler gasification, which was used on large scale in the 1930s and 1950s, later found limited application in some countries. The Shell process, demonstrated commercially in another application with a capacity equivalent to a world-scale ammonia plant, is a potential candidate for ammonia production processes.

In recent years little development work has been done on complete ammonia plant concepts based on coal. The traditional leading ammonia contractors have to rely on proprietary processes licensed from different companies, which similarly tend not to have specific ammonia technology of their own. Again, compared to a steam reforming plant, the degree of integration is considerably lower; power generation facilities are usually separate. Thus it is difficult to identify specific ammonia processes for the individual contractors and the following descriptions serve as examples, without striving for completeness.

The Koppers–Totzek Process gasifies coal dust with oxygen in the temperature range 1500–1600 °C at about atmospheric pressure. For a more detailed description of the gasification, refer to Section 4.1.2.3 and [546], [555]–[561]. The cooled gas, free of coal dust and fly ash, contains about 60 % of CO. The next step is compression to about 30 bar, followed by sulfur removal at –38 °C with chilled methanol (Rectisol process). Steam is added for the shift conversion, carried out stepwise with intermediate heat removal and with a standard HTS catalyst. A second Rectisol stage, operating at –58 °C and 50 bar, removes the CO_2, and the final purification step is a liquid nitrogen wash. Any of the well known converter and synthesis loop concepts may be used, with no purge or minimal purge, due to the practically inert-free makeup gas. Several plants are operating in South Africa [1164], [1165] and India [1166].

The atmospheric-pressure gasification is a considerable disadvantage of this process route, which substantially increases equipment dimensions and costs, as well as the power required for synthesis gas compression. An energy input of 51.5 GJ/t NH_3 (LHV) has been reported. According to [563], the atmospheric ACGP gasifier (Section 4.1.2.3) could lower the consumption to 44 GJ/t NH_3 (HHV).

Lurgi Process. Lurgi [544], [545], [578]–[582], [1167] offers a concept using its proprietary Lurgi dry bottom gasifier, described in Section 4.1.2.3. The moving-bed

generator, which can handle any sort of coal (ash content may exceed 30 %), operates at 30 bar, and the product gas contains up to 15 % CH_4, higher hydrocarbons, troublesome phenolic material, and tars. After washing with process condensates to remove ash and dust, the gas is cooled further with recovery of waste heat. Several process steps treat the separated gas liquor to recover tar, phenols, and some ammonia. Shift conversion, Rectisol process, and liquid nitrogen wash are the further operations in the production of makeup gas. The liquid nitrogen wash produces a methane-rich fraction, which is separately processed in a steam reformer, and the reformed gas rejoins the main stream at the Rectisol unit for purification. The gasification has a power consumption of 32 – 34 GJ/t NH_3, and steam generation consumes 18 – 22 GJ/t NH_3, resulting in a total energy consumption of 50 – 56 GJ/t NH_3.

The Texaco Coal Gasification Process [545], [564] – [571], [1168] – [1172] (see Section 4.1.2.3) originates from Texaco's partial oxidation process for heavy oil fractions and processes a coal – water slurry containing 60 – 70 % coal. A lock hopper system removes ash and glassy slag as a suspension from the quench compartment of the generator. The process can handle bituminous and sub-bituminous coal but not lignite. The further gas purification steps used to arrive at pure makeup gas correspond to those described for an ammonia plant using the Texaco partial oxidation of heavy oil fractions.

Ube Industries commissioned a 1000 t/d ammonia plant in 1984 using Texaco's coal gasification process [1161], [1173]. An energy consumption of 44.3 GJ/t NH_3 is stated, which is lower than the 48.5 GJ/t NH_3 quoted for another Texaco coal gasification-based ammonia plant [544].

The other coal gasification technologies were discussed in Section 4.1.2.3, but so far no newer ammonia concepts are bases on them.

6. Modernization of Older Plants (Revamping)

6.1. Revamping Objectives

With rising feedstock prices and hard competition in the market, many producers have looked for possibilities to "revamp" or modernize their older, less efficient plants so that they can stay competitive. Most revamp projects have been combined with a moderate capacity increase because some of the original equipment was oversized and only specific bottlenecks had to be eliminated, not entailing excessive cost. As the market possibilities for a company do not increase in steps of 1000 or 1500 t/d but slowly and continuously, such a moderate capacity addition will involve less risk and will often be more economical than building a new plant.

For a revamp project first an updated base-line flow sheet of the existing plant should be prepared from which the proposed improvement can be measured [1174]–[1176]. Depending on the objective (energy saving and/or capacity increase) the following guidelines should be kept in mind: maximum use of capacity reserves in existing equipment; shifting duties from overtaxed units to oversized ones; if possible, simple modifications of existing equipment are preferable to replacement; the amount of additional equipment should be kept to a minimum [1175].

6.2. Revamping Options

To give an exhaustive list or description of the individual modification options is beyond the scope of this article, but reviews on this subject and useful information are given in [1027], [1177]–[1192]. Section 5.1.2 describes modifications that lower the energy consumption in newer plant generations compared to the first generation of single-train ammonia plants, and this also represents an overview of the revamp options for existing steam reforming plants.

Just a few of the frequently used revamp possibilities should be mentioned here. In steam reforming plants it is often possible to lower the steam/carbon ratio by using improved reforming catalysts and copper-promoted HT shift catalysts. More active LT shift catalysts lower the residual CO content, which will reduce H_2 loss (methanation) and inert content in the makeup gas. Drying of the makeup gas, addition of hydrogen recovery from purge gas, and installing a more effective CO_2 removal are other options. With the *aMDEA* system, for example, which can be flexibly tailored to fit into existing process configurations, it is, for example, possible to simply replace the MEA solvent with the promoted aMDEA solution, with zero or only minor equipment modification.

Other measures, involving more additional hardware and engineering work, are introduction of combustion air preheating and reducing the primary reformer load.

This latter option is used when the revamp objective is capacity increase and the primary reformer is identified as a bottleneck. One possibility is to increase the duty of the secondary reformer and use air in excess of the stoichiometric demand. Elegant variants of this principle are the *Jacobs BYAS process* [1113], [1124], [1125] and the *Foster Wheeler AM2 process* [1035], [1123], [1193]. Another method is to perform a part of the primary reforming in a pre-reformer [462] – [469] that uses low-level heat. Alternative methods to enlarge the reforming capacity make use of the process heat of the secondary reformer in an exchanger reformer such as *ICI's GHR* [1194] or *Kellogg's KRES* [478]. If oxygen is available, installation of a parallel autothermal reformer or a parallel *Uhde CAR unit* [483], [485] – [488] (see also Section 4.1.1.8) could be considered. Description of executed revamp projects are given in [1126], [1196] – [1201].

Similarly, numerous modernization possibilities exist for partial oxidation plants, and they may even outnumber those for steam reforming plants. Common to both plant types is the potential for improvement of the synthesis loop and converter. Application of indirect cooling and smaller catalyst particles are frequently chosen to reduce energy consumption through lower pressure drop, reduced synthesis pressure, higher conversion, or a combination thereof. Apart from replacing existing converters, in situ modification of the internals of installed converters is a very economic approach. *Topsøe* [1182], [1202] mostly uses its Series 200 configuration; and *Ammonia Casale* [905] – [908], [1203] – [1207] its proprietary ACAR technology, with which more than 90 plants have been revamped so far. With a "split-flow" configuration Kellogg proposed an in situ revamp option to change its four-bed quench converter into a two-stage intercooled converter (with two parallel beds for the second stage) using smaller catalyst particles of 1.5 – 3.5 mm and 3 – 6 mm [1208], [1209]. A promising loop modernization option for the future will be the *Kellogg KAAP process* [398], [1210].

The fact that more than 40 % of world ammonia plants are older than 20 years suggests that there is a major potential for revamp projects, even in plants which have already made modifications.

7. Integration of Other Processes into an Ammonia Plant

There are — at least theoretically — many possibilities to integrate other processes into an ammonia plant. To a limited extent this is possible with an existing ammonia plant, but in this case the production rate of the side product should be small compared to ammonia production. A very simple case with practically no interference with the operation of ammonia production (only a small loss of production if it is not compensated by an adequate increase of synthesis gas generation) is the production of pure hydrogen from the synthesis purge gas by PSA, for example. Carbon monoxide may be produced from a sidestream upstream of the HT shift. With the use of the COSORB process it should be posible to produce in typical 1000 t/d ammonia plant 2000 m^3/h CO with only 2% more feed and 3% additional fuel according to calculations of KTI [650]. Hydrogen production from a sidestream by using PSA is of course possible, too. Designing a grass-root steam reforming plant for a sizeable co-production of, e.g., methanol seems to be economically not very promising, especially if a flexible production rate for the two products is required. Because of the high degree of energy integration in a steam reforming plant an investment penalty is most likely. But in the less integrated partial oxidation plant this seems to be an attractive option, and there are several large installations producing ammonia, methanol, and hydrogen [1214], [1215]. A few years ago, when ammonia prices were low and the methanol prices were sky-rocketing, some producers considered total conversion of an ammonia plant to methanol, but looking at the longer term the prices usualy develop in parallel.

Under favorable conditions, when the front end of an existing ammonia plant has capacity reserves, and the bottleneck is, for example, compression and synthesis, and probably also CO_2 removal, a revamp to incorporate parallel methanol production might be economically attractive. Options for a partial retrofit are described in [1216]; [1496]; an example for a co-production in a side stream with a separate methanol loop is given in Figure 117 [1217].

Integrating ammonia and urea production [1218] has been discussed frequently in the past, in most cases with respect to energy and CO_2 supply. For total conversion of the ammonia, the CO_2 produced in partial oxidation plants suffices but is at deficit in plants based on steam reforming of natural gas.

An integration of ammonia und urea on the process side has been suggested for example by **Toyo Koatsu** [1219], [1220], **M. W. Kellogg** [1221] and **Snamprogetti** [1222] – [1224]. In these ideas the main point of integration is the carbon dioxide removal stage, which is performed by washing with an ammonium carbamate/ammonia solution. The Snamprogetti concept uses a falling film adsorber. A falling film absorber could also be applied for ammonia recovery from the synthesis loop with the aquaeous ammonia being sent directly to the urea reactor. The introduction of the raw CO_2-containing synthesis gas into the urea reactor was even proposed in one publication.

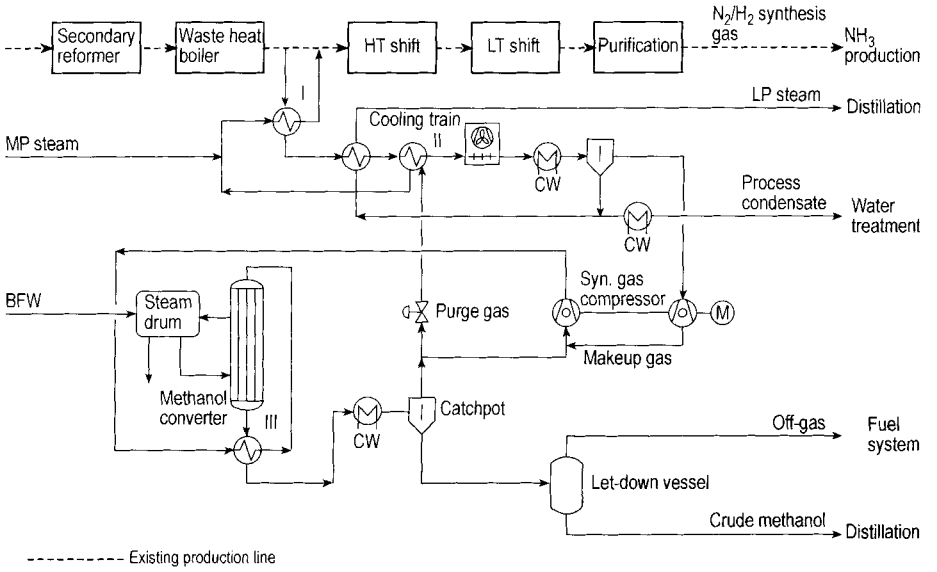

Figure 117. Methanol co-production (sidestream loop)

8. Material Considerations for Equipment Fabrication

8.1. Hydrogen Attack

In several steps of the ammonia production process, especially in the synthesis section, the pressure shells of reaction vessels as well as the connecting pipes are in contact with hydrogen at elevated pressure and temperature with a potential risk of material deterioration [1211]–[1213], [1484].

Chemical Hydrogen Attack. Under certain conditions chemical hydrogen attack [1225], [1226], [1228] can occur. Hydrogen diffuses into the steel and reacts with the carbon that is responsible for the strength of the material to form methane, which on account of its higher molecular volume cannot escape. The resulting pressure causes cavity growth along the grain boundaries, transforming the steel from a ductile to a brittle state. This may finally reach a point where the affected vessel or pipe ruptures, in most cases without any significant prior deformation. This phenomenon was already recognized and principally understood by BOSCH et al. [1] when they developed the first ammonia process. The resistance of steel against this sort of attack can be enhanced by alloy components which react with the carbon to form stable carbides (e.g., molybdenum, chromium, tungsten, and others). The rate of deterioration of the material depends on the pressure of the trapped methane, the creep rate of the material, and its grain structure. Areas highly susceptible to attack are those which have the greatest probability of containing unstable carbides, such as welding seams [1227]. The type of carbides and their activity are strongly influenced by the quality of post-weld heat treatment (PWHT). The risk of attack may exist at quite moderate temperatures (ca. 200 °C) and a hydrogen partial pressure as low as 7 bar.

Numerous studies, experiments and careful investigations of failures have made it possible to largely prevent hydrogen attack in modern ammonia plants by proper selection of hydrogen-tolerant alloys with the appropriate content of metals that form stable alloys. Of great importance in this field was the work of NELSON [1226], [1228], [1229], who summarized available experimental and operational experience in graphical form. These Nelson diagrams give the stability limits for various steels as a function of temperature and hydrogen partial pressure. In [1230], [1231], CLASS gives an extensive survey, still valid today, on this subject. Newer experience gained in industrial applications required several revisions of the original Nelson diagram. For example, 0.25 and 0.5 Mo steels are now regarded as ordinary nonalloyed steels with respect to their hydrogen resistance [1228].

Physical Hydrogen Attack. A related phenomenon is physical hydrogen attack, which may happen simultaneously with chemical attack. It occurs when adsorbed

molecular hydrogen dissociates at higher temperatures into atomic hydrogen, which can diffuse through the material structure. Wherever hydrogen atoms recombine to molecules in the material structure (at second-phase particles or material defects such as dislocations) internal stress becomes established within the material. The result is a progressive deterioration of the material that lowers its toughness until the affected piece of equipment cracks and ultimately ruptures.

The phenomenon is also referred to as hydrogen embrittlement. It is most likely to occur in welds that not received proper PWHT. Holding a weld and the heat-affected zone for a prolonged period at elevated temperature (an operation known as soaking) allows the majority of included hydrogen to diffuse out of the material. But this may not be sufficient if moisture was present during the original welding operation (for example if wet electrodes or hygroscopic fluxes were used), because traces of atomic hydrogen are formed by thermal decomposition of water under the intense heat of the welding procedure. Highly critical in this respect are dissimilar welds, such as those between ferritic and austenitic steels [1232], where the formation of martensite, which is sensitive to hydrogen attack, may increase the risk of brittle fracture.

At higher temperature and partial pressure, hydrogen is always soluble to a minor extent in construction steels. For this reason it is advisable not to cool vessels too rapidly when taking them out of service, and to hold them at atmospheric pressure for some hours at 300 °C so that the hydrogen can largely diffuse out (soaking). In contrast to the hydrogen attack described above this phenomenon is reversible.

It has been reported [1233], [1234] that hot-wall converters in which the pressure shell is in contact with ammonia-containing synthesis gas at 400 °C have developed cracks in circumferential welding seams to a depth nearly approaching the wall thickness in places. This was surprising because the operating conditions for the material (2 1/4Cr-1Mo) were well below the Nelson curve. One investigation [1235] concluded that hydrogen attack had occurred by a special mechanism at temperatures lower than predicted by the Nelson diagram. Nitriding proceeding along microcracks could transform carbides normally stable against hydrogen into nitrides and carbonitrides to give free active carbon, which is hydrogenated to methane. High residual welding stress and internal pressure are considered to be essential for the propagation of the cracks. A rival theory [1234], [1236] attributes the damage to physical hydrogen attack resulting from the use of agglomerated hygroscopic flux in combination with insufficient soaking. However, no problems were experienced for the same converter design in other cases where non-hygroscopic flux was used for welding and a more conservative vessel code was adopted, leading to less stress on account of thicker walls. Recent unpublished observations seem to support the nitriding mechanism.

8.2. Nitriding

Nitriding is a problem specific to the ammonia converter. It occurs in the presence of ammonia on the surface of steel at temperatures above 300 °C [1237] – [1240]. With unalloyed and low-alloy steels, the nitride layer grows with time to a thickness of several millimeters. Austenitic steel, used for the converter basket, develops very thin but hard and brittle nitride layers, which tend to flake off. In the nitrided areas, the risk of formation of brittle surface cracks exists.

8.3. Temper Embrittlement

For heat-resistant steels long-term service at temperatures above 400 °C (e.g., high-pressure steam pipes) can lead to a decline in impact strength. Normally, transition temperatures (precipitous decline of notched bar impact values) of below 0 °C are encountered, but this can increase to 60 °C and more (temper embrittlement).

The susceptibility to temper embrittlement can be reduced by controlling the level of trace elements (Si, Mn, P, Sn) in steels [1241], [1242]. Vessels for which temper embrittlement is anticipated should not be pressurized below a certain temperature.

8.4. Metal Dusting

Metal dusting [1243] – [1249] is a corrosion phenomenon which has come into focus again in the last few years with the introduction of exchanger reformer technology and the operation of steam superheaters in the hot process gas downstream of the secondary reformer waste heat boiler. Conventional carburization is a familiar problem with high-temperature alloys in steam reforming furnaces caused by inward migration of carbon leading to formation of carbides in the metal matrix. It happens at high temperatures, typically above 800 °C, and the carbon originates from cracking of hydrocarbons. In contrast, metal dusting occurs at 500 – 800 °C on iron – nickel and iron – cobalt based alloys with gases containing carbon monoxide. The Boudouard reaction, strongly catalyzed by iron, nickel, and cobalt, is generally regarded as the source of the carbon in this case. It is assumed that thermodynamically favored sites exist for these elements at the surface and enhance the carbon deposition if the gas composition corresponds to a carbon activity > 1 [1247], [1248].

As the name implies, the affected material disintegrates into fine metal and metal oxide particles mixed with carbon. Depending on the defects in a protective oxide film on the metal surface and the ability of the material to sustain this film, an induction period may be observed until metal dusting manifests itself as pitting or general attack. A possible mechanism was proposed by GRABKE [1250] and HOCHMANN [1251].

At least from a theoretical point of view, alloys formulated to form chromium, aluminum, or silicon oxide films should exhibit an increased resistance. Efforts to find solutions for this problem are continuing, but at present the following situation must be accepted: virtually all high-temperature alloys are vulnerable to metal dusting; higher steam/carbon ratios reduces this sort of corrosion; improvements may be expected by additional surface coating (for example with aluminum). With materials such as Inconel 601, 601H, 625 and similar alloys it is at least possible to reduce the attack to a level which is tolerable in practical operation. The active sites at the metal surface which catalyze the Boudourd reaction can be poisoned by H_2S, thus inhibiting the initiation of metal dusting [1248].

8.5. Hydrogen Sulfide Corrosion

Corrosion by hydrogen sulfide in partial oxidation plants can be controlled by the use of austenitic steels, but special care to ensure proper stress relief of welds is advisable to avoid stress corrosion cracking in these plants caused by traces of chlorine sometimes present in the feed oil.

8.6. Stress Corrosion Cracking

Stress corrosion cracking (SCC) of many steels in liquid ammonia is a peculiar phenomenon. It occurs at ambient temperature under pressure as well as in atmospheric storage tanks at – 33 °C. Extensive studies [1252]–[1265] have defined the conditions under which SSC in liquid ammonia is likely to occur and how it may largely be prevented, but the mechanism is so far not fully understood. Preventive measures include maintaining a certain water content in the ammonia and excluding even traces of oxygen and carbon dioxide. Welds in pressurized vessels must be properly stress-relieved, and in atmospheric tanks it is important to select the appropriate welding electrodes, avoid excessive differences of the thickness of plates welded together and choose the correct geometry of welding seams (see also Section 9.1.1).

9. Storage and Shipping

Producing and processing ammonia requires storage facilities to smooth out fluctuations in production and usage or shipments. If manufacture and use occur in separate locations, then appropriate transport must be arranged [1266]. This may be by ocean-going ships, river barges, rail or tank cars, or by pipeline. Ammonia is usually handled in liquid form, but in some cases delivery of ammonia vapor to downstream consumers on site may have some advantage due to savings of refrigeration energy in the ammonia plant. If there is an opportunity for on-site usage or marketing of aqueous ammonia, obtained as a byproduct of purge-gas scrubbing or, less frequently, deliberately produced, storage and handling facilities for this product will also be needed, but compared to liquid ammonia the demand is negligible.

Liquid ammonia is a liquefied gas. Its storage and distribution technologies therefore have much in common with other liquefied gases. Reference [399, vol. IV] summarizes the literature on storage, handling, and transportation of ammonia.

9.1. Storage

Three methods exist for storing liquid ammonia [1267], [1268]:

1) Pressure storage at ambient temperature in spherical or cylindrical pressure vessels having capacities up to about 1500 t
2) Atmospheric storage at −33 °C in insulated cylindrical tanks for amounts to about 50 000 t per vessel
3) Reduced pressure storage at about 0 °C in insulated, usually spherical pressure vessels for quantities up to about 2500 t per sphere

The first two methods are preferred, and there is growing opinion that reduced-pressure storage is less attractive [399]. However, in many cases, the combination of atmospheric and pressure storage may be the most economic concept (Fig. 118). The determining factors for the type of storage – apart from the required size – are temperature and the quantity of ammonia flowing into and out of storage [1269].

Characteristic features of the three types of storage are summarized in Table 40 [402]. For pressurized storage, spheres with a capacity up to 1500 t have been constructed, in which case the ratio tonnes ammonia per tonne of steel will become about 6.5.

Table 40. Characteristic features of ammonia storage tanks

Type	Typical pressure, bar	Design temperature, °C	t ammonia per t steel	Capacity, t ammonia	Refrigeration compressor
Pressure storage	16–18	ambient	2.8	< 270*	none
Semi-refrigerated storage	3–5	ca. 0	10	450–2700	single stage
Low-temperature storage	1.1–1.2	−33	41–45	4500–45 000	two-stage

*) Refers to cylindrical tanks ("bullets"); spherical vessels see Section 9.1.1.

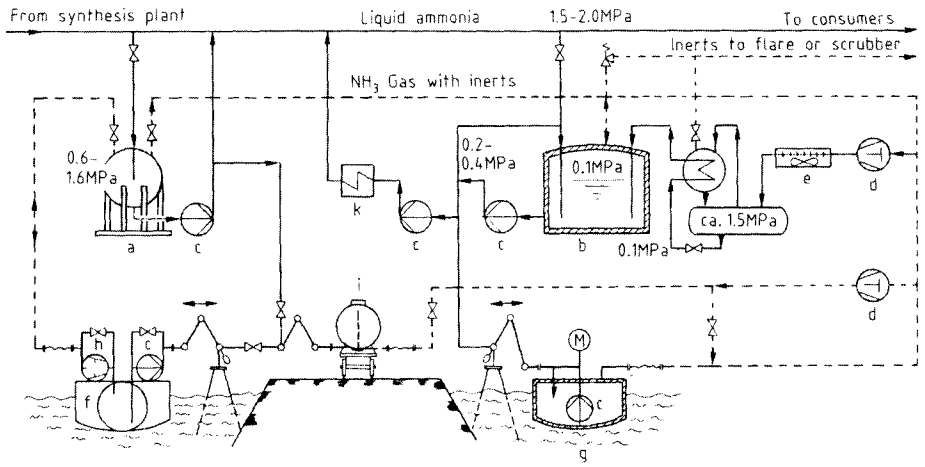

Figure 118. Ammonia terminal with loading and unloading facilities
a) Sphere at ambient temperature; b) Tank at ambient pressure (refrigerated); c) Pumps; d) Compressors; e) Air-cooled condenser; f) Barge with pressure tank; g) Barge for ammonia at ambient pressure; h) Booster; i) Rail car or truck; k) Heater

9.1.1. Pressure Storage

This system is especially suitable for:

- Storing small quantities of ammonia
- Balancing production variations with downstream units processing pressurized ammonia
- Loading and unloading trucks, tank cars, and marine vessels carrying pressurized ammonia
- Entrance to or exit from pipeline systems

Usually, cylindrical pressure vessels are designed for about 2.5 MPa. The larger spherical vessels are designed only for about 1.6 MPa to avoid wall thicknesses above 30 mm. A coat of reflecting paint or, frequently in hot climates, an outer covering of insulation may be used on the vessels to avoid solar radiation heating. Spraying the

vessel with water is very effective against intense solar radiation but does stain and damage the paint. As a rule, liquid ammonia fed to storage from a synthesis loop carries inert gases with it. Besides the prescribed safety relief valves, pressure control is provided for the storage drum by controlled bleeding of the inert gases through a pressure-reducing valve, for example, into a water wash system (Fig. 118).

Sometimes high-strength or fine-grained steels are used in making pressure vessels. These may be susceptible to stress corrosion cracking by ammonia. Safely avoiding this hazard requires careful thermal stress relief after completing all welding on the vessel.

The shape of the vessel depends above all on its capacity:

Cylindrical, usually horizontal for up to about 150 t
Spherical vessels resting on tangentially arranged support columns but also more recently, for static and safety reasons, in a suitably shaped shallow depression for about 250–1500 t.

Ancillary equipment, designed for at least 2.5 MPa (25 bar): meters and flow controls for pressurized ammonia feed and effluent streams; centrifugal pumps for discharging into liquid ammonia supply piping and for liquid ammonia loading; equipment for safe pressure relief for ammonia vapor and inerts (see Fig. 118 and [1268]). Design of pressure storage tanks and the related safety aspects are discussed in [1270].

Stress corrosion cracking (see also in Section 8.6 in pressurized ammonia vessels and tanks is a problem which has been discussed in many papers [1252]–[1265], [1271]–[1276]. The mechanism of this phenomenon, the influence of water, and the role of oxygen are not yet completely understood, in spite of extensive research. A review is given in [1277]. As it is generally accepted that addition of water may inhibit stress corrosion [1263], [1264] it has become a widely used practice to maintain a water content of 0.2 % in transport vessels [1264]. Protection may also be achieved by aluminum or zinc metal spray coating [1275], [1277]. More recent research [1273], [1277], however, has shown that water may not give complete protection.

The prevailing opinion was that stress corrosion should occur in atmospheric storage tanks [1278]. Therefore, it was somewhat surprising when cases of stress corrosion in atmospheric ammonia tanks were reported [1279]–[1281]. Descriptions of further incidents, inspection techniques, and repair procedures can be found in [1276], [1282]–[1289], [1290].

In 1995, the capital investment, including ancillary equipment, for a 1000-t pressurized ammonia storage facility amounted to about \$ 3.5×10^6 (6×10^6 DM).

9.1.2. Low-Temperature Storage

Modern single-train plants need to have large-volume storage facilities available to compensate for ammonia production or consumption outages. Storage equivalent to about 20 days is customary for this. Moreover, transporting large amounts of ammonia by ship or pipeline and stockpiling to balance fluctuations in the ammonia market have

great importance. Therefore, correspondingly large storage facilities are necessary at ship and pipeline loading and unloading points.

For comparable large storage volumes, the capital investment costs for atmospheric pressure storage are substantially lower than for pressure storage. In spite of higher energy costs for maintaining the pressure and for feed into and out of atmospheric storage, it is still more economical than pressure storage. This applies especially to storage of ammonia coming from the synthesis loop at low temperature and loading and unloading of refrigerated ships.

For atmospheric storage at −33 °C single tanks with a capacity up to 50 000 t of ammonia are available [1290]. Design pressure is usually 1.1 – 1.5 bar (plus the static pressure of the ammonia). The cylindrical tanks have a flat bottom and a domed roof and are completely insulated. Refrigeration is provided by recompression of the boil-off, usually with two-stage reciprocating compressors. Incoming ammonia of ambient temperature is flashed to − 33 °C before entering the tank, and the vapors from the flash vessel are also fed to the refrigeration unit. Refrigeration units have at least one stand-by unit, mostly powered by a diesel engine. Single-wall and double wall tanks are used in the industry.

Single-Wall Tanks. The single-wall tank has a single-shell designed for the full operating pressure. Mats or panels of rock wool or foamed organics (e.g., in-situ applied polyurethane foam) are used for insulation of single wall tanks. The outside insulation must be completely vapor tight to avoid icing and requires the highest standards of construction and maintenance to avoid hazardous deterioration by meteorological influences. A metal sheet covering is normally applied, and sometimes a bond wall of reinforced concrete or steel is added [1291], [1292].

Double-wall tanks are known in various designs. In the simplest version an inner tank designed for storage temperature and pressure is surrounded by a second tank. The annular space between the two walls is filled with insulation material, for example, Perlite. The main purpose of the outer shell is to contain and hold the insulation. Today's usual practice is to design the outer shell to the same standard as the inner shell. This so-called double-integrity tank concept provides an additional safety measure as the outer tank can hold the full content if the inner shell fails.

Further safety provisions include surrounding the tanks by dikes or placing them in concrete basins to contain the liquid ammonia in the event of a total failure. Discussions of such secondary containment are found in [1285], [1291] – [1293].

Two principle "double integrity" designs are used as shown in Figure 119. In Figure 119 A and B the inner tank has a solid steel roof and is pressure-tight, whereas the gap between inner and outer shell, which can withstand the full hydrostatic pressure at operating temperature, is only covered by the water-tight insulation. The insulation for the inner shell may fill the total annular space [e.g., lightweight concrete [1294] or Perlite (B)] or may consist of an organic foam attached to the outside of the inner shell (A).

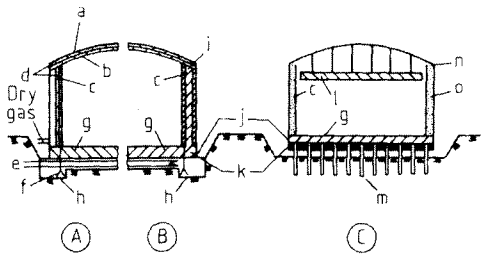

Figure 119. Arrangements of refrigerated ammonia tanks
a) Waterproof roofing; b) Steel roof; c) Inner steel shell; d) Foamed organic materials or rock wool; e) Heating coils; f) Stay bolts; g) Inner steel base; h) Concrete ring wall; i) Loose Perlite or lightweight concrete and rock wool; j) Outer steel shell and base; k) Cellular glass or lightweight concrete; l) Suspended deck with insulation; m) Pile foundation; n) Steel roof and shell or prestressed concrete lined for vapor containment; o) Loose Perlite or insulation on liner or in space

In the design according to Figure 119 C the outer tank is pressure-tight. The inner tank has a suspended roof and the insulation fills the annular gap, which contains an atmosphere of ammonia vapor.

Because of the static loading, cellular glass or lightweight concrete [1294] is used for the floor insulation in all cold tank systems. A foundation as shown in Figure 119 A and B requires underground heating to prevent formation of a continuous ice sheet under the tank, which could lift it. If, as in Figure 119 C, the tank bottom is on piles above ground level, heating is unnecessary.

The tanks are fabricated by welding on site, from steels which retain their notch ductility strength at low temperature. Corresponding to the decreasing static pressure, steel plate thickness in the cylindrical shell is reduced stepwise from bottom to top. Technical details and design questions are treated in [399 Vol IV], [1293], [1295] – [1297]. Influence of climatic conditions on design and operation is considered in [1298]. Specific cases and foundation problems are discussed in [1296], [1299] – [1301]. Retrofitting of existing storage tanks is described in [1302], [1307]. Maintenance and inspection procedures are covered in [1303] – [1309]. For stress corrosion occurred in atmospheric tanks see Section 9.1.1.

A rough budget figure of the capital investment in 1996 for double-integrity tank with a capacity of 20 000 t is around 15×10^6 DM. For large capacity storage (> 20 000 t) presently 600 – 800 DM/t NH_3 have to be invested [1476]. Inclusion of facilities to receive or deliver pressurized ammonia at ambient temperature would add a few millions more. Additional costs may result from high safety standards (e.g., dikes, emmission monitoring systems, ammonia sensors, and computerized control systems) and long transfer lines to shipping terminals.

Energy consumption would also increase considerably, to about 80 kWh/t ammonia throughput. In addition, substantial investment will be necessary for a complete terminal including, for example, a jetty and equipment for ship loading and facilities for loading rail and/or tank cars.

9.1.3. Underground Storage

For years, the liquefied petroleum gas (LPG) industry has used pressurized underground liquefied gas storage. This technique has been applied to ammonia also. DuPont has operated a rock cavern in the United States with a capacity of 20 000 t. Norsk Hydro has one in Norway at 50 000 t. Because of the contaminants occurring in liquid ammonia stored this way and the lack of suitable construction sites, no further storage facilities of this kind have been built for a long time. Underground fertilizer ammonia storage was planned in Russia [1310].

9.1.4. Storage of Aqueous Ammonia

To allow storage and transportation at temperatures up to 35 °C, the concentration of aqueous ammonia should not exceed 25 %, because of its vapor pressure. A small facility uses mostly cylindrical vessels. The capacity of the transporting equipment determines the storage volume, e.g., at least 40 m^3 storage volume for 30 m^3 tank cars. For larger capacities, tanks are used. If it is necessary to avoid contaminating the aqueous ammonia by iron hydroxide, austenitic (stainless) steels may be used instead of the usual carbon steels.

9.2. Transportation

9.2.1. Transportation in Small Containers

The most common containers are:

- Cylindrical steel bottles and pressurized flasks for about 20 – 200 kg anhydrous ammonia to meet the requirements of laboratories, small refrigeration systems, and the like
- Polyethylene canisters, metal casks, and the like for 25 % aqueous ammonia.

9.2.2. Transportation in Trucks and Rail Cars

The most widely used methods are:

With pressure vessels for anhydrous ammonia (maximum allowable operating pressure about 2.5 MPa)
With atmospheric pressure vessels for 25 % aqueous ammonia

With vessels designed for elevated pressure for high-concentration aqueous ammonia (maximum allowable operating pressure in accordance with the ammonia content up to 1.6 MPa).

A modern rail car loading station for anhydrous and aqueous ammonia is described in [1311], [1312].

The distribution in rail cars (capacities normally up to 100 m^3; Jumbo rail cars 150 m^3) and trucks primarily serves to supply smaller processing operations and wholesale merchants. However, rail transport of liquid ammonia may to some extent supplement large marine and pipeline shipments. Reference [1318] examines rail freight cost. Normally, shipping liquid ammonia by truck is used only where other means of transport are not available, e.g., in the agricultural practice of direct fertilization.

9.2.3. Shipping in Ocean-Going Vessels and River Barges

Regarding the transport volume, shipping of anhydrous ammonia is far more important than transport by rail. In 1991, for example, a total of 10×10^6 t of anhydrous ammonia was transported by ocean-going vessels (IFA statistics). Overseas shipping gained great momentum through exports from producers in countries with low natural gas prices or low-price policies [1314]. A comparison of shipping costs is given in [1315]; for more up-to-date information consult the journal *Nitrogen*, published by British Sulfur, which regularly reports shipping prices. Most river barges have loading capacities of 400 to 2500 t and mostly have refrigerated load, but a few are pressure vessels. Ocean-going vessels may transport as much as 50 000 t of fully refrigerated ammonia.

9.2.4. Transport by Pipelines

Transport of large volumes of ammonia by pipeline [1315], [1316] over great distances is far more economical than by river barge or rail. In the USA the MidAmerica Pipeline System (MAPCO) extends from northern Texas, across Oklahoma, Kansas, Nebraska and Iowa and ends in Minnesota, all intensive agricultural areas. The total length is 1754 km. The Gulf Central Pipeline is with 3057 km the longest system and connects the major producers along the Texas and Louisiana Gulf coast with terminals in Arkansas, Iowa, Illinois, Indiana, Nebraska, and Missouri [1317], [1324], [1325]. Another shorter system (132 km) is the Tampa Bay Pipeline (Florida). MidAmerica Pipeline, for example, has a peak delivery capacity of 8000 t/d for a number of destinations [1318], the hold up is about 20 000 t. Maintenance is described in [1319].

As ammonia is transported at a temperature of at least 2 °C (pressure between 22 and 100 bar) it has to be warmed up at the supplier terminal and cooled down again to −33 °C at the receiver terminal. Main branches have diameters of 200 and 250 mm (8 – 10 in). Exact knowledge of the $p - V - T$ properties is important [1320]. Automatic lock valves are installed at intervals of 10 miles, so that the volume which can be released between two valves is limited to 400 t.

The world's longest ammonia pipeline has been in operation since 1983 in Russia, connecting the large production facilities Togliatti/Gordlovka with the terminals Grigorowski/Odessa at the Black Sea over a distance of 2424 km [1315]. Apart from some short pipeline connections, most of them shorter than 50 km, there is no significant pipeline transport in Europe, where ammonia is predominantly further processed in downstream facilities on site and where no widespread direct application to agricultural crops exists.

10. Quality Specifications and Analysis

The quality of the ammonia product depends to some extent on the operating conditions of the production plant and storage. For example, water content from a synthesis loop receiving a dry make-up gas is about zero, whereas plants which receive the feedgas after a methanation without further drying may give a water content of 0.1 – 0.2 %. Oil may be introduced by the seal oil of the synthesis compressor, but on account of its low solubility in liquid ammonia it usually settles out on storage, so that only a minor concentration will remain in commercial deliveries. There are two commercial qualities of anhydrous ammonia: commercial (technical) grade (ammonia as received from production and storage) and refrigeration grade (technical product purified by distillation [1321] or molecular sieve adsorption). Table 41 lists the commercial specifications. The relevant standards are US Specification OA-445a, Supplement 5 (1963) and, in Germany, DIN 8960 (1972) for refrigeration-grade ammonia. To inhibit stress corrosion cracking a water content of at least 0.2 % for shipped and pipelined liquid ammonia is generally recommended and is mandatory in the USA.

Table 41. Minimum quality requirements for ammonia

Quality		Commercial grade		Refrigeration grade	
		USA	FRG	USA	FRG
Purity	wt%, min	99.5	99.5	99.98	99.98 *
Water	wt%, max	0.5	0.2	0.015	0.2
Inerts **	mL/g, max	not spec'd	not spec'd	0.1	0.08
Oil	ppm by wt	5.0	5.0	3.0	not spec'd
Free of H_2S, pyridine, and naphthene					

* Allowable boiling point change on vaporization of 5 – 97 % of the test sample, 0.9 °C

** The noncondensable gases dissolved in ammonia are H_2, N_2, CH_4, and Ar. Their amounts depend on the methods of synthesis and storage. The inerts amount to about 50 mL/kg for atmospheric storage.

Various concentrations and purities of *aqueous ammonia* are on the market. Mostly, the concentration is 25 – 30 % NH_3 and the iron content less than 10 ppm. Shipping in pressure vessels is necessary for ammonia contents above 25 % because of its elevated vapor pressure. For more stringent purity requirements for aqueous ammonia, the containers should be made of seawater-resistant aluminum (magnesium alloyed) or austenitic steels.

Analysis. Ammonia is readily detectable in air in the range of a few parts per million by its characteristic odor and alkaline reaction. Specific indicators, such as Nessler's reagent (HgJ in KOH), can detect ammonia in a concentration of 1 ppm. For the quantitative determination of ammonia in air, synthesis gas, and aqueous solutions, individual (manual) and continuous (recorded) analyses can be made (for a measure-

ment station for automatic determination of ammonium/ammonia, see [1322]). The methods used include, among others:

Acidimetry and volumetric analysis by absorption
Gas chromatography
Infrared absorption
Thermal conductivity measurement
Electrical conductivity measurement
Measurement of heat of neutralization
Density measurement (for aqueous ammonia)

Normally, the water content of liquid ammonia is determined volumetrically as the ammonia-containing residue on evaporation or gravimetrically by fully vaporizing the ammonia sample and absorbing the water on KOH.

The oil content of liquid ammonia can be tested gravimetrically by first evaporating the ammonia liquid and then concentrating the ether extract of the residue. Iron, aluminum, calcium (ammonia catalyst) and other impurities can then be determined in the ether-insoluble residue.

The inert gas content is analyzed volumetrically after the vaporized ammonia has been absorbed in water. Then the inert gas composition is analyzed chromatographically.

11. Environmental, Safety, and Health Aspects

11.1. Environmental Aspects of Ammonia Production and Handling

Measured by its overall environmental impact – air, water and soil pollution, materials and energy consumption – ammonia production is a rather clean technology, with low emissions, low energy consumption due to high-efficiency process design, and no severe cross-media dilemmas, in which improving one environmental effect worsens another. Typical emissions are given in EFMA's publication Production of Ammonia in the series "Best Available Techniques and Control in the European Fertilizer Industry" [1323].

Steam Reforming Ammonia Plants. Table 42 summarizes the achievable emission values for steam reforming ammonia plants [1323].

Table 42. Emissions from steam reforming ammonia plants

			Existing plants	New plants
Emission to air	NO_x (as NO_2)*	ppmv (mL/m^3)	150	75
		mg/Nm^3	300	150
		kg/t NH_3	0.9	0.45
Emission to water	NH_3/NH_4 (as N)	kg/t NH_3	0.1	0.1
Waste material**		kg/t NH_3	< 0.2	< 0.2

* At 3% O_2.** Spent catalysts.

The source of the NO_x emissions is the flue gas of the fired primary reformer, and in plants without a fired tubular reformer NO_x is emitted from fired heaters and auxiliary boilers, but in considerably smaller quantities. However, NO_x emissions from ammonia production, compared to the total amount from human activities, is in fact a marginal quantity. Only about 0.16% of the anthropogenic NO_x emissions come from ammonia production. Emissions to water, generally originating from the condensate from the condensation of surplus process steam ahead of the carbon dioxide removal system, can largely be avoided. Minor concentrations of methanol and amines can be removed and recycled to the reformer feed by stripping with process steam, and the stripped condensate can be recycled to the boiler feed water after polishing with ion exchangers. Steam stripping without recycling to the reformer would produce a cross media effect, because in this case the pollutants would be transferred from water to air. Another possibility is use of the process condensate for feed gas saturation [1033].

Partial oxidation ammonia plants have the same emission sources except for the primary reformer flue gas. The plants have an auxiliary boiler to generate steam for power production and fired heaters, which on account of the sulfur content of the fuel oil release a flue gas containing SO_2 (< 1500 mg/m^3). Other possible emissions are H_2S (< 0.3 ppmv), CO (30 ppmv) and traces of dust. The NO_x content of the flue gas depends on the configuration of the auxiliary boiler and on the extent electric power generation on the site as opposed to outside supply. The total NO_x emission per tonne of product may be somewhat lower than for steam reforming plants.

Noise. An increasing awareness has developed for noise generation and emission from ammonia plants especially in the neighborhood of residential areas [1326]. Many investigations have dealt with noise generation and noise abatement in ammonia plants [1327]–[1331]. The following major sources can be identified: depressurizing of large gas quantities for control or venting, steam blowing, burner noise, resonance vibrations in the flue gas ducts, and noise from compressors, blowers, and pumps. Measures for noise reduction include installing low-noise let-down valves, use of silencers, sound-reducing enclosures for compressors or housing them in closed buildings.

Emission Limits and Guideline Values for Ammonia Production. There are two categories of regulations:

1) Legally binding emission values for certain pollutants associated with ammonia production
2) Guideline values not legally binding but providing the background for requirements laid down in individual operating permits

In Europe such legally binding emission levels relevant to ammonia production exist only in Germany. In the Netherlands and Germany limits for emissions from boilers also apply for ammonia plants, for example for the reformer furnace. The present limit in Germany is 200 mg NO_x/m^3 for furnaces up to 300 MW_{th}. Specific emission guideline values are laid down in the United Kingdom. In the other European countries no national emission limits or guidelines exist; individual operation permits are negotiated, usually orientated on other cases and countries. In the United States, for example, NO_x emission level values are categorized in the Clean Air Act, which defines a significance level for the source according to the total emission (10 to 100 t/a) on the one hand, and assigns a threshold limit to the geographical area (100 t/a to 10 t/a) on the other.

For ammonia in air the authorities in Germany require that the achievable minimum level should correspond to the state of the art; originally projected values in a draft of TA Luft [1332], were not subsequently adopted; some MIK values (maximum imission concentrations) are given in VDI Richtlinie 2310 (Sept. 1974). In Germany there is no maximum ammonia concentration laid down for wastewater, it is only referred to the general interdiction to introduce poisons or harmful substances into

rivers and lakes. A concentration of 1.25 mg NH_3 per liter, stated to be harmful to fish, could serve as a guideline. In the "Catalog of Water Endangering Substances" (Germany) anhydrous ammonia is not listed, but aqueous ammonia is classified in the Water Endangering Group 1 as a weakly endangering substance.

To harmonize European regulations concerning emission value permits for industrial production, the EU commission has proposed a Council Directive Concerning Integrated Pollution Prevention Control (IPPC Directive). A key element is the concept of Best Available Techniques (BAT). This directive requests an exchange between national environmental authorities, industry and nongovernmental organizations with the aim of preparing IPPC BAT Reference Documents (BREFs), which could provide a common accepted basis for emission limit value regulations of the individual EU member states. A BREF for ammonia is being prepared to serve as pilot project. A previous BAT document on ammonia was published in 1990 [1333]. For noise emissions usually local permits are negotiated, whereby in most instances the contribution to the sound level in the surrounding residential areas will be limited. For the limitation of sound levels at working places within the plant occupational safety regulations are valid which also require ear protection above a certain level. The European Fertilizer Manufacturer's Associacion (EFMA) has published a series: "Best Available Techniques for Pollution Prevention and Control in the European Fertilizer Industry". Booklet No. 1 is "Production of Ammonia".

11.2. Safety Features

In ammonia production three potential hazard events can be identified: fire/explosion hazard from the hydrocarbon feed system; fire/explosion hazard due to leaks in the synthesis gas generation and purification, compression, or synthesis section (75 % hydrogen); and toxic hazard from release of liquid ammonia from the synthesis loop. In addition there is also a potential toxic hazard in handling and storing of liquid ammonia. The long history of ammonia production since 1913 has demonstrated that this production technology is a very safe operation. The severe impacts of rare events with explosions seem to be confined to a radius of around 60 m [1323]. The long industrial experience is summarized in a number of national codes and standards which have to be applied for design, material selection, fabrication, operation, and periodic technical inspections of the equipment used. This is especially important for equipment operating at high temperatures and/or pressures. Apart from proper design, skilled and well-trained operators and effective and timely maintenance are essential for safe plant operation. General practice today is to make so-called HAZOP-Studies (HAZOP = hazards and operability) with an experienced team consisting of operating personnel, process engineers (also from contractors), experts in process control, and safety experts (often independent consultants from outside the company) in which, following a very meticulous procedure, apparatus after apparatus

is checked for potential failure and risk possibilities together with a proposal for the appropriate remedies. HAZOP-Studies and risk analysis procedures introduced by ICI [1339] – [1342] for general application in chemical plants proved to be very helpful not only for existing plants but also in the planning phase of new ones. It is especially important to define and configure trip systems and trip strategies for safe plant shut downs in case of offset conditions.

An area which deserves special attention with respect to safety is the storage of liquid ammonia. In contrast to some other liquefied gases (e.g., LPG, LNG), ammonia is toxic and even a short exposure to concentrations of 2500 ppm may be fatal. The explosion hazard from air/ammonia mixtures is rather low, as the flammability limits [1334] – [1338], [1343] of 15 – 27 % are rather narrow. The ignition temperature is 651 °C. Ammonia vapor at the boiling point of – 33 °C has vapor density of ca. 70 % of that of ambient air. However, ammonia and air, under certain conditions, can form mixtures which are denser than air, because the mixture is at lower temperature due to evaporation of ammonia. On accidental release. the resulting cloud can contain a mist of liquid ammonia, and the density of the cloud may be greater than that of air [1334] – [1344]. This behavior has to be taken into account in dispersion models.

Regulations and Guidelines. For maintaining safety in ammonia storage, transfer, and handling many regulations and guidelines exist in the various countries. It is beyond the scope of this article to list them completely and to check for the most up-to-date status. As an illustration only, some relevant regulations in Germany are listed here (for a summary of regulations in the USA, refer to [1345]):

- Verordnung über Druckbehälter, Druckgasbehälter und Füllanlagen (Druckbeh. V vom 27. Febr. 1980)
- Unfallverhütungsvorschriften der Berufsgenossenschaft der chemischen Industrie: e.g. UVV 29 Gase, UVV 20 Kälteanlagen, UVV 39 Arbeiten an Gasleitungen
- Gesetz zum Schutz vor gefährlichen Stoffen (Chem. G. vom 16. September 1980)
- Verordnung über Anlagen zum Lagern, Abfüllung und Umschlag wassergefährdender Stoffe (VAwS von 1983)

The respective "Technische Regelwerke" (technical standards) supplement these regulations and ordnances [1346]:

TRG	Technische Regeln Druckgase
TRB	Technische Regeln Druckbehälter
TRgA	Technische Regeln Gefährliche Arbeitsstoffe
AD	Merkblätter für Druckbehälter (Unterlagen für Auslegung und Berechnung)
SEW	Stahl-Eisen-Werkstoffblätter

Relevant DIN regulations govern design of pressure vessels and other equipment. The German Institute for Standardization (Deutsches Institut für Normung) provides information covering German technical rules and international and foreign standards [1347].

The following regulations are relevant to transportation of ammonia:

GGVE	Gefahrgutverordnung Eisenbahn (FRG)
GGVS	Gefahrgutverordnung Straße (FRG)
RID	Règlement international concernant le transport des marchandises dangereuses par chemin de fer (Europe)
ADR	Accord européen relatif au transport international des marchandises dangereuses par route (Europe)
ADNR	Accord européen relatif au transport international des marchandises dangereuses par navigation sur le Rhin [1348] (Europe)
IMDG	International maritime dangerous goods code [1349]

Publication of GGVE and RID, GGVS and ADR in a synoptic edition is planned [1355].

In addition the Technical Committee of APEA together with a joint Technical Group of ISMA have collected recommendations for erecting and operating ammonia terminals, transfer installations, etc.:

- Safety Recommendations for Large Scale Storage of Ammonia
- Recommendations for the Loading and Unloading of Ammonia Tankers (Maritime Ports)
- Safety Recommendations for the Installation of State Ammonia Tanks on Customers Premises
- Note on the Inflammability of Ammonia
- Safety Recommendations for the Use of Ammonia in Agriculture
- Recommendations Concerning Rubber Hose for Ammonia
- Safety Recommendations for the Construction of Tank-Cars for the Transport of Ammonia by Road

These brochures appeared (1974) in English, French, and German, partly in new editions [1337].

Likewise, in the United Kingdom, a joint working party of renowned companies collected a number of codes of practice published by the CIA:

1) Safe Handling and Transport of Ammonia in Bulk by Road
2) Safe Handling and Transport of Ammonia in Bulk by Rail
3) Demountable Vessels and Containers
4) Transfer Connections
5) Ammonia Storage Installations at Industrial Consumers' Premises
6) Systems and Equipment for the Direct Application of Ammonia in Agriculture
7) Maintenance of Ammonia Systems

In the appendices of the brochures are statutory regulations, recommendations, and bibliographies for reference [1351].

In like manner, for the United States one may mention: safety manuals and standards for the storage, transport, and handling of anhydrous ammonia compiled

by the ANI [1352], and the Chemical Safety Data Sheets of the Manufacturing Chemists Association [1353].

All larger ammonia producers make available technical instructional brochures, in which they also prescribe necessary protective measures and first aid for dealing with ammonia.

Ammonia Spills. In an ammonia spill a portion of the liquid ammonia released flashes as ammonia vapor. This instantaneous flash is followed by a period of slow evaporation of the remaining liquid ammonia [1344], [1354]. In a release from a refrigerated tank operating slightly above atmospheric pressure, the amount of the initial flash is only a few percent of the total, whereas in a release from a pressure vessel at about 9 bar and 24 °C approximately 20 % of the spilled ammonia would flash. Figures for the proportion flashed as a function of pressure and temperature of the spilled ammonia are given in [1354]. This reference also provides quantitative information on temperature development and evaporation rate of small and large ammonia pools at certain wind velocities and also takes radiation influences (sunny or overcast sky, day or night) into account.

Spill experiments on land and on water in various dimensions have been carried out by various companies and organizations. Underwater releases were also studied. Models have been developed to mathematically describe ammonia dispersion in such events [1355] – [1360].

A number of real incidents with tank cars, rail cars, tanks, loading/unloading of ships and barges, and pipeline transport in which major spills occurred is described in [1361] – [1370] and in an excellent review on safety in ammonia storage [1371]. Training of operating personal for ammonia handling with special regard to ammonia spills is important [1369], [1372], [1373].

11.3. Health Aspects and Toxicity of Ammonia

In ammonia production, storage, and handling the main potential health hazard is the toxicity of the product itself. For this reason this section concentrates on ammonia only. Other toxic substances such as carbon monoxide or traces of nickel carbonyl (which may be formed during shut down in the methanation stage) may be only a risk in maintenance operations and need appropriate protection provisions as well as blanketing or flushing with nitrogen.

Human Exposure. The threshold of perception of ammonia varies from person to person and may also be influenced by atmospheric conditions, values as low as 0.4 – 2 mg/m^3 (0.5 – 3 ppm) are reported in [1374], but 50 ppm may easily detected by everybody [1375]. Surveys [1376] found concentrations from 9 – 45 ppm in various

plant areas. Though initially irritated, exposed persons may quickly become accustomed to these concentrations. Another report [1377] gives concentration limits for short time exposures as follows: 100 ppm (10 min); 75 ppm (30 min) 50 ppm (60 min). The time-weighted average Threshhold Limit Value (TLV) of the ACGIH is 25 ppm (or 18 mg/m^3) [1378], [1383]. This recommendation was supplemented by a value for short-time exposure: 35 ppm for 15 min. The MAK value is 50 ppm. A review of the present situation in the United States is given in [1384].

Exposure to higher ammonia concentration has the following effects: 50 – 72 ppm does not disturb respiration significantly [1379]; 100 ppm irritates the nose and throat and causes a burning sensation in the eyes and tachypnoe [1379]; 200 ppm will cause headache and nausea, in addition to the above symptoms [1380]; at 250 – 500 ppm tachypnoe and tachycardia [1380]; at 700 ppm, immediate onset of burning sensations in the eyes [1381]; 1000 ppm causes immediate coughing [1382]. The symptomatology of various exposure levels is also described in [1378], [1383] – [1385]. At 1700 ppm coughing with labored breathing, sometimes with momentary inability to breath (coughing of rescued persons may continue for hours). 2500 to 4500 ppm may be fatal after short exposure; 5000 ppm and higher causes death by respiratory arrest [1371].

The metabolism seems not to be significantly changed after exposure to 800 ppm [1382]. A discussion of metabolism and of acute and chronic health problems caused by ammonia can be found in [1386].

Toxicology. Ammonia is a strong local irritant. On mucous membranes alkaline ammonium hydroxide is formed, which dissolves cellular proteins and causes severe necrosis (corrosive effect).

The primary target organ is the pulmonary system, and the following symptoms can be observed: pharyngitis, laryngitis, tracheobronchitis, nausea, vomiting, increased salivation, reflectoric bradycardia, and life-threatening symptoms, such as edema of the glottis, laryngospasm, bronchospasm, and interstitial lung edema [1387].

Ammonia or ammonium hydroxide can penetrate the cornea rapidly, leading to keratitis, damage of the iris, cataract, and glaucoma [1388].

Oral ingestion of aqueous ammonia can corrode the mucous membranes of the oral cavity, pharynx, and esophagus and cause the shock syndrome, toxic hepatitis, and nephritis. Because of its corrosive action constrictions of the esophagus may result.

Ammonia is absorbed rapidly by the wet membranes of body surfaces as ammonium hydroxide, converted to urea, and excreted by the kidneys [1389]. The capacity of detoxification via urea is sufficient to eliminate the ammonium ion when ammonia is inhaled in nonirritating concentrations. The inhaled ammonia is partly neutralized by carbon dioxide present in the alveoli [1390]. Only a small fraction of the ammonia is exhaled unchanged by the lungs (12.3 % at an inhalation concentration of 230 ppm) [1391]. Repeated inhalation can cause a higher tolerance because the mucous membranes become increasingly resistant [1392]. Additional information on the toxicology of ammonia can be found in [1393] – [1409].

Carcinogenicity. Ammonia failed to produce an increase in the incidence of tumors in Sprague Dawley rats even when the protein ratio in the diet was increased or when urea was added [1410].

Lifetime ingestion of ammonium hydroxide in drinking water by mice was without any carcinogenic effects [1411].

Mutagenicity. Ammonia is not mutagenic in the Ames *Salmonella* system and in *Saccharomyces cerevisiae* [1412].

12. Chemical Reactions and Uses of Ammonia

12.1. Reactions of Ammonia

By addition of a proton ammonia forms the ammonium ion which is similar to the alkali metal ions with respect to its alkaline and salt-forming properties.

The free radical NH_4 has been isolated only in the form of its amalgam (DAVY, 1811) which precipitates the more noble metals, such as copper, cadmium, and zinc, from their solutions. Solutions of ammonium in liquid ammonia are blue and usually exhibit properties similar to liquid ammonia solutions of sodium and potassium.

Aqueous solutions of ammonia react as weak bases because hydroxyl ions result from the addition of a proton or H_3O^+ from the water to the ammonia molecule. However, the equilibrium is very strongly shifted to the side of free ammonia, as may be seen from the equilibrium constant at 18 °C:

$$\frac{[NH_4^+]\,[OH^-]}{[NH_3]} = K\,[H_2O] = K'_{NH_3} = 1.75 \times 10^{-5} \qquad (96)$$

A 1 N solution of ammonium hydroxide has a pH of 11.77 at 18 °C.

Ammonium salts result from reaction with acids in aqueous solution or in the gas phase.

Ammonia is oxidized by oxygen or air, depending on the reaction conditions, to NO, NO_2, or N_2O or to nitrogen and water. On alkaline surfaces, such as quicklime or soda lime, ammonia–air mixtures are oxidized readily at 350 °C to nitrite and further to nitrate. The reaction rate can be increased by adding traces of nickel and cobalt oxides to the catalyst surfaces [1413]. Gaseous ammonia reacts very violently or even explosively with nitrogen oxides to form nitrogen, water, ammonium nitrate or nitrite. The reaction with N_2O requires ignition. The controlled catalytic oxidation of ammonia to produce nitric acid or pure NO for hydroxylamine production is described in [1419]–[1421].

At higher temperatures, especially in the presence of surface-active materials, ammonia forms *hydrogen cyanide* with carbon monoxide, methane, or charcoal. The catalytic oxidation of methane in the presence of ammonia is employed for the industrial production of hydrogen cyanide. With CO_2, SO_3, and P_2O_5, NH_3 forms amides of carbonic acid (e.g., Urea [1422]), sulfuric acid [1423], and phosphoric acid [1424].

Metals may replace one or all of the hydrogen atoms of ammonia. *Sodium amide* ($NaNH_2$), for example, is obtained with evolution of hydrogen by passing ammonia vapor over metallic sodium. Sodium amide reacts with N_2O to form the highly explosive sodium *azide*. An ammonium azide, NH_4N_3, may be prepared also. The *imide*, for example, lithium imide, Li_2NH, results from replacing a further hydrogen

atom by metals. Finally, there are the *nitrides*, such as lithium or magnesium nitride, Li_3N or Mg_3N_2. The nitrides of reactive metals, such as lithium, magnesium, calcium, aluminum, and titanium, are formed directly from the elements at elevated temperature. In many cases, it is better to obtain nitrides through the action of ammonia on the metals or metal compounds at higher temperature. A nitride also may result from thermal decomposition of an amide.

Sulfur, phosphorus, and halogens also can take the place of the hydrogen atoms in ammonia. At relatively low temperatures, halogens react with ammonia to form *nitrogen–halogen compounds* and *ammonium halides*. At higher temperatures the products are nitrogen and hydrogen halides. With sodium hypochlorite, ammonia forms *hydrazine hydrate* (Raschig synthesis) with chloramine, H_2NCl, as an intermediate.

Reactions in liquid ammonia [1414] sometimes proceed differently from those in water because of the solubility difference of many salts between water and ammonia. For example, the reaction

$$2\,AgNO_3 + BaCl_2 \underset{NH_3}{\overset{H_2O}{\rightleftharpoons}} 2\,AgCl + Ba(NO_3)_2 \qquad (97)$$

leads in water to precipitation of silver chloride, and in ammonia, to precipitation of barium chloride. In liquid ammonia, ammonium salts have an "acid" character. For example, alkali and alkaline-earth metals, cerium, lanthanum, manganese, cobalt, nickel, and iron and its alloys are soluble in solutions of ammonium bromide, iodide, cyanide, and thiocyanide, with formation of the corresponding metal amine salt and evolution of hydrogen:

$$2\,NH_4^+ + Mg \longrightarrow Mg^{2+} + 2\,NH_3 + H_2 \qquad (98)$$

Correspondingly, metal amides in liquid ammonia have a "basic" character. The reaction of ammonium salt with metal amide in liquid ammonia is analogous to the neutralization of acid and base in water. The heats of neutralization in ammonia are even larger than in water. The process of hydrolysis corresponds to ammonolysis in ammonia. This results in ammonobasic compounds, for example, in the infusible precipitate $HgNH_2Cl$ from $HgCl_2$.

Liquid ammonia is a good solvent for white phosphorus. Rhombic sulfur is dissolved by liquid ammonia at –11.5 °C. Once dissolved, at lower temperature a blue solution results in which partial ammonolysis of sulfur to sulfur nitride and ammonium sulfides or polysulfides takes place.

Liquid ammonia's ability to dissolve alkali and alkaline-earth metals has been well known for a long time. In concentrated solutions, the metals largely remain in the metallic state. The magnetic properties and the electrical conductivity, which is comparable to that of mercury, confirm this. In the more dilute blue solutions, the metals are completely dissociated to positive metal ions and solvated electrons [1415]. The ammoniacal solutions allow preparation of many compounds otherwise unobtainable

or obtainable only with difficulty. Examples are the sodium selenides, Na_2Se through Na_2Se_6, tellurides up to Na_2Te_4, antimonides, arsenides, polystannides, and polyplumbides. Introducing oxygen into the solution of alkali metals forms peroxides, Na_2O_2, K_2O_2, as well as dioxides, KO_2, RbO_2, and CsO_2. White explosive salts of the hypothetical acetylenediols, such as KO–C≡C–OK, result with carbon monoxide [1416]; with acetylene, NaC≡CH; and with phosphine, KPH_2. Reactions of ammoniacal metal solutions with halogen-containing organic compounds can be used for the synthesis of higher hydrocarbons, amines, and free radicals. For example, reacting triphenylchloromethane with dissolved sodium produces the triphenylmethyl radical $Ph_3C\cdot$.

Generally liquid ammonia is a good solvent for many salts, such as nitrates, nitrites, iodides, cyanides, thiocyanides, and acetates. Ammonium salts are especially soluble. The hydroxides, fluorides, and salts with di- and trivalent anions, such as oxides and sulfides, in general are insoluble. Apart from alkali metals, some other metals and nonmetals are also soluble. A compilation of the solubilities of organic compounds in liquid ammonia shows notable solubility of saccharoses [1417].

Because of its dipole moment, the ammonia molecule interacts with these ions to form solvates in a manner analogous to the water molecule in aqueous solutions. Solutions in liquid ammonia show significant electrical conductance. Pure ammonia, like water, itself has a conductivity that, although limited, is based on dissociation according to:

$$2\,NH_3 \rightleftharpoons NH_4^+\,NH_2^- \qquad (99)$$

Liquid ammonia in combination with water as antisolvent and methylamine as prosolvnet is also an excellent extraction medium for all types of petroleum fractions [1418].

A survey of organic reactions in liquid ammonia appears in [1494].

12.2. Uses of Ammonia

In 1997 about 85 % of ammonia production was consumed for fertilizers. Ammonia is either converted into solid fertilizers (urea; ammonium nitrate, phosphate, sulfate) or directly applied to arable soil.

The industrial use of ammonia is around 15 %. Actually every nitrogen atom in industrially produced chemical compounds comes directly or indirectly from ammonia. An important use of the ammonia nitrogen, partly after conversion to nitric acid, is the production of plastics and fibers, such as polyamides, urea–formaldehyde–phenol resins, melamine-based resins, polyurethanes, and polyacrylonitrile.

Some examples of industrially important uses are the following reactions: With alkyl halides or alcohols *amines* or *imines* can be manufactured. For example, methanol forms mono- through trimethylamine; dichloromethane yields ethylene imine in the presence of calcium oxide. Amines can also be produced by reacting ammonia with alkyl halides in multistage processes [1425].

Acid Amides can be produced by acylating ammonia with esters, acid anhydrides, or the acids themselves (above 100 °C); an important product is formamide from methyl formate. Alternatively acid amides can be synthesized by reacting acid halides with ammonia. Catalytic hydrogenation converts the acid amides to *primary amines*. Ammonia and aldehydes or ketones are the basis for different stable products. With formaldehyde hexamethylenetetramine (urotropine) is obtained; with acetaldehyde, ammono acetaldehyde; with benzaldehyde, hydrobenzamide; with ethylene and propylene oxides, aqueous ammonia reacts to form ethanol- or propanolamine.

The catalytic gas-phase oxidation of olefins in the presence of ammonia on vanadium- or molybdenum-containing catalysts, so-called *ammonoxidation,* results in economic yields of the commercially important *acid nitriles,* for example, acrylonitrile from propylene [1426]. Ammonoxidation of *o*-xylene yields phthalodinitrile in a single reaction step.

Another application is the manufacture of explosives, hydrazine, amines, amides, nitriles and other organic nitrogen compounds, which serve as intermediates for dyes and pharmaceuticals.

Major inorganic products are *nitric acid, sodium nitrate, sodium cyanide, ammonium chloride,* and *ammonium bicarbonate. Urea production* consumed about 40 % of the ammonia produced in 1995.

In the environmental sector ammonia is used in various processes for removing SO_2 from flue gases of fossil-fuel power plants. The resulting ammonium sulfate is sold as fertilizer. In the *selective catalytic reduction process (SCR) the* NO_x in flue gases is reduced in a catalytic reaction of the nitrogen oxides with a stoichiometric amount of ammonia [1427] – [1430]. Also noncatalytic reduction is applied with ammonia or urea solutions.

Ammonia is also applied as a solvent in certain processes. Another application is the *nitriding of steel.* An old an still flourishing business is the use of *ammonia as refrigerant,* based on its low boiling point and its high heat of evaporation. For some time heavy competition came from chlorofluorocarbons (CFCs), but with increasing environmental concern regarding the application of CFCs ammonia's position is strenghening again. Ammonia is applied in a large number of industrial and commercial refrigeration units and air-conditioning installations [1431] – [1434]. In addition to the high specific refrigeration effect, the ammonia has the following advantages: it is noncorrosive; it tolerates moisture, dirt, and oil contaminants; it is cheap and there are many suppliers. A drawback is its toxicity.

The production of smaller volumes of hydrogen/nitrogen mixtures used as protective gases for chemical products [1435] and for metal-working processes [1436] by *decomposition of ammonia* over iron- or nickel-based catalysts at 800 – 900 °C may be an economic alternative where production or purchase of pure hydrogen is too expensive [1437], [1443]. Energy-related applications of ammonia are proposed in [1429].

13. Economic Aspects

13.1. Capacity and Production

About 1.6% of the world consumption of fossil energy (not including combustion of wood) goes into the production of ammonia. In developing countries, ammonia is generally one of the first products of industrialization. As 85% of world nitrogen consumption is for fertilizers it might be expected that ammonia production should develop approximately in proportion to the growth of world population. This was roughly the case in the mid-1980s as can be seen from Figure 120 [404]; since then the rate of increase in production has been markedly slower than that of world population. This has been mainly for economic reasons in developing countries and for ecological reasons in industrialized countries.

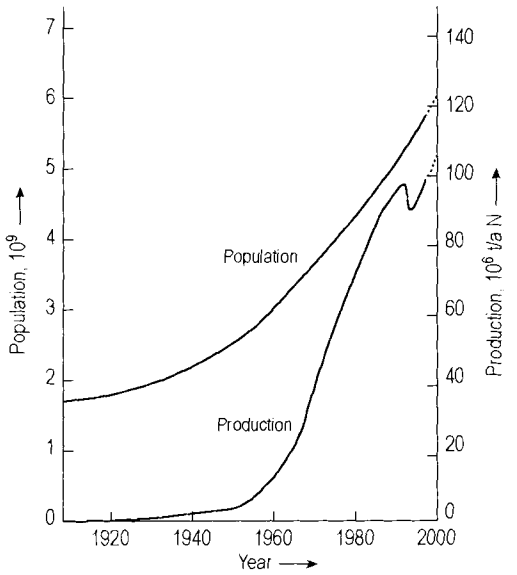

Figure 120. Development of ammonia production and world polulation

The political changes in the former Eastern Bloc caused a dramatic slump in 1991 – 1993. The present forecast figures signalize faster growth for the next few years and, as can be seen from Table 43, an average capacity utilization rate above 82% will be necessary at the end of the century, a value probably not achievable on a global scale. To cope with this situation in the shorter term, plant efficiency in Eastern Europe and some developing countries must be improved. Revamp projects and, in addition to those already under construction, new plants will be necessary to improve supply situation in the medium- to long-term perspective. In the last few years a number of new ammonia projects materialized, but it is difficult to assess what influence the present Asian crises will have. It generally can be expected that in these countries a

Table 43. World ammonia supply/demand balance (10^6 t/a N) [1438] – [1440], [1479]

	Year									
	1985	1990	1991	1992	1994	1995	1996	1998	2000	2001
Capacity	118.5	122.5	122.5	124.5	116.3	117.5	117.9	124.5	131.3	135.7
Demand	92.0	94.4	93.1	93.1	93.4	95.2	97.7	102.7	107.8	110.7
Capacity utilization, %	77.7	78.7	80.2	74.7	80.3	81.0	82.9	82.5	82.7	81.6

retreat from government subsidizing with a shift to more private and bank financing will occure. As this is associated with a more critical attitude towards profitability this development could have some retarding effect on future investments [1445], [1474]. To construct and commission a new ammonia plant takes about 3 years and for legal matters, project financing and authority approvals another 1 – 2 years will be necessary. This means that estimates of capacity development beyond a 4 – 5 years horizon are very uncertain.

Another uncertainty is introduced by the need to replace a great number of older plants for economic and environmental reasons, which might also retard the growth of capacity. This applies for a number of plants all over the world which cannot be revamped economically. Outstanding examples are plants in the People's Republic of China [1480], with a 21 % share in the world ammonia capacity. China's large production comes from around 900 individual plants [1475], which, on average, reach about 65 % of the nominal capacity. Only about 30 plants are modern world-scale plants, more than 50 plants have capacities between 80 000 and 150 000 t/a. The rest are very small plants with capacities often below 30 000 t/a. Most of these tiny village ammonia plants use coal as feedstock which is gasified with outdated watergas/generator gas technology (with some minor improvements), known from early days of ammonia production. The ammonia is recovered in these plants usually as aqua ammonia and converted either to ammonium bicarbonate or ammonium chloride, used as fertilizer for rice growing. Other sources [1482], [1483] state an even higher number for these small plants in China and give their capacities as 3000 – 10 000 t/a. About 65 % of China's total production is based on coal. Since China is deficient in natural gas and oil in the long term, it can be expected that further expansions of ammonia capacity will be coal-based as well, probably with modern technology in world-scale plants. Excluding China, as number and locations of the smaller plants are rather uncertain, the situation in the rest of the world in 1998 is as follows: Ammonia is produced at about 310 locations all over the world. About 470 plants were operated by nearly 250 different companies [1481]. The approximate average plant capacity which results from these figures is around 260 000 t/a NH_3. Situation in 1991 is found in [1447].

The geographical distribution of world ammonia capacity together with the apparent capacity utilization in 1994 is shown in Table 44. Europe and North America, which now together have a 25 % capacity share, lost their leading position (54 % in 1969) to Asia, which now accounts for 38 % (17 % in 1969), as may be seen from Figure 121. This

Table 44. Geographical distribution of ammonia capacity and capacity utilization rate (1994)

	Capacity share, %	Capacity utilization, %
Western Europe	10.3	83
Eastern Europe	7.6	60
Former Soviet Union	17.7	58
Middle East	4.0	85
Africa	3.2	70
North America	14.2	102
Central America	3.3	95
South America	1.8	79
South and East Asia, Oceania	17.4	84
Asia CPE*	20.5	88
World	100	81

* Centrally planned economies.

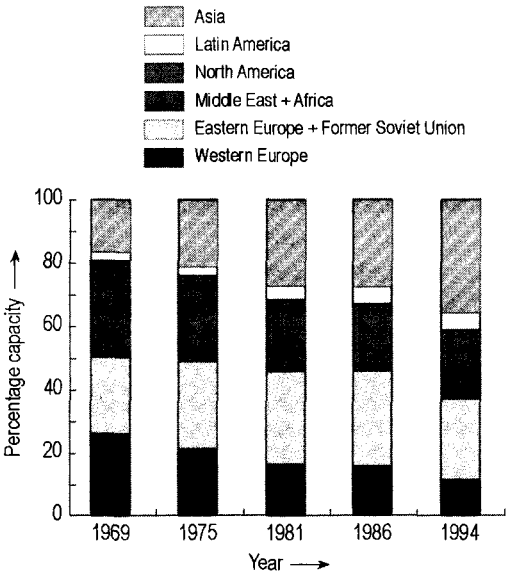

Figure 121. Geographical shift of ammonia world production capacity

development continued and in 1998 more than 40% of the world ammonia capacity is located in Asia.

The major importers of ammonia [1486] are Western Europe (1996: 3.8×10^6 t N) and the United States (1996: 3.4×10^6 t N), whereas, on account of their enormous natural gas reserves, the former Soviet Union (FSU), the Arabian Gulf, and Trinidad are dominant in ammonia export. The former FSU exported, for example, in 1996 4.1×10^6 t N, the Middle East 1.3×10^6 t, Trinidad 1.6×10^6 t N. World ammonia trade in 1996 was around 11×10^6 t N. Values for 1994 are found in [1439].

13.2. Feedstock Choice

Natural gas is by far the most economical feedstock for ammonia production, achieving the lowest energy consumption and requiring the lowest investment [404]. This can also be seen from Table 45, which gives an estimate of ammonia production costs in Northwest Europe for different feedstocks using state-of-the-art technological standards. The lump turn key price for the ammonia plant were assumed as $\$ 180 \times 10^6$ for steam reforming of natural gas, $\$ 270 \times 10^6$ for partial oxidation of vacuum residue and $\$ 400 \times 10^6$ for coal-based plants (Capacity 1800 mt/d).

Table 45. Ammonia production costs from various feedstocks in 1998 (600 000 t/a)

Feedstock (process)	Natural gas (steam reforming)	Vacuum residue (partial oxidation)	Coal (partial oxidation)
Feedstock price, $\$/10^6$ Btu	2.8	1.8	1.5
Total energy consumption, 10^6 Btu/t	27	36	45.5
Feedstock and energy costs, \$/t NH_3	75.6	64.8	68.3
Other cash costs, \$/t NH_3	28.5	41.0	59.0
Total cash costs, \$/t NH_3	104.6	105.8	127.3
Capital related costs*, \$/t NH_3	68.4	100.3	143.3
Total costs, \$/t NH_3	172.5	206.1	270.6
Total capital**, 10^6 \$	250	350	500

* Assumed dept/equity ratio 60:40; depreciation 6%, 8% interest on depts, 16% ROI on equity.

** Total capital (1998) includes turn-key lump sum price for plant and storage, spare parts, catalysts, clients inhouse costs, offsites, working capital (3 months), basis 1,8 DM/\$.

At present there is obviously no chance for other feedstocks to compete with steam reforming of natural gas. Only under very special circumstances, for example, in cooperation with a refinery, might partial oxidation of heavy residues be economically justified. It should be noted that the average energy consumption of the steam reforming plants in operation at present is noticeably higher than the example of the most advanced concept presented in Table 45. In Western Europe the combined cost of feedstock and energy — both are actually natural gas energy — is the major determinant of the production cost. Even with most modern plants gas cost are more than 70% of the cash costs and as much as 40% of the total production costs. Gas prices are linked to a greater or lesser extent to the crude oil price but the present so-called interfuel relationship may change in the future because of the general need for less polluting fuels. Today natural gas is still favorably priced in comparison to other fossil fuels. The medium-term forecast is higher prices in Europe and USA. In the low-cost areas, such as the Middle East, Trinidad and Indonesia, where uses of natural gas competing with ammonia production are not growing to a great extent only a moderate increase of the feedstock price is expected [1444], [1445]. In these countries a certain increase in export-oriented ammonia capacity might be expected for the future.

Table 46. Percentage of world natural gas reserves and consumption for various geographical areas in 1997 [1442]

	% of world reserves [114.8 × 10^{12} m^3]	% of world consumption [2196.7 × 10^9 m^3 (STP)]
Former Soviet Union	39.2	22.4
(Russian Federation)	(33.2)	(15.1)
Middle East	33.7	7.3
North America	5.8	33.7
Europe (incl. North Sea)	3.8	19.0
Africa	6.8	2.3
Central and South America	4.4	3.9
Asia (incl. Australia and New Zealand)	6.3	11.4

Table 47. World Reserves and Consumption Rate of Fossil Feedstocks in 1994 [1442]

	Coal, t	Mineral oil, t	Natural gas, m^3 (STP)
Reserves	1032 × 10^9	140.9 × 10^9	141 × 10^{12}
Consumption per year	4712 × 10^6	3445 × 10^6	2136 × 10^9
Years of expected supply	219	41	66

Nearly three-quarters of world natural gas reserves (1994) are concentrated in two areas: in the former Soviet Union (39%) and the Arabian Gulf (34%) as may be seen from Table 46.

In the very long term, coal has prospects as can be seen from world reserves of fossil energy and their present consumption rate (Table 47).

13.3. Capital Demand for Ammonia Production

The other main contribution to the ammonia production cost are the capital related costs like interests for debts, depreciation and required return on equity. The total capital involved consists of the lump-sum turn- key price for plant and storage facility; an adequate amount of spare parts; catalysts, solvents and lubricants including some reserves; in-house costs for the client for project definition, project supervision, hazard studies, cost for project development and organization, including financing; off-sites; working capital. For non-industrialized and/or remote areas additional investments for infra structure will also be necessary. For the lump-sum turn-key price (LSTK) of a 1800 t/d steam reforming ammonia plant based on natural gas, presently a budget figure of about \$ 170–180 × 10^6 can be taken as a reasonable figure [1476], [1477]. Investment cost for partial oxidation plants are considerably higher. One factor is the need for a cryogenic air separation to produce the required quantity of pure oxygen and nitrogen. For a 1800 t (STP)/d ammonia plant based on heavy oil residues the investment for the air separation unit producing 100 bar oxygen and 75 bar nitrogen is around \$ 55 × 10^6 in Western Europe [1478]. Other expensive units are in the gas

purification, namely Rectisol for sour gas removal, Claus plant with tail gas unit and liquid nitrogen wash. Soot management, metal recovery and wastewater treatment, and in coal gasification plants the feedstock handling and preparation, are substantial cost contributions. As partial oxidation plants may differ considerably in process configuration, especially for coal feedstock, and are less frequently built — sometimes also not on a lump-sum basis — less reliable data are available. For lump-sum turn-key prices for just the ammonia plant the following figures may be used as a rule of thumb: Steam reforming natural gas 100 %, partial oxidation of heavy oil residues 150 %, coal gasification based plant 220 %.

The abovementioned budget price for the natural gas steam reforming plant consist of about 40 % of material, 30 % of labor (civil work and erection) and 30 % of other costs (transport, engineering, insurance, financing, etc.) [1476], [1477]. Geographical location of the plant may of course influence the LSTK price. Material is bought worldwide in a highly competitive market and prices are at first approximation independent of the country of destination, but the total expenditure for material might differ. For example, in a country of high natural gas prices higher investment for energy saving might be economical and vice versa. Also stricter authority regulations for safety and environmental standards in industrialized countries might cause an increase in cost as well as extreme climatic conditions. Higher material transport costs in distant locations might, for example, be compensated for by lower labor costs, e.g., NW Europe 100 %, US Gulf 90%, Trinidad 90%, the Middle East 70 %.

In conclusion it can be said that the influence of plant location on the LSTK price of the "naked" ammonia plant is often overestimated [1476]. This is not the case for the other investments. Assuming a stand-alone plant (no other ammonia plants existing at the site) the following will apply for the required storage capacity: If the capacity is intended for domestic product use only a storage capacity of about 20 days might be sufficient, if it is intended for export at least a capacity of one month would be appropriate. This is naturally different if the plant is erected at a side where already one or more ammonia plants exist and only a minor or even no increase of tank capacity is necessary. Inventory of spare parts and reserve catalysts will differ for the locations as well as the in-house costs, which will depend for example, on the technical capabilities of the client. Off-site costs can be considerable, for example, when facilities for power generation, water purification and supply, buildings for workshop, material storage and administration have to be included on a grass-root site. In some cases these additional costs might be as high as $\$ 50 \times 10^6$. For remote locations additional investments for infrastructure might be necessary, for example, harbor construction, railway tracks and roads, but this would not be justified for just one stand-alone ammonia plant even at a location with extremely low natural gas prices.

Finally an adequate working capital has to be also included in the calculation of production costs. The cash cost of three month production would be a reasonable assumption for the working capital. Keeping all these factors in mind it becomes clear that the numbers in Figure 122 have only orientating character and that each real

ammonia project is a custom-made solution according to the whishes and objectives of the client.

13.4. Other Production Cost Factors

Besides the capital charges, which will depend on equity/debt ratio for the involved capital, interest rates, and anticipated ROI for equity, the other major fixed costs are maintenance, labor, laboratory costs, and overheads. For the annual maintenance costs, usually a percentage of the investment is assumed, generally 3 % for steam reforming plants and 4 % for partial oxidation of heavy feedstocks and coal (this includes material and labor for maintenance). The number of operators depends to some extent on the shift schedule and operating philosophy in the individual company. The number of operators present at a plant has to be sufficient for safe continuous operation and a safe shut down, in the event of a sudden plant trip. The number need not necessarily be sufficient to restart the plant because additional people from off-duty shifts may be called in. Usually 5 – 7 operators are considered as adequate for operating a steam reforming plant; the number in partial oxidation plants is higher. Costs for consumption of catalysts, molecular sieves, inert material, solvents, and lube and seal oil are around 3 \$/t NH_3.

Catalysts have nowadays sufficient service life that change intervals can coordinated with normal turn-arounds. (Years of catalyst service life: primary reformer 2 – 4, secondary reformer > 6, HTS > 6, LTS 2 – 4 (6 with guard bed), methanation > 8, synthesis 10 – 15) (see also [1497]).

An important influence on production cost has, of course, the so-called on-stream factor, the number of production days per year. It is standard practice to assume that a well designed and operated plant should be capable to reach a minimum of 330 days per year, a value on which economic calculations are usually based. Modern plants often achieve higher on-stream factors. A beneficial effect is also that many plants achieve higher capacity than the original design. Plant outages because of operational problems or temporary shut downs for economic reasons because of unfavorable market situation can lower the profitability considerable. The on-stream factor is an average value, because plants should shut down only every 2 to 3 years for a major turn-around for repair and preventive maintenance. Only a very few short unscheduled shut-downs for repair work should occur between two turn-arounds. A start up needs between 15 to 30 hours and consumes a considerable amount of natural gas without an equivalent production (100 000 – 200 000 DM/d).

Overhead costs (administration and general services) also have to be included as cash costs.

13.5. Production Costs for Various Geographical Locations

Figure 122 shows an estimate of ammonia production costs at various locations. In this figure the capital-related costs are based on a debt/equity ratio of 60/40. With 6 % depreciation of fixed assets and spare material, 8 % interest on debts and 16 % ROI on equity, corresponding to a total of about 16.5 % of the total capital involved. The total capital includes the LSTK price for plant and storage, cost of the off-sites for an industrialized site, in-house project costs, spare parts and catalyst reserves, working capital.

Admittedly the picture given in Figure 122 is somewhat simplified, but nevertheless some principal conclusions can be drawn from it: The decisive cost factor is the natural gas price as the investment for the areas compared does not differ significantly for reasons discussed above. With inclusion of the high freight cost from the Arabian Gulf

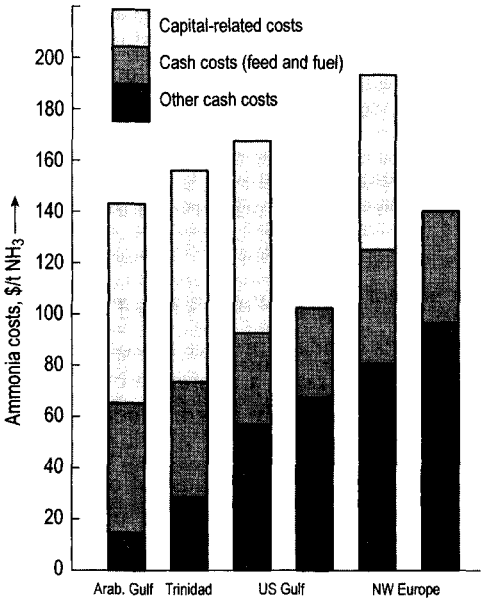

Figure 122. Ammonia production costs at various locations (capacity 600 000 t/a)

	Arab Gulf	Trinidad	US Gulf		NW Europe	
Plant	new	new	new	old	new	old
Natural gas, $/$10^6$ Btu	0.6	1.2	2.2	2.2	2.8	2.8
Feed + fuel, 10^6 Btu/t NH_3	29	28	28	32	27	32
Total capital, 10^6 $	270	250	240	-	250	-
Product use	export	export	domestic	domestic	domestic	domestic

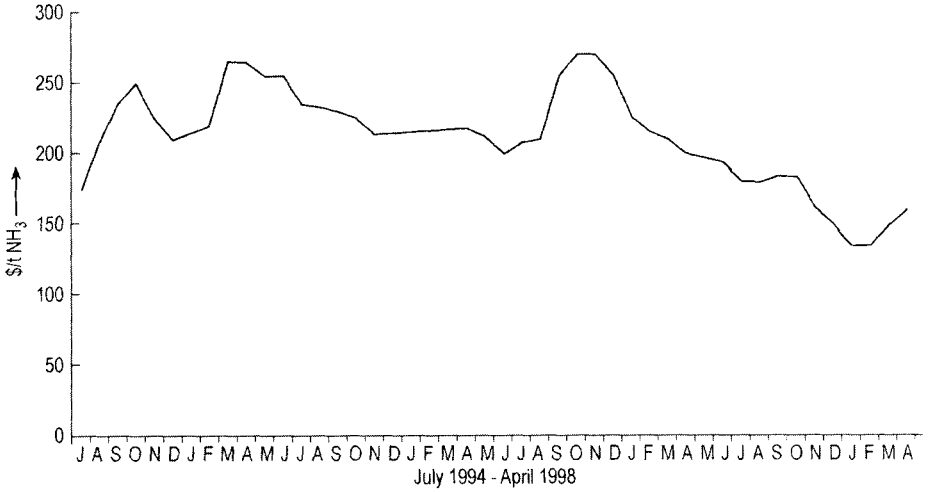

Figure 123. Development of ammonia prices in North-West Europe

a plant there is not competitive against existing world scale capacities in NW Europe and scarcely competitive against a new high efficiency plant in NW Europe. But lower freight rates and higher market prices will make the export to the Asian market out of a new Arabian Gulf plant attractive. Imports to NW Europe come mainly from former Soviet Union (FSU), which in desire of hard currency and on account of their surplus capacity (partially due to lower domestic fertilizer consumption), sell at very competitive prices. As it is rather difficult to guess how the gas will be valued internally (probably 1.6 – 2.3 $/GJ) [1440] an estimate for the production costs in the FSU former was not included in Figure 122. An account of the natural gas situation and prices is presented in [1444]. An advantage are the relatively moderate freight rates from the terminal in Ventspils at the Baltic Sea.

With inclusion of shipping costs, new plant capacities in Trinidad are, according to Figure 122, only marginally competitive against a new plant at the US Gulf, and cannot compete against existing US Gulf productions. But this simple picture might change if the plant is not intended for the free market but for long contract delivery, for example, to the owners own facilities in the United States. India and China are still net importers, Indonesia has surplus capacity, but exports to the Asian market are rather in form of urea than as ammonia. Indonesia and Malaysia together have about 3 % of the proven natural gas reserves, and a reserve/production rate of 30 and 57 respectively. Because of the present Asian financial crisis it is difficult to figure out natural gas prices, but they might range between 0.8 and 1.0 $/10^6 Btu. Production costs are a more or less calculable issue, but the prices are not. When talking of ammonia prices one has to consider that only a part of the ammonia is traded as such, the major part is directly converted by the producers in urea (about 45 %), other solid fertilizers (35 %) or chemical products. As the overseas trade represents only about 8 % of the world

ammonia production plant output, variations in the nitrogen fertilizer imports in Asia (mainly China and India) may at time cause substantial price variations as illustrated with the C & F prices of imports in NW Europe (Figure 123, values from Nitrogen magazine). Also of influence are, of course, the changes in the dollar exchange rates to other currencies.

14. Future Perspectives

It is difficult to venture a prognosis for the future development of ammonia production technology. As about 85 % of the ammonia consumption goes into the manufacture of fertilizers, it is obvious that the future of the ammonia industry is very closely bound up with future fertilizer needs and the pattern of the world supply.

Nitrate pollution, which may become a problem in some countries, is sometimes used as an argument against the use of industrially produced "inorganic" or "synthetic" fertilizers and in favor of more "organic" or "natural" fertilizers. But this is a misconception, because degradation of biomass and manure also leads to nitrate run-off. In addition, the amount of this biological material is far to small to supply the increasing demand of the agriculture necessary to feed the growing world population. The solution to the run-off problem therefore can also not consist in cutting back fertilizer application, which would be disastrous in developing countries, but is likely to lie in a better management of the timing of fertilizer application, requiring a better understanding of the biological nitrogen cycle. Estimates of fixed nitrogen from natural sources and antropogenic activities on global basis are found in [1446], [1450].

14.1. Other Nitrogen Fixation Methods for the Future

A fundamental question is whether there are other options for the future than the present ammonia technology, which involves severe temperatures and pressures. The research for new approaches should strive for the following, admittedly rather ambitious and idealized objectives: ambient reaction conditions, less or no consumption of fossil energy, lower investment, simple application, even in remote developing areas, and wide capacity range. As the major demand is in agriculture, biological processes for in vivo conversion of molecular nitrogen into fixed nitrogen would probably be the first choice. Alternatively abiotic processes (in vitro) with homogenous catalysis under mild reaction conditions could be discussed for ammonia production. In addition there are also some reports [1017], [1451], [1452] of resumed research on direct nitrogen oxidation, as was once used in the Birkeland–Eyde process. The use of a plasma processes instead of an electric arc for radiation in a chemo-nuclear process was also discussed [1453].

14.1.1. Biological Processes

Certain bacteria and blue-green algae are able to absorb atmospheric nitrogen, by themselves or in symbiosis with a host plant, and transform it into organic nitrogen compounds via intermediate ammonium ions, whereby the host plant indirectly supplies the large amount of energy needed. A well known example is the symbiotic relationship between legumes (e.g., peas, beans, soybeans, lupins) and Rhizobium bacteria, which settle in their root nodules. Ammonia synthesis is performed by the enzyme nitrogenase [1455], [1456]. For the synthesis of the nitrogenase in the cell the so-called NIF gene is responsible. Apart from Rhizobium bacteria a number of other organisms have nitrogen fixation potential, living in symbiosis or providing the required energy from their own metabolism. Genetic engineering to extend biological nitrogen fixation to other plant groups pursues various routes [1457], [1458]:

1) Modifying Rhizobium to broaden its spectrum of host plants
2) Transferring the NIF gene to other bacteria which have a broader spectrum of host plants but have no natural nitrogen-fixing capability
3) Engineering soil bacteria to absorb and convert nitrogen to ammonia and release it to the soil [1459]
4) Inserting the NIF gene directly into plants

Especially the last option, to design nitrogen-fixing species of traditional crops such as wheat, rice, and corn, leads to the following questions: Would it be preferable to fix nitrogen in the leaves where energy is available or in the roots, to which carbohydrates have to be transported? If fixation is performed in the leaves, then how can the problem of the proximity of oxygen generated in the photosynthesis and oxygen-sensitive nitrogenase be dealt with? To what extent will the energy required by a plant to fix nitrogen affect overall productivity?

The last question has been discussed in some detail [1460]. For the conversion of molecular nitrogen into ammonia the following stoichiometric equation may be formulated:

$$0.5\ N_2 + 1.5\ H_2O \longrightarrow NH_3 + 0.75\ O_2 \qquad (100)$$

$$\Delta F^0_{298} = +340\ \text{kJ/mol},\ \Delta H^0_{298} = +383\ \text{kJ/mol}$$

The oxidation of glucose generates 3140 kJ/mol and with 100 % efficiency only about 0.11 mol of glucose would be required to produce one mole of ammonia. This ideal can, of course, never be achieved. In the molybdenum-containing nitrogenase a transfer of eight electrons is involved in one catalytic cycle:

$$N_2 + 8\ H^+ + 8\ e^- \longrightarrow 2\ NH_3 + H_2 \qquad (101)$$

As seen from this equation two electrons are "wasted" in forming molecular hydrogen, which also seems to be unavoidable in vivo. This stoichiometry suggests an efficiency of 75 %, but if additional functions associated with fixation are taken into

account, a maximum overall efficiency of 10 – 15 % is estimated for the enzyme, and even less for the bacteria as a whole [1461]. In investigations on Rizobium [1462], [1463] it was shown for the nodulated roots of peas that 12 g of glucose are consumed to produce 1 g of fixed nitrogen. Using this efficiency for the case where all the fixed nitrogen in the plant is supplied only via this route, a yield loss of 18 % would result. Nitrate, for example from a fertilizer, absorbed by the plant is transformed to ammonia involving a free energy change ΔF^0_{298} = +331, which is comparable to the free energy change for converting molecular nitrogen to ammonia, as shown in the stoichiometric equation above.

This is a somewhat surprising result, which suggests that nitrogen supply with nitrate has an energetic advantage over the biological fixation process [1464]. A definite answer to this question will only be possible when genetically engineered nitrogen-fixing plants are available in sufficient amounts for field tests. There is no doubt that in the foreseeable future genetic engineering will succeed in designing nitrogen-fixing plants for agricultural crops, and that these modified plants will be used on a large scale for securing the food supply for a growing number of people in the developing countries.

But until this will become a reality, application of selected natural nitrogen-fixing microorganisms to crops would be an intermediate solution to reduce industrial fertilizer consumption. In the United States field tests with *Azospirillium* applied to corn could demonstrate a considerable increase in harvest yield [1458]. Careful directed application of blue-green algae, (*Anabaena azolla*) and water fern (*Azolla pinata*) in tropical rice fields is also very promising [1465], [1466]. Unlike most diazotropic bacteria, blue-green algae are self-sufficient in that they themselves produce the energy necessary for the nitrogen fixation by photosynthesis.

14.1.2. Abiotic Processes [1460]

Possibilities of converting molecular nitrogen into ammonia in homogeneous solution by using organometallic complexes have been studied from around 1966 onwards. Numerous investigations resulted in the laboratory-scale synthesis of ammonia , but with rather low yields. The prospects of this route are not judged to be very promising in terms of energy consumption and with respect to the costs of the rather sophisticated catalyst systems. Photochemical methods [1467], [1468] to produce ammonia at ambient temperature and atmospheric pressure conditions in presence of a catalyst have up to now attained ammonia yields which are far too low to be economically attractive.

For a detailed review of biological and abiotic nitrogen fixation, see [1469] and [1460]; additional literature references can be found in [1448] – [1450], [1454], [1455].

14.2. Conclusions

Based on the foregoing discussion and the evaluation of present technology (see also [404]) and research efforts one may formulate the scenario for the future development of ammonia production as follows:

1) For the major part, ammonia production in the next 15 to 20 years will rely on the classic ammonia synthesis reaction combining nitrogen and hydrogen using a catalyst at elevated temperature and pressure in a recycle process.
2) It is very likely that genetic engineering will succeed in modifying some classical crops for biological nitrogen fixation and that large-scale application will occur predominantly in areas with strongly growing populations to secure the increasing food demand. This development may be pushed by the fact that compared to the classical fertilizer route less capital and less energy would be needed. This may happen within the next 15 – 20 years, but time estimates are always difficult. But even with the introduction of this new approach, traditional ammonia synthesis will continue to operate in parallel, because it might be necessary to supplement the biological nitrogen fixation with classical fertilizers. In addition, the existing ammonia plants represent a considerable capital investment and a great number of them may reliably operate for at least another 20 to 30 years from a mere technical point of view.
3) Natural gas will remain the preferred feedstock of present ammonia production technology in the medium term (15 – 20 years) as may be assumed from the world energy balance shown in Table 47. Partial oxidation of heavy hydrocarbon residues will be limited to special cases and coal gasification might not play a major role in this period.
4) Ammonia technology will not change fundamentally, at least not in the next 10 to 15 years. Even if there are radical, unforeseeable developments, they will need some time to mature to commercial applicability. With the traditional concepts, the margins for additional improvements have become rather small after years of continuous research and development. Thus further progress may be confined to minor improvements of individual process steps, catalysts and equipment design.
5) The best energy figure so far achieved in commercial production is around 28 GJ/t NH_3. With the new ruthenium-based catalysts M. W. Kellogg claims a figure of 27.2 GJ/t NH_3. Further reduction would need an even more active catalyst to operate at a much lower synthesis pressure, for example, at around 30 bar, which is the usual pressure level of steam reforming. The probability of finding such a catalyst is rather small after all the years of intensive research. Figures between 27 and 28 GJ/t NH_3 already correspond to a rather high efficiency of around 75 % with respect to the theoretical minimum of 20.9 GJ/t NH_3 (calculated as stoichiometric methane demand, see Section 5.1.3).

6) The bulk of ammonia production in the near future will still be produced in world-scale plants of capacity 1000 – 2000 t NH_3/d. Small capacities will be limited to locations where special logistical, financial or feedstock conditions favor them.
7) Most newer technology developments will mainly reduce investment costs and increase operational reliability. Smaller integrated process units, such as exchanger reformers in various configurations, contribute to this reduction and will achieve additional savings by simplifying piping and instrumentation. Progress in instrumentation and computer control could reduce the effective overall energy consumption achieved over the course of a year by tuning plants continuously to optimal operating conditions.

15. References

[1] C. Bosch, Nobel price address 1933.
[2] I. Hay, G. D. Honti, in G. D. Honti (ed.): *The Nitrogen Industry, part I,* Akademiai Kiado, Budapest 1976, pp. 68–73.
[3] F. Ritter, F. Walter in K. Winnacker, E. Weingaertner (eds.): *Chemische Technologie,* **vol. 2,** Carl Hanser, München 1950 pp. 368.
[4] J. Hess, *Chem. Ind. (Berlin)* **45** (1922) 538.
[5] *Chem. Ind. (Berlin)* **48** (1925) 718.
[6] F-W. Kampmann, W. Porz, F-K. Frorath, H. Oertel: *"Calcium Carbide",* in Ullmann's Encyclopedia of Industrial Chemistry, **vol. 4,** VCH Weinheim.
[7] G. Plumpe: *Die I. G. Farbenindustrie — Wirtschaft, Technik und Politik,* Dunker & Humblot, Berlin 1990.
[8] A. Mittasch: Chemische Grundlegung der industriellen Ammoniakkatalyse, Ludwigshafen 1953.
[9] B. Timm, W. Danz in V. Sanchelli (ed.): *"Fertilizer Nitrogen, its chemistry and production",* Reinhold, New York 1964, p. 40.
[10] A. Mittasch, W. Frankenburger, *Z. Elektrochem. Angew. Phys. Chem.* **35** (1929) 920.
[11] F. Haber, G. van Oordt, *Z. Anorg. Allg. Chem.* **43** (1904) 111; **44** (1905) 341; **47** (1905) 42.
[12] W. Nernst, *Z. Elektrochem. Angew. Phys. Chem.* **13** (1907) 521.
[13] F. Jost, *Z. Anorg. Allg. Chem.* **57** (19108) 414.
[14] M. Appl, *"The Haber-Bosch Heritage: The Ammonia Production Technology"* 50th Anniversary of the IFA Technical Conference, September 25–26, 1997, Sevilla, Spain.
[15] F. Haber, R. Le Rossignol, *Ber. Dtsch. Chem. Ges.* **40** (1907) 2144.
[16] P. Krassa, *Chem. Ztg. Chem. Appar.* **90** (1966) 104.
[17] F. Haber, *Z. Elektrochem. Angew. Phys. Chem.* **14** (1908) 181; **20** (1914) 597.
[18] R. Le Rossignol, *Naturwissenschaften* **16** (1928) 1070.
[19] B. Timm, *Chem. Ing. Tech.* **35** (1963) no. 12, 817.
[20] F. A. Henglein, *Chem. Ztg.* **75** (1951) 345–350, 389–392, 407–410.
[21] K. Holdermann: *Im Banne der Chemie – Carl Bosch,* Econ Verlag, Düsseldorf 1953.
[22] M. Appl in W. F. Furter (ed.): *A Century of Chemical Engineering,* Plenum Publ. Corp., New York, 1982 p. 29.
[23] M. Appl : *IIChE Conference,* Hyderabad, 1986; *Indian Chemical Engineer* **XXIX** (1987) no. 1, 7–29.
[24] S. A. Topham: *Catalysis, Science and Technology,* vol. 7, Springer-Verlag, Berlin–Heidelberg–New York–Tokyo pp. 1–50.
[25] A. Nagel et al.: *Stickstoff,* Schriftenreihe der BASF, 2nd ed., 1991.
[26] F. Duftschmidt, F. Markert, *Chem. Ing. Techn.* **32,** (1960), 806–811.
[27] M. Appl, *Nitrogen* **100** (1976) 47.
[28] L. Pauling: *The Nature of the Chemical Bond,* 3rd ed., Cornell University Press, Ithaca, N.Y., 1960.
L. Pauling: *Die Natur der chemischen Bindung,* 3rd ed., Verlag Chemie, Weinheim 1968.
[29] F. Hund, *Z. Phys.* **31** (1925) 95.
[30] L. Haar, *J. Phys. Chem. Ref. Data* **7** (1978) no. 3, 635–792.
[31] *VDI Forschungsh.* 1979, no. 596, VDI-Verlag Düsseldorf.
[32] F. Din: *Thermodynamic Functions of Gases,* **vol. 1,** Butterworths, London 1956.

[33] A. Nielsen: *An Investigation on Promoted Iron Catalysts for the Syntheses of Ammonia,* Gjellerup, Kopenhagen 1968.

[34] M. P. Wukalowitsch et al., *Teploenergetika (Moscow)* **7** (1960) no. 1, 63–69; *Chem. Ing. Tech.* **33** (1961) no. 4, 5, 291, 292.

[35] R. Döring: *Thermodynamische Eigenschaften von Ammoniak (R 717),* Verlag C. F. Müller, Karlsruhe 1978; *Ki Klima + Kälte Ing.,* extra no. 5.

[36] *Landolt-Börnstein,* vol. 2, part 1–10, Springer Verlag, Berlin–Heidelberg–New York 1971.

[37] *Handbuch der Kältetechnik,* **vol. IV,** Springer Verlag, Berlin–Heidelberg–New York 1956.

[38] A. Kumagai, T. Toriumi, *J. Chem. Eng. Data* **16** (1971) no. 3, 293.

[39] R. Wiebe, V. I. Gaddy, *J. Am. Chem. Soc.* **60** (1938) 2300.

[40] E. P. Bartlett, H. L. Cupples, T. H. Tremearne, *J. Am. Chem. Soc.* **50** (1928) 1275.

[41] E. P. Bartlett et al., *J. Am. Chem. Soc.* **52** (1930) 1363.

[42] B. H. Sage, R. H. Olds, W. N. Lacey, *Ind. Eng. Chem.* **40** (1948) 1453.

[43] A. Michels et al., *Appl. Sci. Res.* **A3** (1953) 1.

[44] A. Michels et al., *Appl. Sci. Res.* **A4** (1954) 180.

[45] R. Plank, *Kältetechnik* **12** (1960) 282–283.

[46] W. K. Chung, *Can. J. Chem. Eng.* **55** (1977) no. 6, 707–711.

[47] G. G. Fuller, *Ind. Eng. Chem. Fundam.* **15** (1976) no. 4, 254–257.

[48] B. D. Djordjevic et al., *Chem. Eng. Sci.* **32** (1977) no. 9, 1103–1107.

[49] M. Zander, W. Thomas, *J. Chem. Eng. Data* **24** (1979) 1.

[50] L. J. Christiansen, J. Kjaer: *Enthalpy Tables of Ideal Gases,* Haldor Topsøe, Copenhagen 1982, p. 1.

[51] Dow Chemical Corp., *JANAF Thermodynamical Tables,* 2nd ed., 1971, NSRDS NBS-37.

[52] L. Haar, *J. Res. Natl. Bur. Stand. Sect. A* **72** (1968) 2.

[53] E. R. Grahl, *Pet. Process.* **8** (1953) 562.

[54] R. G. Barile, G. Thodos, *Can. J. Chem. Eng.* **43** (1965) 137–142.

[55] C. G. Alesandrini et al., *Ind. Eng. Chem. Process Des. Dev.* **11** (1972) no. 2, 253.

[56] H. Zeininger, *Chem. Ing. Tech.* **45** (1973) no. 17, 1067.

[57] H. H. Reamer, B. H. Saga, *J. Chem. Eng. Data* **4** (1959) no. 4, 303.

[58] K. V. Reddy, A. Husain, *Ind. Eng. Chem. Process Des. Dev.* **19** (1980) 580–586.

[59] H. Masuoka et al., *J. Chem. Eng. Jpn.* **10** (1977) no. 3, 171–175.

[60] A. T. Larson, C. A. Black, *J. Am. Chem. Soc.* **47** (1925) 1015.

[61] A. Michels et al., *Physica (Utrecht)* **16** (1950) 831–838.

[62] A. Michels et al., *Physica (Utrecht)* **25** (1959) 840.

[63] G. Guerreri, *Hydrocarbon Process.* **49** (1970) no. 12, 74–76.

[64] H. H. Reamer, B. H. Saga, *J. Chem. Eng. Data* **4** (1959) no. 2, 152.

[65] R. Wiebe, T. H. Tremearne, *J. Am. Chem. Soc.* **55** (1933) 975.

[66] F. Heise, *Ber. Bunsenges. Phys. Chem.* **76** (1972) 938.

[67] B. Lefrancois, C. Vaniscotte, *Genie Chim.* **83** (1960) no. 5, 139.

[68] H.-D. Müller, *Z. Phys. Chem. (Leipzig)* **255** (1974) no. 3, 486.

[69] B. I. Lee, M. G. Kesler, *AIChE J.* **21** (1975) no. 3, 510.

[70] K. Konoki et al., *J. Chem. Eng. Jpn.* **5** (1972) no. 2, 103–107.

[71] G. Sarashina, *J. Chem. Eng. Jpn.* **7** (1974) no. 6, 421–425.

[72] R. Heide, *Luft Kältetech.* **7** (1971) no. 3, 128–130.

[73] I. Durant, *J. Chem. Soc.* 1934, no. 135, 730.

[74] Yu. V. Efremov, I. F. Golubev, *Russ. J. Phys. Chem. Eng. (Engl. Transl.)* **36** (1962) no. 5, 521–522.

[75] J. A. Jossi et al., *AIChE J.* **8** (1962) no. 1, 59–63.

[76] H. Shimotake, G. Thodos, *AIChE J.* **9** (1963) no. 1, 63.

[77] B. K. Sun, T. S. Storwick, *J. Chem. Eng. Data* **24** (1979) no. 2, 88.

[78] I. T. Perelsatein, E. B. Parushin, *Kholod. Tekh.*, 1980, no. 6, 34–37.

[79] A. K. Pal, A. K. Barura, *J. Chem. Phys.* **47** (1967) no. 1, 216.

[80] E. A. Mason, L. Mouchik, *J. Chem. Phys.* **36** (1962) no. 10, 2746.

[81] A. B. Rakshit, C. S. Roy, A. K. Barua, *J. of Chemical Physics* **59** (1973) 3633–3688.

[82] D. P. Needham, H. Ziebland, *Int. J. Heat Mass Transfer* **8** (1965) 1387–1414.

[83] A. M. P. Tans, *Ind. Chem.* **39** (1963) no. 3, 141.

[84] R. Afshar, S. Murad, S. C. Saxna, *Chem. Eng. Commun.* **10** (1981) 1–11.

[85] D. A. Kouremenos, *Kältetechnik* **20** (1968) no. 10, 319.

[86] A. O. S. Maczek, P. Gray, *Trans. Faraday Soc.* **66** (1970) 127.

[87] P. Correia et al., *Ber. Bunsenges. Phys. Chem.* **72** (1968) 393.

[88] W. Inkofer et al., 15th AIChE Ammonia Safety Symp., Denver 1970; *Ammonia Plant Saf.* **13** (1971) 67.

[89] L. J. Gillespie, J. A. Beattie, *Phys. Rev.* **36** (1930) 743.

[90] S. Peter, H. Wenzel, *Chem. Ing. Tech.* **45** (1973) no. 9 + 10, 573.

[91] F. Haber, S. Tamaru, *Z. Elektrochem. Angew. Phys. Chem.* **21** (1915) 191.

[92] L. J. Gillespie, J. A. Beattie, *Phys. Rev.* **36** (1930) 1008.

[93] V. G. Telegin, G. M. Lutskii, *J. Appl. Chem. USSR (Engl. Transl)* **37** (1964) 2271.

[94] L. J. Christiansen in W. A. Nielsen (ed.): *Ammonia — Catalysis and Manufacture,* Springer, Heidelberg 1995 pp. 1–16.

[95] I. Granet, *Pet. Refiner* **33** (1954) no. 5, 205.

[96] I. Granet, P. Kass, *Pet. Refiner* **32** (1953) no. 3, 149.

[97] A. K. Pal, A. K. Barua, *J. Chem. Phys.* **47** (1967) 116.

[98] H. R., Christen, *Grundlagen der allgemeinen und anorganischen Chemie,* Verlag Sauerländer, Arau; Diesterweg-Salle, Frankfurt am Main, 4. Auflage, 1973, p. 482.

[99] W. G. Frankenburger, *Catalysis 1954–1960* **3** (1955) 171.

[100] R. Brill et al., *Ber. Bunsenges. Phys. Chem.* **73** (1969) 999.

[101] A. Ozaki, K. Aika: "The Synthesis of Ammonia by Heterogeneous Catalysis," in R. W. F. Hardy et al. (eds.): *A Treatise on Dinitrogen Fixation,* Sect. I and II, Wiley, New York 1979, pp. 169–247.

[102] A. Ozaki, K. Aika: "Catalytic Activation of Dinitrogen," in R. H. Anderson, M. Boudart (eds.): *Catalysis: Science and Technology,* **vol. 1,** Springer Verlag, Berlin–Heidelberg–New York 1981, pp. 87–158.

[103] P. H. Emmett in E. Drauglis, R. I. Jaffee (eds.): *The Physical Basis for Heterogenous Catalysis,* Plenum Publ., New York 1975, p. 3.

[104] K. Tamaru in J. Chatts et al. (eds.): *New Trends in the Chemistry of Nitrogen Fixation,* Academic Press, New York 1980, p. 13.

[105] G. A. Somorjai: *Chemistry in Two Dimensions: Surfaces,* Cornell Press, Ithaca 1981.

[106] G. Ertl, J. Küppers: *Low Electrons and Surface Chemistry,* 2nd ed., VCH Verlagsgesellschaft, Weinheim 1985.

[107] G. Ertl in J. R. Jennings (ed.): *Catalytic Ammonia Synthesis,* Plenum Press, New York – London 1991, pp. 109–131.

[108] P. Stolze in A. Nielsen (ed.): *Ammonia — Catalysis and Manufacture,* Springer-Verlag, Heidelberg 1995, pp. 17–102.

[109] G. Ertl: "Kinetics of Chemical Processes on Well-defined Surfaces," in R. H. Anderson, M. Boudart (eds.): *Catalysis: Science and Technology,* **vol. 4,** Springer-Verlag, Berlin–Heidelberg–New York 1983, pp. 257–282.

[110] M. Boudart, "Kinetics and Mechanism of Ammonia Synthesis," *Catal. Rev. Sci. Eng.* **23** (1981) 1–15.

[111] J. J. F. Scholten et al., *Trans. Faraday Soc.* **55** (1959) 2166.

[112] J. J. F. Scholten, Dissertation, Techn. Hochschule Delft 1959.

[113] P. Mars et al. in J. H. de Boer (ed.): *The Mechanism of Heterogenous Catalysis,* Elsevier, Amsterdam 1960, p. 66.

[114] K. Tanaka, A. Matsumaya, *J. Res. Inst. Catal. Hokkaido Univ.* **2** (1971) 87.

[115] M. I. Temkin, *Adv. Catal.* **28** (1979) 173.

[116] P. H. Emmett, S. Brunauer, *J. Am. Chem. Soc.* **56** (1934) 35.

[117] H. S. Taylor, *J. Am. Chem. Soc.* **53** (1931) 578.

[118] W. Frankenburger, *Z. Elektrochem.* **39** (1933) 45, 97, 269.

[119] K. T. Kozhenova, M. Y. Kagan, *Zh. Fiz. Khim.* **14** (1940) 1250.

[120] P. H. Emmett, S. Braunauer, *J. Am. Chem. Soc.* **59** (1937) 1553.

[121] L. M. Aparicio, J. A. Dumesic: *Topics in Catalysis,* vol. 1, Baltzer AG, Basel 1994, p. 233–252.

[122] D. R. Strongin, G. A. Somorjai in J. R. Jennings (ed.): *Catalytic Ammonia Synthesis,* Plenum Press, New York 1991, pp. 133–178.

[123] G. Ertl, M. Huber, S. B. Lee, Z. Paal, M. Weiss, *Appl. Surf. Sci.* **8** (1981) 373.

[124] T. Nakata, S. Matsushita, *J. Phys. Chem.* **72** (1968) 458.

[125] V. I. Shvachko et al., *Kinet. Katal.* **7** (1966) 635, 734.

[126] Y. Morikawa, A. Ozaki, *J. Catal.* **12** (1968) 145.

[127] R. Westrik, P. Zwieterring, *Proc. K. Ned. Akad. Wet. Ser. B: Palaeontol. Geol. Phys. Chem.* **56** (1953) 492.

[128] R. Brill et al., *Angew. Chem.* **79** (1967) 905.

[129] H. Taube, Dissertation, Freie Universität Berlin 1968.

[130] R. Brill, *Ber. Bunsenges. Phys. Chem.* **75** (1971) 455.

[131] J. A. Dumesic, H. Topsøe, S. Khammouma, M. Boudart, *J. Catal.* **37** (1975) 503; see also [352].

[132] F. Boszo et al., *J. Cat.* **49** (1977) 103.

[133] G. Ertl et al., *J. Vac. Sci. Technol.* **13** (1976) 314.

[134] G. Ertl et al., *Surf. Sci.* **114** (1982) 515.

[135] G. A. Somorjai et al.: *Topics in Catalysis,* vol. 1, Baltzer AG, Basel 1994, p. 215–231.

[136] N. D. Spencer, R. C. Schoonmaker, G. A. Somorjai, *J. Catal.* **74** (1982) 129.

[137] G. Ertl: "Plenary Lecture," in T. Seiyama, K. Tanabe (eds.): *New Horizons in Catalysis, Proc. Int. Congr. Catal. 7th 1980,* Elsevier 1981, p. 21.

[138] F. Bozso, G. Ertl, *J. Catal.* **49** (1977) 18; **50** (1977) 519.

[139] R. Schlögl: "Ammonia Synthesis," in G. Ertl, H. Knözinger, J. Weitcamp (eds.): *Handbook of Heterogeneous Catalysis,* **vol. 4,** Wiley-VCH, Weinheim 1997, pp. 1698–1748.

[140] B. Fastrup: *Topics in Catalysis,* **vol. 1,** Baltzer AG, Basel 1994, p. 273–283.

[141] L. Falicov, G. A. Somorjai, *Proc. Natl. Akad. Sci. USA* **82** (1985) 2207.

[142] G. Ertl et al., *Surf. Sci.* **114** (1982) 527.

[143] G. Ertl et al., *Surface Science* **114** (1982) 527.

[144] S. R. Bare, D. R. Strongin, G. A. Somorjai, *J. Phys. Chem.* **90** (1987) 4726.

[145] D. R. Strongin et al., *J. Catal.* **103** (1987) 289.

[146] M. Bowker: *Topics in Catalysis,* **vol. 1,** Baltzer AG, Basel 1994, p. 265 – 271.
[147] C. Rettner, H. Stein, *Phys. Rev. Let.* **56** (1987) 2768.
[148] C. Rettner, H. Stein, *J. Chem. Phys.* **87** (1987) 770.
[149] J. K. Norskov: *Topics in Catalysis,* **vol. 1,** Baltzer AG, Basel 1994, p. 385 – 403.
[150] M. Grunze et al., *Phys. Rev. Lett.* **53** (1984) 850.
[151] L. J. Whitman, C. E. Bartosch, W. Ho, G. Strasser, M. Grunze, *Phys: Rev. Lett.* **56** (1986) 1984.
[152] L. J. Whitman, C. E. Bartosch, W. Ho, *J. Chem. Phys.* **85** (1986) 3688.
[153] M. Grunze, G. Strasser, M. Golze, *Appl. Phys.* **A 44** (1987) 19.
[154] J. Schütze et al.: *Topics in Catalysis,* **vol. 1,** Baltzer AG, Basel 1994, p. 195 – 214.
[155] M. Boudart: *Topics in Catalysis,* **vol. 1,** Baltzer AG, Basel 1994, p. 405 – 414.
[156] R. Schlögl, *Ammonia Synthesis,* in Handbook of Heteregeneous Catalysis (ed. G. Ertl, H. Knörzinger, J. Weitkamp), **vol. 4,** VCH Weinheim, 1997.
[157] A. Nielsen, *Catal. Rev.,* **4,** (1970) no. 1, 1.
[158] W. A. Schmidt, *Angew. Chem.* **80** (1968) 151.
[159] V. I. Shvachko et al., *Kinet. Katal.* **7** (1966) 635, 734.
[160] R. Brill et al., *Z. Phys. Chem. (Wiesbaden)* **64** (1969) 215.
[161] Y. Morikawa, A. Ozaki, *J. Catal.* **12** (1968) 145.
[162] N. Takezawa, I. Toyoshima, *J. Catal.* **19** (1970) 271.
[163] S. Carra, R. Ugo, *J. Catal.* **15** (1969) 435.
[164] I. I. Tretyakov et al., *Dokl. Akad. Nauk SSSR* **175** (1967) 1332.
[165] G. Parravano, *J. Catal.* **8** (1967) 29.
[166] M. I. Temkin et al., *Kinet. Katal.* **4** (1963) 494.
[167] S. R. Logan, J. Philp, *J. Catal.* **11** (1968) 1.
[168] N. Takezawa, P. H. Emmett, *J. Catal.* **11** (1968) 131.
[169] G. Schulz-Ekloff, *Ber. Bunsenges. Phys. Chem.* **75** (1971) 110.
[170] A. Nielsen et al., *J. Catal.* **3** (1964) 68.
[171] P. E. H. Nielsen, unpublished work, Haldor Topsøe A/S, cited in [253].
[172] S. R. Tennison in J. R. Jennings (ed.): *Catalytic Ammonia Synthesis,* Plenum Press, New York and London 1991, pp. 303 – 364.
[173] K. Aika, K. Tamaru in W. A. Nielsen (ed.): *Ammonia — Catalysis and Manufacture,* Springer-Verlag, Heidelberg 1995, pp. 103 – 148.
[174] J. N. Nwalor, J. G. Goodwin jr.: *Topics in Catalysis,* **vol. 1,** Baltzer AG, Basel 1994, p. 228 – 148.
[175] K. Aika, A. Ozaki, *J. Catal.* **16** (1970) 97.
[176] D. A. King, F. Sebba, *J. Catal.* **4** (1965) 253.
[177] N. Segal, F. Sebba, *J. Catal.* **8** (1967) 105.
[178] K. Aika, A. Ozaki, *J. Catal.* **14** (1969) 311.
[179] G. E. Moore, F. C. Unterwald, *J. Chem. Phys.* **48** (1968) 5409, 5393.
[180] M. R. Hillis et al., *Trans. Faraday Soc.* **62** (1966) 3570.
[181] K. Azuma, *Nature (London)* **190** (1961) no. 4775, 530.
[182] H. Kubota, M. Shindo, *J. Chem. Eng. Jpn.* **23** (1959) 242.
[183] G. Gramatica, N. Pernicone in J. R. Jennings (ed.): *Catalytic Ammonia Synthesis,* Plenum Press, New York – London 1991, pp. 211 – 252.
[184] J. P. Hansen in A. Nielsen (ed.): *Ammonia — Catalysis and Manufacture,* Springer-Verlag, Heidelberg 1995, pp. 149 – 190.
[185] M. I. Temkin, V. Pyzhev, *Acta Physicochim. URSS* **12** (1940) 327.

[186] M. I. Temkin, *Zh. Fiz. Khim.* **24** (1950) 1312.
[187] R. M. Adams, E. W. Comings, *Chem. Eng. Prog.* **49** (1953) 359.
[188] P. H. Emmett, J. T. Kummer, *Ind. Eng. Chem.* **35** (1943) 677.
[189] D. Annable, *Chem. Eng. Sci (Genie Chimique)* **1** (1952) no. 4, 145.
[190] C. Bokhoven et al., *Catalysis 1954 – 1960* **3** (1955) 265.
[191] R. Brill, *J. Chem. Phys.* **19** (1951) 1047.
[192] S. Kiperman, V. S. Granovskaya, *Zh. Fiz. Khim.* **26** (1952) 1615.
[193] M. I. Temkin et al., *Kinet. Katal.* **4** (1963) 224.
[194] A. Ozaki et al., *Proc. R. Soc. London Ser. A* **258** (1960) 47.
[195] M. I. Temkin, N. M. Morozow, E. M. Shapatina, *Kinet. Catal. (Engl. Trans.)* **4** (1963) 565.
[196] ICI: *Catalyst Handbook with Special Reference to Unit Processes in Ammonia and Hydrogen Manufacture,* Wolfe Scientific Books, London 1970.
[197] K. Aika, A. Ozaki, *J. Catal.* **13** (1969) 232.
[198] A. Nielsen, J. Kjaer, B. Hansen, *J. Catal.* **3** (1964) 68.
[199] A. Ozaki, H. S. Taylor, M. Boudart, *Proc. R. Soc. London Ser. A* **258** (1960) 47.
[200] R. Brill, *J. Catal.* **16** (1970) 16.
[201] A. Cappelli, A. Collina, *Inst. Chem. Eng. Symp. Ser.* **35** (1972) 10.
[202] G. Buzzi-Ferraris et al., *Eng. Chem. Sci.* **29** (1974) 1621.
[203] U. Guacci et al., *Ind. Eng. Chem.* **16** (1977) 166.
[204] D. G. Dyson, J. M. Simson, *Ind. Eng. Chem. Fundam.* **7** (1968) 601.
[205] M. Bowker, I. Parker, K. Waugh, *Appl. Catal.* **14** (1985) 101.
[206] M. Bowker, I. Parker, K. Waugh, *Surface Science* **97** (1988) L 233.
[207] P. Stolze, J. K. Norskov, *Phys Rev. Let.* **55** (1985) 2502.
[208] P. Stolze, J. K. Norskov, *Surface Science* **189/190** (1987) 91; *Surface Science* **197** (1988) L 230; *J. Catal.* **110** (1988) 1.
[209] J. A. Dumesic, A. A. Trevino, *J. Catal.* **116** (1989) 119.
[210] P. Stolze, *Phys. Sci.* **36** (1987) 824.
[211] E. Wicke, *Z. Elektrochem.* **60** (1956) 774.
[212] A. Wheeler, *Adv. Catal.* **3** (1951) 249.
[213] T. Akehata et al., *Can. J. Chem. Eng.* **39** (1961) 127.
[214] C. Bokhoven, W. van Raayen, *J. Phys. Chem.* **58** (1954) 471.
[215] J. Hoogschagen, *Ind. Eng. Chem.* **47** (1955) 906.
[216] J. B. Hansen in A. Nielsen (ed.): *Ammonia – Catalysis and Manufacture,* Springer, Heidelberg 1995, p. 184.
[217] D. G. Dyson, J. M. Simon, *Ind. Eng. Chem. Fundam.* **7** (1968) 605.
[218] C. Chu, O. A. Hougen, *Chem. Eng. Sci.* **17** (1962) 167.
[219] C. P. P. Singh, N. D. Saraf, *Ind. Eng. Chem. Process Des. Dev.* **18** (1979) 364.
[220] A. Cappelli, A. Collina, *Inst. Chem. Eng. Symp. Ser.* **35** (1972) 10.
[221] C. Wagner, *Z. Phys. Chem. (Leipzig)* **193** (1943) 1.
[222] E. W. Thiele, *Ind. Eng. Chem.* **31** (1939) 916.
[223] J. Kjaer: *Calculation of Ammonia Converters on an Electronic Digital Computer,* Akademisk Forlag, Kopenhagen 1963.
[224] J. J. Hag, I. M. Palla, *Br. Chem. Eng.* **8** (1963) no. 3, 171.
[225] J. Kubec, J. Burianova, Z. Burianec, *Int. Chem. Eng.* **14** (1974) no. 4, 629.
[226] R. F. Baddour, R. L. T. Brian, B. A. Logeais, J. P. Eymery, *Chem. Eng. Sci.* **20** (1965) 281. R. L. T. Brian, R. F. Baddour, J. P. Eymery, *Chem. Eng. Sci.* **20** (1965) 297.
[227] M. J. Shah, *Ind. Eng. Chem.* **59** (1967) no. 1, 73.

[228] A. D. Stephens, *Chem. Eng. Sci.* **30** (1975) 11.
[229] L. D. Gaines, *Ind. Eng. Chem. Process. Des. Dev.* **16** (1977) no. 3, 381.
[230] T. Huberich, R. Krabetz in A. V. Slack (ed.): *Ammonia,* **part III,** Marcel Dekker, New York – Basel 1977.
[231] A. Mittasch: *Geschichte der Ammoniaksynthese,* Verlag Chemie, Weinheim 1951.
[232] A. Mittasch, *Adv. Catal.* **2** (1950) 82.
[233] C. Bosch, *Z. Elektrochem. Angew. Phys. Chem.* **24** (1918) 361.
[234] K. Aika, J. Yamaguchi, A. Ozaki, *Chem. Lett.* 1973, 161; cited in [102]
[235] S. R. Logan, C. Kemball, *Trans. Faraday Soc.* **56** (1960) 144.
[236] E. P. Perman, *Proc. R. Soc. London* **76** (1905) 167.
[237] F. Haber, G. von Oørdt, *Z. Anorg. Allg. Chem.* **43** (1905) 111.
[238] BASF, DE 249447, 1910.
[239] A. T. Larson, R. S. Tour, *Chem. Metall. Eng.* **26** (1922) 493, 555, 588, 647.
[240] J. A. Almquist, E. D. Crittenden, *Ind. Eng. Chem.* **18** (1926) 1307.
[241] G. L. Bridger et al., *Chem. Eng. Prog.* **43** (1947) 291.
[242] H. Hinrichs, *Br. Chem. Eng.* **12** (1967) 1745.
[243] Indianapolis Center for Advanced Research, US 4235749, 1980.
[244] Topsøe, GB 989242, 1961.
[245] P. D. Rabina et al., *Khim. Prom.* **5** (1969) 350.
[246] The Gas Council London, DE-OS 1931758, 1969 (T. Nicklin, D. Oyden).
[247] Chevron Res. Comp., US 3653831, 1972.
[248] J. L. Carter, C. G. Savini, US 3472794, 1969; SU 173204 (749 751) 23-4, 1961.
[249] The Lummus Comp., US 3992328, 1976; The Lummus Comp., US 3951862, 1976.
[250] Ammonia Casale, IT-A 47920 A, 1979.
[251] ICI, EP-A 7830276, 1979.
[252] Société Chimique de La Grande Paroisse, Azote et Produits Chimiques, US 3839229, 1974.
[253] A. Nielsen: "Ammonia Synthesis: Exploratory and Applied Research," *Catal. Rev. Sci. Eng.* **23** (1981) 17 – 51.
[254] D. C. Silverman, M. Boudart, *J. Catal.* **77** (1982) 208.
[255] C. Peters et al., *Z. Elektrochem.* **64** (1960) 1194.
[256] K. Schäfer, *Z. Elektrochem.* **64** (1960) 1190.
[257] P. H. Emmett, S. Brunauer, *J. Am. Chem. Soc.* **59** (1937) 310; *J. Catal.* **15** (1969) 90.
[258] S. Brunauer, P. H. Emmett, *J. Am. Chem. Soc.* **62** (1940) 1732.
[259] D. C. Silverman, Dissertation, Stanford University 1976.
[260] H. C. Chen, R. B. Anderson, *J. Colloid Interface Sci.* **38** (1972) 535; *J. Catal.* **28** (1973) 161.
[261] G. Ertl, N. Thiele, *Appl. Surf. Sci.* **3** (1979) 99.
[262] R. Hosemann, A. Preisinger, W. Vogel, *Ber. Bunsenges. Phys. Chem.* **70** (1966) 786. H. Ludwiszek, A. Preisinger, A. Fischer, R. Hosemann, A. Schönfel, W. Vogel, *J. Catal.* **51** (1977) 326.
R. Buhl, A. Preisinger, *Surf. Sci.* **47** (1975)344.
[263] W. S. Borghard, M. Boudart, *J. Catal.* **80** (1983) 194.
[264] R. Schlögl in J. R. Jennings (ed.): *Catalytic Ammonia Synthesis,* Plenum Press, New York – London 1991, pp. 19 – 108.
[265] C. Peters, K. Schäfer, R. Krabetz, *Z. Elektrochem.* **64** (1960) 1194.
[266] M. E. Dry, J. A. K. du Plessis, B. M. Leuteritz, *J. Catal.* **6** (1966) 194.
[267] R. Krabetz, C. Peters, *Angew. Chem. Int. Ed. Engl.* **4** (1965) 341.
[268] A. Kazusaka, I. Toyoshima, *Z. Phys. Chem. (Wiesbaden)* **128** (1982) 111.

[269] L. M. Dmitrenko et al., *Proc. Int. Congr. Catal. 4th 1968* **1** (1971) 404.

[270] K. Karaslavova, M. D. Anastasov, *Geterog. Katal. Tr. Mezhdunar. Simp. 3rd 1975,* 1978, 297.

[271] K. Z. Zakieva, P. D. Rabina, J. E. Zubova, I. E. Klaustova, N. Z. Pavlova, L. D. Kusnetzov, *Tr. Mosk. Khim. Tekhnol. Inst. im. D. I. Mendeleeva,* 1973, no. 73, 120.

[272] B. Aleksic, N. Jovanovic, A. Terlecki-Baricevic, *Geterog. Katal. Tr. Mezhdunar. Simp. 3rd 1975,* 1978, 147.

[273] M. G. Berengarten et al., *Kinet. Katal.* **15** (1974) 250.

[274] Yu. N. Artyukh, M. T. Rusov, N. A. Boldyreva, *Kinet. Katal.* **8** (1967) 1319.

[275] P. J. Smith, D. W. Taylor, D. A. Dowden, C. Kemball, D. Tayler, *Appl. Catal.* **3** (1982) 303.

[276] I. D. Kusnetsov, *Chem. Tech. (Leipzig)* **15** (1963) 211.

[277] J. Herrmann et al., *Chem. Tech. (Leipzig)* **18** (1966) 472.

[278] D. G. Ivanov, N. D. Anastasov, *Chem. Tech. (Leipzig)* **15** (1963) 229.

[279] L. Sokol, *Chem. Tech. (Leipzig)* **15** (1963) 214.

[280] U. Zardi, A. Antonini, *Nitrogen* **122** (1979) 33.

[281] M. C. Sze, *Hydrocarbon Process.* **56** (1977) no. 12, 127.

[282] N. Pernicone, G. Liberti, G. Servi in C. Eyraud, M. Escoubes (eds.): *Progress in Vacuum Mikrobalance Techniques,* **vol. 3,** Heyden, London 1975, p. 304.

[283] A. Mittasch, E. Keunecke, *Z. Elektrochem. Angew. Phys. Chem.* **38** (1932) 666.

[284] H. Uchida, I. Terao, K. Ogawa, *Bull. Chem. Soc. Jpn.* **37** (1964) 653.

[285] N. Pernicone, F. Traina: *Preparation of Catalysts,* **vol. 2,** Elsevier, Amsterdam 1979, p. 321.

[286] B. S. Clausen, S. Mørup, H. Tropsøe, R. Candis, E. J. Jensen, A. Baranski, A. Pattek, *J. Phys. (Orsay, Fr.)* **37** (1976) C6-245.

[287] P. D. Rabina, T. Y. Malysheva, L. D. Kusnetzov, V. A. Batyrev, *Kinet. Catal. (Engl. Transl.)* **11** (1970) 1030.

[288] A. Mittasch, E. Keunecke, *Z. Elektrochem. Angew. Phys. Chem.* **38** (1932) 666.

[289] R. Westrik, *J. Chem. Phys.* **21** (1953) 2049.

[290] M. E. Dry, L. C. Ferreira, *J. Catal.* **7** (1967) 352.

[291] F. Garbassi, G. Fagherazzi, M. C. Calcaterra, *J. Catal.* **26** (1972) 338.

[292] A. C. Turnock, H. P. Eugster, *J. Petrol.* **3** (1962) 533.

[293] R. Brill, *Allg. Prakt. Chem.* **17** (1966) 94.

[294] R. Hosemann et al., *Ber. Bunsenges. Phys. Chem.* **70** (1966) 769.

[295] L. v. Bogdandy et al., *Ber. Bunsenges. Phys. Chem.* **67** (1963) 958.

[296] N. Pernicone et al., *Catal. Proc. Int. Congr. 5th 1972* 1973, 1241.

[297] V. Solbakken, A. Solbakken, P. H. Emmett, *J. Catal.* **15** (1969) 90.

[298] K. C. Wough et al.: *Topics in Catalysis,* **vol. 1,** Baltzer AG, Basel 1994, p. 295–301.

[299] G. Ertl: "Zum Mechanismus der Ammoniaksynthese," *Nachr. Chem. Tech. Lab.* **31** (1983) no. 3, 178.

[300] Y. Sasa, M. Uda, I. Toyoshima, *Chem. Lett.* **no. 12,** 1982, 2011.

[301] S. K. Egeubaev et al., *Kinet. Katal.* **6** (1965) no. 4, 676; also see [9] and [269]

[302] M. M. Ivanov et al., *Kinet. Katal.* **9** (1968) 1239; **10** (1969) 349.

[303] J. G. Ommen et al., *J. Catal.* **38** (1975) 120.

[304] A. Ozaki et al., *Catal. Proc. Int. Congr. 5th 1972* **2** (1973) 1251.

[305] E. K. Enikeev, A. V. Krylova, *Kinet. Katal.* **3** (1962) 116; *Chem. Abstr.* **57** (1962) 7965.

[306] G. Ertl, M. Weiss, S. B. Lee, *Chem. Phys. Lett.* **60** (1979) 391.

[307] M. C. Tsai et al., *Surf. Sci.* **155** (1985) 387.

[308] J. A. Dumesic, Dissertation, Stanford University 1974.

[309] T. Yoshioka, J. Koezuka, I. Toyoshima, *J. Catal.* **14** (1969) 281.

[310] Y. E. Sinyak, Thesis, Inst. of Chemical Physics Akad. Sci. USSR, Moscow 1960; cited in [301]
[311] Haldor Topsøe, ZA 645279, 1964; also see [315]
[312] I. P. Nukhlenov et al., *J. Appl. Chem. USSR (Engl. Transl.)* **37** (1964) 248.
[313] V. N. Anokhin et al., *J. Appl. Chem. USSR (Engl. Transl.)* **35** (1962) 29.
[314] A. Baranski et al., *J. Catal.* **26** (1972) 286.
[315] V. Věk, *Chem. Ing. Tech.* **45** (1973) 608.
[316] K. Feind, *Chem. Ing. Techn.* **38** (1966) 1081.
[317] Chemie Linz, US 3965246, 1976.
[318] E. Comandini, A. Passariello, U. Zardi, *Ammonia Plant Saf.* **23** (1981) 44.
[319] Wargons Aktiebolag, Haldor Topsøe, US 3243386, 1961.
[320] Kuhlmann, GB 1080838, 1964.
[321] Kuhlmann, CH 434218, 1964.
[322] Haldor Topsøe, GB 989242, 1961.
[323] ICI, BE 576059, 1959.
[324] IG Farbenind., DE 748620, 1938.
[325] I. V. Nicolescu et al., *Genie Chim.* **82** (1959) 33.
[326] I. V. Nicolescu et al., *Chem. Tech. (Leipzig)* **15** (1963) 226.
[327] S.I.R.I. Societa Italiana Ricerche Industriali, US 4073749, 1978.
[328] ICI, GB 1484864, 1977.
[329] J. E. Jarvan, H. U. Larsen, unpublished work, (Haldor Topsøe A/S) cited in [253].
[330] A. T. Larson et al., *Chem. Trade J. Chem. Eng.* **100** (1937) 403.
[331] G. M. Schwab (ed.): *Handbuch der Katalyse,* **vol. 5: Heterogene Katalyse II,** Springer-Verlag, Wien 1957, p. 566.
[332] A. M. Rubinštejn et al., *Izv. Akad. Nauk SSSR Ser. Khim.* 1966, 1707; *Chem. Zentralbl.* 1968, 8–0639.
[333] A. M. Rubinštejn et al., *Kinet. Katal.* **6** (1965) 285; *Chem. Zentralbl.* 1965, 42–0622.
[334] P. Bussiere, R. Dutartre, G. A. Martin, J. P. Mathieu, *C. R. Hebd. Seances Acad. Sci. Ser. C* **280** (1975) 1133. R. Dutartre, M. Primet, G. A. Martin, *React. Kinet. Catal. Lett.* **3** (1975) 249.
[335] H. Topsøe, J. A. Dumesic, E. C. Derouane, B. S. Clausen, S. Mørup, J. Villadsen, N. Topsøe in: *Preparation of Catalysts,* **vol. 2,** Elsevier, Amsterdam 1979, p. 365.
H. Topsøe et al. in T. Seiyama, K. Tanabe (eds.), *New Horizons in Catalysis, Proc. Int. Congr. Catal. 7th 1980,* Elsevier 1981.
[336] M. Boudart, A. Delbouille, J. A. Dumesic,. S. Khammouna, H. Topsøe, *J. Catal.* **37** (1975) 486.
J. A. Dumesic, H. Topsøe, S. Khammouna, M. Boudart, *J. Catal.* **37** (1975) 503.
J. A. Dumesic, H. Topsøe, M. Boudart, *J. Catal.* **37** (1975) 513.
[337] The Lummus Comp., GB 1529823, 1978.
[338] IG Farbenind., DE 554855, 1928; FR 611139, 1935.
[339] N. W. Sseljakow, SU 48210, 1936; *Chem. Zentralbl.* **1937** II, 119.
[340] N. N. Pschenitzyn et al., *Zh. Prikl. Khim. (Leningrad)* **13** (1940) 76; *Chem. Zentralbl.* 1940, no. II, 1932.
[341] Österreichische Stickstoffwerke, AT 252957, 1964.
[342] M. V. Tovlin et al., *Kinet. Katal.* **7** (1966) 749; *Chem. Zentralbl.* 1966, 42–0597.
[343] H. Flood, D. G. Hill, *Z. Elektrochem.* **61** (1957) 18.
[344] J. Valcha, *Chem. Tech. (Leipzig)* **15** (1963) 222.
[345] Österreichische Stickstoffwerke, GB 833878, 1958.
[346] D. B. Christozvonov et al., *Int. Chem. Eng.* **9** (1969) 387.

[347] SU 169077, 1963.

[348] H. Uchida, N. Todo, *Bull. Chem. Soc. Jpn.* **29** (1956) 20; also see [346]

[349] Z. N. Bardik et al., *Khim. Promst. (Moscow)* **42** (1966) 351.

[350] CS 117658, 1966 (L. Sokol).

[351] P. A. Strelzov et al., *Khim. Promst. (Moscow)* **43** (1967) no. 1, 46.

[352] H. Amariglio, G. Rambeau, in G. C. Bond et al. (eds.): *Proc. Int. Congr. Catal. 6th 1976,* Chemical Society London 1977, p. 1113.

[353] T. L. Joseph, *Trans. AJME* **120** (1936) 72.

[354] P. K. Stangway, H. U. Ross, *Trans. AJME* **242** (1968) 1981.

[355] M. Moukassi et al., *Metall. Trans.* **B14** (1983) 125.

[356] Y. K. Rao et al., *Metall. Trans.* **B10** (1979) 243.

[357] J. O. Edström, *J. ISI* **175** (1953) 289.

[358] A. Baranski, M. Lagan, A. Pattek, A. Reizer, L. J. Christiansen, H. Topsøe in: *Preparation of Catalysts,* **vol. 2,** Elsevier, Amsterdam 1979, p. 353.

[359] O. Gramtica, N. Pernicone in: J. R. Jennings (ed.): *Catalytic Ammonia Synthesis,* Plenum Press, New York and London pp. 211–252.

[360] A. Baranski et al., *J. Catal.* **26** (1972), 286–294.

[361] A. I. Forster, B. J. Cromarty "Theory and practice of steam reforming" *ICI/Katalco/KTI, UOP 3rd Annual International Seminar of Hydrogen Plant Operation,* Chicago, USA (June 1995).

[362] J. R. Rostrup-Nielsen, "Catalytic steam reforming" in J. R. Anderson, M. Boudart (Eds.) *Catalytis, Science and technology,* Springer, Berlin (1984), pp. 1–130.

[363] L. Altrup, *Journal of Catalytis,* **109,** 241–251 (1988).

[364] A. Baranski et al., *Archivum Hutniktva* **25** (1980) 153.

[365] A. Baranski et al., *Appl. Catal.* **3** (1982) 207.

[366] A. Baranski et al., *Appl. Catal.* **19** (1985) 417.

[367] A. Pattek-Janczyk et al., *Appl. Catal.* **6** (1983) 35.

[368] J. A. Burnett et al., *Ind. Eng. Chem.* **45** (1953) 1678.

[369] R. Royen, G. H. Langhans, *Z. Anorg. Allg. Chem.* **315** (1962) 1.

[370] P. H. Emmett, S. Brunauer, *J. Am. Chem. Soc.* **52** (1930) 2682; **62** (1940) 1732.

[371] I. A. Smirnov et al., *Kinet. Katal.* **6** (1965) 351.

[372] I. A. Smirnov, *Kinet. Katal.* **7** (1966) 107.

[373] P. E. Højlund Nielsen, paper at the ACS meeting, Washington 1983.

[374] P. E. Højlund Nielsen inW. A. Nielsen (ed.): *Ammonia — Catalysis and Manufacture,* Springer-Verlag, Heidelberg 1995, pp. 191–199.

[375] P. E. Højlund Nielsen inJ. R. Jennings (ed.): *Catalytic Ammonia Synthesis,* Plenum Press, New York 1991, pp. 285–301.

[376] P. Stolze, *Phys. Sci.* **36** (1983) 824.

[377] P. Stolze, J. K. Nørskov, *J. Vac. Sci. Technol.* **A5** (1987) 581.

[378] T. Kirkerød, P. Skaugset, Abstracts of IV Nordic Symp. on Catalysts, Trondheim 1991.

[379] I. P. Sidorov, K. E. Istomina, *Chem. Abstr.* **54** (1960) 6049.

[380] H. Hinrichs, *Chem. Ing. Tech.* **40** (1968) 723.

[381] L. N. Marakhovets et al., *Izv. Vyssh. Uchebn. Zaved. Khim. Khim. Tekhnol.* **15** (1972) no. 5, 735.

[382] R. Brill et al., *Ber. Bunsenges. Phys. Chem.* **72** (1968) 1218.

[383] J. D. Bulatnikova et al., *Zh. Fiz. Khim.* **32** (1958) 2717.

[384] H. J. Hansen in V. Sauchelli (ed.): *Fertilizer Nitrogen, its Chemistry and Technology,* Reinhold Publ. Co., New York 1964.

[385] I. Dybkjaer, E. A. Gam, AIChE Symposium on Safety in Ammonia Plants, San Francisco, Calif., 1984; *Ammonia Plant Saf.* **25** (1985) 15.
[386] A. Ozaki, *Acc. Chem. Res.* **14** (1981) 16.
[387] F. Haber, *Z. Elektrochem.* **16** (1910) 244.
[388] A. Ozaki, K. Urabe, K. Shimazaki, S. Sumiya: *Preparation of Catalysts,* **vol. 2:** Scientific Basis for the Preparation of Heterogenous Catalysts, Elsevier, Amsterdam 1979, p. 381.
[389] British Petroleum Co., US 4163775, 1979.
[390] F. F. Gadallah et al. in G. Poncelet et al. (eds.): *Preparation of Catalysts,* **vol. 3,** Elsevier, Amsterdam 1983.
[391] GB 1 468 441, 1977.
[392] GB 174 079, 1985.
[393] D. J. Lowe, B. E. Smith, R. N. F. Thornely in. P. M. Harrison (ed.): *Metalloproteins,* **Part I.** Verlag Chemie 1985 p. 207.
[394] O. Glemser, *Naturwissenschaften* **37** (1950) 539.
[395] *Nitrogen* **193** (1991) 17–21.
[396] W. K. Taylor, S. A. Hall, D. G. Heath, ICI/CFDC Technical Symp., Shanghai 1989.
[397] J. P. Shirez, J. R. LeBlanc, Kellogg Ammonia Club Meeting, San Francisco 1989.
[398] T. A. Czuppon, S. A. Knez, 41th AIChE Ammonia Safety Symp., Boston 1996; *Ammonia Plant Saf.* **37** (1997) 34.
[399] A. V. Slack, G. Russel James (eds.): *Ammonia,* part I–IV, Marcel Dekker, New York 1973/74.
[400] S. Strelzoff: *Technology and Manufacture of Ammonia,* Wiley-Interscience, New York 1981.
[401] F. J. Brykowski (ed.): *Ammonia and Synthesis Gas,* Noyes Data Corp., Park Ridge, N.J., 1981, p. 280.
[402] I. Dybkjaer in W. A. Nielsen (ed.): *Ammonia — Catalysis and Manufacture,* Springer-Verlag, Heidelberg 1995, pp. 199–327.
[403] C. W. Hooper in J. R. Jennings (ed.): *Catalytic Ammonia Synthesis,* Plenum Press, New York 1991, pp. 253–283.
[404] M. Appl: *Ammonia, Methanol Hydrogen, Carbon Monoxide — Modern Production Technologies,* CRU, London 1997.
[405] D. Wagner, J. F. Meckel, K. H. Laue in A. I. More (ed.), *Proc. Br. Sulphur Corp. Int. Conf. Fert. Technol. 4th 1981* 1982, 471.
[406] *Nitrogen* 1975, no. 97, 35.
[407] T. Grundt, K. Christiansen in A. I. More (ed.), *Proc. Br. Sulphur Corp. Int. Conf. Fert. Technol. 4th 1981* 1982, 73.
[408] H. Wendt, *Chem. Ing. Tech.* **56** (1984) no. 4, 265.
[409] G. A. Crawford, S. Benzimra, *Fertilizer '85 Conference (British Sulphur),* London, Feb. 1985.
[410] The Ultimate in Ammonia/Urea Studies, Fertecon 1991.
[411] K. J. Mundo, *Chem. Ing. Tech.* **45** (1973) no. 10 a, 632.
[412] T. A. Czuppon, L. J. Buividas, *Hydrocarbon Process.* **58** (1979) no. 9, 197.
[413] J. Y. Livingston, *Hydrocarbon Process.* **50** (Jan. 1971) 126.
[414] H. W. Neukermans, J. P. Schurmans, 26th AIChE Symp. Saf. Ammonia Plants, Montreal 1981.
[415] B. W. Burklow, R. L. Coleman, 21st AIChE Ammonia Safety Symp., Atlantic City, 1976; *Ammonia Plant Saf.* **19** (1977) 21.
[416] M. H. Hyman, *Hydrogen Processing, 47, 7* (1968) 131.
[417] K. Atwood, C. B. Knight, *"Reforming Kinetics and Catalysis"* in V. A. Slack, G. Russel James, Ammonia, Marcel Dekker Inc, New York, 1973, 145–174.

[418] J. R. Rostrup-Nielsen, *Catalysts Today,* **19,** 305–324 (1993).

[419] B. J. Cromarty, "Carbon formation and removal in the primary reforming process", *ICI/ Katalco Technical papers, ICI Group 113W/075/2 CATPREF.*

[420] H. J. Renner, F. Marschner, G. Hochgesandt, "Gas Production" in Ullmann's Encyclopedia of Industrial Chemistry, VCH, Weinheim, **vol. A 12,** p. 190.

[421] Nitrogen **166** (1987) 24–31.

[422] K. Kochloefl, "Steam reforming" in *Handbook of Heterogeneous Catalysis* (ed. G. Ertl, H. Knörzinger, J. Weitkamp), VCH Weinheim, 1997, **vol. 4,** 1819–1931.

[423] J. M. Moe, E. R. Gerhard, *56th AIChE National Meeting,* Mai 1965, Preprint 36d.

[424] D. A. Lihou, *Chem. Process Engineering,* Sept. 1965, 487.

[425] G. W. Bridger, G. C. Chinchen, "Hydrocarbon Reforming Catalysts" in, *Catalysts Handbook,* Wolfe Scientific, London 1970, 82.

[426] M. Appl, H. Gössling, *Chem. Ztg,* **96** (1972), 135.

[427] British Patents 953877; 1 003 707; 1 040 066 (ICI).

[428] B. J. Cormarty, **Nitrogen '91:** "British Sulphur International Conference, Copenhagen (Jun 1991).

[429] *Nitrogen,* **232** (Mar-Apr 1998), 45.

[430] Nitrogen **214** (1995) 38–56.

[431] J. Thuillier, F. Pons, 22nd AIChE Ammonia Safety Symp., Aug 1977, Los Angeles; *Ammonia Plant Saf.* **20** (1978) 89.

[432] S. I. Ziolkowski, "Heat Flux and Pressure Drop", *in A. v. Slack, G. R. James (eds.), Ammonia,* Marcel Dekker, Inc. New York (1973), **Part I,** pp. 213–220.

[433] M. Leva, *Ind. Engng. Chem.* **39,** *(1947) 657.*

[434] J. Beck, Advances in Chemistry and Chemical Engineering, *3rd ed.,* Academic Press, New York (1962) p. 234.

[435] P. T. L. Brian, *AlChE J.,* **9,** 6 (1963).

[436] V. S. Beskovm V. P. Kuzin, M. G. Slinko, *Int. Chem. Engng. 5,* 2 (1965).

[437] S. Ergun, *Chem. Engng. Progress 48,* 2 (1952) 89.

[438] T. Kuen Yen, *Chem. Engng. Progress,* (March 1967) 173.

[439] B. J. Cromarty, "The use of computer simulations in primary steam reformers", *ICI Katalco Technical Paper.*

[440] F. C. Roesler, *Chem. Engng. Sci.,* 22 (1967) 1325.

[441] H. C. Hottel, E. S. Cohen, *AlChE Journ.* **4,** *1,* (1958) 3.

[442] H. C. Hottel, *J. Fuel 34,* (1961) 220.

[443] H. C. Hottel, A. F. Sarofim, *Int, J. Heat Mass Tranfer,* **8** (1965) 1153.

[444] I. Dybkjaer, *Fuel Processing Technology,* 42 (1995) 85–107.

[445] B. R. Fisher, "Failure mechanismus, Inspection techniques and repair methodes; ICI's reformer tube changing policy" *ICI Katalco Technical Papers 31 W/126/2/IMTOF.*

[446] G. Russel James, "Furnace Designs" in *A: V. Slack, G. Russel James (eds.): Ammonia,* **part I** *Marcel Dekker Inc,* New York 1973, 221–251.

[447] The Uhde Reformer, Uhde brochure Hi 118 1500 11/91.

[448] P. W. Farnell, R. J. Huges "Secondary Reforming: *Theory and Application", ICI Katalco, Technical papers, ICI Group 524/1270/0/SREF.*

[449] T. S. Christensen, I. Dybkaer, L. Hansen, I. I. Primdahl, 39th AIChE Ammonias Safety Symposium, October 3–6, 1994, Vancouver, BC, Canada; *Ammonia Plant Saf.* **35** (1995), 205.

[450] Nitrogen **217** (1995), 26–30.

[451] K. L. Blanchard, J. R. LeBlanc, 39th AIChE Ammonia Safety Symposium, October 3–6, 1994, Vancouver, BC, Canada; *Ammonia Plant Saf.* **35** (1995), 195.

[452] J. R. LeBlanc, R. V. Schneider, R. B. Strait, "Production of Methanol" in W.-H., Cheng, H.. H. Kung (Eds.): "Methanol Production and Use", Marcel Dekker, Inc., New York 1994, p. 91–93.

[453] P. W. Farnell, 38th AIChE Ammonia Safety Symposium, Sep. 1993, Orlando; *Ammonia Plant Saf.* **34** (1995).

[454] S. Wirtz, H. D. Marsch, M. Severin; *Nitrogen* **222** (1996) 33–35.

[455] J. M. Rhine, R. J. Tucker, "Modelling of Gas-Fired Furnaces and Boilers", McGraw-Hill in Associatione with British Gas plc London (1991), p. 191.

[456] L. Olsen, I. I. Primdahl, Institute of Energy Symposium on Modelling – Profitable Application to Industrial Processes, Birmingham, England, June 23, 1992.

[457] R. G. Cockerham, G. Percival, *Trans. Inst. Gas. Eng.* **107** (1957/58) 390/433.

[458] H. Jockel, B. E. Triebskorn, *Hydrocarbon Process.* **52** (1973) no. 1, 93.

[459] W. Rall, *Erdöl Kohle Erdgas Petrochem.* **20** (1967) no. 5, 351.

[460] H. Jockel, *GWF Gas Wasserfach* **110** (1969) no. 21, 561.

[461] T. Ishiguro, *Hydrocarbon Process.* **47** (1968) no. 2, 87.

[462] N N. Clark., W. G. S. Henson, 32rd AIChE Ammonia Safety Symp., Minneapolis; *Ammonia Plant Saf.* **28** (1987) 99.

[463] B. J. Cromatry, *Nitrogen* **191** (1991)30 – 34.

[464] R. Vannby, S. Winter-Madsen, 36th AIChE Ammonia Safety Symp., Nov. 1991, Los Angeles; *Ammonia Plant Saf.* **32** (1987) 122.

[465] B. J. Cromatry, B. J. Crewdson, *The Application of Pre-reforming in the Ammonia and Hydrogen Industries*, ICI Catalco Tech. Paper, 59W/0590/0/CAT2.

[466] K. Elkins, *Feedstock Flexibility Options*, ICI Catalco Tech. Paper, 313/035/0REF.

[467] P. W. Farnell, *Pre-Reforming — a Retrofit Case Study*, ICI Catalco Tech. Paper, 291W/025/0/IMTOF.

[468] W. D. Verduijn, 37th AIChE Ammonia Safety Symp., San Antonio 1992; *Ammonia Plant Saf.* **33** (1993) 165.

[469] S. E. Nielsen, I. Dybkaer, 41th AIChE Ammonia Safety Symp., Boston 1996; *Ammonia Plant Saf.* **37** (1997) 125.

[470] B. J. Cromarty, B. J. Crewdson, "The application of pre-reforming in the ammonia and hydrogen industries" ICI Katalco Technical Papers (59W/0590/0/CAT2).

[471] *Nitrogen* **178** (1989) 30 – 39.

[472] K. J. Elkins, I. C. Jeffery, D. Kitchen, A. Pinto, "Nitrogen '91", *International Conference (British Sulphur)*, Copenhagen, June 4 – 6, 1991.

[473] P. M. Armitage, J. Elkins, D. Kitchen, AIChE Ammonia Safety Symp., Los Angeles 1991; *Ammonia Plant Saf.* **32** (1992) 111.

[474] D. Kitchen, K. Mansfield, Eurogas 92, Trondheim 1992.

[475] R. Schneider, Kellogg Ammonia Club Meeting, San Diego 1990.

[476] J. R. LeBlanc, Asia Nitrogen: British Sulphur Intern. Conf., Singapore 1996.

[477] *Ammonia*, Kellogg brochure, HG 1/96.

[478] J. R. LeBlanc, R. Schneider, K. W. Wright, 40th AIChE Ammonia Safety Symp., Tucson [1995].

[479] M. W. Kellogg, EP-A 106076, 1983 (C. van Dijk et al.)

[480] M. Sosna, I. Bondar, B. Gunko, B. J. Grotz, 38th AIChE Ammonia Safety Symposium, Sep. 1993, Orlando, *Ammonia Plant Saf.* **34,** (1995).

[481] B. J. Grotz, Frankini, J. Magallenes, HTI Quaterly (Winter 94/95).

[482] *Nitrogen* **200** (1992) 39.

[483] *Nitrogen* **214** (1995) 38 – 56.

[484] R. Vannby, S. E. L. Winter Madsen "New developments in synthesis gas production", Topsoe company publication.

[485] H. D. Marsch, N. Thiagarajan, 33rd AIChE Ammonia Safety Symp., Denver 1988; *Ammonia Plant Saf.* **29** (1989) 195.

[486] H. J. Herbort, Uhde Ammonia Symp., Dortmund 1992.

[487] N. Thiagarajan, Uhde Ammonia Symp., Dortmund 1992.

[488] H. D. Marsch, N. Thiagarajan, 37th AIChE Ammonia Safety Symp., San Antonio 1992; *Ammonia Plant Saf.* **33** (1992) 108.

[489] *Chem. Eng. (N.Y.)* **73** (1966) 24.

[490] *Hydrocarbon Process.* **63** (1984) no. 4, 103.

[491] I. Dybkær, *Fuel Processing Technology* **42** (1995) 85 – 107.

[492] E. Bartholome, H. Nonnemacher, The Fifth World Petroleum Congress, May 1959..

[493] P. Degand, V. Julemont, J. P. Schurmans, 36th AIChE Ammonia Safety Symposium, Nov 1991 Los Angeles; *Ammonia Plant Saf.* **32** (1992) 129.

[494] *Nitrogen* **195** (1992) 22 – 36.

[495] T. Tomita, M. Kitugawa, *Chem. Ing. Tech.* **49** (1977) no. 6, 469.

[496] *Nitrogen* **144** (1983) 33.

[497] T. Tomita et al., Special Paper 9, 11th World Petroleum Congress, London 1983.

[498] *Nitrogen* **168** (1987) 29 – 37.

[499] *Nitrogen* **186** (1990) 21 – 30.

[500] O. J. Quartulli, *Hydrocarbon Process.* **44** (1965) no. 4, 151.

[501] J. Davies, D. A. Lihou, *Chem. Process Eng. (London)* **52** (1971) no. 4, 71.

[502] H. D. Marsch, H. J. Herbort, *Hydrocarbon Process.* **61** (1982) no. 6, 101.

[503] A. I. Forster, B. J. Cromatry, *The Theory and Practice of Steam Reforming,* ICI/Catalco/KTI/UOP, 3rd Int. Seminar on Hydrogen Plant Operation, Chicago 1995.

[504] G. W. Bridger, W. Wyrwas, *Chem. Process Eng. (London)* **48** (1967) no. 9, 101.

[505] F. Marschner, H. J. Renner, *Hydrocarbon Process.* **61** (1982) no. 4, 176.

[506] J. R. Rostrup-Nielsen, 17th AIChE Ammonia Safety Symp., Aug 1972, Minneapolis; *Ammonia Plant Saf.* **15** (1973) 82.

[507] G. W. Bridger, *Oil Gas J.* **74** (Feb. 16, 1976) 73; 20th AIChE Ammonia Safety Symp., Boston 1975; *Ammonia Plant Saf.* **18** (1976) 24. *Ammonia Plant Saf.* **18** (1976) 24.

[508] D. P. Rounthwaite, *Plant Oper. Prog.* **2** (1983) no. 2, 127.

[509] *Nitrogen* **174** (1988) 23 – 24.

[510] *Nitrogen* **166** (1987) 24 – 31.

[511] *Nitrogen* **167** (1987) 31 – 36.

[512] H. Fricke, *Chem. Ztg.* **96** (1972) 123.

[513] S. Strelzoff, *Hydrocarbon Process.* **53** (1974) no. 12, 79.

[514] E. Supp, M. Brejc, "Gas Production" in, Ullmann's Encyclopedia of Industrial Chemistry, VCH Weinheim, 5th edition, **vol. A 12,** p. 190.

[515] K. T. Lee "Partial oxidation of Hydrocarbons" in A. V. Slack, G. Russel James (ed) Ammonia, **Part I**, 293 – 294, Marcel Dekker, New York, 1973.

[516] Fertilizer Manual ed. by United Nations Industrial Development Organization (UNIDO), Vienna Austria and International Fertilizer Development Center (IFDC); Muscle Schoals, Alabama (USA) Klewer Academic Publishers, Dordrecht, The Netherlands, 1998.

[517] G. E. Weismantel, L. Ricci, *Chem. Eng. (N.Y.)* **86** (1979) no. 21, 57.

[518] Du Bois Eastman, "The production of synthesis gas by partial oxydation" *Fifth World Petroleum Congress, 1959, New York, Proceed, Section IV, p. 153–161.*
[519] S. C. Singer, L. W. Ter Har, *Cemical Engng. Progress,* **57,** 7 (1961), 68–74.
[520] "Shell gasification" *(Gas Processing Handbook) Hydrocarbon Processing,* **63** (4), 90 (1984).
[521] *Lurgi Gas Production Technology: The Shell Process* Lurgi comp. brochure 189e/6.92/2.20.
[522] C. Higmann, *Perspectives and Experience with Partial Oxidation of Heavy Residues,* Lurgi company brochure.
[523] *Hydrocarbon Process.* **63** (1984) no. 4, 90.
[524] *Integrated Gasification Combined Cycle Process,* Lurgi information paper, 1995.
[525] W. Liebner, N. Hauser, ERPI Conference on Power Generation and the Environment, London 1990.
[526] C. Higmann, G. Grünfelder, Conference on Gasification Power Plants, San Francisco 1984.
[527] W. Soyez, 33rd AIChE Ammonia Safety Symp., Denver 1988; *Ammonia Plant Saf.* **29** (1989) 19.
[528] G. J. van den Berg et al., *Hydrocarbon Process.* **45** (1966) no. 5, 193.
[529] L. W. ter Haar, *Ind. Chim. Belge* **33** (1968) 655.
[530] P. D. Becker et al., *Chem. Process Eng. (London)* **52** (1971) no. 11, 59.
[531] C. L. Reed, C. J. Kuhre, *Hydrocarbon Process.* **58** (1979) no. 9, 191.
[532] *Uhde's Design of the Texaco Oil Gasification,* Krupp – Uhde comp. brochure TOPG 2A/AB, 1995.
[533] *Hydrocarbon Process.* **58** (1979) no. 4, 168.
[534] H. Fricke, *Chem. Ztg.* **96** (1972) 123.
[535] E. Supp, M. Brejc, "Gas Production" in *Ullmann's Encyclopedia* of Industrial Chemistry, VCH Weinheim, **vol. A 12.**
[536] W. Liebner, *Tenth Refinery Technology Meeting,* February 11–13, Mumbay, India, 1998.
[537] R. Lohmüller, *Chem. Ing. Tech.* **56** (1984) no. 3, 203.
[538] C. I. Kuhre, C. I. Shearer, *Hydrocarbon Process.* **50** (1971) no. 12, 113.
[539] L. J. Buividas, J. A. Finneran, O. J. Quartulli, *Chem. Eng. Prog.* **70** (1974) no. 10, 21; *Ammonia Plant Saf.* **17** (1975) 4.
[540] *Nitrogen* **83** (1973) 40.
[541] C. P. Marion, J. R. Muenger, *Energy Prog.* **1** (1981) no. 1–4, 27.
[542] H. J. Madsack, *Hydrocarbon Process.* **61** (1982) no. 7, 169.
[543] *Nitrogen* **226** (1997) 47–56.
[544] *Nitrogen* **161** (1986) 23–27.
[545] E. Supp: *How to Produce Methanol from Coal,* Springer-Verlag, Heidelberg 1989.
[546] *Nitrogen* **126** (1980) 32–39.
[547] R. Reimert, G. Schaub, "Gas Production" in *Ullmann's Encyclopedia of Industrial Chemistry,* VCH Weinheim, **vol. A 12,** p. 214–236.
[548] *Nitrogen* **126** (1980) 32.
[549] L. J. Buividas, *Chem. Eng. Prog.* **77** (1981) no. 5, 44; *Ammonia Plant Saf.* **23** (1981) 67.
[550] *Ammonia from Coal,* Bull. Y-143, Tennessee Valley Authority, Muscle Shoals, Ala. 1979.
[551] D. A. Waitzman, *Chem. Eng. (N.Y.)* **85** (1978) 69.
[552] F. Brown, *Hydrocarbon Process.* **56** (1977) no. 11, 361.
[553] H. Teggers, H. Jüntgen, *Erdöl Kohle Erdgas Petrochem.* **37** (1984) no. 4, 163.
[554] V. Happe, "Partial Oxidation of Coal" in A. V. Slack, G. Russel James (eds) "Ammonia", **Part I,** 325–354, Marcel Dekker, New York, 1973.
[555] H. Staege, *Tech. Mitt. Krupp Werksber.* **40** (1982) no. 1, 1.

[556] *Hydrocarbon Process.* **63** (1984) no. 4, 94.

[557] H. J. Michaels, H. F. Leonard, *Chem. Eng. Prog.* **74** (1978) no. 8, 85.

[558] H. Staege, *Hydrocarbon Process.* **61** (1982) no. 3, 92.

[559] J. E. Franzen, E. K. Goeke, *Hydrocarbon Process.* **55** (1976) no. 11, 134.

[560] A. D. Engelbrecht, Tennessee Valley Authority Symposium in Muscle Shoals, Alabama 1979.

[561] *Nitrogen* 1985, no. 156, 35.

[562] H. Schmidt-Traub, H. C. Pohl, *Chem. Ing. Tech.* **55** (1983) no. 11, 850. *Hydrocarbon Process.* **63** (1984) no.no. 4, 95.

[563] W. L. E. Davey, E. L. Taylor, M. D. Newton, P. S. Larsen, P. S. Weitzel, Asia Nitrogen '98, Brit. Sulphur Internat. Conference, Kuala Lumpur, Feb. 22–24, 1998. Proceed. **vol. 2**, p. 165.

[564] T. W. Nurse, *5th International Symposium Large Chemical Plants,* Antwerpen 1982.

[565] B. Cornils et al., *Chem. Ing. Tech.* **52** (1980) no. 1, 12.

[566] *Hydrocarbon Process.* **63** (1984) no. 4, 97.

[567] W. Konkol et al., *Hydrocarbon Process.* **61** (1982) no. 3, 97.

[568] D. E. Nichols, P. C.Williamson in A. I. More (ed.), *Proc. Br. Sulphur Corp. Int. Conf. Fert. Technol. 4th 1981* 1982, 53.

[569] B. Cornils et al., *CEER Chem. Econ. Eng. Rev.* **12** (1980) no. 6–7, 7.

[570] E. T. Child, Tennessee Valley Authority Symposium in Muscle Shoals, Alabama 1979.

[571] B. Cornils et al., *Hydrocarbon Process.* **60** (1981) no. 1, 149.

[572] *Hydrocarbon Process.* **63** (1984) no. 4, 96.

[573] M. J. van der Burgt, *Hydrocarbon Process.* **58** (1979) no. 1, 161.

[574] C. A. Bayens, 36th AIChE Ammonia Safety Symposium, Los Angeles 1991; *Ammonia Plant Saf.* **32** (1992) 268.

[575] *Clean Coal Technology,* International Power Generation, 1990.

[576] M. J. van der Burgt, J. E. Naber, *Ind. Chem. Bull.* (1983) 104–105.

[577] J. N. Mahagaokar, J. N. Phillips, A. Kreweinghaus, 10th ERPI Conf. on Coal Gasification, 1986.

[578] T. J. Pollaert, *Chem. Eng. Prog.* **74** (1978) no. 8, 95.

[579] *Hydrocarbon Process.* **60** (1980) no. 11, 130.

[580] M. K. Schad, C. F. Hafke, *Chem. Eng. Prog.* **79** (1983) no. 5, 45.

[581] H. Hiller, *Erdöl Kohle Erdgas Petrochem.* **28** (1975) no. 2, 74.

[582] P. D. Becker, Tennessee Valley Authority Symposium in Muscle Shoals, Alabama 1979.

[583] W. Schäfer et al., *Erdöl Kohle Erdgas Petrochem.* **36** (1983) no. 12, 557.

[584] *Hydrocarbon Process.* **61** (1982) no. 4, 151.

[585] *Hydrocarbon Process.* **61** (1982) no. 4, 133.

[586] K. A. Theis, E. Nitschke, *Hydrocarbon Process.* **61** (1982) no. 9, 233. *Hydrocarbon Process.* **63** (1984) no. 4, 93.

[587] P. Speich, H. Teggers, *Erdöl Kohle Erdgas Petrochem.* **36** (1983) no. 8, 376.

[588] M. Appl: *Ammonia, Methanol Hydrogen, Carbon Monoxide – Modern Production Technologies, CRU London 1994,*4. Hydrogen, p. 102–115.

[589] "Wasserstofftechnologie – Perspektiven für Forschung und Entwicklung" (Hydrogen technology – Perspectives for research and development), Dechema 1985, p. 105–133 (ISBN 3-921567-69-6).

[590] G. Sandstede, *Chemie-Ingenieur Technik,* **61,** 5, 349–361, 1989.

[591] L. Bisset, *Chemical Engineering,* **84** (21), 177 (1977).

[592] D. J. Bogards, J. S. Campbell, "Design and operation of CO shift, naphtha and natural gas" in *A. V. Slack, G. Russel James (eds.): Ammonia, part II, Marcel Dekker Inc,* New York 1974, p. 25–71.

[593] G. W. Bridger, G. C. Chinchen, "Hydrocarbon Reforming Catalysts" in *Catalyst Handbook, Wolf Scientific Book, London 1970, 97–125.*

[594] L. Loyd, D. E. Riddler, M. W. Twigg, Catalyst Handbook (2nd ed.), ICI. *Wolf Publ. Ltd., London, 1989.*

[595] J. R. Jennings, M. W. Twigg, in "Selected developments in catalysis" (ed. j. R. Jennings), Blackwell Sci. Publ., Oxford 1985, chapt. 4, p. 102–127

[596] P. S. Pedersen, J. H. Carstensen, J. Boghild-Hansen, 34th AIChE Ammonia Safety Symp., San Francisco 1989; *Ammonia Plant Saf.* **30** (1990) 139.

[597] R. E. Stockwell, *FINDS* **vol. V,** n. 4, fourth quater, 1990, p. 22.

[598] S. J. Catchpole et al., *Modern Catalyst Systems for Increased Ammonia Production and Efficiency,* ICI Catalco Tech. Paper.

[599] M. Schneider, K. Kochloefl, J. Pohl, O. Bock, *Europ. Pat. Appl.* o 353 453, SÜD-CHEMIE AG, München, Germany, May 17, 1984.

[600] A. Tamaru, Y. Oshima, K. Honda, *German Pat. Appl.* DE 3 835 345 A 1 *Mitsubishi Kasai Co, Tokyo, Oct. 17, 1989.*

[601] A. Andreew, V. Idakiev, D. Mihajlova, D. Shopov, Appl. Catal., 1985, 22, 385–387.

[602] D. S. Newsome, Cat. Rev.-Sci. Eng., **21,** (1980) 275–318.

[603] K. Kochloefl, "Water gas shift and COS removal in *Handbook of Heterogeneous Catalysis (ed. G. Ertl, H. Knörzinger, J. Weitkamp), VCH Weinheim,* 1997, vol. 4, 1831–1843.

[604] G. C. Chinchen, *European patent application,* A 0 062410, 1982 (ICI).

[605] D. G. Rethwisch, J. A. Dumesic, *Appl. Catal.,* 1986, 21, 97–109.

[606] F. M. Gottschalk, R. g. Copperthwaite, M. van der Riet, G. J. Hutchings, *Appl. Catal.,* 1988, 381, 103–108.

[607] F. M. Gottschalk, R. g. Copperthwaite, G. J. Hutchings, *Appl. Catal.,* 1989, 51, 103–108.

[608] C. L. Thomas, "Catalytic processes and proven catalysts" Academic Press, New York 1970, p. 104–105.

[609] D. Allen "CO conversion catalyst" in *A. V. Slack, G. Russel James (eds.): Ammonia,* **part II,** Marcel Dekker Inc, New York 1974, p. 3–23.

[610] H. Bohlbro, "An investigation on the kinetics of the conversion of CO with H_2O over iron-based catalysts, 2nd ed. *Gjellerup, Copenhagen,* 1969.

[611] M. D. Ruthven, *Canad. Chem. Eng.,* 1969, 47, 327.

[612] G. C. Cinchen, R. H. Logan, M. S. Spencer, *Appl. Catal.,* 1984, 12, 69–89, 97–103.

[613] H. Brohlo, J. Catal., 1979, 3, 207.

[614] K. Atwood, M. R. Arnold, E. G. Appel, *Ind. Eng. Chem.,* 42, 1600 (1950).

[615] R. Habermehl, FINDS, Volume VIII, no 4, Fourth Quater 1993, 25.

[616] H. Roos, H. Wanjek, 34th AIChE Ammonia Safety Symp., San Francisco 1989; *Ammonia Plant Saf.* **30** (1990) 187.

[617] D. Kitchen, W. G. Henson, J. K. Madsen, 34th AlChE Ammonia Safety Symposium, San Francisco 1989, *Ammonia Plant Saf.,* **30** (1990), 105.

[618] D. Kitchen, A. Pinto, H. van Praag, 34th AlChE Ammonia Safety Symposium, San Francisco 1989, *Ammonia Plant Saf.,* **29** (1989), 212.

[619] J. R. Rostrup-Nielsen et al., 37th AIChE Ammonia Safety Symp., San Antonio 1992; *Ammonia Plant Saf.* **33** (1993).

[620] J. B. Hansen, P. S. Pedersen, J. H. Carstensen, 33rd AIChE Ammonia Safety Symp., Denver 1988; *Ammonia Plant Saf.* **29** (1989) 304.

[621] W. C. Lundberg, 23rd AIChE Ammonia Safety Symp., Miami Beach, 1978, *Ammonia Plant Saf.* **21** (1979) 105.

[622] P. W. Young, B. C. Clark, 17th AIChE Ammonia Safety Symp., Minneapolis 1972; *Ammonia Plant Saf.* **15** (1973) 18.

[623] I. Dybkjaer in A. I. More (ed.), *Proc. Br. Sulphur Corp. Int. Conf. Fert. Technol. 4th 1981* 1982, 503.

[624] T. Salmi, R. Hakkarainen, *Appl. Catal.*, 1989, 49, 285–306.

[625] T. van Herwijnen, W. A. De Jong J. Catal, 1980, 63, 83–93.

[626] R. Habermehl, *FINDS*, Volume VII, n. 4, fourth Quarter, 1992, p. 26.

[627] J. M. Stell et al., *The Operation of High, Low and Intermediate Temperature Catalysts*, ICI Catalco/KTI/UOP Hydrogen Plant Seminar, Chicago 1995.

[628] *Nitrogen* **232**, (1998), 47.

[629] J. Ilg, B. Kandziora, 41st AIChE Ammonia Safety Symp., Boston 1996; *Ammonia Plant Saf.* **37** (1997) 341.

[630] D. F. Balz, H. F. Gettert, K. H. Gründler, *Plant Oper. Prog.* **2** (1983) no. 1, 47.

[631] J. M. Moe, *Chem. Eng. Prog.* **58** (1962) no. 3, 33.

[632] *Nitrogen* **40** (1966) 28.

[633] A. P. Ting, Shen-Wu-Wan, *Chem. Eng. (N.Y.)* **76** (1969) no. 11, 185.

[634] J. F. Lombard, *Hydrocarbon Process.* **48** (Aug. 1969) 111.

[635] L. Lloyd, M. V. Twigg, *Nitrogen* **118** (1979) 30.

[636] *Nitrogen* **133** (1981) 27.

[637] P. N. Hawker, *Hydrocarbon Process.* **61** (1982) no. 4, 183.

[638] *Nitrogen* **226** (1997) 43–46.

[639] F. Lorenz, F. Wodtke, F. L. Ebenhoech, E. Giesler, H. Kirner, *German Pat*, 1 667 386, BASF AG, April 15, 1967..

[640] W. Auer, *Erdöl Kohle Erdgas Petrochem.* **24** (1971) 145.

[641] *Hydrocarbon Process.* **61** (1982) no. 4, 154.

[642] I. Dybkjaer, H. Bohlbro, 23rd AIChE Ammonia Safety Symp., Maiami Beach 1978; *Ammonia Plant Saf.* **21** (1979) 145.

[643] BASF, DE-AS 1250792, 1959.

[644] I. Dybkjaer, in: *Ammonia from Coal Symposium*, TVA Muscle Schoals Alabama, USA p. 133.

[645] C. L. Aldridge, T. Kalina *German Pat*, 2 054 946, Exxon research and engineering Co, Linden, USA November 7, 1971.

[646] J. S. Merriam, C. B. Hoog, *US Patent.* 253 941, United Catalysts Inc., Louisville, USA April 14 1981; *Europ. Pat. Appl.* 0 062 912, April 8, 1982.

[647] H. Schäfer, *FINDS*, **vol. VII,** no 4, Fourth Quater, 1992.

[648] P. Hou, D. Mecker, H. Wiese, J. Catal. 1983, 80, 280–285.

[649] V. Berispeck, "Studies on an alkali-impregnated Co-Mo catalyst for water gas shift conversion and methanation", *M. S., Thesis, Virginia Polytechnic Institute and State University, Blacksburg, VA*, USA, 1975.

[650] "Carbon monoxide production technologies", *KTI Newsletter* (Winter 1987).

[651] K. J. Stokes, *Nitrogen* **131** (1981) 35. K. J. Stokes in A. I. More (ed.): *Proc. Br. Sulphur Corp. Int. Conf. Fert. Technol. 4th 1981* 1982, 525.

[652] K. F. Butwell et al., *Chem. Eng. Prog.* **69** (1973) no. 2, 57–61.

[653] *Nitrogen* **96** (1975) 33.

[654] *Nitrogen* **102** (1976) 40.
[655] K. F. Butwell, D. J. Kubek, P. W. Sigmund, 23th AIChE Ammonia Safety Symp., Miami Beach, 1978; *Ammonia Plant Saf.* **21** (1979)156; *Chem. Eng. Prog.* **75** (1979) no. 2, 75. K. F. Butwell, D. J. Kubek, *Hydrocarbon Process.* **56** (1977) no. 10, 173.
[656] J. R. Fair, D. E. Steinmeyer, W. R. Penney, B. B. Crocker, "Gas Absorption and Gas-Liquid System Design", in R: H. Perry, D. W. Green, J. O. Maloney (eds.) "Perry's Chemical Engineering Handbook ", MacGraw-Hill, New York, International edition, 1997, pp. 14-1ff.
[657] H. E. Benson, R. W. Parrish, *Hydrocarbon Process.* **53** (1974) no. 4, 81.
[658] H. E. Benson in A. V. Slack, G. J. James (eds.): *Ammonia,* **part II,** Marcel Dekker, New York 1974, p. 159.
[659] B. S. Grover, E. S. Holmes: "Nitrogen 86," *Br. Sulphur Conf.,* Amsterdam 1986, Proceedings of the Conf., p. 101.
[660] R. K. Bartoo, S. J. Ruzicka: "Fertilizer '83," *Br. Sulphur Corp. 7th Int. Conf.,* London 1983, Proceedings of the Conf., p. 129.
[661] US 4035 166, 1977 (F. C. van Hecke).
[662] L. C. Crabs, R. Pouillard, F. C. van Hecke, 24th AIChE Ammonia Safety Symp., San Francisco 1989; *Ammonia Plant Saf.* **22** (1980) 185.
[663] *Hydrocarbon Process.* **61** (1982) no. 4, 95 – 102.
[664] R. N. Maddox, M. D. Burns, *Oil Gas J.* **66** (1968) no.4 91.
[665] G. Giammarco, in A. V. Slack (ed.): *Ammonia,* **part II,** Marcel Decker New York 1974, p. 171.
[666] L. Tomasi, *Nitrogen* **199** (1992) 35.
[667] *Hydrocarbon Process.* **63** (1984) no. 4, 57 – 64.
[668] A. G. Eickmeyer in A. V. Slack, G. J. James (eds.): *Ammonia,* **part II,** Marcel Dekker, New York 1974.
[669] *Nitrogen* **180** (1989) 20 – 30.
[670] C. C. Song et al., 36th AIChE Ammonia Safety Symp., Los Angeles 1991; *Ammonia Plant Saf.* **32** (1992) 187.
[671] S. Linsmayer, *Chem. Tech. (Leipzig)* **24** (1972) no. 2, 74.
[672] K. Elberling, W. Gabriel, *Chem. Tech. (Leipzig)* **29** (1977) no. 1, 43.
[673] T. M. Gemborys, 39th AIChE Ammonia Safety Symp., Vancouver 1994.
[674] M. J. Mitariten, C. M. Wolf, T. J. DePaola, ICI Catalco/UOP Hydrogen Plant Seminar, Chicago 1995.
[675] P. Clough: "Asia Nitrogen," *Br. Sulphur Conf.,* Bali 1994, Proceedings of the Conf., p. 191 – 193.
[676] J. N. Iyengar, D. E. Keene, 38th AIChE Ammonia Safety Symp., Orlando 1993; *Ammonia Plant Saf.* **34** (1994).
[677] US 4702 898 (B. S. Grover).
[678] R. K. Bartoo, T. M. Gemborys: "Nitrogen 91," *Br.Sulphur Conf.,* Copenhagen 1991, Proceedings of the Conf., p. 127 – 139.
[679] R. K. Bartoo, *Removing Acid gas by the Benfield Process,* UOP Comp brochure, GP 5132–1M-11/93.
[680] R. K. Bartoo, *Chem. Eng. Prog.* **80** (1984) no. 10, 35
[681] *Nitrogen* **229** (Sep.-Oct 1997), 37–52.
[682] A. G. Eickmeyer, "Catacarb" in *A. V. Slack, G. Russel James (eds.): Ammonia,* **part II,** Marcel Dekker Inc, New York 1974, p. 165–169.

[683] G. Giammarco, "Giammarco-Vetrocoke" in *A. V. Slack, G. Russel James (eds.): Ammonia,* **part II,** Marcel Dekker Inc, New York 1974, p. 171–182.
[684] R. E. Meissner, U. Wagner, *Oil Gas J.* **81** (Feb. 7, 1983) 55.
[685] K. Volkamer, E. Wagner, F. Schubert, *Plant Oper. Prog.* **1** (1982) no. 2, 134.
[686] K. Volkamer, U. Wagner: "Fertilizer '83," *Br. Sulphur Corp. 7th Int. Conf.,* London 1983, Proceedings of the Conf., p. 139.
[687] W. Gerhard, W. Hefner, 33rd AIChE Ammonia Safety Symp., Denver 1988; *Ammonia Plant Saf.* **29** (1989) 73.
[688] D. W. Stanbridge, Y. Ide, W. Hefner, AIChE Ammonia Safety Symp., Anaheim 1984.
[689] R. Welker, R. Hugo, R. Meissner, 41st AIChE Ammonia Safety Symp., Boston 1996; *Ammonia Plant Saf.* **37** (1997) 330.
[690] R. Welker, R. Hugo, B. Büchele: "Asia Nitrogen 96", Singapore 1996.
[691] G. Ripperger, J. C. Stover, AIChE Spring National Meeting, Boston 1996.
[692] J. E. Nobles, N. L. Shay: "Nitrogen 88," *Br. Sulphur Int. Conf.,*Geneva 1988.
[693] W. Hefner, R. E. Meissner, 37th AIChE Ammonia Safety Symp., San Antonio 1992; *Ammonia Plant Saf.* **33** (1993) 101.
[694] D. K. Judd, *Hydrocarbon Process.* **57** (1978) no. 4, 122.
[695] C. G. Swanson, 23th AIChE Ammonia Safety Symp., Miami Beach, 1978; *Ammonia Plant Saf.* **21** (1979)152.
[696] C. G. Swanson, F. C. Burkhard, 23th AIChE Ammonia Safety Symp., Denver 1983; *Ammonia Plant Saf.* **24** (1984) 16.
[697] V. A. Shah, *Energy Progress* **8** (1988) 67–70.
[698] R. J. Hernandez, T. L. Huurdemann: "Nitrogen 88," *Br. Sulphur Int. Conf.,* Geneva 1988.
[699] T. L. Huurdemann, V. A. Shah, 34th AIChE Ammonia Safety Symp., San Franzisco 1989.
[700] V. A. Shah, *Hydrocarbon Process.* **67** (1988).
[701] R. J. Hernandez, T. L. Huurdemann, *Chem. Eng.* **5** (1989) 154–156.
[702] *Fertilizer Focus* **5** (1988) 27.
[703] G. C. Swanson, 23rd AIChE, Ammonia Safety Symposium, Miami Beach Nov. 1978; *Ammonia Plant Saf.* **21** (1979), 152.
[704] J. L. Lewis, H. A. Truby, M. B. Pascoo, *Hydrocarbon Process.* **58** (1979) no. 4, 112.
[705] R. W. Bucklin, R. L. Schendel, *Energy Progr.* **4** (1984) no.3, 137.
[706] J. L. Lewis, H. A. Truby, M. B. Pasco, *Oil Gas J,* 72 (June 24, 1974) 120.
[707] B. Sehrt, P. Polster, *Chem. Tech. (Leipzig)* **32** (1980) no. 7, 345.
[708] T. P. Cook, "Fluor", in *A. V. Slack, G. Russel James (eds.): Ammonia* **part II,** Marcel Dekker Inc, New York 1974, p. 249–252.
[709] "Schwefel-Rückgewinnung", in *Lurgi company brochure* 1542d/5.94/3.10.
[710] "Sulfur", Ullmann, Sed., vol 25, pp. 523–525.
[711] *The Rectisol Process for Gas Purification,* Lurgi brochure 1676 e/5.95/10.
[712] *Rectisol for Gas Treating,* Lurgi Express Information O 1051/12.72.
[713] G. Ranke, Linde Berichte aus Wissenschaft und Technik.
[714] H. Haase, *Chem. Anlagen Verfahren* **10** (1970) 59.
[715] W. Linde, G. Ranke, H. Jungfer: "Rectisol" in A. V. Slack, G. J. James (eds.): *Ammonia* **part II** Marcel Dekker, New York 1974 p. 233–241.
[716] M. Kriebel, "Gas Production" in *Ullmann's Encyclopedia of Industrial Chemistry,* VCH, Weinheim, **vol. A 12,** p. 207, 262–264.
[717] L. W. Dailey, "Purisol" in *A. v. Slack, G. Russel James (eds.): Ammonia,* **part II,** Marcel Dekker Inc, New York 1974, p. 243–248.

[718] M. Kriebel, "Gas Production" in *Ullmann's Encyclopedia of Industrial Chemistry,* VCH, Weinheim, **vol. A 12,** p. 257.

[719] J. P. Klein, *Erdöl Kohle Erdgas Petrochem.* **23** (1970) no. 2, 84.

[720] H. W. Schmidt, H. J. Henrici, *Chem. Ztg.* **96** (1972) no. 3, 154.

[721] K. E. Zarker, "Sufinol" in A. V. Slack, G. Russel James (eds.): *Ammonia,* **part II,** Marcel Dekker Inc, New York p. 219–232.

[722] M. Kriebel, "Gas Production" in *Ullmann's Encyclopedia of Industrial Chemistry,* VCH, Weinheim, **vol. A 12,** p. 261–262.

[723] K. J. Stokes, 24th AIChE Ammonia Safety Symp., San Francisco, 1979; *Ammonia Plant Saf.* **22** (1980)178.

[724] B. G. Goar, *Oil Gas J.* **69** (July 12, 1971) 75.

[725] A. L. Kohl, F. C. Riesenfeld: *Gas Purification,* Gulf Publ. Co., Houston, Tex. 1979.

[726] G. Hochgesand, *Chem. Ing. Techn.* **40** (1968) 43; *Ind. Eng. Chem.* **62** (1970), 7–37.

[727] S. Strelzoff, *Chem. Eng. (N.Y.)* **82** (1975) no. 19, 115.

[728] D. Werner, *Chem. Ing. Techn.* **53** (1981) no. 2, 73.

[729] K. G.Christensen, *Hydrocarbon Process.* **57** (1978) no. 2, 125.

[730] H. Thirkell in A. V. Slack, G. Russel James (eds.): *Ammonia,* **part II,** Marcel Dekker, New York 1974, p. 117.

[731] S. Strelzow: *Technology and Manufacture of Ammonia,* Wiley, New York 1981, p. 193.

[732] F. C. Brown, C. L. Leci, *Proc. Fertilizer Soc.* **210** (1982) 1.

[733] *Nitrogen* **180** (1989) 20.

[734] H. W. Schmidt, *Chem. Ing. Tech.* **40** (1968) 425.

[735] D. W. Allen, W. H. Yen, 17th AIChE Ammonia Safety Symp., Minneapolis, August 1972; *Ammonia Plant Saf.* **15** (1973) 96.

[736] A. J. M. Janssen, N. Siraa, J. M. Blanken, 25th AIChE Ammonia Safety Symp., Portland, 1980; *Ammonia Plant Saf.* **23** (1981)19.

[737] H. Y. Allgood, "Copper liquid scrubbing" in *A. V. Slack, G. Russel James (eds.): Ammonia* **part II,** Marcel Deckker Inc, New York 1974, p. 289–309.

[738] B. J. Cromarty, "Methanotor catalyst and operation" ICI Katalco Technical Paper, ICI Group 385W/126/0/METH.

[739] *Chemical Economy and Engineering Review,* **12** no.(6–7), 33–36, (Jun/Jul 1980).

[740] C. M. Buckthorp, *Nitrogen* **113** (1978) 34.

[741] *Nitrogen* **123** (1980) 39.

[742] J. C. Bonacci, T. G. Otchy, 22th AIChE Ammonia Safety Symp., Denver, 1977; *Ammonia Plant Saf.* **20** (1978) 165.

[743] J. H. Colby, G. A. White, P. N. Notwick, 23th AIChE Ammonia Safety Symp., Miami Beach 1978; *Ammonia Plant Saf.* **21** (1979)138.

[744] *Nitrogen* **197** (1992) 18–25.

[745] P. Soregaard-Andersen, O. Hansen, 36th AIChE Ammonia Safety Symp., Los Angeles 1991. *Ammonia Plant Safety* **32** (1992), 177.

[746] *Nitrogen* **217** (1995) 41–48.

[747] US 3442 613, 1969 (B. J. Grotz).

[748] *Nitrogen* **144** (1983) 30.

[749] B. J. Grotz, *Nitrogen* **100** (1976) 30.

[750] *Nitrogen* **182** (1989).

[751] B. J. Grotz, G. Good, *(1980) Chem. Age* (London) (November, 14), 18.

[752] C. K. Wilson et al., *Nitrogen* **151** (1984) 31.

[753] B. I. Grotz, *Hydrocarbon Process.* **46** (1967) no. 4, 197.

[754] W. Scholz, *DECHEMA-Monogr.* **58** (1968) 31.

[755] W. Förg, *Chem. Anlagen + Verfahren* 1970 no. (March), 33.

[756] *Nitrogen* **95** (1975) 38.

[757] S. Haseba et al., 10th AIChE Ammonia Safety Symp., Minneapolis 1965; *Ammonia Plants* **8** (1966) 14.

[758] S. R. Krolikowski, *Chem. Eng. (London)* 1965 no. 186, 40.

[759] F. Corr, F. Dropp, E. Rudelstorfer, *Hydrocarbon Process.* **58** (1979) no. 3, 119.

[760] D. H. Werner, G. A. Schlichthärle, 24th AIChE Ammonia Safety Symp., Minneapolis san Francisco, November 1979; *Ammonia Plant Saf.* **22** (1980) 12.

[761] *Nitrogen* **121** (1979) 37.

[762] J. L. Heck, *Oil Gas J.* **78** (Feb. 11, 1980) 122.

[763] P. Taffe, J. Joseph, *Chem. Age* 1978 (October) 14.

[764] P. R. Savage, *Chem. Eng. (N.Y.)* **82** (1978) no. 25, 68D.

[765] R. Rehder, P. Stead, FAI Seminar 1985, The Fertilizer Association of India, New Dehli, Tech II-2/1.

[766] W. F. van Weenen, J. Tielroy, *Nitrogen* **127** (1980) 38.

[767] *Oil Gas J.* **19** (1981) 270.

[768] W. F. van Weenen, J. Tielroy, *Chem. Age India* **31** (1980) no. 12, Dev-2/1.

[769] J. Voogd, FAI Seminar 1985, The Fertilizer Association of India, New Dehli, Tech 11–1/1.

[770] D. J. Carra, R. A. McAllister, *Chem. Eng. (N.Y.)* **70** (1963) 62.

[771] "Compressors" in *Encyclopedia of Chemical Engineering,* **vol. 10**, Marcel Dekker, New York 1979, 157–409.

[772] E. E. Ludwig, "Compressors" in *Applied Design for Chemical and Petrochemical Plants,* **vol. 3** , Gulf. Houston, 1983, pp. 251–396.

[773] C. A. Vancini: *La Sintesi dell Amoniaca,* Hoepli, Milano 1961, p. 497.

[774] J. L. Kennedy, *Oil Gas J.* **65** 1967, no. 46, 105; no. 48, 95; no. 1, 72; no. 51, 76. *Oil Gas J.* **66** 1968, no. 4, 76.

[775] G. P. Williams, W. W. Hoehing, *Chem. Eng. Prog.* **79** (1983) no. 3, 11.

[776] G. A. J. Begg, *Chem. Process Eng. (London)* **49** (1968) no. 1, 58.

[777] F. Fraschetti et al., *Quad. Pignone* 1967, no. 9, 5.

[778] *Chem. Eng. (N.Y.)* **73** (1966) no. 9, 126.

[779] P. Kerklo, *Hydrocarbon Process.* **61** (1982) no. 10, 112.

[780] H. Strassmann, Uhde Ammonia Symp., Dortmund 1992.

[781] C. Dickinson, *Why dry running gas seals?* J. Crane Inc. Comp. Publ.

[782] W. Koch, *Dry Gas Seal – Principles – Capabilities – Application,* J. Crane Inc. Comp. Publ.

[783] S. Gray, B. Baxter, G. Jones, "Magnetic Bearings can Increase Availability, Reduce Oil and Maintenance Costs," Power Engineering, 1990.

[784] R. R. Poricha, D. G. Rao, *Technology (Sindri, India)* **3** (1966) 96.

[785] H. Förster, *Chem. Tech. (Leipzig)* **23** (1971) 157.

[786] *Hydrocarbon Process. Pet. Refiner* **45** (1966) no. 5, 179.

[787] *Eur. Chem. News* **11** (1967) no. 270, 26.

[788] W. Plötner, *Chem. Tech. (Leipzig)* **24** (1972) 324.

[789] A. F. Wilck, *Energy Tech.* **23** (1971) no. 5, 161.

[790] I. M. Kalnin, *Luft Kältetech.* **8** (1972) no. 3, 142.

[791] W. L. Luther, *Ingenieur Digest* **10** (1971) no. 1, 60.

[792] H. E. Gallus, *Brennst. Wärme Kraft* **23** (1971) no. 4, 172.

[793] F. Fraschetti, U. Filippini, P. L. Ferrara, *Quad. Pignone* **9** (1967) 5.

[794] G. A. J. Begg, *Chem. Proc. Eng. (London)* **49** (1968) no. 1, 58.

[795] A. Vitti, *Het Ingenieursblad* **40** (1971) 619.

[796] P. L. Ferrara, A. Tesei, *Quad. Pignone* **25** (1978) 131.

[797] J. Salviani et al., in A. V. Slack, G. Russel James (eds.): *Ammonia,* **part III**, Marcel Dekker, New York 1974, p. 7.

[798] *Nitrogen* **55** (1968) 37.

[799] S. Labrow, *Chem. Proc. Eng.* (London) **49** (1968) no. 1, 55.

[800] H. Foerster, *Chem. Technol.* **23** (1971) 93.

[801] H. Foerster, *Chem. Technol.* **23** (1971) 157.

[802] W. Plötner, *Chem. Technol.* **24** (1972) 324.

[803] *Nitrogen* **181** (1981) 23.

[804] S. D. Caplow, S. A. Bresler, *Chem. Eng.* (New York) **74** (1967) no. 7, 103.

[805] F. Fraschetti, P. L. Ferrara, U. Philippini, "Centrifugal compressor arrangement and drive systems" in A. V. Slack, G. Russel James (eds.): *Ammonia* **part III**, Marcel Dekker Inc, New York 1977, p. 11–45.

[806] H. B. Hile, "Large ammonia plant centrifugal compressor operation" in *A. V. Slack, G. Russel James (eds.): Ammonia* **part III**, Marcel Dekker Inc, New York 1977, p. 47–54.

[807] K. J. Stokes, *Chem. Eng. Prog.* **75** (1979) no. 7, 88.

[808] GB 1134 621, 1968 (D. R. Twist, D. W. Stanbridge).

[809] S. Ujii, M. Ikeda, *Hydrocarbon Process.* **60** (1981) no. 7, 94.

[810] W. Rall, 35th AIChE Ammonia Safety Symp., San Diego 1990, *Ammonia Plant Saf.* **31** (1991), 247.

[811] H. Uchida, M. Kuraishi, *Bull. Chem. Soc. Jpn.* **23** (1955) 106.

[812] R. F. Baddour et al., *Chem. Eng. Sci.* **20** (1965) 281.

[813] C. van Heerden, *Ind. Eng. Chem.* **45** (1953) 1242.

[814] H. Inoue, T. Komiya, *Int. Chem. Eng.* **8** (1968) no. 4, 749.

[815] H. Bakemeier et al., *Chem. Ing. Tech.* **37** (1965) 427.

[816] I. Porubszky et al., *Br. Chem. Eng.* **14** (1969) no. 4, 495.

[817] F. Horn, *Chem. Ing. Tech.* **42** (1970) no. 8, 561.

[818] V. Hlavacek, *Ind. Eng. Chem.* **62** (1970) no. 7, 8.

[819] J. Kjaer: *Measurement and Calculation of Temperature and Conversion in Fixed-bed Catalytic Reactors,* Gjellerup, Kopenhagen 1958.

[820] G. F. Froment, *Chem. Ing. Tech.* **46** (1974) no. 9, 374.

[821] J. E. Jarvan, *Ber. Bunsenges. Phys. Chemie* **74** (1970) no. 2, 74.

[822] J. Kjaer, Computer Methods in Catalytic Reactor Calculations, Haldor Topsøe, Vedaek 1972.

[823] J. E. Jarvan, *Oil Gas J.* **76** (1978) no. 5, 178.

[824] J. E. Jarvan, *Oil Gas J.* **76** (1978) no. 3, 51.

[825] C. P. P. Singh, D. N. Saraf, *Ind. Eng. Chem. Process Des. Dev.* **18** (1979) no. 3, 364.

[826] J. Simiceanu, C. Petrila, A. Pop, *Chem. Tech.* (Leipzig) **35** (1983) no. 12, 628.

[827] K. Lukas, D. Gelbin, *Chem. Eng.* (London) **7** (1962) 336.

[828] M. J. Shah, *Ind. Eng. Chem.* **59** (1967) 72.

[829] L. D.Gaines, *Ind. Eng. Chem. Process Des. Dev.* **18** (1979) no. 3, 381.

[830] L. D. Gaines, *Chem. Eng. Sci.* **34** (1979) 37.

[831] K. V. Reddy, A. Husain, *Ind. Eng. Chem. Process Des. Dev.* **21** (1982) no. 3, 359.

[832] L. M. Shipman, J. B. Hickman, *Chem Eng. Progr.* **64** (1968) 59.

[833] R. F. Baddour et al., *Chem. Eng. Sci.* **20** (1965) 281.

[834] P. L. Brian, R. F. Baddour, J. P. Emery, *Chem. Eng. Sci.* **20** (1965) 297.
[835] G. A. Almasy, P. Jedlovsky, *Chem. Eng.* (London) **12** (1967) 1219.
[836] I. Porubsky, E. Simonyi, G. Ladanyi, *Chem. Eng.* (London) **14** (1969) 495.
[837] A. Murase, H. L. Roberts, A. O. Converse, *Ind. Eng. Chem. Process Des. Dev.* **9** (1970) 503.
[838] D. Balzer et al., *Chem. Technik* (Leipzig) **23** (1971) 513.
[839] D. R. Levin, R. Lavie, *Ind. Chem. Symp. Ser.* **87** (1984) 393.
[840] A. Nielsen: *Advances in Catalysis,* **vol. V**, Academic Press, New York 1953, p. 1.
[841] H. Hinrichs, J. Niedetzky, *Chem. Ing. Tech.* **34** (1962) 88.
[842] L. Fodor, *Chim. Ind. Genie Chim.* **104** (1971) 1002.
[843] *Nitrogen* **140** (1982) 30.
[844] U. Zardi, *Hydrocarbon Process.* **61** (1982) no. 8, 129.
[845] J. J. Hay, I. M. Pallai, *Br. Chem. Eng.* **8** (1963) 171.
[846] P. L. T. Brian et al., *Chem. Eng. Sci.* **20** (1965) 297.
[847] W. Hennel, *Chem. Tech. (Leipzig)* **15** (1963) 293.
[848] L. B. Hein, *Chem. Eng. Prog.* **48** (1952) no. 8, 412.
[849] N. S. Zayarnyi, *Int. Chem. Eng.* **2** (1962) no. 3, 378.
[850] A. Murase et al., *Ind. Eng. Chem. Process Des. Dev.* **9** (1970) no. 4, 503.
[851] J. B. Allen, *Chem. Process Eng. (London)* **46** (1965) no. 9, 473.
[852] Gmelins Handbuch der Anorganischen Chemie (1935), Stickstoff, nitrogen system 4, **vol. 2**, Verlag Chemie, Berlin, p. 405.
[853] C. Rumscheidt, H. H. Saenger, K. Winnacker, "Der Stickstoff und seine anorganischen Verbindungen" in K. Winnacker, E. Weingaertner (eds) "Chemische Technologie". Carl Hanser Verlag, München 1950, **vol. 2**, p. 188–190.
[854] C. A. Vancini: *Synthesis of Ammonia,* Macmillan, London 1971, p. 235.
[855] I. Hay, G. D. Honti: *The Nitrogen Industry,* **vol. 1,** Akadememiai Kiado, Budapest 1976.
[856] *Nitrogen* **72** (1971) 34.
[857] C. A. Vancini: *Synthesis of Ammonia,* Macmillian, London 1971, p. 249.
[858] US 2953 371, 1958 (A. Christensen, R. D. Rayfield).
[859] D. L. Astanovski, L. Z. Astanovski, *Nitrogen,* **232** (1998) 33–38.
[860] US 3041 151, 1962 (A. Christensen).
[861] US 3050 377, 1962 (A. Christensen).
[862] US 2861 873, 1976 (G. A. Worn).
[863] US 3032 139, 1976 (M.Vilceanu, C. Bors).
[864] H. Hinrichs et al., *DECHEMA Monogr.* **68** (1971) 493–500.
[865] P. Lesur, *Nitrogen* **108** (1977) 29.
[866] C. A. Vancini: *Synthesis of Ammonia,* Macmillan, London 1971, p. 236, 240, 244.
[867] A. V. Slack "Commercial ammonia processes"; A. V. Slack, G. J. James, *Ammonia,* **Part III** Marcel Dekker, New York 1974, p. 291–369.
[868] *Nitrogen* **75** (1972) 33.
[869] US 3475 136, 1969 (G. P. Eschenbrenner, C. A. Honigsberg).
[870] S. Strelzow: *Technology and Manufacture of Ammonia,* Wiley, New York 1981, p. 34.
[871] US 3694 169, 1972 (R. Fawcett, A. W. Smith, D. Westwood).
[872] D. E. Riddler, 16th AIChE Ammonia Safety Symp., Atlantic City 1971; *Ammonia Plant Saf.* **14** (1972), 57.
[873] US 3633 179, 1972 (D. D. Metha, E. J. Miller).
[874] I. Dybkaer inH.I. Lasa (ed.): *Chemical Reactor Design and Technology,* Nasa ASI Series E: Applied Sciences, no. 110, Nijhoff Publ., Dordrecht 1986.

[875] V. Vek, 7th Int. Symp. Large Chem. Plants, Brugge 1988, p. 77.
[876] V. Vek, *Chem. Ing. Tech.* **45** (1973) 608.
[877] V. Vek, *Ind Eng. Chem. Process Des. Dev.* **16** (1977) 412.
[878] DE 3334 777, 1984 (K. Ohasaki, J. Zanma, H. Watanabe).
[879] *Nitrogen* **31** (1964) 22.
[880] T. Wett, *Oil Gas J.* **69** (1971) 70.
[881] *Chem. Eng (New York)* **78** (1971) 90.
[882] US 3372 988, 1968 (H. J. Hansen).
[883] A. Nielsen, 16th AIChE Ammonia Safety Symp., Atlantic City 1971.
[884] A. V. Slack in A. V. Slack, G. J. James (eds.): *Ammonia,* **part III,** Marcel Dekker, New York 1974, p. 345.
[885] A. V. Slack in A. V. Slack, G. J. James (eds.): *Ammonia,* **part III,** Marcel Dekker, New York 1974, p. 354.
[886] US 3754 078, 1975 (H. Hinrichs et al.).
[887] US 3918 918, 1975 (H. B. Kohn, G. Friedman).
[888] O. J. Quartulli, G. A. Wagner, *Hydrocarbon Process.* **57** (1978) no. 12, 115.
[889] US 3567 404, 1971(L. C. Axelrod et al.).
[890] G. P. Eschenbrenner, G. A. Wagner, 16th AIChE Ammonia Safety Symp., Atlantic City 1971; *Ammonia Plant Saf.* **14** (1972) 51.
[891] C. A. Vancini: *Synthesis of Ammonia,* Macmillan, London 1971 p. 232.
[892] US 2898 183, 1959 (G. Fauser).
[893] S. Strelzow: *Technology and Manufacture of Ammonia,* Wiley, New York 1981, p. 27.
[894] H. W. Graeve, *Chem. Eng. Prog.* **77** (1981) no. 10, 54; *Ammonia Plant Saf.* **23** (1981) 78.
[895] *Nitrogen* **81** (1973) 29, 37.
[896] H. Hinrichs, H. Lehner, *Chem. Anlagen + Verfahren* 1972, no. 6, 55.
[897] F. Förster, *Chem. Eng. (N.Y.)* **87** (1980) no. 9, 62.
[898] *Nitrogen* **101** (1976) 42.
[899] Topsøe Topics, June 1976.
[900] I. Dybkjaer, E. A. Gam, 29th AIChE Ammonia Safety Symp., San Francisco 1994; *Ammonia Plant Saf.* **25** (1985) 15.
[901] I. Dybkjaer, E. A. Gam, *CEER Chem. Econ. Eng. Rev.* **16** (1984) 29.
[902] Haldor Topsoe US 4181 701, 1980 (E. A. Gam).
[903] Haldor Topsoe US 2710 247, 1981.
[904] I. Dybkjaer, J. E. Jarvan, Nitrogen 97, British Sulphur Conference, Geneva 1997.
[905] *Nitrogen* **169** (1987) 33.
[906] E. Commandini, U. Zardi, Fertilizer Latin America, Int. Conf. British Sulphur , Caracas 1989.
[907] L. Sutherland, B. Wallace, 33rd AIChE Ammonia Safety Symp., Denver 1988.
[908] G. Pagani, U. Zardi, FAI Seminar 1988, The Fertilizer Society of India, New Dehli, S II/1–19.
[909] K. A. Clayton, N. Shannahan, B. Wallace, 35th AIChE Ammonia Safety Symp., San Diego 1990.
[910] N. Shannahan, *Hydrocarbon Process* **68** (1989) 60.
[911] S. E. Handman, J. R. LeBlanc, *Chem. Eng. Prog.* **79** (1983) no. 5, 56.
[912] H. Stahl, *Symposium of the Fertilizer Society,* London 1982, Proceedings, p. 61.
[913] US 4452760, 1984 (R. B. Peterson, R. Finello, G. A. Denavit).
[914] US 3892 535, 1975 (W. Hennel, C. Sobolewsk).
[915] W. A. Glover, J. P. Yoars, *Hydrocarbon Process.* **52** (1973) no. 4, 165; 17th AIChE Ammonia Safety Symp., Minneapolis 1972; *Ammonia Plant Saf.* **15** (1973) 77.

[916] *Nitrogen* **82** (1973) 34.
[917] GB 1134 621, 1989 (D. R. Twist, D. W. Stanbridge).
[918] W. A. Glover, J. P. Yoars, *Hydrocarbon Process* **52** (1973) 165.
[919] US 3721 532, 1973 (L. E. Wright, A. E. Pickford).
[920] US 3851 046, 1975 (L. E. Wright, A. E. Pickford).
[921] US 4 744 966, 1988 (B. J. Grotz).
[922] EP 268 469, 1988 (B. J. Grotz).
[923] K. C. Wilson, B. J. Grotz, *J. Tech. Dev.* **14** (1990) 54.
[924] B. J. Grotz, L. Grisolia, *Nitrogen* **199** (1992) 39.
[925] F. Horn, L. Küchler, *Chem. Ing. Tech.* **31** (1959) 1.
[926] H. Bakemeier, R. Krabetz, *Chem. Ing. Tech.* **34** (1962) 1.
[927] R. Jackson, *Chem. Eng. Sci.* **19** (1964) no. 19, 253.
[928] D. C. Dyson et al., *Canadian J. Chem. Eng. Sci.* **45** (1967) 310.
[929] L. D. Gaines, *Ind. Eng. Chem. Process Des. Dev.* **16** (1977) no. 3, 381.
[930] I. Dybkjaer in A. Nielsen: *Ammonia — Catalysis and Manufacture,* Springer-Verlag, New York 1995, p. 251.
[931] Ammonia — Energy Integration in Ammonia Plants, Uhde Engineering News 2–91, Hi 111 9 1000 91, 1991.
[932] M. J. P. Bogart in A. I. More (ed.), *Proc. Br. Sulphur Corp. Int. Conf. Fert. Technol. 4th 1981* 1982, 141.
[933] M. J. P. Bogart, *Plant Oper. Prog.* **1** (1982) no. 3, 147.
[934] M. J. P. Bogart, *Hydrocarbon Process.* **57** (1978) no. 4, 145.
[935] W. Malewski, *Chem. Ztg.* **95** (1971) 186.
[936] K. Bohlscheid, *Chem. Prod.* **8** (1979) no. 3.
[937] G. Holldorff, *Hydrocarbon Process.* **58** (1979) no. 7, 149.
[938] Pullman Inc., DE-OS 2741851, 1978 (C. L. Becker).
[939] G. Pagani, U. Zardi, *Hydrocarbon Process.* **51** (1972) no. 7, 106–110.
[940] F. Saviano, V. Lagana, P. Bisi, *Hydrocarbon Process.* **60** (1981) no. 7, 99.
[941] H. Hinrichs, *Chem. Ztg. Chem. Appar.* **86** (1962) 223.
[942] H. Neth et al., *Chem. Eng. Prog.* **78** (1982) no. 7, 69.
[943] *Chem. Week* **116** (Feb. 19, 1975) 29.
[944] A. Finn, *Nitrogen* **175** (1988) 25 –32.
[945] R. Harmon, W. H. Isalski, 25th AIChE Ammonia Safety Symp., Portland 1980; *Ammonia Plant Saf.* **23** (1981) 39.
[946] A. Haslam, P. Brook, H. Isalski, L. Lunde, *Hydrocarbon Process.* **55** (1976) no. 1, 103.
[947] *Nitrogen* **102** (1976) 35.
[948] R. Banks, *Chem. Eng. (N.Y.)* **84** (1977) no. 21, 90.
[949] A. A. Haslam, W. H. Isalski, 19th AIChE Ammonia Safety symp., Salt Lake City 1974; *Ammonia Plant Saf.* **17** (1975) 80.
[950] R. Harmon in A. I. More (ed.), *Proc. Br. Sulphur Corp. Int. Conf. Fert. Technol. 4th 1981* 1982, 113.
[951] R. Banks, 22th AIChE Ammonia Safety Symp., Denver 1977; *Ammonia Plant Saf.* **20** (1978) 79.
[952] *Oil Gas J.* **77** (March 5, 1979) 182.
[953] W. H. Isalski, *Nitrogen* **152** (1984) 100.
[954] R. Harmon, W. H. Isalski, 25th AIChE Ammonia Safety Symp., Portland 1980; *Ammonia Plant Saf.* **23** (1981) 39.

[955] C. A. Combs, 25th AIChE Ammonia Safety Symp., Portland 1980; *Ammonia Plant Saf.* **23** (1981) 32.

[956] R. Fabian, D. Tilman, *Linde Ber. Techn. Wiss.* **59** (1986) 6.

[957] C. A. Combs, 25th AIChE Ammonia Safety Symp., Portland 1980; *Ammonia Plant Saf.* **23** (1981)32.

[958] D. L. MacLean, C. E. Prince, Y. C. Chae, *Chem. Eng. Prog.* **76** (1980) no. 3, 98; 24th AIChE Ammonia Safety Symp., San Francisco 1979; *Ammonia Plant Saf.* **22** (1980) 1.

[959] Y. C. Chae, G. S. Legendre, J. M. van Gelder in A. I. More (ed.), *Proc. Br. Sulphur Corp. Int. Conf. Fert. Technol. 4th 1981* 1982, 457.

[960] *Nitrogen* **130** (1981) 40.

[961] *Nitrogen* **136** (1982) 29.

[962] R. L. Schendel, C. L. Mariz, J. Y. Mak, *Hydrocarbon Process.* **62** (1983) no. 8, 58.

[963] D. L. MacLean, D. J. Stockey, T. R. Metzger, *Hydrocarbon Process.* **62** (1983) no. 8, 47.

[964] H. Knieriem Jr., *Hydrocarbon Process.* **59** (1980) no. 7, 65.

[965] M. D. Rosenzweig, *Chem. Eng. (N.Y.)* **88** (1981) no. 24, 62.

[966] G. Schulz, H. Michele, U. Werner, *Chem. Ing. Tech.* **54** (1982) no. 4, 351.

[967] A. K. Fritzsche, R. A. Narayan, *CEER Chem. Econ. Eng. Rev.* **19** (1987) 19.

[968] W. A. Koros, R. A. Narayan, *Chem. Eng. Progr.* (1995) 68 - 81.

[969] *Hyrocarbon Process.* **62** (1983) 43 - 62.

[970] G. Q. Miller, M. J. Mitariten, ICI Catalco/KTI/UOP Hydrogen Plant Seminar, Chicago 1995.

[971] *Nitrogen* **121** (1979) 37 - 43.

[972] G. Low, "Revamping Ammonia Plant" (ed. K. Dunn), Supplement to *Nitrogen* **147** (1984).

[973] Union Carbide Corp., US 4077780, 1976.

[974] *Chem. Eng. (London)* 1979, no. 345, 395.

[975] K. Knoblauch et al., *Erdöl Kohle Erdgas Petrochem.* **32** (1979) 551.

[976] J. G. Santangelo, G. T. Chen, *Chemtech* **13** (1983) no. 10, 621.

[977] J. J. Sheridan, III, et al., *Less Common Met.* **89** (1983). 447.

[978] R. J. Berry, *Chem. Eng. (N.Y.)* **86** (1979) no. 15, 62.

[979] W. H. Isalski, G. J. Ashton in A. I. More (ed.), *Proc. Br. Sulphur Corp. Int. Conf. Fert. Technol. 4th 1981* 1982, 125.

[980] S. Lynn, C. Alesandrini, 18th AIChE Ammonia Safety Symp., Vancouver 1973; *Ammonia Plant Saf.* **16** (1974) 80.

[981] I. Dybkjaer in A. Nielsen: *Ammonia — Catalysis and Manufacture,* Springer-Verlag, New York 1995, p. 231.

[982] O. J. Quartulli, J. B. Fleming, J. A. Finneran, *Hydrocarbon Process.* **47** (1968) 153.

[983] O. J. Quartulli, J. B. Fleming, J. A. Finneran, *Nitrogen* **58** (1969) 25.

[984] I. Dybkjaer in A. Nielsen (ed.): *Ammonia — Catalysis and Manufacture,* Springer-Verlag, New York 1995, p. 227, 228.

[985] H. Weber et al., *Chem. Ing. Tech.* **56** (1984) no. 5, 356.

[986] H. W. Graewe, 25th AIChE Ammonia Safety Symp., Portland 1980; *Ammonia Plant Saf.* **23** (1981) 78.

[987] H. W. Graewe, *Chem. Eng. Progr.* **77** (1981) no. 10, 54.

[988] K. Nassauer, M. Fix, AFA/Abu — Qir Ammonia/Urea Technol. Symp., 1996.

[989] "Plant and process engineering equipment – Components and plant circuitry", *Steinmüller company brochure* P 8604-06-0510/89 (1989)

[990] "Waste heat recovery for reformed gas and synthesis gas cooling in modern ammonia plants", *Borsig AG, company brochure.*

[991] "K. Nassauer, "Process gas waste heat boilers" *Borsig AG, company brochure* 290151 AC.

[992] *Nitrogen* **176** (1988) 25.

[993] H. Lachmann, D. Fromm, 32nd AIChE Ammonia Safety Symp., Minneapolis 1987; *Ammonia Plant Saf.* **28** (1988) 39.

[994] G.R. Prescott et al., 33rd AIChE Ammonia Safety Symp., Denver 1988; *Ammonia Plant Saf.* **29** (1989) 253.

[995] NH_3—Gas—Synthesis, Balke-Dürr comp. brochure, CBA 100o-7.91, 1991.

[996] T. Timbres et al., 34th AIChE Ammonia Safety Symp, San Francisco 1989; *Ammonia Plant Saf.* **30** (1990) 200.

[997] Balcke-Dürr, Company Leaf-let 31.07.1990.

[998] Synloop Wast Heat Boiler in Ammonia Plants — Unique Hot/Cold Tube Sheet Design, Babcock Borsig comp. brochure.

[999] M. Podhorsky et al., 40th AIChE Ammonia Safety Symp., Tucson 1995; *Ammonia Plant Saf.* **36** (1996) 321.

[1000] K. H. Deuse, *Ingenieursblad* **40** (1971) no. 21, 614 (Prospectus of Borsig: Process Gas Waste Heat Boilers).

[1001] M. Podhorski, "Hydraulic expansion of tubes", *International Conference on Expanded and Rolles Joint technology, Toronto* (1993).

[1002] J. Becker, *Verfahrenstechnik* 3, 8 (1969), 335.

[1003] Shell POX Waste heat boilers Standard Fasel-Lentjes, Company brochure 1996.

[1004] L. Silberring, *Nitrogen* **120** (1979) 35.

[1005] P. Hinchley, *Chem. Eng. (N.Y.)* **86** (1979) no. 17, 120. P. Hinchley, *Proc. Inst. Mech. Eng.* **193** (1979) no. 8.

[1006] H. Lachmann, 25th AIChE Ammonia Safety Symp., Portland 1980; *Ammonia Plant Saf.* **23** (1981) 51.

[1007] O. J. Quartulli, W. Turner, *Nitrogen* **80** (1972) 28.

[1008] O. J. Quartulli, W. Turner, *Nitrogen* **81** (1973) 32.

[1009] J. B. LeBlanc, M. N. Shah, L. J. Buividas, *Hydrocarbon Process.* **59** (1980) no. 4, 68-G.

[1010] *Hydrocarbon Process.* **62** (1983) no. 11, 81.

[1011] E. Futterer, E. Pattas, *Chem. Ztg.* **98** (1974) no. 9, 438.

[1012] K.-J. Mundo, *Chem. Anlagen + Verfahren* 1972, no. 6, 49.

[1013] J. D. Rankin, J. G. Livingstone, 25th AIChE Ammonia Safety Symp., Portland 1980; *Ammonia Plant Saf.* **23** (1981) 203.

[1014] J. S. Campbell, J. W. Marshall, *Nitrogen* 1976, no. 103, 33.

[1015] O. J. Quartulli, D. Wagener, *Erdöl Kohle Erdgas Petrochem.* **26** (1973) no. 4, 192.

[1016] U. Zardi, A. Antonini, *Nitrogen* **122** (1979) 33.

[1017] G. D. Honti, 4th Int. Conf on Fertilizer Technol., London 1981, Conf. Proc., Brit. Sulphur (ed. A. More) p. 1.

[1018] F. Saviano, W. Lagana, P. Bisi, *Hydrocarbon Process.* **60** (1981) 99.

[1019] I. Dybkjaer, ECN Europ. Chemical News: Fertilizers 83 (suppl.), 1983, p.15.

[1020] G. R. James, K. J. Stokes, *Chem. Eng. Progr.* **62** (1984)81.

[1021] J. M. Blanken, 33rd AIChE Ammonia Safety Symp., Denver 1988; *Ammonia Plant Saf.* **29** (1989) 273.

[1022] F. C. Brown, *Nitrogen* **100** (1976) 65.

[1023] K. J. Mundo, *Erdöl, Kohle, Erdgas Petrochemie* **31** (1978) 74.

[1024] *Nitrogen* **182** (1989) 25.

[1025] L. J. Buividas, *Hydrocarbon Process.* **58** (1979) no. 5, 257.

[1026] G. D. Honti in A. I. More (ed.), *Proc. Br. Sulphur Corp. Int. Conf. Fert. Technol. 4th 1981* 1982, 1.

[1027] G. R. James, 31st Annual Meeting, The Fertilizer Industry Round Table, USA 1981 G. R. James, K. J. Stokes, *Chem. Eng. Prog.* **80** (1984) no. 6, 33.

[1028] I. Dybkjaer, *Eur. Chem. News* 1983, no. Feb. 21, 15 (Fertilizers '83 Suppl.).

[1029] A. Pinto, P. L. Rogerson, *Chem. Eng. Prog.* **73** (1977) no. 7, 95.

[1030] K. J. Mundo, *Erdöl Kohle Erdgas Petrochem.* **31** (1978) no. 2, 74.

[1031] J. R. LeBlanc, *Hydrocarbon Process.* **63** (1984) no. 7, 69.

[1032] A. Nielsen et al., *Plant Oper. Prog.* **1** (1982) no. 3, 186.

[1033] J. G. Livingstone, A. Pinto, *Chem. Eng. Prog.* **79** (1983) no. 5, 62.

[1034] ICI, EP-A 93502, 1983 (A. Pinto).

[1035] P. H. Brook: "Fertilizer '83," *Br. Sulphur Corp. 7th Int. Conf.*, London 1983, Proceedings of the Conf., p. 159.

[1036] G. Pagani, G. Brusasco, G. Gramatica in A. I. More (ed.), *Proc. Br. Sulphur Corp. Int. Conf. Fert. Technol. 4th 1981* 1982, 195.

[1037] Pullman Inc., US 4079017 (D. B. Crawford, C. L. Becker, J. R. LeBlanc); US 4162290, 1979 (D. B. Crawford, C. L. Becker, J. R. LeBlanc).

[1038] S. Uji, M. Ikeda, *Hydrocarbon Process.* **60** (1981) no. 7, 94.

[1039] E. Nobles, J. C. Stover, *Chem. Eng. Prog.* **80** (1984) no. 1, 81. E. Nobles, J. C. Stover, *Ammonia Plant Saf.* **24** (1984) 41.

[1040] *Nitrogen* **162** (1986).

[1041] J. G. Livingstone, A. Pinto, 27th AIChE Ammonia Safety Symposium, Los Angeles 1982; *Chem. Eng. Progr.* **79** (1983) 62–66.

[1042] W. K. Taylor, A. Pinto, 31st AIChE Ammonia Safety Symposium, Boston 1986; *Ammonia Plant Saf.* **27** (1987) 43.

[1043] "Ammonia–Uhde's low energy technology", *Uhde engineering news 1–91 (1991).*

[1044] S. Weems, D. H. Ball, D. E. Griffin, *Chem. Eng. Prog.* **75** (1979) no. 5, 64; 23th AIChE Ammonia Safety Symp., Miami Beach 1978; *Ammonia Plant Saf.* **21** (1979) 39.

[1045] G. Collier, J. D. Voelkers, D. E. Griffin, *Ammonia Plant Saf.* **22** (1980) 206.

[1046] F. Yazhari, *Hydrocarbon Process.* **61** (1982) no. 5, 187.

[1047] P. Tjissen, 21nd AIChE Ammonia Safety Symp., Atlantic City 1976; *Ammonia Plant Saf.* **19** (1977) 155.

[1048] G. R. Nieman, L. C. Daigre, III, 18th AIChE Ammonia Safety Symp., Vancouver 1973; *Ammonia Plant Saf.* **16** (1974) 45.

[1049] C. C. Yost, C. R. Curtis, C. J. Ryskamp, 24th AIChE Ammonia Safety Symp., San Francisco 1979; *Ammonia Plant Saf.* **22** (1980) 200.

[1050] *Nitrogen* **65** (1970) 32.

[1051] T. L. Huurdeman, 33rd AIChE Ammonia Safety Symp., Denver 1988; *Ammonia Plant Saf.* **29** (1989) 234.

[1052] R. L. Allen, jr., G. A. Moser, 36th AIChE Ammonia Safety Symp., Los Angeles 1991; *Ammonia Plant Saf.* **32** (1992) 170.

[1053] D. Dekmush et al., 37th AIChE Ammonia Safety Symp., San Antonio 1992; *Ammonia Plant Saf.* **33** (1993)278.

[1054] S. Madhaven, *Plant /Oper. Progr.* **3** (1984) no. 1, 14.

[1055] S. M. Solomon, 29th AIChE Ammonia Safety Symp., San Francisco 1984; *Ammonia Plant Saf.* **25** (1985) 129.

[1056] S C. Moore, T. M. Piper, C. C. Chen,30th AIChE Ammonia Safety Symp., Seattle 1985; *Ammonia Plant Saf.* **26** (1986) 56.
[1057] *Nitrogen* **169** (1987) 35.
[1058] S. Mani, S. K. Shoor, H. S. Pedersen, 33rd AIChE Ammonia Safety Symp., Denver 1988; *Ammonia Plant Saf.* **29** (1989) 244; *Plant /Oper. Progr.* **8** (1989) 33.
[1059] G. Grossman, J. Dejaeger, 37th AIChE Ammonia Safety Symp., Los Angeles 1991; *Ammonia Plant Saf.* **32** (1992) 164.
[1060] I. Dybkjaer in A. Nielsen (ed.): *Ammonia Catalysis and Manufacture* Springer, New York 1995 p. 263.
[1061] I. Dybkjaer in A. Nielsen (ed.): *Ammonia Catalysis and Manufacture* Springer, New York 1995 p. 258 – 261; 269 – 271 .
[1062] P. Radke, *Nitrogen* **225** (1997) 27.
[1063] *Oilweek (Calgary, Alberta)* (May 23, 1983) 12.
[1064] *Chem. Week* **134** (March 21, 1984) 15.
[1065] *Nitrogen* **189** (1989) 25.
[1066] J. R. LeBlanc, *Chem. Econ. Eng. Rev.* **18** (1986) no. 5, 22.
[1067] *Fertilizer Focus* **4** (1987) no. 10, 40.
[1068] J. R. LeBlanc, *Energy Prog.* **5** (1985) no. 1, 4.
[1069] M. Appl: *Ammonia, Methanol, Hydrogen, Carbon Monoxide — Modern production Technologies* CRU Publ., London 1997, p. 44, 45.
[1070] J. R. LeBlanc, 29th AIChE Symposium on Safety in Ammonia Plants, San Francisco, Calif., 1984; *Ammonia Plant Saf.* **25** (1985) 29.
[1071] *CEER Chem. Econ. Eng. Rev.* **11** (1979) no. 5, 24.
[1072] I. Dybkjaer in A. Nielsen (ed.): *Ammonia Catalysis and Manufacture* Springer, New York 1995 p. 288, 289.
[1073] I. Dybkjaer, Fertilizer Latin America Int. Conf., Caracas 1989; Brit. Sulphur Corp. Proc., vol. 1, p. 77.
[1074] I. Dybkjaer, FAI Seminar 1990, The Fertilizer Assoc. of India, New Delhi, p. SIII–1.
[1075] T. Bajpai, *Nitrogen 88, Brit. Sulphur 12th Int. Conf.,* Geneva 1988.
[1076] T. S. Hariharan, *J. Tech. Dev.* **7** (1987) no. 4, 42.
[1077] S. R. Sahore, T. S. Krishnan, *Fertilizer News* **15** (1989).
[1078] I. Dybkjaer, *Fertilizer Industry Ann. Rev.* **XIII** (1990) 42a.
[1079] I. Dybkjaer, IFA Technical Conf., The Hague 1992.
[1080] I. Dybkjaer, IFA – FADINAP Regional Conf. for Asia and Pacific, Bali 1992
[1081] *Hydrocarbon Process.* **62** (1983) no. 11, 79.
[1082] F. Brown, Proceedings no. 218, The Fertilizer Society, London 1983.
[1083] *Hydrocarbon Process.* **60** (1981) no. 11, 132.
[1084] *The Uhde Reformer: High Pressure, High Temperature Service* Uhde Brochure Hi 18 1500 11/ 1991.
[1085] Energy Efficient Ammonia Production*Uhde Eng. News.***3** (1991)
[1086] Ammonia Plant – Energy Integration*Uhde Eng. News.***2** (1991).
[1087] *Uhde's Ammonia Technology* Uhde Brochure Hi 18 1500 11/1991; RRD, 1992.
[1088] Ammonia, Uhde's Low Energy Technology*Uhde Eng. News.***1** (1991).
[1089] R. Hakmann,FAI Seminar 1990, The Fertilizer Assoc. of India, New Delhi, p. SIII–3.
[1090] J. Dejaeger, E. Das, 38th AIChE Ammonia Safety Symp., Orlando 1993; *Ammonia Plant Saf.* **34** (1994) 145.

[1091] F. C. Brown in A. I. More (ed.), *Proc. Br. Sulphur Corp. Int. Conf. Fert. Technol. 4th 1981* 1982, 39.

[1092] P. A. Ruziska, C. C. Song, 29th AIChE Ammonia Safety Symp., San Francisco 1984; *Ammonia Plant Saf.* **25** (1985) 22.

[1093] P. A. Ruziska, P. Dranze, C. C. Song, Nitrogen 86, Brit. Sulphur conf., Amsterdam 1986.

[1094] *Chem. Eng. (N.Y.)* **86** (1979) no. 26, 88.

[1095] L. J. Ricci, *Chem. Eng. (N.Y.)* **86** (1979) no. 3, 50, 54.

[1096] *Oil Gas J.* **76** (1978) no. 49, 34.

[1097] P. Taffe, *Chem. Age (London)* **117** (Dec. 15, 1978) 8.

[1098] V. Pachaiyappan, *Fertilizer News* 1979, 41.

[1099] V. Lagana, *Chem. Eng. (N.Y.)* **85** (1978) no. 1, 37.

[1100] B. J. Grotz, *Nitrogen* **100** (1976) 71.

[1101] B. Grotz, G. Good, *Chem. Age* (London) **121** (Nov. 14, 1980) p. 18.

[1102] *Nitrogen* **144** (1983) 30.

[1103] K. C. Wilson et al., *Nitrogen* **151** (1984) 31.

[1104] K. C. Wilson, B. J. Grotz, J.Richez, Nitrogen 86, Brit. Sulphur Conf., Amsterdam 1986.

[1105] B. J. Grotz, *Nitrogen* **217** (1995) 41 - 48.

[1106] K. G. Christensen, B. J. Grotz, K. G. Gosnell, *Nitrogen* **181** (1989) 31 - 36.

[1107] W. Glover, J. P. Yoars, *Hydrocarbon Process.* **52** (1973) no.no. 4, 165.

[1108] W. Glover, J. P. Yoars, 17th AIChE Ammonia Safety Symp., Minneapolis 1972; *Ammonia Plant Saf.* **15** (1973) 77.

[1109] K. G. Christensen, B. J. Grotz, K. G. Gosnell, Fertilizer Latin America Int. Conf., Caracas 1989; Brit. Sulphur Corp. Proc., vol. 1.

[1110] B. J. Grotz, L. Grisolia, *Nitrogen* **199** (1992) 39.

[1111] ICI, EP-A 49967, 1982 (A. Pinto).

[1112] *Chem. Week* **132** (Jan. 5, 1983) 23.

[1113] *Hydrocarbon Process.* **62** (1983) no. 11, 80.

[1114] J. G. Livingstone, A. Pinto, 27th AIChE Ammonia Safety Symp., Los Angeles 1982; *Chem. Eng. Progr.* **79** (May 1983) 62 – 66.

[1115] Fertilizer Industry Annual Review, vol. XI, 1988

[1116] S. A. Topham, S. A. Hall, D. G. Heath, ICI/CFDC Tech. Symp., Shanghai 1989.

[1117] W. K. Taylor, A. Pinto, *Commisioning C–I–Ls Ammonia Plant,* 31st AIChE Ammonia Safety Symp., Boston 1986; *Ammonia Plant Saf.* **27** (1987) 43; *Plant/Operations Prog.* **6** (1987) 106 – 111.

[1118] M. P. Robert, C. W. Hooper, ICI/CFDC Tech. Symp., Shanghai 1989.

[1119] K. J. Elkins et al., Asia Nitrogen, Int. Conf., (Brit. Sulphur) Bali 1994.

[1120] K. J. Elkins et al., *ICIs AMV Ammonia Technology* ICI Catalco tech. paper 246W/126/3/AMM.

[1121] *Nitrogen* **162** (1989) 32 - 37.

[1122] J. G. Livingstone, A. Pinto, Fertilizer 83, Int. Conf. (Brit. Sulphur), London 1988.

[1123] D. L. Banquy, 24th AIChE Ammonia Safety Symp., Denver 1983; *Ammonia Plant Saf.* **24** (1984) 8.

[1124] F. C. Brown, *Eur. Chem. News* 1982, no. 15, 10 (Process Review Suppl.).

[1125] Humphreys & Glasgow Ltd., GB-A 2126208 A, 1983 (C. L. Winter).

[1126] F. C. Brown, C. Topham, Proc. Europ. Conf. on Energy Efficient Prod. of Fertilizers, Bristol 1990, p. 1.

[1127] *Jacobs Ammonia Technology,* Jacobs company brochure, 1996.

[1128] *Chem. Eng. (N.Y.)* **88** (1981) no. 10, 33.

[1129] P. Conolly, *Chem. Age (London)* **122** (Feb. 6, 1981) 12. *Eur. Chem. News* **36** (1981) no.no. 967, 16.

[1130] Pullman Inc., US 4148866, 1979 (C. L. Becker); US 4153673, 1979 (C. L. Becker).

[1131] *Nitrogen* **178** (1989) 30–39.

[1132] J. M. Halstead, A. Pinto, FAI Seminar, Delhi 1988.

[1133] S. P. Sergeev, *Nitrogen,* **233** (1998) 31–34

[1134] A. Pinto, J. M. S. Moss, T. C. Hicks, 34th AIChE Ammonia Safety Symp., San Francisco 1989; *Ammonia Plant Saf.* **30** (1990) 152.

[1135] K. Elkins, I. R. Barton, 39th AIChE Ammonia Safety Symp., Vancouver 1994; *Ammonia Plant Saf.* **35** (1995) 276; *Operational Performance of the ICI Leading Concept Ammonia (LCA) Process,* ICI Catalco tech. paper 274W/126/3/LCA.

[1136] T. C. Hicks, A. Pinto, *Fertilizer News* (1989) 37.

[1137] T. Miyasugi et al., *Chem. Eng. Prog.* **80** (1984) no. 7, 41. T. Miyasugi et al., *Ammonia Plant Saf.* **24** (1984) 64.

[1138] W. F. van Weenen, J. Tielroy, *Nitrogen* **127** (1980) 38.

[1139] *Oil Gas J.* **79** (1981) no. 18, 270.

[1140] S. Ratan, K. S. Jungerhans, KTI Symp., Scheveningen 1991.

[1141] J. J. Westenbrink, J. Voogd, Nitrogen 86, Brit. Sulphur Int. Conf., Amsterdam 1986.

[1142] J. J. Westenbrink, J. Voogd, FAI Seminar, New Delhi 1995.

[1143] W. F. van Weenen, J. Tielroy, *Proc. Fertilizer Soc.* (London) (1980) no. 191, 1.

[1144] W. F. van Weenen, J. Tielrooy, *32nd Ann. Meet., The Fertilizer Industry Round Table,* USA 1982, p. 268.

[1145] *Nitrogen* **208** (1994) 44–49.

[1146] M. Lembeck, Asia Nitrogen 96: Brit. Sulphur Int. Conf., Singapore 1996.

[1147] M. Lembeck, *Fertilizer News* (1993) 15.

[1148] *The Linde Ammonia Concept,* Linde Comp. publ. 1995.

[1149] J. Ilg, B. Kandziora, 41st AIChE Ammonia Safety Symp., Boston 1996; *Ammonia Plant Saf.* **37** (1997) 341.

[1150] M. Spear, *Chem. Eng. (London)* 1979, no. 340, 29.

[1151] P. R. Savage, *Chem. Eng. (N.Y.)* **85** (1978) no. 25, 68 D.

[1152] *ECN Euro Chem News* **20** (1978) 39.

[1153] F. C. Brown, Proc. Dev. Symp. 1978, The Inst. of Engineers, p. 1.

[1154] W. Armbruster, *Erdöl Kohle Erdgas Petrochem.* **33** (1980) no. 3, 118.

[1155] G. Kammholz, G.-A. Müller, *Erdöl Kohle Erdgas Petrochem.* **26** (1973) no. 12, 695.

[1156] H. E. Butzert, *Chem. Eng. Prog.* **72** (1976) no. 1, 56; 20th Ammonia Safety Symp., Boston 1975; *Ammonia Plant Saf.* **18** (1976) 78.

[1157] E. Supp, *Nitrogen* **109** (1977) 36.

[1158] J. Morrison, *Oil Gas J.* **67** (Feb. 24, 1969) 76.

[1159] *CEER Chem. Econ. Eng. Rev.* **12** (1980) no. 6–7, 33.

[1160] J. Dybkjaer, J. Hansen *Chem. Age India* **31** (1980) no. (12): DEV. 3/1

[1161] T. Sueyama, T. Tsujino, Fertilizer 85: Brit. Sulphur Int. Conf., London 1985.

[1162] G. F. Skinner in A. I. More (ed.), *Proc. Br. Sulphur Corp. Int. Conf. Fert. Technol. 4th 1981* 1982, 491.

[1163] Humphreys & Glasgow Ltd., GB-A 2126573 A, 1983 (F. C. Brown).

[1164] R. A. Sharpe, *Hydrocarbon Process.* **55** (1976) no. 11, 171.

[1165] L. J. Partridge, *Chem. Eng. Prog.* **72** (1976) no. 8, 57; 20th AIChE Ammonia Safety Symp., Boston 1975; *Ammonia Plant Saf.* **18** (1976) 73.

[1166] S. McQueen, *Chem. Eng. (N.Y.)* **85** (1978) no. 25, 68 H.

[1167] Lurgi Express Information Ö 1323/5.79, Ammonia Plant Based on Coal.

[1168] *Chem. Eng. News* **57** (1977) no. 23, 27.

[1169] G. W. Alves, D. A. Waitzmann, *Erdöl Kohle Erdgas Petrochem.* **35** (1982) no. 2, 70.

[1170] D. Netzer, J. Moe, *Chem. Eng. (N.Y.)* **84** (1977) no. 23, 129.

[1171] D. A. Waitzman et al., Fall Annual Meeting of the AIChE, Washington, D.C., Oct. 30, 1983.

[1172] T. Matsunami, paper presented to the Internat.Fertilizer Industry Assoc., Johannesburg, South Africa, March 1983.

[1173] *Ubes Texaco Process Coal Gasification Plant,* Ube comp. brochure 1984.

[1174] D. C. Thomson, 4th Int. Conf. on Fertilizer Technol., London 1991, Conf. Proc., part 1, p. 1.

[1175] J. A. Tonna, F. C. Brown, T. W. Nurse, *Nitrogen 91: Brit. Sulphur Conf.,* Copenhagen 1991, p. 127 – 139.

[1176] S. Madhavan, B. Landry, *Nitrogen 91: Brit. Sulphur Conf.,* Copenhagen 1991, p. 127 – 139.

[1177] R. W. Parrish, *Process Improvements,* Gulf Coast Ammonia Producers Meeting, Baton Rouge 1991.

[1178] J. R. LeBlanc, *Hydrocarbon Process.* **65** (1986) no. 8, 39 – 44.

[1179] M. Jung, *Nitrogen* **191** (1991) 42 – 52.

[1180] *Nitrogen* **141** (1983) 38.

[1181] F. C. Brown, *ECN Europ. Chem. News, Proc. Rev.* **8** (1982).

[1182] I. Dybkjaer, Fertilizer Latin America, Int. Conf. Brit Sulphur, Caracas 1989.

[1183] A. Nielsen et al., *Plant/Oper. Progr.* **1** (1982) no. 3, 186.

[1184] H. Graewe, *Nitrogen 88: 12th Int. Conf. Brit. Sulphur,* Geneva 1988, p. 77.

[1185] A. M. Dark, E. A. Stallworthy, *Nitrogen* **153** (1985) 25

[1186] D. Singh, *Process Plant Eng.* **73** (1986) Jan–March.

[1187] J. R. LeBlanc, *Hydrocarbon Process.* **63** (1984) no. 7, 69..

[1188] R. Darjat, J. R. LeBlanc, Nitrogen 88: 12th Int. Conf. Brit. Sulphur, Geneva 1988, p. 77.

[1189] C. L. Becker in A. I. More (ed.), *Proc. Br. Sulphur Corp. Int. Conf. Fert. Technol. 4th 1981* 1982, 537.

[1190] J. R. LeBlanc, *Hydrogen Process.* **63** (1984) no. 7, 69.

[1191] S. I. Wang, N. M. Patel, 28th Ammonia Safety Symp., Denver 1983; *Ammonia Plant Saf.* **24** (1984) 1. S. I. Wang, N. M. Patel, *Plant Oper. Prog.* **3** (1984) no. 2, 101.

[1192] G. Low, *Nitrogen* **147** (1984)1 – 32 (Suppl. "Revamping Ammonia Plants").

[1193] Foster Wheeler, US 4296 085, 1981 (D. L. Banquy).

[1194] D. Kitchen, A. Pinto, 35th AIChE Ammonia Safety Symp., San Diego 1990; *Ammonia Plant Saf.* **31** (1991) 219.

[1195] *Nitrogen* **214** (1996) 46.

[1196] H. Bendix, L. Lenz, 33rd AIChE Ammonia Safety Symp., Denver 1988; *Ammonia Plant Saf.* **29** (1989) 221.

[1197] D. L. MacLean, C. E. Prince, Y. C. Chae, 24th AIChE Ammonia Safety Symp., San Francisco 1979; *Ammonia Plant Saf.* **22** (1980) 1, *Chem. Eng. Progr.* 1980, 98 – 104.

[1198] R. G. Howerton, 24th AIChE Ammonia Safety Symp., San Francisco 1979; *Ammonia Plant Saf.* **22** (1980) 9.

[1199] N. W. Patel, S. I. Wang, K. J. Kittelstad, 33rd AIChE Ammonia Safety Symp., Denver 1988; *Ammonia Plant Saf.* **29** (1989) 33.

[1200] M. Tsujimoto et al., 34th AIChE Ammonia Safety Symp., San Francisco 1989; *Ammonia Plant Saf.* **30** (1990) 167.
[1201] M. Tsujimoto et al., *Nitrogen 91: Brit. Sulphur Conf.*, Copenhagen 1991, p. 127–139.
[1202] R. L. Newland, J. D. Pierce, D. M. Borzik, 32nd AIChE Ammonia Safety Symp., Minneapolis 1987; *Ammonia Plant Saf.* **28** (1988) 53.
[1203] U. Zardi, E. Commandini, C. Gallazzi in A. I. More (ed.), *Proc. Br. Sulphur Corp. Int. Conf. Fert. Technol. 4th 1981* 1982, 173.
[1204] Ammonia Casale, DE-OS 3146778, 1981 (U. Zardi, E. Commandini).
[1205] E. Commandini, U. Zardi: "Fertilizer '83", *Br. Sulphur Corp. 7th Int. Conf.*, London 1983, Proceedings of the Conf., p. 179.
[1206] *Fertilizer News* (1987) (December) 19.
[1207] F. C. Brown, U. Zardi, G. Pangani, *Nitrogen 88: 12th Brit. Sulphur Int. Conf.*, Geneva 1988, p. 1159–139.
[1208] The M. W. Kellogg ammonia converter retrofit, Kellogg company brochure HG/2.5M/3–88 (1988)
[1209] R. G. Howerton, S. A. Noe, *33rd AIChE Ammonia Safety Symposium*, Denver, Oct 1988; *Ammonia Plant Saf.* **29** (1989) 157.
[1210] T. Czuppon et al., 38th AIChE Ammonia Safety Symp., Orlando 1993; *Ammonia Plant Saf.* **34** (1994).
[1211] B. Szantay, E. Jahab in G. D. Honti (ed.): *The Nitrogen Industry*, Akademiai Kiado, Budapest 1976, p. 701–706.
[1212] C. A. Vancini: *La Sintesi dell Amoniaca*, Hoepli, Milano 1961, p. 769.
[1213] *Nitrogen* **16** (1962) 48.
[1214] H. Jungfer, "Synthesegas aus Raffinerie-Rückständen, Konzeption und Betriebsergebnisse von Lindeanlagen zur Partiellen Oxidation", *Linde-Bericht aus Technik und Wissenschaft*, Nr. 57 (1985), 15–20 (ISBN 0024-3728).
[1215] Lurgi, References – *Gas- and Synthesis gas Technology, Lurgi Brochure* 1569e/9.93/4.10.
[1216] M. Appl: *Ammonia, Methanol Hydrogen, Carbon Monoxide – Modern Production Technologies*, CRU London 1997, 3. Methanol, p. 98–99.
[1217] D. Claes, N. Frisse, R. Hakman "Methanol co-production as a revamp otopn for an ammonia plant" *FAI Symposium "Advances in Fertilizer Production"*, New Delhi (April 1995).
[1218] I. Dybkjaer "Ammonia Production Processes" in W. A. Nielsen (ed.): *Ammonia – Catalysis and Manufacture*, Springer, Heidelberg, 1995, p. 300–302.
[1219] *Nitrogen* **43** (1966) 26.
[1220] *Nitrogen* **64** (1970) 17.
[1221] O. J. Quartulli, L. C. Axelrod, R. Randall, (1971) Het Ingenieursblad, 40 (21), 642.
[1222] V. Lagana, U. Zardi, Proc. Fert., Soc. London, (1977), 167, 1.
[1223] V. Lagana, Chem. Eng. (NY) (1978), 85 (1), 167, 1.
[1224] G. Farinola, V. Lagana, Hydrocarbon Processing (1979), 58 (9), 202.
[1225] W. Hausmann et al., *Stahl Eisen* **107** (1987) no. 12, 45–53.
[1226] W. A. Bonner, *Hydrocarbon Process.* (1951) no. 5, 165.
[1227] B. Granville, *Welding in the World* **31** (1993) no. 5, 308.
[1228] API Publication 941, 2nd ed., American Petroleum Institute, Washington, D.C., June 1977; last ed. April 1990.
[1229] G. A. Nelson, *Transactions of ASME* **56** (1977) 205–213.
[1230] I. Class, *Stahl Eisen* **80** (1960) no. 11, 17.
[1231] I. Class, *Stahl Eisen* **85** (1965) 149.

[1232] G. R. Prescott, *Plant Oper. Prog.* **1** (1982) no. 2, 94.
[1233] A. Heuser, 36th AIChE Ammonia Safety Symp., Los Angeles 1991; *Ammonia Plant Saf.* **32** (1992) 243.
[1234] G. R. Prescott, 37th AIChE Ammonia Safety Symp., Los Angeles 1991; *Ammonia Plant Saf.* **32** (1992) 217.
[1235] G. H. Wagner, A. Heuser, G. Heinke, 36th AIChE Ammonia Safety Symp., Los Angeles 1991; *Ammonia Plant Saf.* **32** (1992) 252.
[1236] G. R. Prescott, B. J. Grotz, 39th AIChE Ammonia Safety Symp., Vancouver 1994; *Ammonia Plant Saf.* **35** (1995) 116.
[1237] H. D. Marsch, *Plant Oper. Prog.* **1** (1982) no. 3, 152.
[1238] U. Jäkel, W. Schwenk, *Werkst. Korros.* **22** (1971) no. 1, 1.
[1239] S. Y. Sathe, T. M. O'Connor 32nd AIChE Ammonia Safety Symp., Minneapolis 1987; *Ammonia Plant Saf.* **28** (1988) 115.
[1240] C. A. van Grieken, 33rd AIChE Ammonia Safety Symp., Denver 1988; *Ammonia Plant Saf.* **29** (1989) 145.
[1241] Y. Murakami, T. Nomura, J. Watanabe, *MPC/ASTM Symposium on the Application of 2 1/4 Cr-1 Mo Steel for Thick Wall Pressure Vessels,* Denver, Col. 1980. J. Watanabe et al., *29th Petroleum Mechanical Engineering Conf.,* Dallas, Tex. 1974. G. Grote, *Chem. Ing. Tech.* **55** (1983) no. 2, 93.
[1242] R. Bruscato, *Weld. J. (Miami)* **49** (1970) no. 4, 148.
[1243] J. A. Richardson, *Nitrogen* **205** (1993) 49 – 52.
[1244] H. Stahl, S. G. Thomson, 40th AIChE Ammonia Safety Symp., Tucson 1995; *Ammonia Plant Saf.* **36** (1996) 180.
[1245] T. Shibasaki et al., 40th AIChE Ammonia Safety Symp., Tucson 1995; *Ammonia Plant Saf.* **36** (1996) 165.
[1246] R. J. Gommans, T. L. Huurdeman, 39th AIChE Ammonia Safety Symp., Vancouver 1994; *Ammonia Plant Saf.* **35** (1995) 145.
[1247] J. DeJaeger, L. Guns, J. Korkhaus, 39th AIChE Ammonia Safety Symp., Vancouver 1994; *Ammonia Plant Saf.* **35** (1995) 134.
[1248] J. A. Richardson, Boudouard Carbon and Metal Dusting, ICI Catalco Tech. paper.
[1249] O. J. Dunmore, *Proc. of UK Corrosion Conf.,* 1982.
[1250] H. Grabke, R. Krajak, J. C. Nava Paz, *Corrosion Science* **35** (1993) 1141.
[1251] R. F. Hochmann, 4th Int. Congr. on Metal Corrosion, Nat. Corr. Engineers, 1972.
[1252] A. W. Loginow, E. H. Phelps, *Corrosion (Houston)* **18** (1962) 299.
[1253] L. Lunde, 28th AIChE Ammonia Safety Symp., Denver 1983; *Ammonia Plant Saf.* **24** (1984) 154. J. M. Blanken, 28th AIChE Ammonia Safety Symp., Denver 1983; *Ammonia Plant Saf.* **24** (1984) 140.
[1254] *Plant Oper. Prog.* **2** (1983) no. 3, 247.
[1255] Dechema-Werkstoff-Tabelle/Chem. Beständigkeit, keyword "Ammoniak," sheet 4, Nov. 1978.
[1256] I. Class, K. Gering, *Werkst. Korros.* **25** (1974) no. 5, 314.
[1257] A. W. Loginow, *Mater. Perform.* **15** (1976) no. 6, 33.
[1258] B. E. Wilde, *Corrosion-NACE* **37** (1981) no. 3, 131.
[1259] R. S. Brown, *Plant Oper. Prog.* **1** (1982) no. 2, 97.
[1260] T. Kawamoto et al., *IHI Eng. Rev.* **10** (1977) no. 4, 17.
[1261] N. K. Roy, *Fert. Technol.* **18** (1981) no. 1+2, 1.
[1262] P. B. Ludwigsen, H. Arup, *Corrosion (Houston)* **32** (1976) no. 11, 430.
[1263] E. H. Phelps, *Ammonia Plant Saf.* **16** (1974) 32.

[1264] E. H. Phelps, 18th AIChE Ammonia Safety Symp., Vancouver 1973; *Ammonia Plant Saf.* **16** (1974) 32.

[1265] E. A. Olsen, 13th AIChE Ammonia Safety Symp., Montreal 1968; *Ammonia Plant Saf.* **11** (1969) 46.

[1266] W. v. d. Heuvel, G. v. d. Lindenbergh, *Ingenieursblad* **43** (1974) no. 18, 540–546.

[1267] C. C. Hale, *Nitrogen* **119** (1979) 30–36.

[1268] C. C. Hale, *Nitrogen* **125** (1980) 5.

[1269] T. Huberich, *Plant Oper. Prog.* **1** (1982) no. 2, 117–122.

[1270] I. K. Suri, R. K. Bohla, *Fertilizer News* (1986) (May), 52

[1271] E. H. Phelps, 16th AIChE Ammonia Safety Symp., Atlantic City 1971; *Ammonia Plant Saf.* **14** (1972) 109.

[1272] H. Arup, 21st AIChE Ammonia Safety Symp., Atlantic City 1976; *Ammonia Plant Saf.* **19** (1977) 73.

[1273] L. Lunde, R. Nyborg, 27th AIChE Ammonia Safety Symp., Vancouver 1994; *Ammonia Plant Saf.* **35** (1995) 50; *Plant/Oper. Progr.* **6** (1967) 11–16.

[1274] J. D. Stephens, F. Vidalin, 32nd AIChE Ammonia Safety Symp., Minneapolis 1987; *Ammonia Plant Saf.* **28** (1988) 9.

[1275] L. Lunde, R. Nyborg, 34th AIChE Ammonia Safety Symp., San Francisco 1989; *Ammonia Plant Saf.* **30** (1990) 60.

[1276] J. Blanken, 22nd AIChE Ammonia Safety Symp., Denver 1983; *Ammonia Plant Saf.* **20** (1978) 32.

[1277] L. Lunde, R. Nyborg, The Fertilizer Society, London 1991, Proc. no. 307.

[1278] H. Arup, 21st AIChE Ammonia SAfety Symp., Atlantic City 1976; *Ammonia Plant Saf.* **19** (1977) 73.

[1279] J. R. Byrne, F. E. Moir, R. D. Williams, 33rd AIChE Ammonia Safety Symp., Denver 1988. *Ammonia Plant Saf.* **29** (1989) 122.

[1280] M. Appl et al., 34th AIChE Ammonia Safety Symp., San Francisco 1989; *Ammonia Plant Saf.* **30** (1990) 22.

[1281] R. A. Selva, A. H. Heuser, 21st AIChE Ammonia Safety Symp.; *Ammonia Plant Saf.* **30** (1990) 39.

[1282] K. A. van Krieken, 20th AIChE Ammonia Safety Symp., Boston 1976; *Ammonia Plant Saf.* **18** (1976) 15.

[1283] A. Cracknell, 24th AIChE Ammonia Safety Symp., San Francisco 1979; *Ammonia Plant Saf.* **22** (1980) 63.

[1284] R. S. Brown, *Plant/Oper. Progr.* **1** (1982) 97.

[1285] D. C. Guth, D. A. Clark, 29th AIChE Ammonia Safety Symp., San Francisco 1994; *Ammonia Plant Saf.* **25** (1984) 60.

[1286] D. C. Guth, D. A. Clark, *Plant/Oper. Progr.* **4** (1985) 16.

[1287] S. Hewerdine, The Fertilizer Society, London 1991, Conf. Proc. no. 308, p. 1.

[1288] B. G. Burke, D. E. Moore, 21st AIChE Ammonia Safety Symp., San Francisco 1989; *Ammonia Plant Saf.* **30** (1990) 91.

[1289] M. J. Conley, S. Angelsen, D. Williams, 35th AIChE Ammonia Safety Symp., San Diego 1990; *Ammonia Plant Saf.* **31** (1991) 159.

[1290] C. C. Hale, 18th AIChE Ammonia Safety Symp., Vancouver 1978; *Ammonia Plant Saf.* **16** (1974)23; 23th AIChE Ammonia Safety Symp., Miami Beach 1978; **21** (1979) 61; 28th AIChE Ammonia Safety Symp., Denver 1983; **24** (1984) 181; C. C. Hale, *Nitrogen* **150** (1984) 27.

[1291] J. J. Aarts, D. M. Morrison, 25th AIChE Ammonia Safety Symp., Portand 1980; *Ammonia Plant Saf.* **23** (1981) 124.
[1292] N. A. Hendricks, 23rd AIChE Ammonia Safety Symp., Miami Beach 1978; *Ammonia Plant Saf.* **21** (1979)69.
[1293] J. M. Shah, *Plant Oper. Prog.* **1** (1982) no. 2, 90.
[1294] K. Feind, 22nd AIChE Ammonia Safety Symp., Denver 1977; *Ammonia Plant Saf.* **20** (1978) 46.
[1295] Code of Practice for the Large Scale Storage of Fully Refrigerated Anhydrous Ammonia in the UK, Chemical Industries Association, London 1975.
[1296] J. R. Thomson, 34th AIChE Ammonia Safety Symp., San Francisco 1989; *Ammonia Plant Saf.* **30** (1990) 241.
[1297] J. R. Thomson, R. N. Carnegie, 33rd AIChE Ammonia Safety Symp., Denver 1988; *Ammonia Plant Saf.* **29** (1989) 116.
[1298] C. C. Hale, *Plant Oper. Prog.* **1** (1982) no. 2, 107.
[1299] E. T. Comeau, M. L. Weber, 21st AIChE Ammonia Safety Symp., Atlantic City 1976; *Ammonia Plant Saf.* **19** (1977) 63.
[1300] K. A. Wick, J. B. Withaus, H. C. Mayo, 22nd AIChE Ammonia Safety Symp., San Francisco 1979; *Ammonia Plant Saf.* **22** (1980) 54.
[1301] O. A. Martinez, S. Madhavan, D. J. Kellett, 31th AIChE Ammonia Safety Symp., Boston 1986; *Ammonia Plant Saf.* **27** (1987) 162; *Plant Oper. Prog.* **6** (1967) 129
[1302] C. C. Hale, J. A. Josefson, D. E. Mattick, 29th AIChE Ammonia Safety Symp., San Francisco 1984; *Ammonia Plant Saf.* **25** (1985) 172.
[1303] P. N. Arunachalam, *Fertilizer News* **57** (1986).
[1304] I. Dayasagan, *Fertilizer News* **60** (1986) no.
[1305] P. P. Briggs, J. M. Richards, III, E. G. Fiesinger, 30th AIChE Ammonia Safety Symp., Seattle 1985; *Ammonia Plant Saf.* **26** (1986) 89.
[1306] F. Prasek, 32nd AIChE Ammonia Safety Symp., Minneapolis 1987; *Ammonia Plant Saf.* **28** (1988) 66.
[1307] R. C. A. Wiltzen, 35th AIChE Ammonia Safety Symp., San Diego 1990; *Ammonia Plant Saf.* **31** (1991) 28.
[1308] R. H. Squire, 35th AIChE Ammonia Safety Symp., San Diego 1990; *Ammonia Plant Saf.* **31** (1991) 131.
[1309] S. B. Ali, R. E. Smallwood, 35th AIChE Ammonia Safety Symp., San Diego 1990; *Ammonia Plant Saf.* **31** (1991) 142.
[1310] V. V. Kharlamov, Yu. M. Tsymbal, *Zh. Vses. Khim. Ova.* **28** (1983) no. 4, 433–438.
[1311] G. Schlichthärle, T. Huberich, *Plant Oper. Prog.* **2** (1983), no. 3, 165–167.
[1312] A. A. Arseneaux, 29th Ammonia Safety Symp., San Francisco 1984; *Ammonia Plant Saf.* **25** (1985) 150.
[1313] W. R. Southard et al., Interstate Commerce Comission, U.S. Govt., Informal Study of Freight Rate Structure Fertilizer and Fertilizer Products, **vol. II.**
[1314] R. F. Schrader, *Nitrogen* **117** (1979) 26.
[1315] T. P. Hignett, *Transportation and Storage of Ammonia,* Fertilizer Industry Round Table, Washington 1979.
[1316] C. C. Hale, *Nitrogen 88: 12th Brit. Sulphur Int. Conf.,* Geneva 1988.
[1317] *Nitrogen* **140** (1982) 20.
[1318] G. V. Rohleder, 13th Ammonia Safety Symp., Montreal 1968; *Ammonia Plant Saf.* **11** (1967) 35.

[1319] W. A. Inkofer, 13th Ammonia Safety Symp., Montreal 1968; *Ammonia Plant Saf.* **11** (1967) 40.
[1320] W. A. Inkofer, G. M. Wilson, J. E. Adams, 15th Ammonia Safety Symp., Denver 1970; *Ammonia Plant Saf.* **13** (1971) 67.
[1321] T. F. Kohlmeyer, *Gas Wärme Int.* **19** (1970) no. 1, 15–20.
[1322] R. Leschbaer, H. Schumann, *DECHEMA-Monogr.* **80** (1976) no. 1639–1669, part 2, 747–748.
[1323] *Best Available Techniques for Pollution Prevention and Control in the European Fertilizer Industry,* Booklet 1: Production of Ammonia, European Fertilizer Manufacturers Assoc., 1995.
[1324] Fertilizer Manual ed. by United Nations Industrial Development Organization (UNIDO), Vienna Austria and International Fertilizer Development Center (IFDC), Muscle Schoals, Alabama (USA) Klewer Academic Publishers, Dordrecht, The Netherlands, 1998.
[1325] C. C. Hale, W. H. Lichtenberg, 32nd AIChE Ammonia Safety Symposium; Minneapolis, 1987, *Ammonia Plant Saf.* **28,** (1980) 76.
[1326] D. Eckhold et al., *Chem. Tech. (Leipzig)* **24** (1972) no. 2, 92.
[1327] L. V. Caserta, *Chem. Eng. Prog.* **68** (1972) no. 5, 41.
[1328] T. Dear, 18th AIChE Ammonia Safety Symp., Vancouver 1973; *Ammonia Plant Saf.* **16** (1974) 108.
[1329] R. Werchan, 20th AIChE Ammonia Safety Symp., Boston 1975; *Ammonia Plant Saf.* **18** (1976) 87.
[1330] J. G. Seebold, *Hydrocarbon Process.* **51** (1972) no. 3, 97.
[1331] E. E. Allen, *Gas World* **172** (1970) no. 4501, 431.
[1332] TA, Technische Anleitung zur Reinhaltung der Luft vom Dezember 1983.
[1333] *Environmental Quality of Life,* Technical Note on the best Available Technology not Entailing Excessive Costs for Ammonia Production, *EC Report EUR 13002 EN, 1990.*
[1334] R. F. Griffiths, G. D. Kaiser, *J. Hazard Mater* **6** (1982) 197.
[1335] C. Charp, Agricult. Anhydrous Ammonia Technol. Use Proc. Symp., San Louis 1966, p. 21.
[1336] G. F. P. Harris, P. E. MacDermott, *Inst. Chem. Eng. Symp. Ser.* **49** (1977) 29.
[1337] Association des Producteurs Europeens d'Azote (APEA), Sekretariat Schweizerische Treuhandgesellschaft, St. Jakobstraße 25, Basel, Postfach, 1974.
[1338] W. J. De Coursey et al., *Can. J. Chem. Eng.* **40** (1962) 203.
[1339] C. D. Swann, M. L. Preston, *Loss Prev. Proc Ind.,* **vol. 8.** No. 6, 349–353, 1995, Elsevier Science Ltd.
[1340] R. D. Turney, *TransChem.,* **vol. 68.** Part B, Feb 1990, 12–16.
[1341] R. A. McConnel, 36th AIChE Ammonia Safety Symposium, Nov 1991, Los Angeles; *Ammonia Plant Saf.* **32** (1992), 104.
[1342] A. L. Ormond, *J. ChemE Loss Prev. Bulletion, Issue 126, Dec 1995.*
[1343] E. Banik, *Explosivstoffe* **5** (1957) no. 2, 29.
[1344] J. M. Blanken, 24th Ammonia Safety Symp., San Francisco 1979. *Chem. Eng. Progr.* **76** (1980) 89–104.
[1345] *Oil Gas J.* **70** (Sep. 4, 1972) 86.
[1346] Hauptverband der gewerblichen Berufsgenossenschaften: *Technische Regelwerke,* Carl Heymanns Verlag, Köln.
[1347] DIN Deutsches Institut für Normung e.V., Deutsches Informationszentrum für techn. Regeln (DITR), Berlin.
[1348] Binnenschiffahrtsverlag GmbH, 4100 Duisburg-Ruhrort, Haus Rhein, Dammstraße 15–17.
[1349] IMO, International Maritime Organization, London.

[1350] Bundesanzeigerverlag GmbH, Postfach, 5000 Köln 1.
[1351] Chemical Industries Association Limited, Alembic House, 93 Albert Embankment, London SE 1 7 TU.
[1352] Agricultural Nitrogen Institute, 703 Dupont Building, 22 South Second Str., Memphis, Tennessee.
[1353] Manufacturing Chemists Association, 1825 Connecticut Avenue, N.W., Washington, D.C.
[1354] W. L. Ball, 14th AIChE Ammonia Safety Symp., Portland 1969; Ammonia Plant Saf. **12** (1970), 1.
[1355] A. Resplandy, *Chim. Ind. Genie Chim.* **102** (1969) 691.
[1356] H. C. Goldwire, *Chem. Eng. Progr.* **82** (1986) 35.
[1357] P. K. Raj, J. H. Hagopian, A. S. Kalekar, 19th AIChE Ammonia Safety Symp., Salt Lake City 1969; *Ammonia Plant Saf.* **17** (1970) 102.
[1358] J. C. Statharas et al., *Process Safety Progr.* **10** (1993) 118.
[1359] K. P. Raj, R. C. Reid, *Environ. Sci. Technol.* **12** (1978) 1422.
[1360] National Research Council Panel on Response to Causalities Involving Shipborne Hazards, AD-A075203, 1979, p. 1.
[1361] H. v. Bell, *Chem. Eng. Prog.* **78** (1982) no. 2, 74–77.
[1362] K. A. Vick, J. B. Witthaus et al., *Chem. Eng. Prog. Techn. Man.* **22** (1980) 54–62.
[1363] B. H. Winegar, *Chem. Eng. Prog. Tech. Man.* **22** (1980) 226–230.
[1364] F. J. Heller, *Chem. Eng. Prog. Tech. Man.* **23** (1981) 132–145.
[1365] R. J. Eiber, *Chem. Eng. Prog. Tech. Man.* **23** (1981) 146–156.
[1366] J. J. O'Driscol, 19th AIChE Ammonia Safety Symp., Salt Lake City 1974; *Ammonia Plant Saf.* **17** (1975) 119–122.
[1367] R. F. Griffiths, G. D. Kaiser, *J. Hazard. Mater.* **6** (1982) no. 1/2, 197–212.
[1368] P. P. K. Raj, R. C. Reid, *Environ. Sci. Technol.* **12** (1978) no. 13, 1422–1425.
[1369] M. L. Greiner, *Plant Oper. Prog.* **3** (1984) no. 2, 66; 28th AIChE Ammonia Safety Symp., Denver 1984; *Ammonia Plant Saf.* **24** (1984) 109.
[1370] J. E. Lessenger, *Plant Oper. Prog.* **4** (1985) no. 1, 20.
[1371] A. Nielsen: *Ammonia — Catalysis and Manufacture,* Springer, New York 1995, 329–346.
[1372] C. C. Hale, W. H. Lichtenberg, 24th AIChE Ammonia Safety Symp., San Francisco 1979; *Ammonia Plant Saf.* **22** (1980) 35.
[1373] P. J. Baldock, *Chem. Eng. Prog. Loss Prev.* **13** (1980) 35–42.
[1374] M. Y. Nuttonson, PB–209478, 1 (1972)
[1375] M. B. Jacobs: *The analytical Toxicology of Industrial Inorganic poisons,* **509** Interscience, Wiley N.Y. (1967).
[1376] National Inst. for Occupational Safety and Health, Rockville 1974, PB-246669, p. 1.
[1377] National Research Council, Committee on Toxicology, Washington, PB-244336, p. 1.
[1378] L. Legters, (1980), AD-A094501 p. 1
[1379] I. M. Alpator, *Prom. Toksikol. i. Klinika Prof. Zabol. Khim. Etiol.* **200** (1962).
[1380] L. Matt, *Med. Inaugural Diss,* Würzburg (1889).
[1381] A. C. S. Fieldner, S. H. Katz, S. P. Kinney, *in Noxious Gases,* **125** 2nd rev. ed. Reinhold, N.Y. (1943).
[1382] L. Silvermaur, L. Whittenberger, I. Muller, *I. Industr. Hyg.* **31** (1949) 74.
[1383] J. E. Lessenger, *Plant/Oper. Progr.* **4** (1985) 20.
[1384] R. A. Michaels, Nitrogen **228** (1997) 27–31.
[1385] J. C. Barber, 22nd AIChE Ammonia Safety Symp., Denver 1977; *Ammonia Plant Saf.* **20** (1978) 5.

[1386] J. E. Ryer-Powder, 35rd AIChE Ammonia Safety Symposium, San Diego 1990; *Ammonia Plant Saf.* **31** (1991) 93.

[1387] M. Coplin, *Lancet* **241** (1949) 95.

[1388] W. M. Grant, *Arch. Ophthal.* **44** (1950) 399.

[1389] T. Sollmann, *A Manual of Pharmacology*, 6th ed., Saunders, Philadelphia 1944.

[1390] R. C. Wands, in G. D. Clayton, F. E. Clayton: *Patty's Industrial Hygiene and Toxicology*, **vol. 2 B**, Wiley Interscience, New York 1981, p. 3045–3052.

[1391] K. B. Lehmann, *Arch. Hyg.* **17** (1893) 329.

[1392] P. Trendelenburg in A. Heffter: *Handbuch der experimentellen Pharmakologie*, **vol. I**, p. 470, Springer, Berlin 1923.

[1393] I. M. Alpator, *Gig. Tr. Prof. Zabol.* **2** (1964) 14.

[1394] D. P. Stombaugh, H. S. Teague, W. L. Roller, *I. Anim. Sci.* **6** (1969) 844.

[1395] H. F. Smith, *Amer. Industr. Hyg. Quart.* **17** (1956) 145.

[1396] C. P. Carpenter, H. F. Smith Jr., U. C. Pozzani, *J. Industr. Hyg.* **31** (1949) 343.

[1397] V. I. Mikhailow, *Probl. Kosmich. Biol. Akad. Nauk SSSR* **4** (1965) 531.

[1398] E. M. Boyd, M. L. McLachlin, W. F. Perry, *J. Industr. Hyg.* **26** (1944) 29.

[1399] S. D. Silver, F. P. McGrath, *I. Industr. Hyg.* **30** (1948) 7.

[1400] K. B. Lehmann, *Arch. Hyg.* **5** (1886) 68.

[1401] I. H. Weatherby, *Proe. Soc. Exp. Biol.* **81** (1952) 300.

[1402] R. A. Coon, R. A. Jones, L. J. Jenkins, I. Siegel, *Toxicol. Appl. Pharmacol* **16** (1970) 646.

[1403] K. S. Warren, S. Schenker, *J. Lab. Clin. Med.* **64** (1964) 442.

[1404] W. D. Lotspeich, *Amer. J. Physiol.* **206** (1965) 1135.

[1405] P. Vinay, E. Alignet, C. Pichette, M. Watford, G. Lemieux, A. Gougoux, *Kidney Intern.* **17** (1980) 312.

[1406] D. Z. Levine, L. A. Nash, *Amer. J. Physiol.* **225** (1973) 380.

[1407] K. S. Warren, *J. Clin. Invest.* **37** (1958) 497.

[1408] J. Oliver, E. Bourke, *Clin. Sci. Molec. Med.* **48** (1975) 515.

[1409] J. Yoshida, K. Nakame, R. Nakamura, *Nippon Chikusangakukaiko* **28** (1957) 185.

[1410] D. C. Topping, W. J. Visek, *J. Nat.* **106** (1976) 1583.

[1411] B. Toth, *Int. J. Cancer* **9** (1972) 109.

[1412] Litten Bionetics, *NTIS, PB-245*, 506 (1975) Washington D.C.

[1413] K. A. Hofmann: *Anorganische Chemie*, 20th ed., Vieweg & Sohn, Braunschweig 1969.

[1414] J. Jander: *Chemie in wasserfreiem flüssigem Ammoniak*, Vieweg & Sohn, Braunschweig – Interscience, New York 1963.

[1415] J. P. Lenieur et al., *C. R. Acad. Sci. Ser. C* **268** (1969) no. 20, 1791.

[1416] E. Weiss, W. Buchner cited in [1413]

[1417] F. W. Bergstrom, *Ind. Eng. Chem.* **24** (1932) 57.

[1418] P. Barton et al., *Ind. Eng. Chem. Process Des. Dev.* **7** (1968) no. 3, 366.

[1419] Michael Thiemann et al.: *"Nitric Acid, Nitrous Acid, and Nitrogen Oxides"*, in Ullmann's Encyclopedia of Industrial Chemistry 5ed., **vol. A 17**, pp. 293–340.

[1420] G. D. Honti "Nitric Acid" in G. D. Honti (ed.): The Nitrogen Industry, Akademiai Kiado, Budapest 1976.

[1421] C. Keleti, "Nitric Acid and Fertilizer Nitrates" (Fertilizer Science and Technology Series, **vol. 4**) Marcel Dekker, New York, 1985.

[1422] J. H. Meesen, H. Petersen: *"Urea"* in Ullmann's Encyclopedia of Industrial Chemistry 5ed., **vol. A 27**, pp. 333–366.

[1423] H. Müller: *"Sulfuric Acid and Sulfur Trioxide"* in Ullmann's Encyclopedia of Industrial Chemistry, 5ed., **vol. A 25,** pp. 635–704.

[1424] K. Schrödter et al.: *"Phosphoric Acid and Phosphates"* in Ullmann's Encyclopedia of Industrial Chemistry , 5ed., **vol. A 19,** pp. 465–504.

[1425] U. Müller, A. Greiner, *Chem. Tech. (Leipzig)* **18** (1966) no. 6, 327.

[1426] P. W. Langvardt: *"Acrylonitrile"* in Ullmann's Encyclopedia of Industrial Chemistry, 5ed., **vol. A 1,** pp. 177 – 187.

[1427] T. Wakabayashi, *Ammonia Plant Saf.* **20** (1978) 17.

[1428] *Erdöl Kohle Erdgas Petroch.* **37** (1984) no. 4, 143. *Chem. Ing. Tech.* **56** (1984) no. 8, A 407.

[1429] H. J. Bomelburg, *Plant Oper. Prog.* **1** (1982) no. 3, 175.

[1430] *Chem. Ing. Tech.* **56** (1984) no. 4, A 154.

[1431] K. Dietrich, *Kältetech. Klim.* **22** (1970) no. 6, 184.

[1432] H. L. v. Cube, *Kältetechnik* **16** (1964) no. 3, 76.

[1433] F. Özvegyi, *Kälte (Hamburg)* **23** (1970) no. 6, 298.

[1434] A. Miller, *Kälte (Hamburg)* **20** (1967) no. 6, 275.

[1435] H. Borrmann, *Chem. Ing. Tech.* **40** (1968) 1192.

[1436] C. Hollmann, *Gas Wärme* **9** (1960) 267.

[1437] G. Kurz, *Proc. Eng.* (1976) no. Oct., 97.

[1438] M. N. Park., *Nitrogen 88: Brit. Sulphur International Conference,* Geneva Mar 1988.

[1439] "World Ammonia Production, Consumption and Trade", Statistical supplement, *Nitrogen* **217** (1995) 22.

[1440] "Five year outlook for Ammonia 1995 – 2000", British Sulphur.

[1441] M. Appl, *Ammonia, Methanol, Hydrogen, Carbon monoxide – Modern Production Technologies* CRU Publishing Ltd, London 1997 63 – 65.

[1442] "BP Statistical Review of the world Energy", British Petroleum Co., June 1995.

[1443] "Hydrogen" in Ullmann's Encyclopedia of Industrial Chemistry, VCH Weinheim, **vol A 13,** p. 358.

[1444] F. J. Wollmer, *Ammonia Casale's 75th Anniversary Symposium,* Lugano, Switzerland, Nov. 1996.

[1445] B. Brentnall, "Nitrogen Projects: Gas, Capital, and What Else? *Asia Nitrogen '98, British Sulphur International Conference. Kuala Lumpur.* Feb 22–24, 1998.

[1446] K. Isermann in A. I. More (ed.), *Proc. Br. Sulphur Corp. Int. Conf. Fert. Technol. 4th 1981* 1982, 571.

[1447] Nitrex Statistik 1991, Nitrex AG, Zürich.

[1448] A. Quispel: *The Biology of Nitrogen Fixation,* Elsevier/North Holland Publ. Comp., Amsterdam – Oxford – New York 1974.

[1449] Emerging Technologies no. 1: Nitrogen Fixation. An Analysis of Present Research and Implications for the Future. Technical Insights Inc., Fort Lee, New Jersey.

[1450] R. W. F. Hardy, U. D. Havelka, *Science (Washington, D.C.)* 1975, no. 4188, 633.

[1451] G. J. Leigh in A. I. More (ed.), *Proc. Br. Sulphur Corp. Int. Conf. Fert. Technol. 4th 1981* 1982, 662.

[1452] R. F. Baddour, R. S. Timmins: *The Application of Plasmas to Chemical Processing,* Mass. Inst. Technol. Press, Cambridge 1967.

[1453] D. R. Safrany, *Chem. Eng. Prog. Symp. Ser.* **67** (1971) no. 112, 91, 103.

[1454] *Nitrogen* **144** (1983) 32.

[1455] *The Energetics of Biological Nitrogen Fixation,* Workshop Summaries I, Plant, Physiology, Am. Soc. of Plant Physiologists, Rockville, Maryland, USA.

[1456] D. F. Shanmugam, F. O'Gara, D. Andersen, R. C. Valentine: "Biological Nitrogen Fixation," *Am. Rev. Plant Physiol.* **29** (1978) 263.

[1457] H. J. Rehm: "Beiträge der modernen Biotechnologie und Biochemie zur Ernährung," *VCI-Schriftenreihe Chemie + Fortschritt* 1983, no. 3, 18.

[1458] *Nitrogen* **146** (1983) 24.

[1459] J. R. Postgate: "Fertilizer '83," *Br. Sulfur Corp. 7th Int. Conf.*, London 1983, Proceedings of the Conf., p. 119.

[1460] G. J. Leigh, in *Catalytic Ammonia Synthesis*, ed. by J. R. Jennings, Plenum Press New York and London 1991, 365 – 387.

[1461] J. S. Pathe, C. A. Atkins, R. M. Rumbird, in A. H. Gibson, W. E. Newton (eds.): *Current Perspectives in Nitrogen Fixation*, Australian Academy of Science, Canberra 1981.

[1462] V. P. Gutschick, Long term strategies for supplying nitrogen to crops; Informal report LA-6700–19S, Los Alamos Scientific Laboratory, Los Alamos, NM, USA, 1977.

[1463] R. F. Michin, S. J. Pate, *J. Exp. Bot.* **24** (1973) 259.

[1464] M. J. Merrik, *J. R. Agric. Soc. Engl.* **147** (1986) 202.

[1465] M. Tamaguchi: "Biological Nitrogen Fixation in Flooded Rice Fields," in Nitrogen and Rice, International Rice Research Institute, Manila, Philippines, 1979, p. 193 – 204.

[1466] K. Gopalakrishna Pillai, D. B. B. Chaudary, K. Krishnamurty: "Bio-Fertilizers in Rice Culture – Problems and Prospects for Large Scale Adaptation", *Fert. News* **25** (1980) 40 – 45.

[1467] *Chem. Eng. News* **55** (1977) no. 40, 19.

[1468] G. N. Schrauzer, T. D. Guth, *J. Am. Chem. Soc.* **99** (1977) 7189.

[1469] "Nitrogen Fixation" in Ullmann's Encyclopedia of Industrial Chemistry, **vol. A 18,** VCH Weinheim.

[1470] C. Gleitzner, *Solid State Ionics,* **38** (1990) 33–141.

[1471] M. Et-Tabiru, B. Dupré, C. Gleitzner, *Metallurgical Trans,* **19B** (1988) 311–371.

[1472] H. Schenck, H. P. Schulz, *Arch. Eisenhüttenwesen,* **31** (1960) 691–702.

[1473] J. Schütze, W. Mahdi, B. Herzog, R. Schlögl, *Top. Catal.* 230 (1994), 95 – 96.

[1474] B. Brentnall, "The investment climate of nitrogen fertilizers", Krupp-Uhde Fertilizer Symposium 1998, Dortmund, June 11–13, 1998.

[1475] L. Connock, *Nitrogen,* **226,** (1997) 47–56.

[1476] Krupp-Uhde, private communication.

[1477] R. Saure, "Ammonia from hydrogen-rich off-gases", Krupp-Uhde Fertilizer Symposium 1998, Dortmund, June 11–13, 1998.

[1478] Linde AG, Juliy 1998, private communication.

[1479] P. L. Louis, *66th IFA Annual Conference,* 1998, May 11–14, Toronto.

[1480] L. Maene, "The nitrogen fertilizer markets of Asiain global context – status and outlook", *Asia Nitrogen '98, British Sulphur International Conference,* Kuala Lumpur, 1998, Feb 22–24.

[1481] Capacity statistics by Factories, Situation May 1998, *Nitrex-Complex.*

[1482] K. P. Wang. "The People's Republic of China". US Bureau of Mines, Washington, D. C., 1975.

[1483] "American Rural Small-Scale Industry Delegation", 1977. Rural Rural Small-Scale Industry in the People's Republic of China, Chapter VI, University of California Press, Berkley and Los Angeles, CA, USA.

[1484] G. Heinke, G. H. Wagner, Mat.-Wiss. und Werkstofftechnik, **27** (1996) 259–266.

[1485] S. Fritsch, "Synthesis Gas Production, Comparison of four Synthesis Gas Routes: Steam Reforming, Combined Autothermal Reforming and Partial Oxidation", Krupp-Uhde Fertilizer Symposium 1998, Dortmund, June 11–13, 1998.

[1486] *Nitrogen* **232** (1998) 12.
[1487] J. Richardson, FINDS, X (2) 28 (Second Quarter 1995).
[1488] M. W. Kellogg Press release, Houston July 28, 1998; "Trinidad KAAP Ammonia Plants", M. W. Kellogg presentation September 3, 1998 at Charleston Place Hotel, Charleston, SC.
[1489] J. Xu, G. F. Froment, *AIChE J* **35** (1989). 88 – 86.
[1490] T. Mohri, K. Takamura, T. Shibasaki, 37th AIChE Ammonia Safety Symposium, San Antonio (Sep-Oct 1992); *Ammonia Plant Saf.* **33** (1993). 86 – 100.
[1491] B. J. Cromarty, 36th AIChE Ammonia Safety Symposium, Los Angeles (Nov 1991); *Ammonia Plant Saf.* **32** (1992), 197 – 208.
[1492] "Paralloy H39WM (25/35 Cr/Ni + Nb Microalloy)" Paralloy Technical Paper.
[1493] Schmidt + Clemens, Data Sheets for "Märker G 4852 Micro" and "Märker ET 45 Micro".
[1494] *H. Smith "Organic Reactions in Liquid Ammonia", Vieweg & Sohn, Braunschweig – Interscience*, New York 1963.
[1495] T. Takagi, *Jap. Chem. Q* **4** (4) (1968) 47.
[1496] S. K. Mukherjee, Nitrogen 188, Brit. Sulphur Conf., Geneva, March 27 – 29, 1988.
[1497] R. Habermehl, *FINDS* **vol. IX,** number 3, Third Quater 1994, 24.
[1498] R. Lavie, *Plant/Oper. Prog.* **6 (2)** (1987) 118; *Chem. Eng. Sci.* **40 (11)** (1985), 2019.
[1499] R. US Pat 4537760 (R. Lavie).

Index